ESTIMATION AND CONTROL WITH CENSORED DATA

by

Cory Ignatius Miller

A dissertation submitted to the Faculty of the University of Delaware in partial fulfillment of the requirements for the degree of Doctor of Philosophy in Electrical and Computer Engineering

Winter 2015

ESTIMATION AND CONTROL WITH CENSORED DATA

by

Cory Ignatius Miller

Approved: ______________________________

Dr. Kenneth E. Barner, Ph.D.
Chair of the Department of Electrical and Computer Engineering

Approved: ______________________________

Dr. Babatunde A. Ogunnaike, Ph.D.
Dean of the College of Engineering

Approved: ______________________________

James G. Richards, Ph.D.
Vice Provost for Graduate and Professional Education

I certify that I have read this dissertation and that in my opinion it meets the academic and professional standard required by the University as a dissertation for the degree of Doctor of Philosophy.

Signed: ______________________________

Dr. Ryan M. Zurakowski, Ph.D.
Professor in charge of dissertation

I certify that I have read this dissertation and that in my opinion it meets the academic and professional standard required by the University as a dissertation for the degree of Doctor of Philosophy.

Signed: ______________________________

Dr. Abhyudai Singh, Ph.D.
Member of dissertation committee

I certify that I have read this dissertation and that in my opinion it meets the academic and professional standard required by the University as a dissertation for the degree of Doctor of Philosophy.

Signed: ______________________________

Dr. Charles G. Boncelet, Ph.D.
Member of dissertation committee

I certify that I have read this dissertation and that in my opinion it meets the academic and professional standard required by the University as a dissertation for the degree of Doctor of Philosophy.

Signed: ______________________________

Dr. Mark D. Ilg, Ph.D.
Member of dissertation committee

ACKNOWLEDGEMENTS

I would like to thank Dr. Ryan Zurakowski and Dr. Michael Piovoso for sharing their generous knowledge and experience, for their assistance in all matters of academic pursuit, and for their continued guidance and support. I thank Dr. Bethany Allik for her inspiration and dedication towards creation of the Tobit Kalman Filter. Thank you to the U.S. Army Research Laboratory, Guidance Technologies Branch for enabling the production of this research.

Lastly, thank you to my family, especially my father Thomas Miller, for fostering a scientific mindset and natural curiosity of the world. Thank you for providing for my education at all levels, and encouraging pursuit of ever higher academic and professional success.

TABLE OF CONTENTS

LIST OF TABLES

LIST OF FIGURES

ABSTRACT

Censored measurements are a particular form of output nonlinearity in which the measured output is a continuous function of the state within a certain dynamic range, and is constant outside this range. Such measurements can take the form of output saturation, dead zone, occlusion, and limit of detection. Common systems that may produce censored measurements include low cost inertial sensors with limited dynamic range, imagers with fixed field of view, chemical and biological measurements with limit-of-detection constraints, analog to digital converters, and received signal strength from transmission sources. Estimating the true state of the underlying dynamic system via these censored outputs is a challenging problem that is often overlooked or avoided. Traditional optimal state estimators such as the Kalman filter become biased when presented with the output nonlinearity induced by censored measurements. As a consequence, when output feedback is implemented using these estimators the resulting closed-loop system may become unstable if the system output approaches or enters the censored region.

The Tobit Kalman filter is a novel adaptation of the classical standard Kalman filter for optimal state estimation in the presence of output censoring. With known censoring limits, using a Tobit Kalman filter will result in stable, unbiased state estimation despite censoring. This allows for the application of new and traditional control techniques for system regulation. In this defense new developments of the Tobit Kalman filter and its applications towards control will be reviewed. It will be shown that the Tobit Kalman estimator is a stable unbiased estimator under certain constraints. It will be demonstrated that a Tobit Kalman observer can be used in conjunction with linear output feedback techniques to perform set-point control to values that may not

be directly measureable. Applications of such capability towards novel vision based target tracking and mobile receiver localization and control will be explored.

Novel estimation techniques in the presence of output censoring will be introduced, including the use of multiple fields of view and variable censoring limits. It will be shown that the Tobit Kalman filter can be used to effectively alter censoring limits in order to meet desired state estimation specifications. Advantages of time varying control of censoring limits include minimization of state estimation uncertainty vs. actuation cost, autonomous tracking of multiple targets, and optimal power consumption for measurement systems.

Continuation of this work will be to optimally distribute multiple censoring limits, with seamless integration of differing censoring models, in order minimize state uncertainty over a given region. Optimal control laws will be formulated to alter the trajectory of censoring limits in order to minimize total state uncertainty while tracking multiple states over a given time. Extension to non-linear estimation and control will be performed.

Chapter 1

INTRODUCTION TO CENSORED DATA ESTIMATION

Consider a basic outdoor thermometer not uncommon to any backyard deck or patio. Mercury filled, small, and fixed with a simple scale of zero to one hundred degrees. This simple and inexpensive device has its uses, but it also has its limitations. The temperature may drop to well below zero on a cold winter night, and in summer the temperature may rise well above one hundred on a sunny afternoon. In either case, the thermometer cannot give a more accurate reading than either of its extremes. If the thermometer stays at zero for long enough, intuition leads us to believe that the true temperature actually colder. Likewise, a thermometer saturated at one hundred degrees is more than enough to indicate that it isn't pleasant outside. Examples such as this are so commonplace and routine in one's daily environment that the implications of the underlying sensor limitations are largely ignored.

This simple scenario presented above is a classic example of censored data. The thermometer only presents a limited dynamic range from which measurements can be taken. Too hot or too cold and information is lost, only the limits can be measured, and the true signal has to be inferred. Using the simple thermometer to control room temperature is a typical example of engineering away from the problem. Intuition says that if my measurement limits are between two values, then if I keep my area of interest, in this case room temperature, well below the maximum and well above the minimum, then this censoring will not present itself.

The question is, can this be done better?

First it is shown how systems with these censoring limitations were handled previously. Then the Tobit Kalman Filter is derived and it will be shown that signals can be estimated even when they approach and exceed censoring limits. It is shown that this filter is a stable estimator. Going beyond the estimation itself, it is shown that these estimates can be used in closed-loop feedback to accomplish stable control, even with censored measurements. Set points can be reached even if they are in the censored region, given certain restrictions. This means that not only can a device such as the limited thermometer be used to estimate air temperatures below zero or above one hundred, but one could even use it to control room temperatures into these regions as well. Other motivating examples apart from this one are discussed in detail.

1.1 What is Censored Data?

Censored data is data in which regions exist where the true underlying signal cannot be directly measured. Censored measurements are differentiated from missing measurements by the fact that when the true state enters a censored region a measurement is returned, however this measurement is deterministic and biased. The thermometer for example, has two censored regions. When the true air temperature is below zero the thermometer only returns zero, and when the true air temperature is above one hundred the thermometer can only return one hundred. When the true air temperature is between zero and one hundred then a continuous measurement can be made that is unbiased.

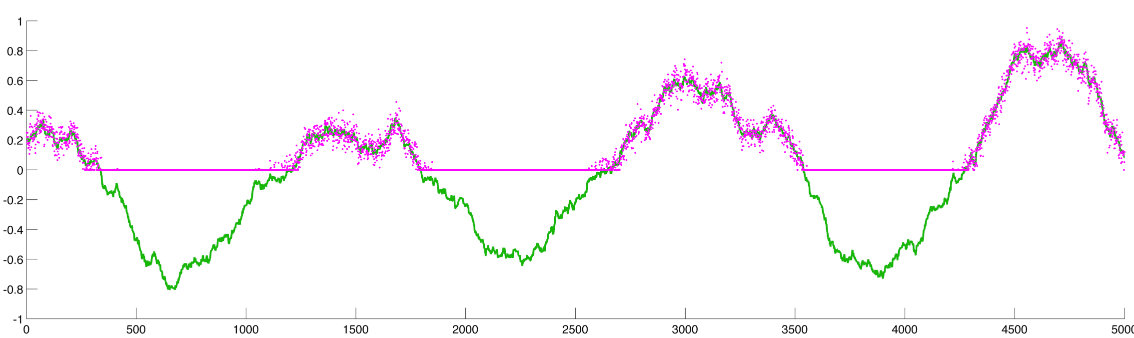

Figure 1.1: Left Censored Data. When the true signal (green) is below the censoring limit, the censoring limit itself is returned as a measurement (magenta).

Censoring may take many different forms. For a single dimensional variable, right censoring occurs when there is only one censoring limit in which all true values above this limit result in measurement of the limit itself. Likewise, left censoring occurs when all true values below the censoring limit result in measurement of the limit itself. Left and right censoring is very common in engineering practice. For example, using a simple electric circuit with a five volt DC power input may result in the ability to only read electrical signals up to five volts. Thus any generated electrical signal, such as that created by common sensors like accelerometers and magnetometers, may be clipped (censored) at five volts. The true signal, if measured without censoring, may be on the order of zero to eight volts. Saturation censoring occurs when both left and right censoring are present at one time, with a region of continuous measurement between. The thermometer is an example of saturation censoring. Deadzone censoring is akin to saturation censoring, except the roles of the censored and uncensored regions are reversed. That is, there is some upper limit above which a measurement can be made, and some lower limit below which a measurement can be made, and a region in between in which a censored value is returned. This type of censoring is common in joystick controls, in which a small area about the neutral position is forced to zero, in order to enforce that there exists a region in which no control is generated. Occlusion censoring occurs in two-dimensions when there exists a closed region in which the true signal cannot be measured. This type of censoring can occur in a vision based system when a target is known to be behind an object, but cannot be directly observed. Frame censoring is akin to occlusion censoring, except the roles of the censored and uncensored regions are reversed. This type of censoring can also occur in a vision based system, when the target exits the field of view. The different types of censoring are presented in table 1.1.

1.2 Basic Handling of Censored Data

The question now arises, what to do if censored data is encountered? The most basic approach to handling censored data in practical applications is to accept them

Table 1.1: Methods of Censoring and Their Definition

Censoring Method	Mathematical Definition
Right Censored	$y_t = \begin{cases} \beta x_t + u_t, & \beta x_t + u_t < T \\ T, & \beta x_t + u_t \geq T \end{cases}$
Left Censored	$y_t = \begin{cases} \beta x_t + u_t, & \beta x_t + u_t > T \\ T, & \beta x_t + u_t \leq T \end{cases}$
Saturation	$y_t = \begin{cases} \beta x_t + u_t, & T_l < \beta x_t + u_t < T_h \\ T_l, & \beta x_t + u_t \leq T_l \\ T_h, & \beta x_t + u_t \geq T_h \end{cases}$
Deadzone	$y_t = \begin{cases} \beta x_t + u_t, & \beta x_t + u_t < T_l \text{ or } \beta x_t + u_t > T_h \\ T_c, & T_l < \beta x_t + u_t < T_h \end{cases}$

as they are. This means giving no preferential treatment to the one measurement over any other, whether censoring is present or not. This approach has the benefit of being computationally and algorithmically very simple. There are no special logical arguments, no additional knowledge to be known beforehand or to be inferred online, and no change to any algorithms that may have been developed with a no-censoring assumption. However this assumption can lead to some very damaging results, because as to be discussed in detail, including censored measurements without special consideration leads to biased estimation of the underlying signal. In short this is due to the fact that censored data measurements not only represent measurements of the true signal directly at the censoring limit, but also all measurements of the true signal in the censored region. Thus, fundamentally, censored measurements must be weighted differently then uncensored measurements when included in any signal estimation algorithm. Failure to do so leads to biases in signal estimation, which may lead to unstable control if the signal is used in an output feedback system.

An alternative approach to handling censored data is to drop the censored measurements from consideration, equating a censored measurement with a missed measurement. This method essentially classifies all censored measurements as invalid measurements. There are two major deficiencies with this approach. One is that uncensored measurements are heavily favored, resulting biased estimation of the true signal. The second is that the information inherent in a censored measurement is being lost. A censored measurement contains information about what region the true signal resides in. Depending on the characteristics of the measurement process this information can be used to estimate the underlying true signal, and at the very least inform about where the signal is not. A missed measurement however fundamentally contains no information. However, the advantage of using this dropped measurement approach over the naive approach presented previously is that good estimation results can still be performed if one has a good model of how the signal is evolving. This is because with a dropped measurement an open-loop prediction can be performed to estimate the signal over time. Instead of relying on accurate signal measurements to estimate the true signal at all times and in all of space, one can take sporadic uncensored measurements and predict using the signal model when missing or dropped measurements are encountered. As shown by [24], and as will be discussed further, this approach can also lead to heavily biased results and unstable feedback control.

A third approach, which largely removes the estimation problem from consideration, is to engineer the system away from known censoring regions. As was discussed with the air-conditioning example, if one assumes that room temperature will only fluctuate between a certain pre-defined range, and sensors are used to measure accurately within this range, then it can be assumed that censoring cannot occur and is not taken into consideration. Often a trade-off is consciously made in order to achieve such a result. For example, in measuring an electrical signal, one can implement a divider to restrict the input range of a given signal, however at the expensive of measurement resolution. So one may be able to guarantee that censored measurements cannot not be generated, but the resulting uncensored measurements may lose precision and be subjected to an increased signal to noise ratio, leading to a system which may become intractable.

1.3 Naive Output Feedback with Censored Measurements

Consider a typical output feedback controller structure given below in figure 1.2. The creation, use, and performance of a such a linear controller structure is explored in detail in chapter four. Consider now however, the implications of keeping the controller and plant structure the same, and the introduction of a censoring block on the output feedback line, as shown in figure 1.3.

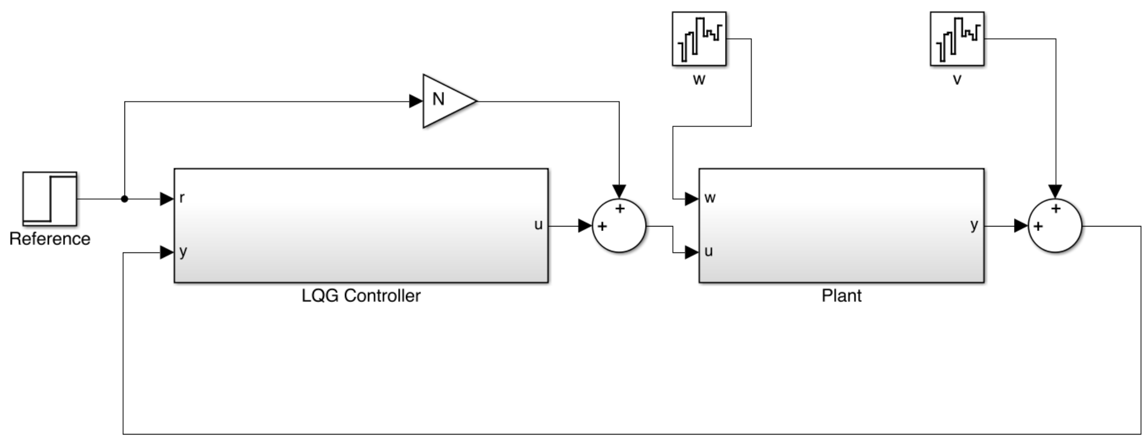

Figure 1.2: Typical output feedback configuration with desired reference, controller with estimator, plant to be controlled, and output feedback.

One would expect that, if the controller and plant are not modified accordingly, then different results are generated between the two systems given the same reference. After all, the output "seen" by the two controllers is now different. The first, uncensored, closed loop system will follow the principals of linear systems given that the controller is correctly designed for the given plant. The second, censored, closed loop system now has an un-modeled nonlinear function on the output line. Therefore, as is shown in later discussion, a naive linear controller and estimator produce biased estimates of the states to be controlled. These biased state estimates then feed into the plant, whose outputs may again become censored, and the cycle repeats. If not

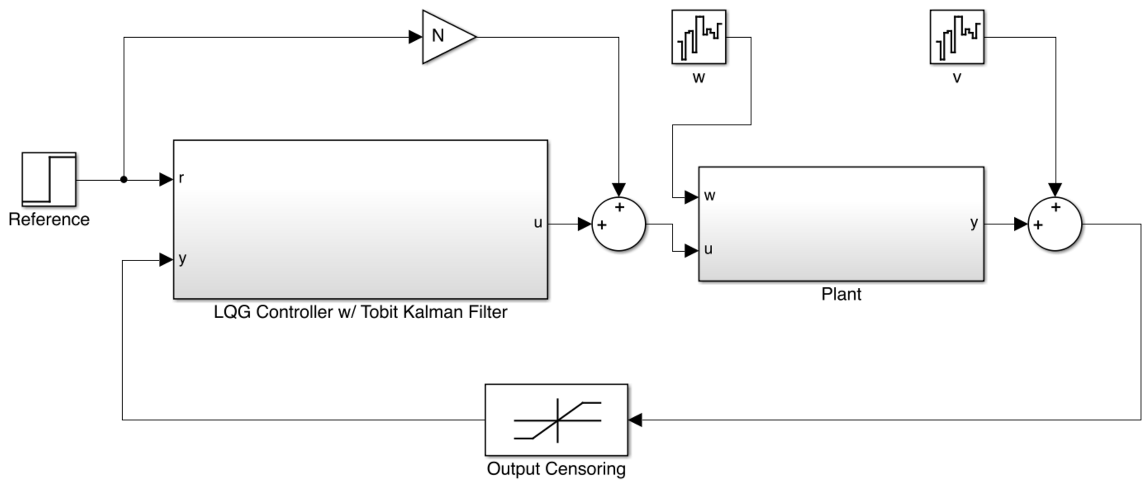

Figure 1.3: Typical output feedback configuration, with the addition of censoring on the plant output.

accounted for by choice of a more appropriate controller and state estimation algorithm, then unstable control can be generated quite rapidly. This dissertation explains the process of how output censoring may cause the state estimates to become biased, how an unbiased state estimator for censored data can be created, how that estimator can compensate for output censoring present in a closed loop controller, and for which systems and circumstances the new censoring compensated closed loop estimator and controller is stable. Furthermore, performance of closed loop controllers with censoring is demonstrated, with examples of how censoring invariably degrades controller performance compared to an optimal uncensored system. Novel control techniques using parameters thus far never seen before in control theory are introduced. First however, background material regarding classical estimation techniques for uncensored linear systems is presented.

Chapter 2

INTRODUCTION TO KALMAN FILTERING

In this chapter some basic concepts of state estimation is discussed. Classical estimation using Kalman filer is introduced. The first approach to using the Kalman filter with censored data is presented, in which a filter is derived for the express purpose of tracking multiple identical objects which exit an imager field of view.

2.1 The Kalman Filter

The Kalman filter, named after Rudolph E. Kalman, developed during the late 1950s and early 1960s with contributions by Richard S. Bucy, as a means for recursive estimation of unknown system states given a series of noisy state measurements. Being a recursive estimator means that the Kalman filter encapsulates all past information of the state's time history into a finite set of variables that are only dependent on the current and previous state estimates and state estimate covariances. In other words, an optimal unbiased estimate of the unknown state can be predicted without the need to keep all past measurements in memory. Only the previous state estimate and state estimate covariance is needed to calculate the current state estimate and state estimate covariance given an up-to-date measurement. This property makes the Kalman filter attractive for a large number of engineering applications. It's recursive nature results in a low, fixed memory footprint, with a small and deterministic computational complexity. The Kalman filter is built off an underlying Bayesian Model which can be applied to a large number of systems and diverse applications. Given an assumed linear state-space model, with known parameters, the Kalman filter recursively produces optimal unbiased state estimates.

2.1.1 Defining the System Model and Filter Terms

In order to derive the Kalman filter framework it is first necessary to define the system model that is to estimated. Start with a typical linear continuous time state space formulation as shown in 2.1.

$$\begin{aligned} \dot{\mathbf{x}} &= \mathbf{Ax} + \mathbf{Bu} + \mathbf{Gw} \\ \mathbf{y} &= \mathbf{Cx} + \mathbf{Du} + \mathbf{Hv} \end{aligned} \tag{2.1}$$

This is a linear system in which evolution of state $\mathbf{x}$ is a linear combination of the current state with input $\mathbf{u}$ and process disturbance $\mathbf{w}$. Likewise, output $\mathbf{y}$ is a linear function of current state $\mathbf{x}$ with input $\mathbf{u}$ and output disturbance $\mathbf{v}$. System matrices $\mathbf{A}, \mathbf{B}, \mathbf{G}, \mathbf{C}, \mathbf{D}, \mathbf{H}$ are linear and may or may not be time varying.

In discrete time a system of similar formulation is given by 2.2

$$\begin{aligned} \mathbf{x_{k+1}} &= \mathbf{Ax_k} + \mathbf{Bu_k} + \mathbf{Gw_k} \\ \mathbf{y_k} &= \mathbf{Cx_k} + \mathbf{Du_k} + \mathbf{Hv_k} \end{aligned} \tag{2.2}$$

For the purposes of the following discussion only consider the discrete time case with time invariant system matrices and the following assumptions :

- There is no input to the system; $\mathbf{u} = 0$
- Initial condition of $\mathbf{x}(\mathbf{0}) = \mathbf{x_0}$ with covariance $\mathbf{P_0}$
- Process disturbance $\mathbf{w}$ is uncorrelated zero mean white noise; $\mathbf{E}\left[\mathbf{w_k w_k^T}\right] = \mathbf{Q}$
- Output disturbance $\mathbf{v}$ is uncorrelated zero mean white noise; $\mathbf{E}\left[\mathbf{v_k v_k^T}\right] = \mathbf{R}$

The goal of the Kalman filter estimation problem is to find the best estimate of $\mathbf{x_k}$ given past measurements $\mathbf{y_{k-1}}, \mathbf{y_{k-2}}, ..., \mathbf{y_{k_0}}$.

2.1.2 The Two Stages

The Kalman filter can be thought of as a two stage process. First, a prediction stage is run in which *a priori* state estimates and state estimate covariances are calculated based off the system model and the previous state estimates. Second, the Update stage is performed in which the state measurements are taken, an error is calculated between that which was observed and that which was expected, a new weighting factor (Kalman gain) is calculated, and the *a posteriori* state estimate and state error covariances are calculated. The update stage effectively "updates" the *a priori* prediction to the *a posteriori* estimate given the new information from the observed measurement, and is sometimes referred to as the "correction" stage.

The *a priori* state estimate is given by :

$$\begin{aligned}
\mathbf{\hat{x}_{k|k-1}} &= \mathbf{E}\left[\mathbf{x_{k|k-1}}|\{\mathbf{y_{k-1}}, \mathbf{y_{k-2}}, ..., \mathbf{y_{k_0}}\}\right] \\
&= \mathbf{A\hat{x}_{k-1|k-1}} \\
\mathbf{P_{k|k-1}} &= \mathbf{E}\left[\left(\mathbf{x_k} - \mathbf{\hat{x}_{k|k-1}}\right)\left(\mathbf{x_k} - \mathbf{\hat{x}_{k|k-1}}\right)^{\mathbf{T}}\right] \\
&= \mathbf{AP_{k-1|k-1}A^T} + \mathbf{Q}
\end{aligned} \tag{2.3}$$

The *a priori* state estimate is purely a function of the previous state estimate and system model, and is not a function of $\mathbf{y}$, for measurements at the current time-step have yet to be taken. The update stage begins by the calculation of the innovation, followed by the calculation of the optimal Kalman gain, and concluding with the update of the *a posteriori* state estimate. The innovation process is carried out when the current measurement $\mathbf{z_k}$ is taken and the innovation $\mathbf{\tilde{y}_k}$ is calculated according to 2.4.

$$\mathbf{\tilde{y}_k} = \mathbf{z_k} - \mathbf{C\hat{x}_{k|k-1}} \tag{2.4}$$

The innovation term represents the new information gained by the taking of measurement $\mathbf{z_k}$. The optimal Kalman gain is then calculated by 2.5.

$$\mathbf{K_k} = \mathbf{P_{k|k-1}C_k^T}\left(\mathbf{C_kP_{k|k-1}C^T} + \mathbf{R}\right)^{-1} \tag{2.5}$$

Finally, the update procedure is completed by correcting the *a priori* prediction with the optimally weighted innovation to produce the *a posteriori* state estimate and state covariance for the current time step.

$$\begin{aligned}\mathbf{\hat{x}_{k|k}} &= \mathbf{\hat{x}_{k|k-1}} + \mathbf{K_k \tilde{y}_k} \\ \mathbf{P_{k|k}} &= \mathbf{E}\left[\left(\mathbf{x_k} - \mathbf{\hat{x}_{k|k}}\right)\left(\mathbf{x_k} - \mathbf{\hat{x}_{k|k}}\right)^{\mathbf{T}}\right] \\ &= \left(\mathbf{I} - \mathbf{K_k C}\right)\mathbf{P_{k|k-1}}\end{aligned} \tag{2.6}$$

The complete Kalman filter can be written more compactly in the following recursive form :

$$\begin{aligned}\mathbf{\hat{x}_{k|k}} =& \mathbf{A\hat{x}_{k-1|k-1}} + \left(\left(\mathbf{AP_{k-1|k-1}A^T} + \mathbf{Q}\right)\mathbf{C^T}\right)\left(\mathbf{C}\left(\mathbf{AP_{k-1|k-1}A^T} + \mathbf{Q}\right)\mathbf{C^T} + \mathbf{R}\right)^{-1}\left(\mathbf{z_k} - \mathbf{CA\hat{x}_{k-1|k-1}}\right) \\ \mathbf{P_{k|k}} =& \Big(\mathbf{I} - \left(\left(\mathbf{AP_{k-1|k-1}A^T} + \mathbf{Q}\right)\mathbf{C^T}\right)\left(\mathbf{C}\left(\mathbf{AP_{k-1|k-1}A^T} + \mathbf{Q}\right)\mathbf{C^T} + \mathbf{R}\right)^{-1}\mathbf{C}\Big)\left(\mathbf{AP_{k-1|k-1}A^T} + \mathbf{Q}\right)\end{aligned} \tag{2.7}$$

Assuming that the initial conditions for state and state covariance are accurate, and the system is correctly modeled, then the Kalman filter produces optimal unbiased state estimates $\mathbf{\hat{x}_{k|k}}$ given noisy measurements $\mathbf{z_k}$. An interesting consequence of the Kalman filter definition is that state error covariance $\mathbf{P_{k|k}}$, therefore Kalman gain $\mathbf{K}$, is not dependent on observed measurements. Thus, if the system is time invariant, then Kalman gain $\mathbf{K}$ and state error covariance $\mathbf{P_{k|k}}$ converge to steady state values. These values may be calculated a head of time by solving the discrete time algebraic Ricatti equation. This enables the filter performance and feasibility to be characterized beforehand. Knowledge of the steady values of the Kalman filter also allows direct implementation of these steady state parameters, instead of the time varying covariances and gains shown above. Although optimal performance cannot be achieved with a steady state filter, the reduced computational complexity is often desired in practical application of the Kalman filter.

Now it is demonstrated through example how the Kalman filter can used in novel ways, in particular in application towards computer vision based target tracking.

2.2 Using the Kalman Filter for Tracking Multiple Similar Targets

2.2.1 Introduction

Vision-based tracking provides a unique set of advantages, but also introduces a new set of challenges. A particularly significant set of problems arise when tracking multiple objects of similar or identical appearance over long periods of time. Examples of such scenarios include the identification and tracking of windows on a building facade, similar vehicles in a large convoy, or birds in a flock. Identity confusion, which is identified here as the inadvertent switch from the tracking of one object to another object of similar appearance, is possible, as there is little to distinguish between individual objects aside from the physics of their motion and previous measurements. Characteristics that would typically be used by traditional trackers, such as color, shape, and features, cannot be relied upon to uniquely identify individual objects, as these are shared traits. Tracking algorithms that rely primarily upon brute force detection and matching between sample frames are subject to large errors when encountered with missing or erroneous data. The tracking performance is further degraded when objects of interest leave the field of view or become occluded. When occluded objects are reintroduced to the image frame, they must be correctly identified in order to continue to propagate their estimated motion, otherwise they must be treated as new entities.

There has been a large amount of previous work done for tracking objects in computer vision, signal and image processing and radar applications [10, 32]. Inspired by tracking problems in video streams where there exists complicated scenarios such as interacting humans, animals, insects and objects in crowded environments [20, 33, 29, 17, 22] , previous vision research as led to the development of many techniques to mitigate these issues. Filtering techniques for tracking objects in imagery include Kalman filters, Particle filters [14] , optical flow, image segmentation via active contours and supervised learning [32]. In [21] target tracking was done for a stationary system. The measurements where linked to the estimates together via a "validation region" derived from Kalman filter covariances. Unlike [21] , this work addresses the complication of a moving camera, and particularly seeks to mitigate the complication of objects exiting and reentering the image frame. For dealing with such systems where data can be missing for periods of time, papers such as [24] access the statistical convergence properties of the estimate error covariance and give expected arrival rate of observations to guarantee convergence.

A modified Kalman filter algorithm is derived for the tracking of multiple similar objects when imaged from a moving camera. The definition of objects of interest can vary depending on the underlying vision algorithm employed, and are only represented in the filtering process by their x,y position and velocities respectively. As such, an object of interest can be represented by the center of mass of various geometric shapes (such as rectangles or windows), or could be feature points detected using advanced computer vision algorithms such as SIFT, SURF [4], etc. Assume that the objects of interest are relatively stationary in the scene and that the camera is moving with inertia. Due to the generic definition of the objects of interest, the vision algorithm for the detection of the objects is not of concern. This formulation is robust to erroneous, spurious, and missing detections, regardless of the underlying detection system.

Three key modifications are proposed to the standard Kalman filter structure. The first involves the use of error thresholding between estimate and measurement for the purpose of identifying erroneous detection or occlusion. The second is the use of linear prediction for propagating object state estimation in such circumstances. The third modification is the estimation of the dynamics of valid measurements and their use as an exogenous feedback term for corrections to the state estimation of occluded objects. The propagation of state estimation using these modifications can then be used to match measurements to predictions and maintain identity between similar objects within the scene.

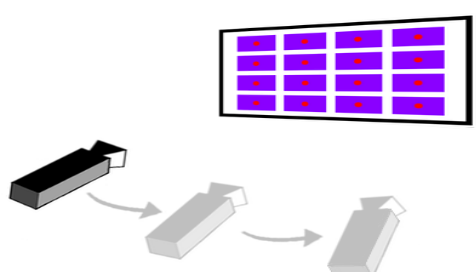

Figure 2.1: Camera moving w.r.t. static objects in the scene. The purple rectangles represent the identical objects to be tracked.

2.2.2 Algorithm Overview

From here on forward, define a measurement as a detected object of interest in video frame k. Due to the formulation of the filter, the terms ”object of interest” and ”point of interest” is used interchangeably. An occluded point is defined as an object of interest that is either estimated to be outside the field of view, is hidden within the field of view by some obstacle, or has otherwise failed to be detected by the vision algorithm. A spurious point is defined as a detected object that is only present for a short period of time, and may or may not be desired for tracking. An erroneous point is a false detection by the vision algorithm which may or may not be spurious, or a valid detection that is unwanted for tracking. As previously explained, the objects to track could vary depending on a large expanse of applications, and is determined by the vision algorithm. In this solution the objects to track are identified by single points in the image plane. There are many associations single points may represent, whether it be center of mass of a contour, the corner of a window or feature points from a SURF , SIFT or Harris detector. Various sets used in this paper are defined in Table 2.1 .

Table 2.1: Variables and their Usage

Set Name	Definition
$\mathbf{Y}$	Kalman estimates (Ordered)
$\mathbf{M}$	Candidate measurements (Unordered)
$\mathbb{Y} \subset \mathbf{Y}$	Kalman estimates with match (ordered)
$\mathbb{M} \subset \mathbf{M}$	Measurements with match (ordered)
$\mathbf{Y} - \mathbb{Y}$	Occluded or missing Kalman estimates
$\mathbf{M} - \mathbb{M}$	Spurious measurements
$\mathbf{T}$	Error Thresholds (Ordered)

At time step $k = 1$ it is assumed that the location of N objects desired for tracking is determined by an independent algorithm and are stored in set $\mathbf{M}$. The tracking and identification algorithm begins with the initialization of N parallel Kalman filters, with a one to one mapping of Kalman filters to set $\mathbf{M}$. Furthermore, set $\mathbf{Y} = \mathbf{M}$, creating a trivial bijective mapping from estimation to measurement.

The initial ordering of these objects is maintained throughout tracking, and is the basis for the avoidance of identity confusion. The process for the identification and tracking of the objects of interest can be decomposed into three fundamental phases of Prediction, Measurement, and Update.

In the prediction phase the N Kalman filters use the Kalman state estimates from iteration $k - 1$ to update $\mathbf{Y}$, based on the standard Kalman filter prediction procedure.

The vision algorithm is then run on frame k to begin the measurement phase, with L detected objects being stored in $\mathbf{M}$ in an unpredictable order. An injective mapping is then created from $\mathbf{Y} \to \mathcal{M}$, matching Kalman estimates to nearest candidate measurements. A second injective mapping is created from $\mathcal{M} \to \mathcal{Y}$, to ensure candidate measurements are mapped to only one Kalman estimate. Finally, error thresholding is applied to remove invalid pairings, resulting in a bijective mapping from $\mathbb{Y} \to \mathbb{M}$. Any measurements that are not paired with an estimate are declared as spurious measurements, and any estimates that are not paired are declared occluded/missing. The bijective mapping thus establishes an order among a subset of the new measurements which is correspondent to a subset of the Kalman estimates, allowing their associated Kalman filters to continue to the update phase and avoiding identity confusion amongst the objects of interest.

Lastly, the recently ordered set of measurements are used to update the Kalman filter state estimations. Kalman estimates that have a corresponding measurement are updated with the standard Kalman filter update formulation, creating an estimation for object state at $k + 1$. Estimates that are declared as occluded are updated with a linear prediction based on their most recent state estimation. Additionally, occluded objects are updated with an exogenous input u dependent on the state estimates of the non-occluded objects.

2.2.3 Mathematical Formulation

Here the mathematical formulation to account for spurious, erroneous, and occluded objects is described. Each object of interest is tracked using its own Kalman filter, as is explained in section 2.2.

Focusing on a single object, begin with a constant velocity model, which is based off the assumption of static objects being imaged by a camera moving with inertia. Assume a high sampling rate with respect to the motion of the camera, and as such instantaneous changes in velocity are not expected.

Using a standard discrete Kalman filter the constant velocity model can be written as

$$\mathbf{x_i(k+1|k) = Ax_i(k|k) + w(k)} \tag{2.8}$$

with x_i denoting the state of the ith object that is being tracked and k representing discrete time. As for the covariance and Kalman gains; $\mathbf{P(k|k)}$ is the posterior error covariance matrix, $\mathbf{S(k)}$ the innovation covariance, $\mathbf{K(k)}$ the Kalman gain. $\mathbf{R}$ is the measurement noise covariance and $\mathbf{Q}$ is the process noise covariance [5].

$$\begin{aligned} p_i(w) &= N(0,Q) \\ p_i(v) &= N(0,R) \\ \mathbf{e_i(k)} &= \mathbf{x_i(k) - x_i(k|k)} \\ \mathbf{P_i(k|k)} &= \mathbf{E(e_i(k)e_i(k)^T)} \end{aligned} \tag{2.9}$$

with $\mathbf{x_i(k|k)} = \begin{bmatrix} x_i & \Delta x_i & y_i & \Delta y_i \end{bmatrix}$ containing the filter's estimate of location and velocity of the ith object being tracked, and

$$\mathbf{A} = \begin{bmatrix} 1 & 1 & 0 & 0 \\ 0 & 1 & 0 & 0 \\ 0 & 0 & 1 & 1 \\ 0 & 0 & 0 & 1 \end{bmatrix} \tag{2.10}$$

to complete the constant velocity model.

The Kalman estimation equations are

$$\mathbf{y_i}(\mathbf{k}) = \mathbf{C}\mathbf{x_i}(\mathbf{k}) + \mathbf{v}(\mathbf{k}) \tag{2.11}$$

with $\mathbf{C} = \begin{bmatrix} 1 & 0 & 0 & 0 \\ 0 & 0 & 1 & 0 \end{bmatrix}$.

The measurement phase consists of two portions, one being the detection of objects using a computer vision algorithm, and the second being the mapping of these measurements to existing Kalman estimates. It is not assumed that the vision algorithm returns the detected objects in a consistent order between frame iterations, and therefore to correctly propagate the Kalman filter estimations over time it is necessary to perform a matching routine between detected points of interest and their associated filter.

Let $\mathbf{Y}$ be the set of Kalman estimates from the previous prediction phase, and $\mathbf{M}$ be the set of candidate measurements. First, create an injective mapping from $\mathbf{Y} \to \mathbf{M}$ $\{y_i, m_j\}$ where $j = \arg\min_j \|y_i - m_j\|_2$. The set of all measurements m_j with a mapping from Y is denoted $\mathcal{M}$. Next, create an injective mapping from $\mathcal{M} \to \mathbf{Y}$ $\{m_j, y_i\}$ where $i = \arg\min_i \|y_i - m_j\|_2$. The set of Kalman estimates with a mapping from $\mathcal{M}$ is denoted $\mathcal{Y}$. There now exists a bijective mapping between $\mathcal{Y}$ and $\mathcal{M}$. Define two subsets $\mathbb{Y} \subset \mathcal{Y}$, $\mathbb{M} \subset \mathcal{M}$ where $y_k \in \mathbb{Y}, m_k \in \mathbb{M} \iff \|y_k - m_k\|_2 < T_i$, where T_i is the threshold defined by the threshold function. The bijective mapping between $\mathbb{Y}$ and $\mathbb{M}$ now defines the pairing of Kalman estimates with their associated trusted measurement. The set $\mathbf{Y} - \mathbb{Y}$ is the set of Kalman estimates with missing or occluded measurements, and the set $\mathbf{M} - \mathbb{M}$ is the set of spurious measurements.

In general, the procedure above is defined for when the individual Kalman filters have converged. If a given Kalman filter has not yet converged, as is the case in first few iterations, then it is not valid to match current measurements to Kalman estimations. Therefore, in these instances match current measurements to previous measurements in order to maintain order. The same algorithm structure is applied, except for the substitution of $m_i(k-1)$ for $y_i(k)$ in $\mathbf{Y}$. This relies upon the assumption that measurements are initially not moving with high dynamics, and occlusion or dropouts are not present. This algorithm, illustrated in Fig. 2.2, also prevents identity confusion between nearby Kalman estimates, assuming reasonable bounds on displacement error.

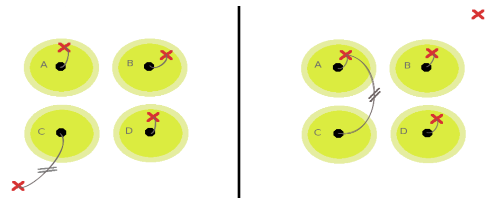

Figure 2.2: In the left frame the bijective mapping results in a match between Kalman estimates (A,B,C,D), and their nearest measurement. The match for estimate C is removed due to error thresholding. Kalman filters A,B,D proceed with standard Kalman filter correction using their associated measurements, while Kalman filter C proceeds with linear prediction + feedback. In the right frame Kalman filters A and C are matched to the same measurement through the first injective mapping. The second injective mapping causes pairing with Kalman estimate A to remain, while Kalman estimate C is declared occluded.

The constant velocity model and Kalman filter track objects satisfactorily unless there are spurious points, dropouts or occlusions. Through the bijective mapping and error thresholding, a point that is spurious, missing or occluded does not present a suitable measurement for the associated Kalman filter. In this case the system propagates as a linear system using its previous state estimation. The pairing between y_k and m_k is applied to threshold T_i as defined by,

$$\|y_k - m_k\|_2 < T_i \tag{2.12}$$

where T_i is a linearly increasing value when objects are occluded for extended periods of time. This allows objects that are occluded for several frames to be subjected to a more lenient threshold and accepted as candidate objects upon reintroduction into the field of view.

$$T_i = T_o + \alpha * O_i(k) \tag{2.13}$$

T_o is the default error threshold, $O_i(k)$ is equal to the number of frames object i is occluded in a given sequence, and α is a scaling factor.

The spurious measurements are treated as outliers and removed from being inputs to the system to prevent the Kalman filter from converging erroneously and to avoid identity confusion. The advantage to this method is that occlusions are not propagated to the Kalman updates because they fail to meet the error threshold. Kalman filter objects that have missing measurements are updated with the current linear model and the update step of the Kalman filter is reduced to,

$$\begin{aligned} \mathbf{x(k|k)} &= \mathbf{x(k|k-1)} \\ \mathbf{P(k|k)} &= \mathbf{P(k|k-1)} \end{aligned} \tag{2.14}$$

as shown in [8]. This allows the Kalman filter to propagate without deteriorating the values of the estimates, although reaction to changing dynamics is diminished.

The threshold provided a mechanism such that the object's motion model is resistant to spurious or occluded points. However, in the event that some objects in the set to be tracked are partially occluded, the states of the other non-occluded objects can assist in providing updates on dynamics of the occluded objects which are otherwise unobservable. The operating assumption here is of planar and or distant objects, resulting in a large correlation between all of the tracked objects velocities. If these assumptions are not valid, this feedback can be carried out using 6-DOF information about the camera motion if it is available.

Introduced now is the technique of using the correlation of the objects' velocities to infer how occluded objects are behaving. As seen in Fig. 2.3 if a standard Kalman filter was used to update occluded points, and the camera changed its heading velocity to the opposite direction, the Kalman filter would continue to propagate the estimates toward the direction of the initial velocity. The solution to this problem is to use the information of the other objects trajectories to assist the occluded ones by way of an input term $\mathbf{u}$ which uses values of states from the parallel Kalman filters.

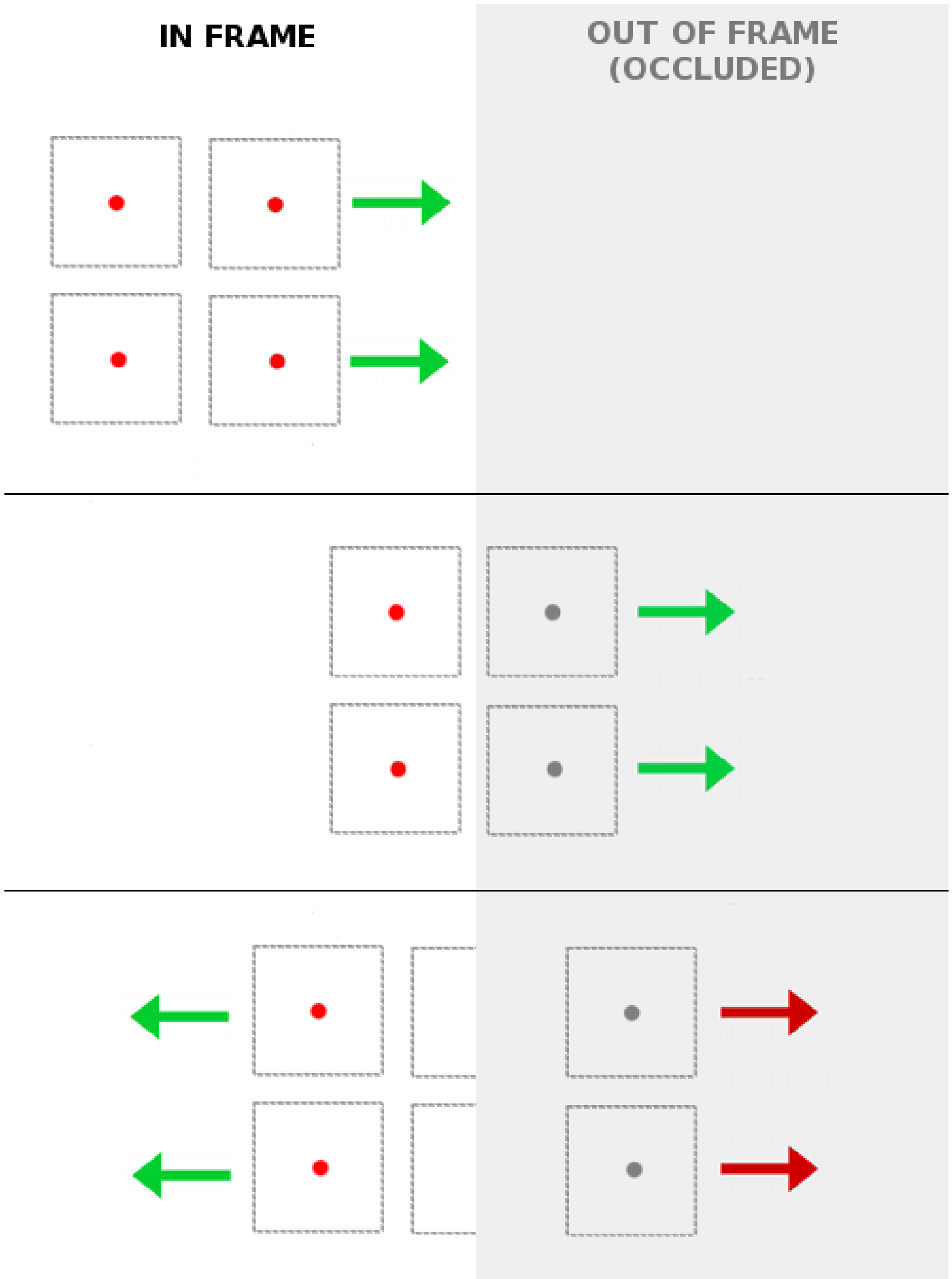

Figure 2.3: Four centers of mass initially move coherently to the right. The two right centers of mass become occluded and continue propagation to the right. The four centers of mass then coherently change direction back to the left. Without feedback correction, the estimates of the right centers of mass are unaffected and continue propagating to the right, leading to large errors upon reintroduction into the frame and possible identity confusion.

The definition of $\mathbf{B}$ and $\mathbf{u}$ matricies

$$\mathbf{x_i(k|k-1) = Ax_i(k-1|k-1) + Bu_i(k) + w(k)} \tag{2.15}$$

$\mathbf{B} = \mathbf{diag}(\mu,\ \mathbf{1},\ \mu,\ \mathbf{1})$ with $\mu \approx 0$.

$$\mathbf{u_i(k)} = \begin{bmatrix} x_i - \frac{1}{N-1}\sum_{n\neq i} x_n \\ \Delta x_i - \frac{1}{N-1}\sum_{n\neq i} \Delta x_n \\ y_i - \frac{1}{N-1}\sum_{n\neq i} y_n \\ \Delta y_i - \frac{1}{N-1}\sum_{n\neq i} \Delta y_n \end{bmatrix} \epsilon_i \quad \forall y_i \in \mathbb{Y} \tag{2.16}$$

The $\mathbf{u_i(k)}$ is an error between the occluded state and the mean of all the other non occluded states. If this vector is increasing or is large then the occluded system relies on the $\mathbf{u_i(k)}$ to propagate the system.

The function ϵ_i is dependent on whether or not Kalman estimate i is declared occluded.

$$\epsilon_i = \begin{cases} 1, & \text{if } i \text{ is within the frame} \\ 0, & \text{otherwise} \end{cases} \tag{2.17}$$

The purpose of ϵ_i is to ensure that the control input for object i is only used should that object become occluded. If object i is occluded, then the state estimates of the non-occluded objects are used as feedback to correct state estimation for object i. This approach works well if motion is primarily translational and objects are not occluded for extended periods of time. If these assumptions fail, good performance can be obtained using feedback based on 6-DOF information about the camera motion.

2.2.4 Experimental Results

Experiments to validate filter performance were performed using OpenCV 2.3.1 on Mac OS X. Simulation data was generated using OpenCV drawing functions, with multiple scenarios being used to evaluate the tracking of object points under various conditions. Truth data was saved for each scenario for use in later analysis. No artificial noise was generated when making the simulated data, in order to evaluate the filter performance solely on controlled parameters.

In this implementation, each individual object of interest is assigned its own Kalman filter. If N points of interest are being tracked, then N parallel Kalman filters are automatically initialized and run. While it is possible to structure the estimation procedure as one large Kalman filter, there are many advantages to the parallel framework described. Primarily, it is more computationally efficient to run multiple parallel Kalman filters as opposed to one large filter. Also, it is easier to drop or add objects of interest when Kalman filters are independent and parallel. Two experiments were run to validate the propositions of this paper. The first involves dynamic movement of the objects of interest within the camera frame, with no occlusions. This was to validate the ideal performance of the filter, verify the constant velocity modeling assumption, and to verify the matching algorithm correctly maintained the identities of individual objects without confusion. The second experiment involves dynamic movement of the objects of interest, with the added complication of partial occlusion from the frame and reintroduction of the occluded objects. This was to correctly verify the behavior of the feedback correction term and its application to the tracking of occluded and otherwise unobservable objects. In this experiment, four squares of identical size and color move at a velocity of one pixel per frame in both the x and y direction. Corner detection was run using a Shi-Tomasi algorithm, and the detected corners were identified as objects of interest. In each frame, a random number of spurious detections (up to a limit of 100) at random locations were added to the set of candidate measurements $\mathbf{M}$, as shown in Fig. 3.1. Despite the ideal nature of the simulated data, the corner detection algorithm does not return the detected corners in the same order between frames. Without any identity preserving mechanism, individual corners may easily be confused with each other and result in erroneous and unstable Kalman filter updates. As seen in Figs. 2.5 and 2.6, the Filter performance and error convergence are excellent under these conditions. In this next experiment four squares are moved right, horizontally across the image frame, simulating a camera moving towards the left in reference to

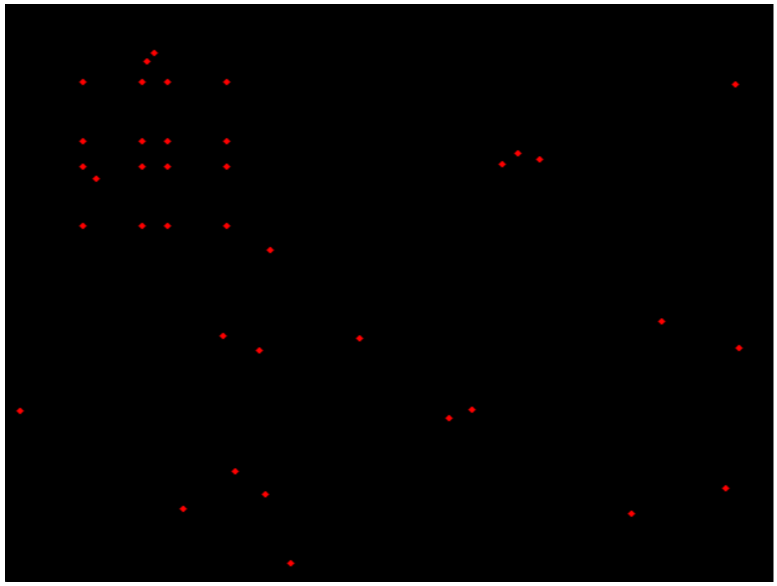

Figure 2.4: Visual representation of the candidate measurements returned by the underlying vision algorithm in one frame. Sixteen points of interest are desired for tracking, corresponding to the four corners of four rectangles moving in unison, and are determined by the initialization procedure. In each frame, the vision algorithm returns any number of unordered candidate measurements. The mapping algorithm proposed ignores spurious measurements, pairs Kalman estimates with appropriate new measurements, and declares which Kalman estimates have an occluded or missing measurement.

the stationary objects of interest. The center of mass of each square is detected using a modified OpenCV rectangle detector. As the right two squares move horizontally out of the frame their centers of masses become occluded. Using traditional filtering, the right two occluded rectangles would continue to propagate horizontally to the right, even if in truth the squares reversed direction and began movement towards the left, shown in Fig. 2.3. This would eventually cause very large errors upon re-entry of the right two rectangles into the field of view, and may potentially lead to confusion as to how each center of mass may be identified. Using the given formulation, once the right two centers of mass became occluded they would be linearly propagated to right, and remain identical in behavior to the standard Kalman filter. However, if the left centers of mass, which remain visible, change velocity, the exogenous feedback term u

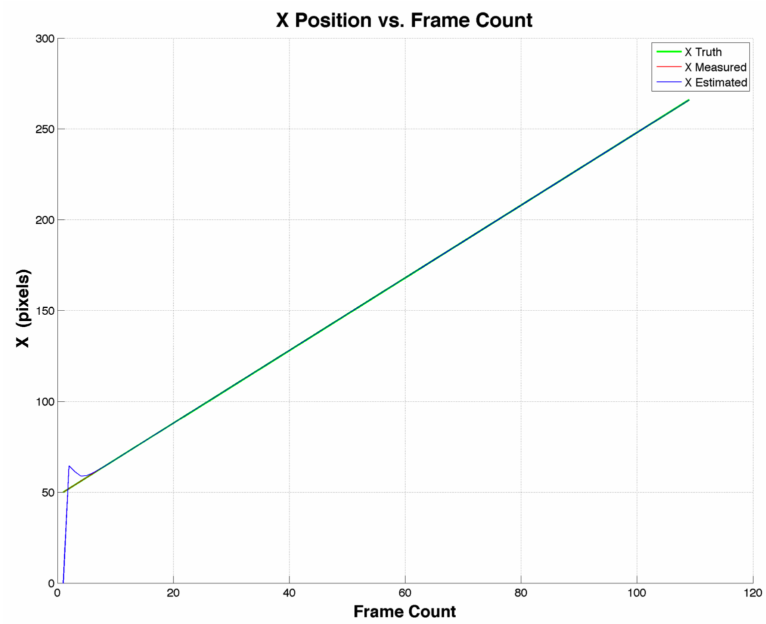

Figure 2.5: No occlusion. Filter performance while tracking x position of interest point 1 as it moves from top left of frame to bottom right with constant velocity (see previous figure).

begins correcting the estimated location of the occluded points. The error upon re-entry between estimate and measurement is then much lower, and identity confusion is avoided, as shown in Fig.2.7 and 2.8.

This experiment shows the performance characteristics of a standard Kalman filter with no measurement mapping versus the proposed modified Kalman filter. In each scenario the top left corner of a rectangle was tracked as the rectangle was moved diagonally across the frame. At every twenty frames, for three consecutive frames, the measurement was purposefully substituted with an erroneous constant value, in order to simulate the failure of the detection algorithm and the presence of an erroneous disturbance to the filter. The original filter follows this disturbance, and then re-converges back to truth when the measurements are valid again. However, in the modified Kalman filter, the disturbance is detected, rejected, and linear prediction is followed instead until a valid measurement returns. This results in no error, for the filter has converged before the disturbance appears, and the linear prediction is

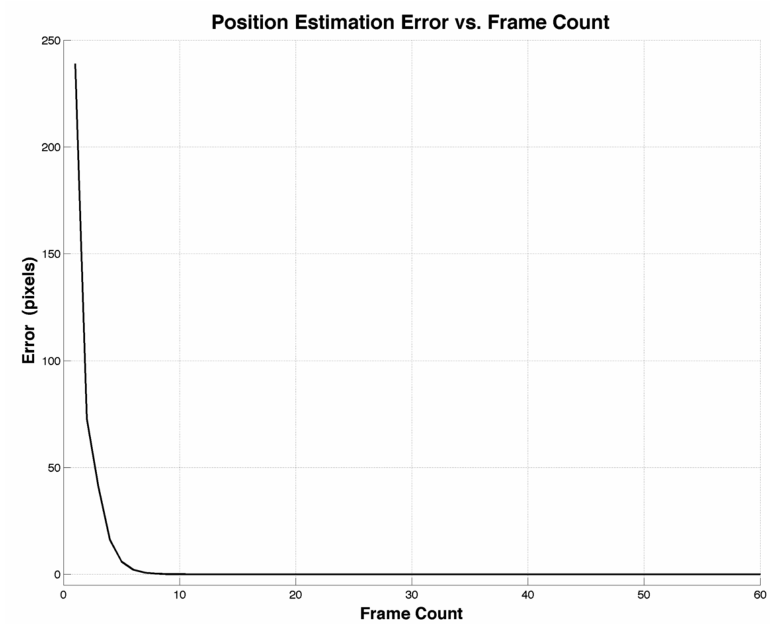

Figure 2.6: No occlusion. Filter error while tracking x position of interest point 1 as it moves from top left of frame to bottom right with constant velocity.

accurate (see Fig. 2.9) .

2.2.5 Conclusions

As the simulation results show, the proposed Kalman filter tracking algorithm successfully tracks objects of interest even in the presence of spurious and missing measurements and partial occlusion. Traditional filtering does not take advantage of the coherent motion of stationary interest points when imaged from a moving camera, and as such is ill suited for the estimation of data which is occluded. By using selective linear prediction and incorporating the dynamics of valid measurements as feedback to the state estimation of occluded interest points the filter is able to successfully estimate the position and velocity of multiple similar objects, even when not directly within in the field of view. Furthermore, the proposed mapping algorithm between unordered candidate measurements and ordered Kalman estimates successfully maintains the identity of each tracked object for correct filter propagation, even when those objects are of similar or identical appearance.

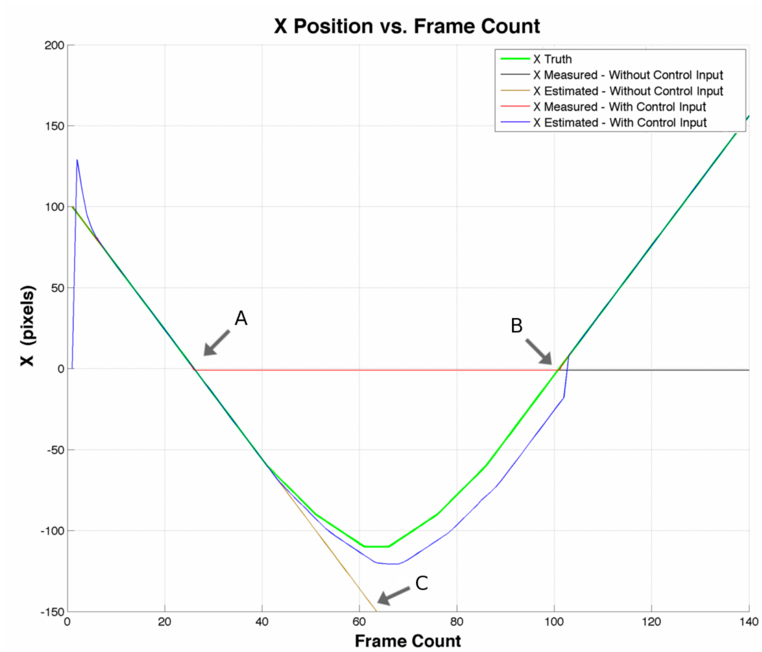

Figure 2.7: Dynamic motion, with occlusion. Filter error while tracking interest point 1 as it move horizontally left and leaves the image frame. Measurement becomes occluded (A), and returns to the field of view some time later (B). While occluded, error is prevented from accumulating by feedback term u. Without feedback, the standard Kalman filter continues to propagate a linear estimation while object measurements are not available (C). After reintroduction into the frame the point is correctly mapped to Kalman filter 1 and the estimate converges.

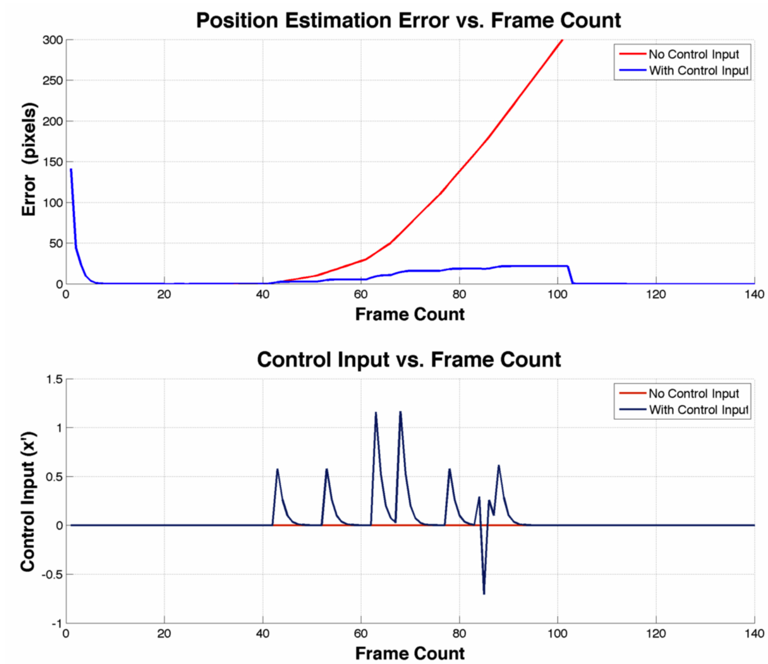

Figure 2.8: Dynamic motion, with occlusion. Filter error while tracking interest point 1 as it move horizontally left and leaves the image frame. Without feedback, the standard Kalman filter error grows unbounded, as linear estimation is propagated while in truth the object as changed velocity. With feedback, the error is kept small and reacts to changes in velocity of non-occluded objects, and after reintroduction into field of view the error converges.

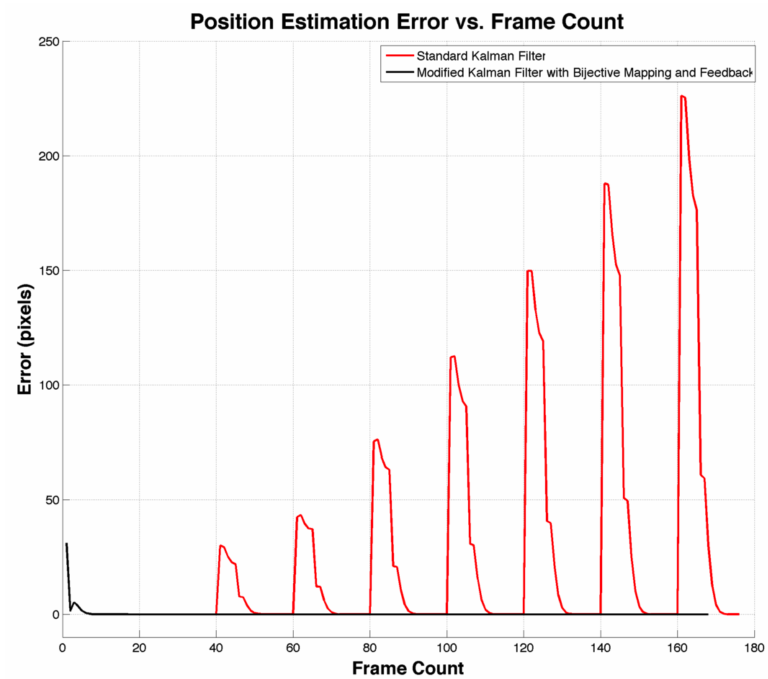

Figure 2.9: Comparison between standard and modified Kalman filters under spurious object detection. During this experiment, at periodic intervals, measurement of the object is manually disturbed to a constant value. Since the object is moving within the frame, this causes the standard Kalman filter error to grow upon each disturbance interval, as the spurious measurement is erroneously used as input to the Kalman filter. With the proposed modifications, the mapping algorithm and error thresholding prevent the erroneous measurement from being used to propagate the Kalman filter, and instead a linear prediction is used for updating. Since the filter has converged before introduction of the spurious measurement, the linear prediction results in no loss of accuracy.

Chapter 3

THE TOBIT KALMAN FILTER

3.1 Kalman Filtering With Censored Measurements

Kalman Filter [15] has become ubiquitous in tracking and estimation. Many estimation applications, especially those using low cost commercial of-the-shelf sensors (COTS), are subject to a specific type of measurement nonlinearity called censoring. When censored measurements are introduced into the standard Kalman filter, the estimates become biased.

A similar measurement nonlinearity which has been previously considered is intermittent measurement. A formulation of the Kalman filter designed for the intermittent measurement case is presented in [25, 16]. This formulation reduces to a linear estimator when measurements are missing. The estimator in [25] provides the minimum state error variance filter given all past observations and arrival sequences, and is an improvement on Jump Least Square (JLS) theory [27] which gives a minimum state error variance filter assuming only the observations and the knowledge of the previous arrival. Both of these previous formulations relied on the assumption that missed measurements were uncorrelated with the state value. The problem with this solution in a censored measurement model is that the censored measurement is correlated to the state value. More specifically it is correlated to the state value as is it relates to the threshold between censored and non censored regions, the measurement model and the noise on the measurement. Tobit model censoring may be formulated as an intermittent measurement problem, but because the dropped measurements are correlated with the state values, the result remains a biased estimate of the state.

One difficulty in using a Kalman filter for censored measurements is that the measurement noise is not Gaussian near the censoring region. If the state variable is a constant near the censored region, noise on the measurements causes some of the measurements to be censored, and the standard Kalman filter produces a biased estimate of the state because the Kalman filter assumption of zero mean white Gaussian noise is no longer valid. Past work has been done to design estimators from the likelihood function that work when the Gaussian observation noise is state-dependent. The work in [28] created an iterative Kalman filter to solve the nonlinear least square problem of the likelihood function. In the censored measurement case a linear Kalman filter can be interpolated.

Censoring can be generalized as an output nonlinearity, and general output nonlinearities can be addressed using the Extended Kalman filter (EKF) or the particle filter. However, the state-measurement equation for censoring has a sharp discontinuity at the threshold value of the censoring region, which is a problem for the EKF as the gradient does not exist at this discontinuity. The particle filter formulated for partially observed Gaussian state space models is presented in [3]. Particle filters are much more computationally expensive than an extended Kalman filter or linear Kalman filter because they require the use of a weighted set of samples called particles to generate the posteriori distribution $p(x_k|y_{1:k})$. Furthermore, the sharp discontinuity in the measurement model for censored data means that a large number of particles are necessary to adequately model the system in this region. The method described in this paper avoids the use of numerical approximation methods such as the particle filter by directly computing the relevant posteriori distributions from the censored data measurement model. The resulting filter has a similar computational burden to the standard Kalman filter, which allows it to be used in computation-limited environments such as embedded systems.

3.2 Classical Tobit Regression

Despite many obvious examples of censored data in estimation and tracking, the Tobit model has not received much attention in the field of signal processing or control theory. It has been widely used, however, in the fields of medicine and economics. The model was first proposed in 1958 by James Tobin as a regression model for household expenditure data [30], a dependent variable which could not be observed below a certain limit. The standard Tobit model formulation is

$$y_t = \begin{cases} \beta x_t + u_t, & \beta x_t + u_t > T \\ T, & \beta x_t + u_t \leq T \end{cases} \tag{3.1}$$

Where $\beta \in \mathbb{R}^{1\times n}$ is vector of constants, $x_t \in \mathbb{R}^{n\times 1}$ is the input vector at time t, y_t is a scalar output, u_t Gaussian random number with zero mean and variance σ_u^2. The use of ordinary least squares to estimate the β or σ_u from the output would be inconsistent because the entire population of the dependent variable is not being observed. Many methods have been devised to solve for the parameters of the Tobit model, including Tobin's original maximum likelihood estimator. An analysis of the method and the consistency of the estimates is presented in [1].

The Tobit model has been extensively studied in the field of Econometrics, and there exist many methods to identify Tobit model parameters and compute expectations of censored data sequences.[11, 19, 2, 7, 1, 26, 23]. Most of these methods require knowledge of the entire measurement history; a recursive estimator such as the Kalman Filter has not previously been developed for this type of measurement nonlinearity.

3.3 From the Kalman Filter to the Tobit Kalman Filter

3.3.1 Problem Formulation

To define the censoring problem consider the evolution of a scalar output state sequence as,

$$\begin{aligned} x_k &= Ax_{k-1} + w_{k-1} \\ y_k^* &= Cx_k + v_k \\ y_k &= \begin{cases} y_k^*, & y_k^* > T \\ T, & y_k^* \leq T \end{cases} \end{aligned} \tag{3.2}$$

$x_k \in \mathbb{R}^{n\times 1}$ is the state vector and y_k is the scalar measurement . The $A \in \mathbb{R}^{n\times n}$ is the state transition matrix and the $C \in \mathbb{R}^{1\times n}$ is the measurement state transition matrix. The w_k and v_k are Gaussian random vectors with zero mean, they have covariance $Q \in$

$\mathbb{R}^{n\times n}$ and $R = \sigma^2$, respectively. Where σ is the standard deviation of the measurement noise. The Kalman filter is optimal in the Gaussian sense; however when the noise distribution on y_k is a censored Gaussian, the filter is not only suboptimal; but because the noise is correlated to the state value, the system violates the assumptions of the Kalman filter. The closer the state is to the threshold value the more censored the Gaussian distribution on y_k becomes.

3.3.2 Problem Formulation in the Tobit Case

Using Equation 3.2, define y_k as the censored observation and y_k^* as the latent variable. The probability distribution of a censored variable with normally distributed noise is:

$$f(y_k|x_k) = \frac{1}{\sigma}\phi(\frac{y_k - Cx_k}{\sigma})u(y_k - T) + \delta(T - y_k)\Phi(\frac{T - Cx_k}{\sigma}) \tag{3.3}$$

where

$$\phi(\frac{y_k - Cx_k}{\sigma}) = \frac{1}{\sqrt{2\pi}}e^{-\frac{(y_k - Cx_k)^2}{2\sigma^2}} \tag{3.4}$$

and

$$\Phi(\frac{y_k - Cx_k}{\sigma}) = \int_{-\infty}^{y_k} \frac{1}{\sqrt{2\pi}}e^{-\frac{(z_k - Cx_k)^2}{2\sigma^2}}dz_k \tag{3.5}$$

are the probability density function and the cumulative distribution function of a Gaussian random variable whose mean is Cx_k. δ is the Dirac delta function. The $u(\alpha)$ is a step function and is equal to $u(\alpha) = 1$ when $\alpha \geq 0$ and $u(\alpha) = 0$ when $\alpha < 0$. The delta function at $T - y_k$ is present when measurements at the censoring limit are recorded, this function is absent in a truncated model.

The likelihood function for the standard Tobit model is,

$$L = \prod_{y_k^* \leq T} [1 - \Phi(\frac{Cx_k - T}{\sigma})] \prod_{y_k^* \geq T} \sigma^{-1}\phi(\frac{y_k - Cx_k}{\sigma}) \tag{3.6}$$

as formulated by Tobin in his pioneering work [30].

The mean of the measurements is given by:

$$
\begin{aligned}
E(y_k|y_k > T, x_k, \sigma) &= \sigma^{-1}\frac{1}{1-\Phi(\frac{T-Cx_k}{\sigma})}\int_T^{+\infty} z\phi(\tfrac{z-Cx_k}{\sigma})dz \\
&= Cx_k + \sigma\lambda((T-Cx_k)/\sigma)
\end{aligned}
\tag{3.7}
$$

This differs from the true value of the latent variable by a bias of $\sigma\lambda((T - Cx_k)/\sigma)$ where $\lambda(\alpha) = \frac{\phi(\alpha)}{[1-\Phi(\alpha)]}$ is the inverse Mills ratio (IMR) [1].

The expected measured value when censored measurements are included is:

$$
\begin{aligned}
E[y_k|x_{k|k-1}, \sigma] &= P[y_k > T|x_{k|k-1}, \sigma]E[y_k|y_k > T, x_{k|k-1}, \sigma] \\
&\quad + P[y_k = T|x_{k|k-1}, \sigma]E[y_k|y_k = T, x_{k|k-1}, \sigma] \\
&= \Phi(\tfrac{Cx_k-T}{\sigma})[Cx_k + \sigma\lambda((T-Cx_k)/\sigma)] \\
&\quad + \Phi(\tfrac{T-Cx_k}{\sigma})T
\end{aligned}
\tag{3.8}
$$

The variance of the expected measured value is derived in [6] and can be written as:

$$
\begin{aligned}
&Var[y_k|y_k > T, x_k, \sigma] = \\
&E[y_k^2|y_k > T, x_k, \sigma] - [E[y_k|y_k > T, x_k, \sigma]]^2
\end{aligned}
\tag{3.9}
$$

$$
E[y_k^2|y_k > T, x_k, \sigma] = \sigma^{-1}\frac{1}{1-\Phi(\frac{T-Cx_k}{\sigma})}\int_T^{+\infty} z^2\phi(\tfrac{z-Cx_k}{\sigma})dz \tag{3.10}
$$

so

$$
Var[y_k|y_k > T, x_k, \sigma] = \sigma^2[1 - \eth(\frac{T-Cx_k}{\sigma})] \tag{3.11}
$$

where

$$
\eth(\tfrac{T-Cx_k}{\sigma}) = \lambda(\tfrac{T-Cx_k}{\sigma})[\lambda(\tfrac{T-Cx_k}{\sigma}) - (\tfrac{T-Cx_k}{\sigma})] \tag{3.12}
$$

Note that $Var[y_k|x_k, \sigma] = Var[y_k|y_k > T, x_k, \sigma]$ since $Var[y_k|y_k < T, x_k, \sigma] = 0$.

3.3.3 Problem Formulation in the Bayesian Sense

The Bayesian derivation of the Kalman filter can be found in several sources, including [5]. The Bayesian filter under a Markov assumption computes the state estimate $\hat{x}_k$ of the true state x_k at time k given measurements y_k. The Markov assumption states,

$$P(x_k|y_k...y_0, x_{k-1}...x_0) = P(x_k|y_k, x_{k-1}) \tag{3.13}$$

and the conditional probability of the measurements is,

$$P(y_k|y_{k-1}...y_0, x_k...x_0) = P(y_k|x_k) \tag{3.14}$$

For a Kalman filter, of interest is how the measurements are projected on the state estimates and future state estimates. The distribution of interest is

$$P(x_k|y_{k-1}) = \int P(x_k|x_{k-1})P(x_{k-1}|y_{k-1})dx_{k-1} \tag{3.15}$$

which is the predict step of the filter; the update state may be written as

$$P(x_k|y_k) = \frac{P(y_k|x_k)P(x_k|y_{k-1})}{P(y_k|y_{k-1})} \tag{3.16}$$

The recursion in equations 3.15 and 3.16 result in the Kalman filter when the noise on the measurement model and the process model are jointly Gaussian. To compute the value of $E(x_k|y_k)$ the Kalman filter computes the minimum mean squared error estimate which is,

$$\hat{x_k} = E(x_k|y_k) = \bar{x}_k + K(y_k - \bar{y}_k) \tag{3.17}$$

Where $\bar{y}_k$ and $\bar{x}_k$ are the mean values of the measurements and states respectively .

In the censored measurement model however the noise is a censored Gaussian in the measurement equations, resulting in the distribution given by Equation 3.3.

This noise function results in a nonlinear relationship between the measurements and state values, and Equation 3.17 does not hold. In the next section, an alternative update schedule which recursively calculates $E(x_k|y_k)$ for Tobit censored measurements is developed.

3.3.4 The Tobit Kalman Filter

The previous section reviewed the basis of the Kalman filter using Bayes' rule. In this section the optimal Kalman formulation for Tobit censored measurements is derived. The derivation is similar to the derivation for the standard Kalman filter; however,the censoring results in new definitions for the measurement residual, and consequently for the optimal Kalman gain and the state estimate covariance. Below is the notation for the hidden Markov model with the state $\mathbf{x_k} \in \mathbb{R}^{n\times 1}$ being hidden and $\mathbf{y_k} \in \mathbb{R}^{m\times 1}$ being the measurement on the system.

$$\begin{aligned} \mathbf{x_k} &= \mathbf{A}\mathbf{x_{k-1}} + \mathbf{w_{k-1}} \\ \mathbf{y^*_k} &= \mathbf{C}\mathbf{x_k} + \mathbf{v_k} \\ \mathbf{y_k} &= \begin{cases} \mathbf{y^*_k}, & \mathbf{y^*_k} > \mathbf{T} \\ \mathbf{T}, & \mathbf{y^*_k} \leq \mathbf{T} \end{cases} \end{aligned} \tag{3.18}$$

The matrix $\mathbf{A} \in \mathbb{R}^{n\times n}$ is the state transition matrix and $\mathbf{C} \in \mathbb{R}^{m\times n}$ is the measurement model. The noise w_k and v_k are zero mean white Gaussian noise with covariance matrix $\mathbf{Q} \in \mathbb{R}^{n\times n}$ and $\mathbf{R} \in \mathbb{R}^{m\times m}$ respectively.

3.3.4.1 The Predict Stage

The prior estimate of the state and it's probability distribution may be written

$$\mathbf{P}(\mathbf{x_{k|k-1}}) \sim \mathcal{N}(\mathbf{E}(\mathbf{x_{k|k-1}}), \mathbf{Var}(\mathbf{x_{k|k-1}})) \tag{3.19}$$

where $\mathbf{x_{k|k-1}} \in \mathbb{R}^{n\times 1}$ is the state estimate vector of $\mathbf{x_k}$ given all estimates and measurements up to time $k-1$. The predict equation of the state may be written as

$$\mathbf{E}(\mathbf{x_{k|k-1}}) = \mathbf{E}(\mathbf{A}\mathbf{x_{k-1|k-1}} + \mathbf{w_k}) = \mathbf{A}\mathbf{x_{k-1|k-1}} \tag{3.20}$$

$\mathbf{x_{k-1|k-1}}$is the estimate of $\mathbf{x_{k-1}}$. The state error covariance given measurements and state information up to time $k-1$ may be written as

$$\begin{aligned} \mathbf{cov}(\mathbf{x_{k|k-1}} - \mathbf{x_k}) &= \mathbf{cov}(\mathbf{A}\mathbf{x_{k-1|k-1}} + \mathbf{w_k} - \mathbf{A}\mathbf{x_{k-1}}) \\ &= \mathbf{A}\mathbf{Var}(\mathbf{x_{k-1|k-1}})\mathbf{A^T} + \mathbf{Q} \\ &= \mathbf{A}\mathbf{\Psi_{k-1|k-1}}\mathbf{A^T} + \mathbf{Q} \end{aligned} \tag{3.21}$$

where $\mathbf{Q}$ is the model covariance matrix and $\mathbf{\Psi_{k-1|k-1}}$ is the previous a posteriori estimate of the state error covariance.

3.3.4.2 The Update Stage

The optimal Kalman filter must minimize the state error covariance, $\mathbf{\Psi_{k|k}}$. The update stage corrects the state estimate using current measurements. The update step reduces the state error covariance, whereas the predict step results in a widening of the state error covariance. The Kalman correction step to obtain the current estimate given all observations up to time k may be written as

$$\mathbf{x_{k|k}} = \mathbf{x_{k|k-1}} + \mathbf{K_k}(\mathbf{y_k} - \mathbf{E}(\mathbf{y_k})) \tag{3.22}$$

The value of $E(y_k)$ was calculated for a scalar case for a censored value in Equation 3.8; in this notation $\mathbf{E}(\mathbf{y_k}) \in \mathbb{R}^{m\times 1}$ is a vector, each scalar component can be censored at any given time and have different threshold limits $\mathbf{T} = [T(1), T(2), ..., T(m)]$ with $T(l)$, $y_k(l)$ representing the lth component of arrays $\mathbf{T}$ and $\mathbf{y_k}$ respectively.

To find $\mathbf{K_k}$ in Equation 3.22 minimize the state error covariance,

$$\begin{aligned} \mathbf{\Psi_{k|k}} &= \mathbf{cov}(\mathbf{x_k} - \mathbf{x_{k|k}}) \\ &= \mathbf{cov}(\mathbf{x_k} - \mathbf{x_{k|k-1}} - \mathbf{K_k}(\mathbf{y_k} - \mathbf{E}(\mathbf{y_k}))) \end{aligned} \tag{3.23}$$

A Bernoulli random variable is introduced to model the occurrence of a censored measurements versus an actual measurement. The variable $p_k(l) = 1$ when the measurement is not censored and $p_k(l) = 0$ when the measurement is equal to the threshold value. The measurement model can be written as

$$p_k(l) = \begin{cases} 1, & Cx_k(l) + u_t(l) > T(l) \\ 0, & Cx_k(l) + u_t(l) \leq T(l) \end{cases} \tag{3.24}$$

At any given time step the measurement represents the state by $Cx_k(l) + u_k(l)$ with probability $E(p_k(l))$. In matrix notation the Bernoulli random matrix is diagonal $\mathbf{p_k} \in \mathbb{R}^{m \times m}$ so the measurements arrive by the following equation

$$\mathbf{y_k} = \mathbf{p_k}(\mathbf{C}\mathbf{x_k} + \mathbf{v_k}) + (\mathbf{I_{m\times m}} - \mathbf{p_k})\mathbf{T} \tag{3.25}$$

where $\mathbf{I_{m\times m}}$ is is the identity matrix. Substituting into Equation 3.22 yields

$$\begin{aligned} \mathbf{\Psi_{k|k}} &= \mathbf{cov}(\mathbf{x_k} - \mathbf{x_{k|k}}) \\ &= \mathbf{cov}(\mathbf{x_k} - \mathbf{x_{k|k-1}} - \mathbf{K_k}(\mathbf{p_k}(\mathbf{C}\mathbf{x_k} + \mathbf{v_k}) + \\ &(\mathbf{I_{m\times m}} - \mathbf{p_k})\mathbf{T} - \mathbf{E}(\mathbf{y_k}))) \end{aligned} \tag{3.26}$$

To simplify the notation in the derivation set the Kalman error to

$$\mathbf{G_k} = \mathbf{p_k}(\mathbf{C}\mathbf{x_k} + \mathbf{v_k}) + (\mathbf{I_{m\times m}} - \mathbf{p_k})\mathbf{T} - \mathbf{E}(\mathbf{y_k}) \tag{3.27}$$

so the covariance of the state estimate becomes

$$\begin{aligned} &\mathbf{\Psi_{k|k}} = \mathbf{E}((\mathbf{x_k} - \mathbf{x_{k|k-1}} - \mathbf{K_k}\mathbf{G_k})(\mathbf{x_k} - \mathbf{x_{k|k-1}} - \mathbf{K_k}\mathbf{G_k})^{\mathbf{T}}) \\ &= \mathbf{\Psi_{k|k-1}} - \mathbf{E}((\mathbf{x_k} - \mathbf{x_{k|k-1}})\mathbf{G_k^T})\mathbf{K_k^T} \\ &-\mathbf{K_k}\mathbf{E}(\mathbf{G_k}(\mathbf{x_k} - \mathbf{x_{k|k-1}})^{\mathbf{T}}) + \mathbf{K_k}\mathbf{E}(\mathbf{G_k}\mathbf{G_k^T})\mathbf{K_k^T} \end{aligned} \tag{3.28}$$

with

$$\mathbf{\Psi_{k|k-1}} = \mathbf{E}((\mathbf{x_k} - \mathbf{x_{k|k-1}})(\mathbf{x_k} - \mathbf{x_{k|k-1}})^{\mathbf{T}}) \tag{3.29}$$

$$\mathbf{R_{xe_k}} = \mathbf{E}((\mathbf{x_k} - \mathbf{x_{k|k-1}})\mathbf{G_k^T}) \tag{3.30}$$

$$\mathbf{R_{ee_k}} = \mathbf{E}(\mathbf{G_k G_k^T}) \tag{3.31}$$

Next take the trace and the derivative of equation 3.28 and set the result equal to zero to find the optimal Kalman gain.

$$\begin{aligned} \mathbf{Tr}(\mathbf{\Psi_{k|k}}) &= \mathbf{Tr}(\mathbf{\Psi_{k|k-1}}) - \mathbf{2Tr}(\mathbf{R_{xe_k} K_k^T}) \\ &+\mathbf{Tr}(\mathbf{K_k R_{ee_k} K_k^T}) \\ \frac{\mathbf{d}}{\mathbf{dK_k}}\mathbf{Tr}(\mathbf{\Psi_{k|k}} &= -\mathbf{2Tr}(\mathbf{R_{xe_k}}) + \mathbf{2Tr}(\mathbf{K_k R_{ee_k}}) \\ \mathbf{K_k} &= \mathbf{R_{xe_k} R_{ee_k}^{-1}} \end{aligned} \tag{3.32}$$

which results in the familiar projection equation. In a standard linear Kalman filter the values of $\mathbf{R_{xe}}$ and $\mathbf{R_{ee}}$ are functions of $\mathbf{\Psi}$, $\mathbf{H}$ and $\mathbf{R}$. Because measurements are not linearly related to the state vector in or around a censored region explicit values for $\mathbf{R_{xe}}$ and $\mathbf{R_{ee}}$ must be found. The function for $\mathbf{R_{xe}}$ is,

$$\begin{aligned} \mathbf{R_{xe_k}} &= \mathbf{E}((\mathbf{x_k} - \mathbf{x_{k|k-1}})((\mathbf{Cx_k} + \mathbf{v_k})^{\mathbf{T}}\mathbf{p_k} + \\ &\quad \mathbf{T^T}(\mathbf{I_{m\times m}} - \mathbf{p_k}) - \mathbf{E}(\mathbf{y_k})^{\mathbf{T}})) \\ &= \mathbf{E}(\mathbf{x_k x_k^T C^T p_k}) + \mathbf{E}(\mathbf{x_k v_k^T p_k}) + \mathbf{E}(\mathbf{x_k T^T}(\mathbf{I_{m\times m}} - \mathbf{p_k})) \\ &-\mathbf{E}(\mathbf{x_k})\mathbf{E}(\mathbf{y_k})^{\mathbf{T}} - \mathbf{E}(\mathbf{x_{k|k-1} x_k^T C^T p_k}) - \mathbf{E}(\mathbf{x_{k|k-1} v_k^T p_k}) + \\ &\mathbf{E}(\mathbf{x_{k|k-1} T^T}(\mathbf{I_{m\times m}} - \mathbf{p_k})) - \mathbf{E}(\mathbf{x_{k|k-1}})\mathbf{E}(\mathbf{y_k})^{\mathbf{T}}) \end{aligned} \tag{3.33}$$

The probability of the measurement being non censored is a function of the distance between the latent measured variable and the threshold value. The expected value of $p_k(l,l)$ may be written as

$$E(p_k(l,l)) = \Phi(\frac{Cx_k(l) - T(l)}{\sigma(l)}) \tag{3.34}$$

Where $Cx_k(l)$ is the l^{th} element of the measurement vector and $\sigma(l)$ is the variance of the noise on that element. In principle this requires knowledge of the true state value. The following assumption allows us to relax this dependence and use the estimated state value instead.

Assumption 1

Assume that the state prediction permits a sufficiently accurate estimate of the probability of censoring:

$$E(p_k(l,l)) = \Phi(\tfrac{Cx_k(l)-T(l)}{\sigma(l)}) \approx \Phi(\tfrac{Cx_{k|k-1}(l)-T(l)}{\sigma(l)}) \tag{3.35}$$

Assumption 2

For simplicity, assume no cross-dependence in the measurements. Consequently, R is diagonal and:

$$cov(y_k(d), y_k(l)) = 0 \;\forall\; d, l \tag{3.36}$$

3.3.4.3 The Update Stage, continued

The above assumptions allows us to estimate $\mathbf{p_k}$ at each iteration and obtain values of $\mathbf{R_{xe}}$ and $\mathbf{R_{ee}}$ without the knowledge of $\mathbf{x_k}$. Where Assumptions 1 and 2 hold,

$$\mathbf{E}(\mathbf{p_k}) = \mathbf{Diag}\begin{pmatrix} \Phi(\frac{Cx_{k|k-1}(1)-T(1)}{\sigma(1)}) \\ \Phi(\frac{Cx_{k|k-1}(2)-T(2)}{\sigma(2)}) \\ \vdots \\ \Phi(\frac{Cx_{k|k-1}(m)-T(m)}{\sigma(m)}) \end{pmatrix}. \tag{3.37}$$

Revisiting $\mathbf{R_{xe_k}}$, and using $\mathbf{E}(\mathbf{x_{k|k-1}v_k^T}) = \mathbf{0_{n\times n}}$ since $\mathbf{v_k}$ is uncorrelated white Gaussian noise and $\mathbf{E}(\mathbf{x_{k|k-1}}) = \mathbf{x_{k|k-1}}$, $\mathbf{E}(\mathbf{x_k}) = \mathbf{x_{k|k-1}}$ and

$$\begin{aligned}\mathbf{E}(\mathbf{x_k x_k^T}) &= \mathbf{E}((\mathbf{x_k} - \mathbf{E}(\mathbf{x_{k|k-1}}))(\mathbf{x_k} - \mathbf{E}(\mathbf{x_{k|k-1}}))^{\mathbf{T}}) \\ &\quad + \mathbf{E}(\mathbf{x_k})\mathbf{E}(\mathbf{x_k})^{\mathbf{T}} \\ &= \mathbf{\Psi_{k|k-1}} + \mathbf{x_{k|k-1}x_{k|k-1}^T}\end{aligned} \tag{3.38}$$

$$
\begin{aligned}
&\mathbf{R_{xe_k}} = (\mathbf{\Psi_{k|k-1}} + \mathbf{x_{k|k-1}x^T_{k|k-1}})\mathbf{C^T E(p_k)} \\
&+\mathbf{x_{k|k-1}T^T(I_{m\times m} - E(p_k))} - \mathbf{x_{k|k-1}E(y_k)^T} \\
&-\mathbf{x_{k|k-1}x^T_{k|k-1}C^T E(p_k)} \\
&+\mathbf{x_{k|k-1}T^T(I_{m\times m} - E(p_k))} + \mathbf{x_{k|k-1}E(y_k)^T)} \\
&= \mathbf{\Psi_{k|k-1}C^T E(p_k)^T}
\end{aligned}
\tag{3.39}
$$

Repeat the above steps for $\mathbf{R_{xe}}$ to compute $\mathbf{R_{ee}}$

$$
\begin{aligned}
&\mathbf{R_{ee_k}} = \mathbf{E(p_k)C(\Psi_{k|k-1}} + \mathbf{x_{k|k-1}x^T_{k|k-1})C^T E(p_k)} \\
&+\mathbf{E(p_k v_k v_k^T p_k)} + \mathbf{E(p_k)Cx_{k|k-1}T^T(I_{m\times m} - E(p_k))} \\
&-\mathbf{E(p_k)Cx_{k|k-1}E(y_k)^T} + \mathbf{(I_{m\times m} - E(p_k))Tx^T_{k|k-1}C^T E(p_k)} \\
&+\mathbf{(I_{m\times m} - E(p_k))TT^T(1 - E(p_k))} - \mathbf{(I_{m\times m} - E(p_k))TE(y_k)^T} \\
&-\mathbf{E(y_k)x^T_{k|k-1}C^T E(p_k)} - \mathbf{E(y_k)(I_{m\times m} - E(p_k))T^T} \\
&+\mathbf{E(y_k)E(y_k)^T} \\
&= \mathbf{E(p_k)C\Psi_{k|k-1}C^T E(p_k)^T} + \mathbf{E(p_k v_k v_k^T p_k)^T}
\end{aligned}
\tag{3.40}
$$

where $\mathbf{E(p_k v_k v_k^T p_k)^T}$ is related to the scalar Equation 3.11. If Assumption 2 holds, this is a diagonal matrix written as:

$$
\mathbf{E(p_k v_k v_k^T p_k)^T} = \mathbf{Diag}\begin{pmatrix} Var[y_k(1)|x_{k|k-1}(1), \sigma(1)] \\ Var[y_k(2)|x_{k|k-1}(2), \sigma(2)] \\ \vdots \\ Var[y_k(m)|x_{k|k-1}(m), \sigma(m)] \end{pmatrix}
\tag{3.41}
$$

where $Var[y_k(i)|x_{k|k-1}(i), \sigma(i)]$ is calculated according to Equation 3.11. Substituting this optimal Kalman gain into Equation 3.28 yields the simplified covariance update equations:

$$
\mathbf{\Psi_{k|k}} = (\mathbf{I_{m\times m}} - \mathbf{E(p_k)K_k C})\mathbf{\Psi_{k|k-1}}
\tag{3.42}
$$

The complete Tobit Kalman filter is:

$$\begin{aligned}
\mathbf{x_{k|k-1}} &= \mathbf{A x_{k-1|k-1}} \\
\mathbf{\Phi_{k|k-1}} &= \mathbf{A \Psi_{k-1|k-1} A^T + Q} \\
\mathbf{x_{k|k}} &= \mathbf{x_{k|k-1} + R_{xe_k} R_{ee_k}^{-1} (y_k - E(y_k))} \\
\mathbf{\Psi_{k|k}} &= \mathbf{(I_{m \times m} - E(p_k) R_{xe_k} R_{ee_k}^{-1} C) \Psi_{k|k-1}}
\end{aligned} \tag{3.43}$$

where $\mathbf{R_{xe_k}}$ is given by Equation 3.39, $\mathbf{R_{ee_k}}$ is given by Equation 3.40, $\mathbf{E(y_k)}$ is given by Equation 3.8, and $\mathbf{E(p_k)}$ is given by Equation 3.37.

3.3.5 Equivalence to the Standard Kalman Filter

The Tobit Kalman filter converges to the standard Kalman filter when the state value is far away from the censoring region,

$$\lim_{\frac{\mathbf{x_{k|k-1}-T}}{\sigma} \to \infty} \begin{cases}
\mathbf{\Phi}(\frac{\mathbf{Cx_{k|k-1}-T}}{\sigma}) = [\mathbf{1\,1} \ldots]^{\mathbf{T}} \\
\mathbf{E(y_k) = Cx_{k|k-1}} \\
\mathbf{R} = \sigma^{\mathbf{2}} \\
\mathbf{R_{xe} = C\Psi_{k|k-1}} \\
\mathbf{R_{ee} = C\Psi_{k|k-1}C^T + R} \\
\mathbf{\Psi_{k|k} = (I_{m \times m} - K_k C)\Psi_{k|k-1}}
\end{cases} \tag{3.44}$$

so this formulation is a generalization of a standard Kalman filter. For state estimates close to the censoring region the convergence is proportional to the distance to the censoring limit and the measurement noise.

3.3.6 Estimation with the Tobit Kalman Filter

In this section the results from two experiments show the potential of the Tobit Kalman filter. The first simulation is estimating constant value in the uncensored region with a measurement noise large enough to cause a large proportion of measurements to be censored. The next simulation is a Brownian motion model which have disturbances as well as additive noise. The Tobit Kalman filter is compared to the the intermittent measurements Kalman filter which is outlined in [16] . This filter operates as a Kalman filter until a missing measurement occurs, then it only predicts the current state and covariance matrix and does not perform the *a posteriori* update; so $\mathbf{x_{k|k}} = \mathbf{x_{k|k-1}}$ and $\mathbf{\Psi_{k|k}} = \mathbf{\Psi_{k|k-1}}$. The filter compared to here treats censored measurements as missing measurements. Also used as a comparison is the standard Kalman filter that treats censored values as regular measurements.

3.3.6.1 A Note on Computation

A Kalman filter for censored data has been derived by making an assumption on the predictability of the amount of censorship. It is important to note that this formulation only requires the extra complexity of computing m normal PDFs and m normal CDFs at each iteration. These extra computations only need to be performed once per iteration, after the predict stage.

3.3.6.2 Estimate a Constant Value

This example estimates a constant value of -.1 near a censoring region, with noise $\sigma = .1$. The initial conditions are $x_0 = .1$ and $\Psi_0 = .05$, with $Q = 10^{-14}$.

As shown in Figure 3.1 the Tobit Kalman filter converges to the true value. All other methods are biased with their estimates remaining in the uncensored region.

In Figure 3.2 the experiment is repeated with a constant value of +0.1 with the same noise value and initial conditions. Even when the value is above the censoring limit, the other two methods result in a biased estimate, while the Tobit Kalman filter is unbiased.

3.3.6.3 Brownian Motion

Brownian motion often leads to saturation issues in both MEMS sensors and tracking with computer vision. The model is simple yet shows the tracking performance of the proposed method in a disturbance-driven model. The data are generated from,

$$y_k^* = \alpha y_{k-1}^* + \eta_k \tag{3.45}$$

Choose $\alpha = .999$ to dampen the natural divergence of the model, keeping it close to the censoring limit. η is a normally distributed random variable with variance 0.01, and the measurements have noise $\sigma = .05$ and are left-censored at $T = 0$. The initial conditions are $\mathbf{x_0} = \mathbf{.05}$ and $\mathbf{\Psi_0} = \mathbf{.05}$.

As shown in Figure 3.3, the standard Kalman filter's estimates converge to the censoring limit when the measurements are censored for a sufficient period. The Intermittent Measurements Kalman Filter only updates when measurements are not censored, resulting in an unstable covariance matrix as described in [16]. The divergence in the state error covariance matrix for the Intermittent Measurements formulation can be seen between samples 350 and 400. By comparison, the state error covariance of the Tobit Kalman filter grows much more slowly. Its size remains bounded by the distance from the estimated latent variable position from the censoring limit even during long periods of censored measurements.

3.3.6.4 Oscillator

The following example has dynamics following Equation 5.40 with the state space matrices

$$A = \alpha \begin{bmatrix} cos(\omega) & -sin(\omega) \\ sin(\omega) & cos(\omega) \end{bmatrix} \tag{3.46}$$

$$C = \begin{bmatrix} 1 & 0 \end{bmatrix} \tag{3.47}$$

This experiment shows a robust tracking ability with a known model and unknown disturbance that enters the system through $\mathbf{w_k}$. In this example, $\alpha = 1$, the disturbance is normally distributed with variance of 0.01 and is uncorrelated to the measurement noise which is normally distributed with variance of 0.1. The initial conditions are $\mathbf{x_0} = [\mathbf{0}\ \mathbf{0}]^\mathbf{T}$ and $\mathbf{\Psi_0} = \mathbf{.05I_{2x2}}$

Figure 3.4 show that when the measurements are being censored the output of the Tobit Kalman filter closely tracks the actual values while the Kalman filter for the intermittent measurements method has a positive bias due to its placing heavy emphasis on stray non censored data. Around sample 1350 in the figure the intermittent measurements Kalman filter quickly converges to a stray measurement due to an inflated $\mathbf{\Psi}$, caused by the update stage not being computed for several samples. The Tobit Kalman filter would accept this noise measurement as spurious an not converge to it rapidly.

In the second half of Figure 3.4 the estimate of the unmeasured second state is plotted against its true value.

3.4 Estimation with a Time-Varying Censoring Limit

The question is now put forward, what happens if the censoring limit is time-varying? As mentioned briefly in the preceding derivation, the structure of the Kalman filter formulations for time-varying and time-invariant systems are identical. The time-invariant system, and subsequent filter, is a special-case of the more general time varying system, in which system matrices are constant over time. Thus, use of the time-invariant system allows for the dropping of time indices from the system matrices, permitting cleaner notation and convergence to steady state values under the appropriate conditions.

The Tobit Kalman filter also does not have a change in formulation between time-varying and time-invariant systems, in accordance with the standard Kalman filter. This duality also extends to the censoring limit T. However, unlike the standard Kalman filter, it will be shown that the presence of censoring means that it cannot be assumed that a time-invariant Tobit Kalman filter converges to a steady state. However, if control of censoring limit T is possible, without error, then a predictable steady Tobit Kalman filter can be achieved. Thus far been assumed that the censoring limit is known a priori with no error. Consideration of a filter with a time-varying stochastic censoring limit is considered to be beyond the scope of this work and is a topic of considerable future research.

3.4.1 The Steady State Kalman Filter

It is well known that with time invariant systems with white stationary process noise and white stationary measurement noise, the standard Kalman filter gain and covariance may converge to steady state values, given certain conditions.

Given the LTI system

$$\begin{aligned}\mathbf{x_{k+1}} &= \mathbf{A x_k} + \mathbf{G w_k} \\ \mathbf{y_k} &= \mathbf{C x_k} + \mathbf{v_k}\end{aligned} \tag{3.48}$$

With

$$\begin{aligned}\mathbf{E}(\mathbf{w_k w_k^T}) &= \mathbf{Q} \\ \mathbf{E}(\mathbf{v_k v_k^T}) &= \mathbf{R}\end{aligned} \tag{3.49}$$

Summarizing the Kalman filter definition given previously, then

$$\begin{aligned}\mathbf{\hat{x}_{k+1|k+1}} &= \mathbf{A\hat{x}_{k+1|k}} + \mathbf{K_{k+1}}\left(\mathbf{z_{k+1}} - \mathbf{C\hat{x}_{k+1|k}}\right) \\ \mathbf{K_k} &= \mathbf{AP_{k|k-1}C^T}\left(\mathbf{CP_{k|k-1}C^T} + \mathbf{R}\right)^{-1} \\ \mathbf{P_{k+1|k}} &= \mathbf{AP_{k|k-1}A^T} - \mathbf{K_k CP_{k|k-1}A^T} + \mathbf{GQG^T}\end{aligned} \tag{3.50}$$

Under the conditions that $\mathbf{Q}$ is positive definite, $\left(\mathbf{A}, \mathbf{G}\sqrt{\mathbf{Q}}\right)$ is controllable, $(\mathbf{A}, \mathbf{C})$ is observable, then it can be shown that :

- There exists a steady state Kalman filter
- $\lim_{\mathbf{k}\to+\infty} \mathbf{P_{k+1|k}} = \mathbf{P_\infty^-}$
- $\lim_{\mathbf{k}\to+\infty} \mathbf{K_k} = \mathbf{K_\infty}$
- $\mathbf{P_\infty^-}$ is the solution to the algebraic Ricatti equation given by :
  $\mathbf{P_\infty^-} = \mathbf{AP_\infty^-A^T} - \mathbf{AP_\infty^-C^T}\left(\mathbf{CP_\infty^-C^T} + \mathbf{R}\right)^{-1}\mathbf{CP_\infty^-A^T} + \mathbf{GQG^T}$
- $\mathbf{K_\infty} = \mathbf{P_\infty^-C^T}\left(\mathbf{CP_\infty^-C^T} + \mathbf{R}\right)^{-1}$
- $\mathbf{P_\infty^-}$ is unique, finite, and positive-semidefinite
- $\mathbf{P_\infty^-}$ is independent of $\mathbf{P_0}$, given that $\mathbf{P_0} \geq \mathbf{0}$
- The resulting steady state Kalman filter is asymptotically unbiased

Often, for reasons of convenience and computational speed, the final steady state formulation of the Kalman filter is utilized in practical estimation applications. Although rate of convergence from initial conditions may be slower, the tradeoff for lower memory footprint and faster computation is largely beneficial for long term applications in which initial conditions are of little concern. As long as the given conditions on system dynamics and noise parameters are met, convergence is guaranteed and initial error may be of little consequence. Furthermore, utilization of fixed Kalman gain $\mathbf{K}_\infty$ allows for leveraging of many linear control techniques to analyze estimator and closed-loop performance, as shown in the next chapter.

3.4.2 The Steady State Tobit Kalman Filter

The presence of censoring, even time-invariant censoring, precludes the Tobit Kalman filter from converging to a steady state for time-invariant systems. This is because the condition that measurement noise is stationary and white is violated when the true state is near the censored region. Thus, variance $\mathbf{R}$ is no longer a time-invariant parameter, thus covariance $\mathbf{P}$ and Tobit Kalman gain $\mathbf{K}$ does not converge. The Tobit measurement variance is given by 3.11.

However, this result is not altogether disappointing. One would expect that when the true state enters the area near the censoring region, and measurements begin to become censored, that practical state information is being lost and error covariance should therefore rise, reflecting higher state estimation uncertainty when near or in the censored region. As has already been shown, naive use of a Kalman filter with a time-invariant system in the presence of censoring leads to convergence to steady state covariance and gain, however the model from which these values result is no longer valid. Therefore state estimation with the standard Kalman filter becomes biased while giving no indication that censoring is present via its error covariance. The Tobit Kalman filter, although not converging to a steady state, increases its state error covariance accordingly to counter-act the reduction of useful information due to censoring. Thus the Tobit Kalman filter can react to censoring in such a manner that the Tobit gain updates, the error covariance grows, and a more accurate measure of state uncertainty can be calculated.

But the question still remains, what if censoring limit T can be changed? One would imagine that if T is managed in such a way that the censoring region always remains a fixed distance away from the state and state estimates, that Tobit parameters relying upon this relationship will stabilize. In fact, if T is controlled in such a manner that a certain expectation of censoring is maintained at all times, it is found that the inverse mills ratio and Tobit variance remain fixed. Thus, the conditions for a steady state filter are recovered, and a modified Ricatti equation can be used to calculate a new steady state Tobit Kalman filter. For example, consider the system given by :

$$\begin{aligned} \mathbf{x_k} &= \mathbf{A x_{k-1}} + \mathbf{B u_k} + \mathbf{w_{k-1}} \\ \mathbf{y^*_k} &= \mathbf{C x_k} + \mathbf{D u_k} + \mathbf{v_k} \\ \mathbf{y_k} &= \begin{cases} \mathbf{y^*_k}, & \mathbf{y^*_k} < \mathbf{T} \\ \mathbf{T}, & \mathbf{y^*_k} \geq \mathbf{T} \end{cases} \end{aligned} \tag{3.51}$$

The Tobit *a priori* state estimate $\bar{x}$ and state estimate covariance $\bar{\Psi}$ given by :

$$\begin{aligned} \bar{\mathbf{x}} &= \mathbf{A}\hat{\mathbf{x}} + \mathbf{B u} \\ \bar{\mathbf{\Psi}} &= \mathbf{A}\hat{\mathbf{\Psi}}\mathbf{A^T} + Q \end{aligned} \tag{3.52}$$

For convenience, define the estimated latent measurement and probability of measurement being uncensored as :

$$\begin{aligned} \bar{\mathbf{Y}} &= \mathbf{C}\bar{\mathbf{x}} + \mathbf{D u} \\ \alpha_i &= \tfrac{(T_i - \bar{Y}_i)}{\sigma_i} \\ \mathbf{E_{pk}} &= \mathbf{diag}\begin{pmatrix} \Phi(\alpha_1) \\ \Phi(\alpha_2) \\ \cdots \end{pmatrix} \end{aligned} \tag{3.53}$$

The inverse mills ratio, expected measurement, and measurement variance can then be defined as :

$$\mathbf{E}(\mathbf{y}) = \begin{pmatrix} \phi(\alpha_1)(\bar{Y}(1) - \sigma_1 IMR(1)) + \Phi(\alpha_1) \\ \phi(\alpha_2)(\bar{Y}(2) - \sigma_2 IMR(2)) + \Phi(\alpha_2) \\ ... \end{pmatrix}$$
$$\mathbf{IMR} = \begin{pmatrix} \frac{\phi(\alpha_1)}{\Phi(\alpha_1)} \\ \frac{\phi(\alpha_2)}{\Phi(\alpha_2)} \\ ... \end{pmatrix} \tag{3.54}$$
$$\mathbf{V} = \mathbf{diag}\begin{pmatrix} \sigma_1^2(1 - IMR(1)^2 - IMR(1)\alpha_1)) \\ \sigma_2^2(1 - IMR(2)^2 - IMR(1)\alpha_2)) \\ ... \end{pmatrix}$$

Then the Tobit Kalman filter can be rewritten as :

$$\begin{gathered} \mathbf{R_{xe}} = \bar{\mathbf{\Psi}}\mathbf{C^T}\mathbf{E_{pk}^T} \\ \mathbf{R_{ee}} = \mathbf{E_{pk}}\mathbf{C}\bar{\mathbf{\Psi}}\mathbf{C^T}\mathbf{E_{pk}^T} + \mathbf{V} \\ \mathbf{K} = \mathbf{Rxe}(\mathbf{Ree})^{-\mathbf{1}} \\ \hat{\mathbf{x}} = \bar{\mathbf{x}} + \mathbf{K}(\mathbf{y} - \mathbf{E}(\mathbf{y})) \\ \hat{\mathbf{\Psi}} = (\mathbf{I_{NxN}} - \mathbf{K}\mathbf{E_{pk}}\mathbf{C})\bar{\mathbf{\Psi}} \end{gathered} \tag{3.55}$$

If T is chosen such that $\mathbf{E_{pk}} = \mathbf{\Xi}$ for a given $\mathbf{\Xi}$, then $\alpha = \Phi^{-1}(\Xi)$, and the inverse mills ratio and variance remain constant. This is accomplished by defining

$$\mathbf{T} = \bar{\mathbf{Y}} + \sigma\mathbf{\Phi^{-1}}(\mathbf{\Xi}) \tag{3.56}$$

Which results in

$$\begin{gathered} \mathbf{V} \to \upsilon \\ \mathbf{C} \to \mathbf{\Xi}\mathbf{C} \\ \mathbf{K} \to \bar{\mathbf{\Psi}}(\mathbf{\Xi}\mathbf{C})^{\mathbf{T}}\bar{\mathbf{\Psi}}((\mathbf{\Xi}\mathbf{C})\bar{\mathbf{\Psi}}(\mathbf{\Xi}\mathbf{C})^{\mathbf{T}} + \upsilon)^{-\mathbf{1}} \end{gathered} \tag{3.57}$$

With a linear time invariant system, given the definition of T above for a given Ξ, a Tobit Kalman filter is defined which mirrors a standard Kalman filter for a modified time invariant system. Measurement matrix $\mathbf{C}$ has been replaced by $\mathbf{\Xi C}$ and measurement variance R goes to υ. Using the assumption that υ is stationary, then a steady state Tobit Kalman filter can be found if the corresponding conditions are met, namely that $\left(\mathbf{A}, \sqrt{\mathbf{Q}}\right)$ is controllable and $(\mathbf{A}, \mathbf{\Xi C})$ is observable. Furthermore, the new Tobit steady state gain $\mathbf{K}_\infty$ and error covariance $\bar{\mathbf{\Psi}}^-_\infty$ can be found by solving the Ricatti equation with the corresponding Tobit parameters.

Since the expectation of censoring and the inverse mills ratio are now calculable to a pre-determined value, the expected measurement can the be defined as

$$E[y] = \Xi(C\hat{x} - \sigma\hat{\lambda}) + (1 - \Xi)T \tag{3.58}$$

and therefore, the state estimate is then given by

$$\begin{aligned} \dot{x} &= A\hat{x} + L(z - E[y]) \\ &= A\hat{x} + L(z - (\Xi(C\hat{x} - \sigma\hat{\lambda}) + (1 - \Xi)T)) \end{aligned} \tag{3.59}$$

where the expection of the measurement z is given by

$$E[z] = (\gamma(Cx - \sigma\lambda) + (1 - \gamma)T)) \tag{3.60}$$

Assume initial convergence of the state and state estimate, then $\gamma \approx \Xi$ and $\lambda \approx \hat{\lambda}$, and therefore

$$\begin{aligned} \dot{\hat{x}} &= A\dot{\hat{x}} + L(\Xi Cx - \Xi C\hat{x}) \\ &= (A - L\Xi C)\hat{x} + L(\Xi Cx) \end{aligned}$$

That is, the original uncensored dynamics of the filter are recovered, save for the addition of the censoring factor Ξ, which is determined by the user.

The same principals apply for the discrete time system, leading to

$$\mathbf{T_k} = \mathbf{C\hat{x}_k} + \sigma\mathbf{\Phi^{-1}}(\mathbf{\Xi}) \tag{3.61}$$

and, assuming initial convergence,

$$\begin{aligned}
\mathbf{x_{k+1}} &= \mathbf{Ax_k} + \mathbf{w_k} \\
\mathbf{\hat{x}_{k+1}} &= (\mathbf{A} - \mathbf{L\Xi C})\mathbf{\hat{x}_k} + \mathbf{L}(\mathbf{\Xi C x_k})
\end{aligned}$$

3.4.3 Application of a Time Varying Censoring Limit

Usage of a time varying censoring limit with the preceding definition has powerful implications. By specifying the parameter Ξ, the user can dictate the level of censoring present at any given time, assuming the implications of physically realizing the desired value T are disregarded for the time being. Because the level of censoring is constant, the all Tobit related parameters resolve to fixed values, and a steady state Tobit Kalman filter can be found if the sufficient conditions are met.

For example, consider the scenario of tracking a noisy oscillating signal, such as that from a common place accelerometer. The general approach to avoid censoring and capturing the highest dynamic range would be to run the associated analog to digital converter at its maximum power level, say five volts. However, in the interests of saving power for mobile applications, it may be far more desirable to run the ADC at three volts, and trade the limited dynamic range for longer battery life. With Tobit Kalman filter this tradeoff is no longer necessary. One can either run at the lower power level indefinitely, and use the full Tobit Kalman filter to estimate the signal when accelerometer enters the censored region of three to five volts. Another approach would be to dynamically change the power level at all times to accomplish a specified level of censoring, therefore state estimation accuracy, and maintain optimum battery life while doing so. Both scenarios are shown below, and it is shown that highly accurate signal tracking can be performed without the need for the full five volt dynamic range.

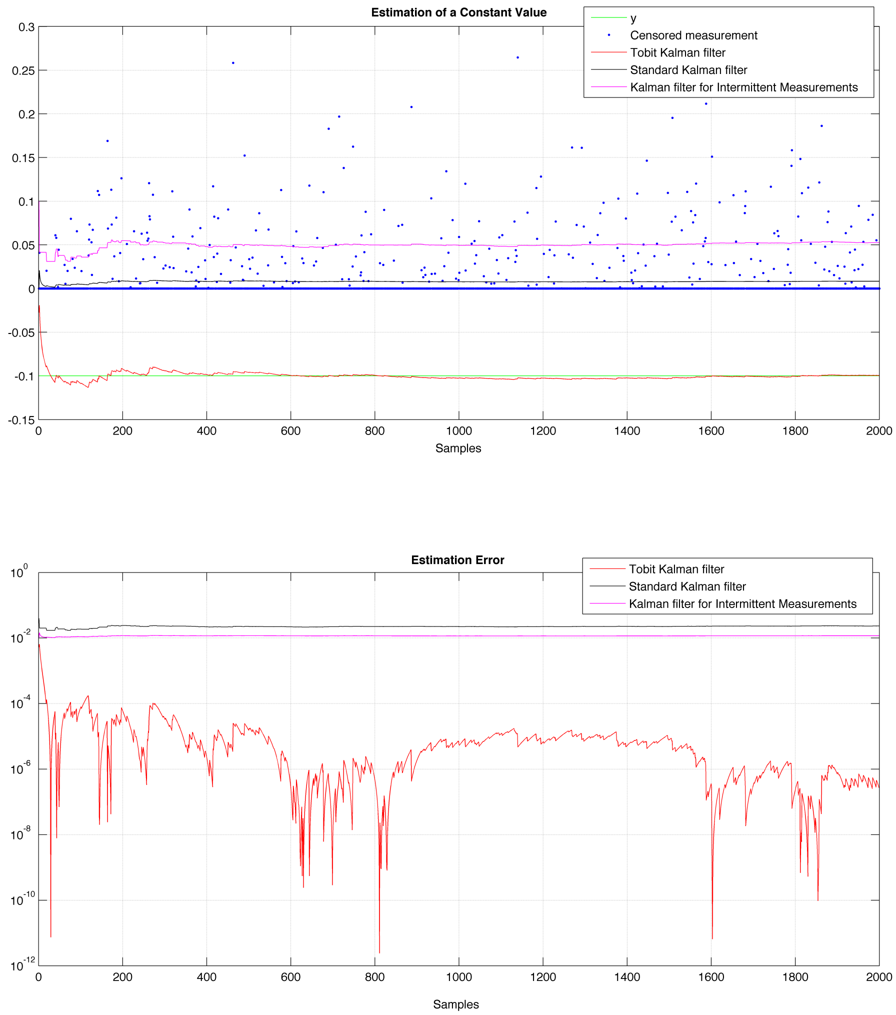

Figure 3.1: Constant value below the censoring limit

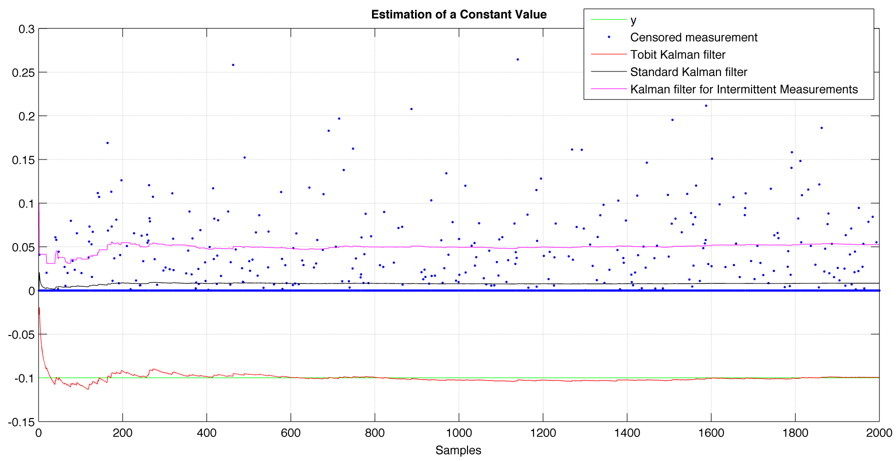

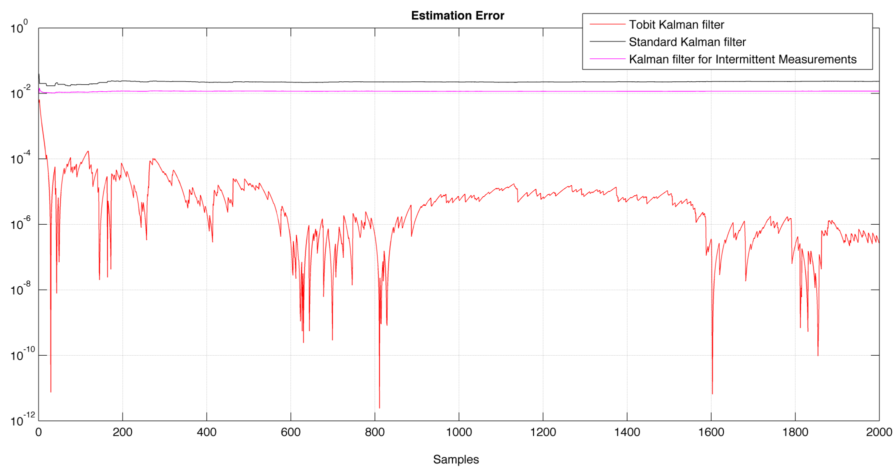

Figure 3.2: Constant value above the censoring limit

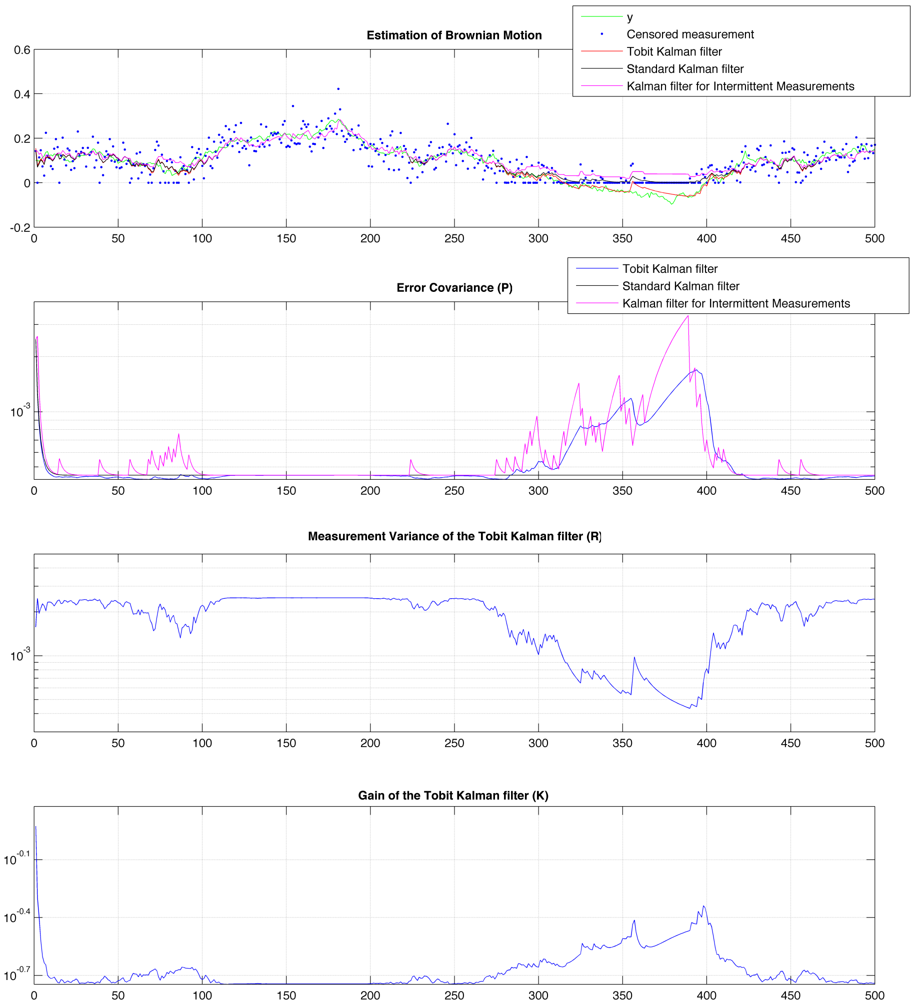

Figure 3.3: Brownian Motion

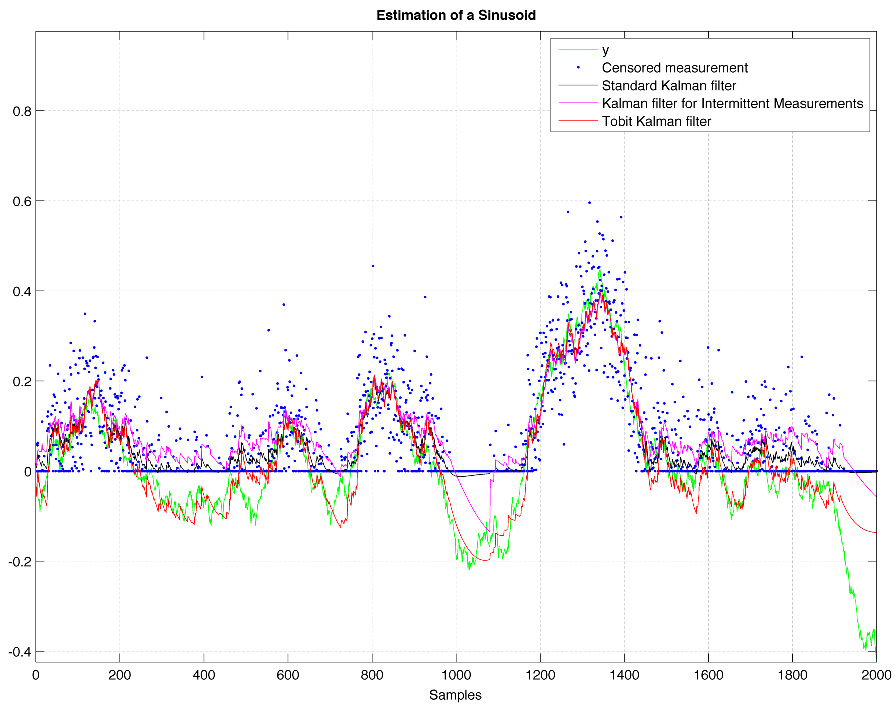

Figure 3.4: Sinusoidal Model

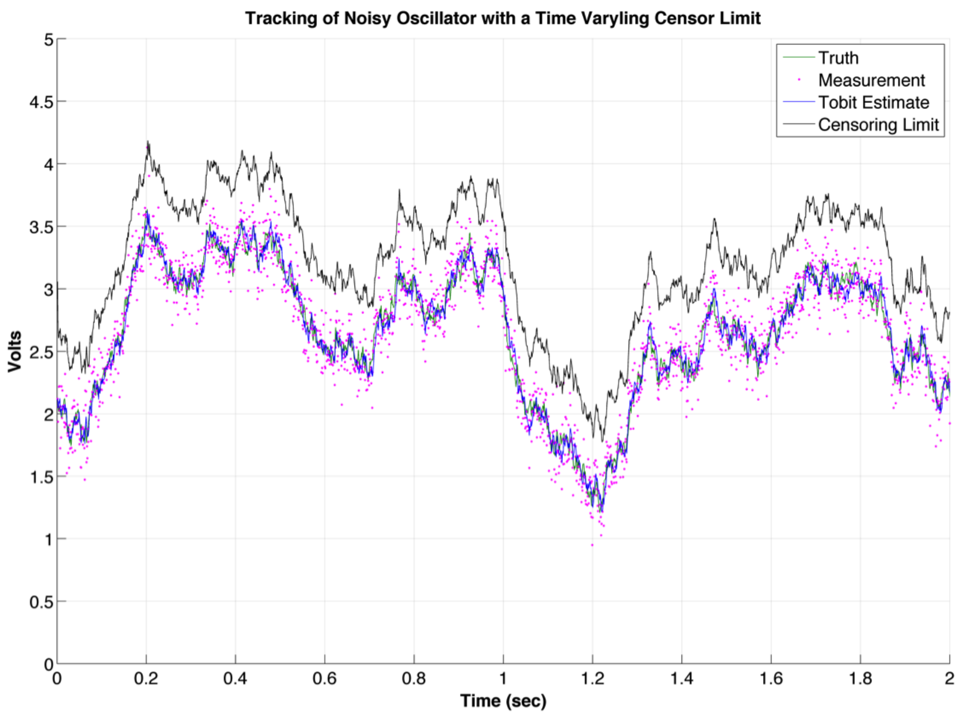

Figure 3.5: Changing the censoring limit T to maintain a constant expectation of censoring.

Chapter 4

INTRODUCTION TO LINEAR CONTROL THEORY

This chapter covers introductory material related to linear systems theory and basic linear control design. Topics ranging from linear system representation to stability and output feedback are covered. This background material is presented with the intent of providing what is necessary to understand the more advanced concepts and conjectures to put forth in later chapters. A more detailed and rigorous discussion of these topics can be found in any undergraduate control course textbook.

4.1 Basic Concepts of Linear Control Theory

In order to understand the control concepts and designs to be discussed, it is first necessary to understand the basic underlying principals of linear systems; namely their representation and properties.

4.1.1 State-Space Linear Systems

A linear state-space system takes the form of :

$$\begin{aligned} \dot{x}(t) &= A(t)x(t) + B(t)u(t), \quad x \in \Re^n, u \in \Re^k \\ y(t) &= C(t)x(t) + D(t)u(t), \qquad\qquad y \in \Re^m \end{aligned} \tag{4.1}$$

Here $x(t)$ is the system state, $u(t)$ is the input, and $y(t)$ is the output. Each signal is a function of time and may be represented as continous (as shown), or discrete. For continuous time t belongs to the set of all real numbers, whereas in discrete time t belongs to the set of integers. A *scalar* signal is that in which the signal is of dimension one. Thus, a scalar input would be u in which $k = 1$, also known as a *single input*. An input with $k > 1$ is called *multiple input*. Likewise, a *single output* is a scalar signal y with $m = 1$, otherwise the output is known as *multiple output*. Therefore, a multi-dimensional *multiple-input multiple-output* (MIMO) system has $k > 1, m > 1$, and a scalar *single-input single-output* (SISO) system has $k = 1, m = 1$.

If the system matrices $A(t), B(t), C(t), D(t)$ are constant for all time t, and are thus not a function of time, then the system is called *linear time-invariant* (LTI). For such systems the time index may be dropped for convenience. Otherwise, the system is *linear time-varying* (LTV).

For discrete time linear state-space systems

$$\begin{aligned} x(t+1) &= A(t)x(t) + B(t)u(t), \quad x \in \Re^n, u \in \Re^k \\ y(t) &= C(t)x(t) + D(t)u(t), \qquad\qquad y \in \Re^m \end{aligned} \tag{4.2}$$

All terms and relations defined previously for the continuous time system hold for the discrete time system as well. The only difference being that for discrete time systems the time index is defined over the domain of all integers, as previously noted. Therefore the state equations for continuous time systems represents a differential equation, whereas the discrete time system represents a difference equation.

4.1.2 Local Linearization of Nonlinear Systems

A nonlinear state-space system is a more generalized form of 4.1 in which the continuous time differential equation takes the form of :

$$\begin{aligned} \dot{x}(t) &= f(x, u, t), \quad x \in \Re^n, u \in \Re^k \\ y(t) &= g(x, u, t), \qquad\qquad y \in \Re^m \end{aligned} \tag{4.3}$$

Linear state-space systems are special cases of 4.3 in which the function f is linear. However, linear systems are often approximations to more complex nonlinear systems. A common method of analyzing nonlinear systems is to create a local linear approximation to the nonlinear system. How to use to equilibrium points to do so is covered next.

An equilibrium point of 4.3 is any point $(x^{eq}, u^{eq}) \in \Re^n \times \Re^k$ such that $f(x^{eq}, u^{eq}) = 0$. At such a point, 4.3 has a defined solution given by $u(t) = u^{eq}$, $x(t) = x^{eq}$, and

$y(t) = g(x^{eq}, u^{eq})$ for all time $t \geq 0$. Any perturbation $\delta u(t)$ added to input u^{eq}, and or perturbation δx^{eq} away from initial condition $x(0) = x^{eq}$, results in a slight perturbation of output y from equilibrium output y^{eq}. To understand the effect of these perturbations define the following :

$$\begin{aligned} u(t) &= u^{eq} + \delta u(t), \quad \forall t \geq 0 \\ x(0) &= x^{eq} + \delta x^{eq} \end{aligned} \tag{4.4}$$

Then,

$$\begin{aligned} \delta x(t) &:= x(t) - x^{eq} \\ \delta y(t) &:= y(t) - y^{eq} \\ &= g(x, u) - y^{eq} \\ &= g\left(x^{eq} + \delta x, u^{eq} + \delta u\right) - g(x^{eq}, u^{eq}) \end{aligned} \tag{4.5}$$

Taylor series expansion of $f(\cdot)$ and $g(\cdot)$ is then performed about the aforementioned equilibrium point (x^{eq}, u^{eq}), resulting in :

$$\begin{aligned} \delta \dot{x} &= \tfrac{\partial f(x^{eq}, u^{eq})}{\partial x} \delta x + \tfrac{\partial f(x^{eq}, u^{eq})}{\partial u} \delta u + \mathcal{O}\left(||\delta x||^2\right) + \mathcal{O}\left(||\delta u||^2\right) \\ \delta y &= \tfrac{\partial g(x^{eq}, u^{eq})}{\partial x} \delta x + \tfrac{\partial g(x^{eq}, u^{eq})}{\partial u} \delta u + \mathcal{O}\left(||\delta x||^2\right) + \mathcal{O}\left(||\delta u||^2\right) \end{aligned} \tag{4.6}$$

The higher order terms in 4.6 can be dropped, resulting in the local linearization of 4.3 about equilibrium point (x^{eq}, u^{eq}) as given by :

$$\begin{aligned} \delta \dot{x} &= A\delta x + B\delta u \\ \delta y &= C\delta x + D\delta u \end{aligned} \tag{4.7}$$

Where,

$$\begin{aligned} A &:= \tfrac{\partial f(x^{eq},u^{eq})}{\partial x} \\ B &:= \tfrac{\partial f(x^{eq},u^{eq})}{\partial u} \\ C &:= \tfrac{\partial g(x^{eq},u^{eq})}{\partial x} \\ D &:= \tfrac{\partial g(x^{eq},u^{eq})}{\partial u} \end{aligned} \tag{4.8}$$

Matrices A,B,C, and D are called the *Jacobian matrices* of system. The system given by use of the Jacobian matrices in 4.7 is an LTI system, which expresses the relationship of the *perturbations* on the state, input, and output of 4.3. Note also that 4.7 is a *local linearization*, and as such, is only valid for a small region about the equilibrium point.

The local linearization for discrete time systems is analogous to that of the continuous time systems considered before. The difference being that the discrete time nonlinear system and discrete time local linearization are both now given by difference equations as opposed to differential equations. Following the previous methodology, the discrete time invariant system given by 4.9 can be linearized about equilibrium point (x^{eq}, u^{eq}), resulting in local linearization given by 4.10, with Jacobian matrices defined by 4.8.

$$\begin{aligned} x^+ &= f(x,u), \quad x \in \Re^n, u \in \Re^k \\ y &= g(x,u), \qquad\qquad y \in \Re^m \end{aligned} \tag{4.9}$$

$$\begin{aligned} \delta x^+ &= A\delta x + B\delta u \\ \delta y &= C\delta x + D\delta u \end{aligned} \tag{4.10}$$

4.1.3 Solutions to LTI Systems Using the Exponential Matrix

Consider the simple time-invariant system given by 4.11. This is a linear time invariant homogenous system, in which the solution for $x(t)$ is given by a linear map from initial condition $x(0)$ by use of the matrix *state transition matrix* $\Phi(x, x_0)$, (4.12).

$$\dot{x} = Ax, \quad x(t_0) = x_0 \in \Re^n \tag{4.11}$$

$$x(t) = \phi(t, t_0)x_0, \quad x_0 \in \Re^n, t \geq 0 \tag{4.12}$$

The LTI and LTV systems the state transition matrix encompasses the complete dynamics of x from initial condition (x_0, t_0) to desired point (x, t) via the integration given by 4.13.

$$\begin{aligned} \phi(t, t_0) &:= I + \int_{t_0}^{t} A ds_1 + \int_{t_0}^{t} \int_{t_0}^{s1} A^2 ds_2 ds_1 + \dots \\ &= \sum_{k=0}^{\infty} \frac{(t-t_0)^k}{k!} A^k \end{aligned} \tag{4.13}$$

For CLTI systems 4.13 simplifies to a matrix exponential of A, defined by 4.14, and leading an exact solution for the state transition matrix given by 4.15.

$$e^A := \sum_{k=0}^{\infty} \frac{1}{k!} A^k \tag{4.14}$$

$$\phi(t, t_0) = e^{A(t-t_0)} \tag{4.15}$$

By use of the matrix exponential for CLTI systems, there is now a defined solution for $x(t)$ for all $t \geq 0$. Replacing the state transition matrix of 4.12 with the matrix exponential definition of 4.15, results in the following complete description of the solution to non homogenous linear time invariant systems for all $t \geq 0$ 4.16.

$$\begin{aligned} x(t) &= e^{A(t-t_0)}x_0 + \int_{t_0}^{t} e^{A(t-\tau)} B(\tau)u(\tau)d\tau \\ y(t) &= Ce^{A(t-t_0)}x_0 + \int_{t_0}^{t} Ce^{A(t-\tau)} B(\tau)u(\tau)d\tau + Du(t) \end{aligned} \tag{4.16}$$

Solutions to discrete time linear systems follow from that of continuous time systems, with the state transition matrix being defined via summation rather than integration.

4.2 Stability

Now that a solution for linear time varying and linear time invariant homogenous systems has be defined, the next question to answer is when do these systems permit stable solutions? First, the very notion of stability is discussed and two differing definitions are defined; stability in the Lyapunov sense, and bounded-input bounded-output stability.

In general, when one wishes to determine the stability of solutions to linear systems, one seeks conditions which guarantee well behaved evolution of the systems state over time. For systems meeting certain conditions, stronger notions of stability such $x(t) \to 0$ as $t \to \infty$, may be guaranteed. The notion of stability in the Lyapunov sense is presented first, in which the affect of initial conditions on the stability of the homogenous system is considered. Then bounded-input bounded-output (BIBO) stability is defined, which focuses attention on the input-output behavior of the system over time.

4.2.1 Lyapunov Stability

Conditions of stability in the Lyapunov sense pertain to the stability of homogeneous systems with regards to initial conditions. That is, in the absence of input u, how does the system evolve over time t from initial condition (x, t_0). Systems which are well-behaved, i.e. do not grow without bound to infinity, are said to be stable. Systems which permit stability without restriction on the initial state are said to be *globally* stable, whereas systems which permit stability only defined regions are said to be *locally* stable.

A *marginally stable* system meets the criteria as defined in 4.17.

$$\begin{aligned} x(t_0) &= x_0 \in \Re^n \\ x(t) &= \Phi(t, t_0)x_0, \forall t \geq 0 \end{aligned} \tag{4.17}$$

A system which is marginally stable has a closed form solution for all times $t \geq 0$, however no conditions on the value of this solution are given.

An *asymptotically stable* system meets the criteria as defined in 4.18.

$$x(t) \to 0 \text{ as } t \to \infty \tag{4.18}$$

A system which is asymptotically stable is marginally stable, with the additional property that the solution converges to the origin as t goes to infinity. In this sense, the system is "well behaved". When the system remains asymptotically stable given any initial condition in the set of all possible initial conditions, the system is said to *globally asymptotically stable*. Otherwise, the system is said to be *locally asymptotically stable* about x_0.

An *exponentially stable* system meets the criteria as defined in 4.19.

$$\begin{gathered} \exists \text{ constants } c, \lambda > 0 \text{ such that } \forall x(t_0) = x_0 \in \Re^n \\ \| x(t) \| \leq ce^{-\lambda(t-t_0)} \| x(t_0) \| \end{gathered} \tag{4.19}$$

A system which is exponentially stable is asymptotically stable, with the additional property that the solution converges to the origin in finite time. That is, there exists some function which converges to the origin and upper bounds the systems solution. When the system remains exponentially stable given any initial condition in the set of all possible initial conditions, the system is said to *globally exponentially stable*. Otherwise, the system is said to be *locally exponentially stable* about x_0. Exponential stability is the strongest condition for system stability in the Lyapunov sense.

When the eigenvalues of A have strictly negative real parts it is said that A is a *stability matrix*. It can be shown that homogeneous CLTI systems where A is a stability matrix are exponentially stable. This can be seen in 4.20 by using the solution for $x(t)$ given by that of 4.16 with zero input, and setting λ equal to the maximum eigenvalue of A, therefore :

$$\| e^{At} \| \leq \; ce^{-\lambda t}, \; \forall t \in \Re$$
$$\| x(t) \| = \| e^{A(t-t_0)} x_0 \| \leq \| e^{A(t-t_0)} \| \| x_0 \| \leq \; ce^{-\lambda(t-t_0)} \| x_0 \|, \; \forall t \in \Re \tag{4.20}$$

The magnitude of the state is upper bounded by an exponential function which decays at a rate determined by the maximum eigenvalue of A. Since this upper bound is always decaying, the system is always decaying, and eventually converges to zero. Thus the system is exponentially stable.

The definitions for marginal stability, asymptotic stability, and exponential stability hold for discrete time systems as well. As for CLTI systems, exponential stability for DLTI systems can be shown if again A is a stability matrix. This follows from the discussion of 4.20, except now

$$\| x(t) \| \leq c\lambda^{t-t_0} \| x(t_0) \| \tag{4.21}$$

4.2.2 Stability of Linearization

In the previous section the stability of linear systems was discussed, but what can be inferred about the stability of systems with the non-linear form of 4.3? As shown in section 4.1.2, this type of system may be linearized by use of the Jacobian A to the following form :

$$\dot{x} = f(x), x \in \Re^n$$
$$\dot{\delta x} = A\delta x \tag{4.22}$$

As before, the perturbation about the equilibrium point is defined as $\delta x := x - x^{eq}$. If A is conditioned as in the previous section then

$$\begin{aligned} \| x(t) - x^{eq} \| &\leq ce^{-\lambda(t-t_0)} \| x(t_0) - x^{eq} \|, \; \forall t \geq t_0 \\ \| \delta x \| &\leq ce^{-\lambda(t-t_0)} \| x(t_0) - x^{eq} \| \end{aligned} \tag{4.23}$$

A ball of radius epsilon can then be shown to exist such that

$$x(t) \in \epsilon \Rightarrow \dot{v} \leq -\tfrac{1}{2} \| \delta x \|^2$$

for suitable Lyapunov function candidates v. Should the norm term remain positive for all $x(t)$, then the Lyapunov derivative remains negative for all t, representing a decrease in system energy overtime, and therefore system stability.

4.2.3 Bounded-Input Bounded-Output Stability

The previous discussion on stability in the Lyapunov sense considered only the evolution from initial conditions and pertained only to homogeneous systems. BIBO stability however address the stability of non-homogeneous systems without regard to initial conditions. The notion of BIBO stability is defined by :

$$\sup_{t \in [0,\infty]} \| y_f(t) \| \leq g \sup_{t \in [0,\infty]} \| u(t) \| \tag{4.24}$$

If a system is stable in the BIBO sense then a finite input produces a finite output, for all time t.

4.3 State Feedback

Having presented a preliminary discussion on the nature of linear system representation and stability, consider now a discussion of various feedback control techniques via the utilization of input u. The goal of any feedback system is to drive the system to a desired state in a stable manner. Furthermore, it is desired that stable feedback control laws can be guaranteed to exist, that certain performance characteristics can be understood and calculated, and that optimal feedback laws can be found to accomplish given criteria.

Begin this discussion on feedback by considering the following definition for u, in which the control input is taken to be a proportional gain on the full system state x, given by :

$$u = -Kx \tag{4.25}$$

Which in turn results in :

$$\begin{aligned} \dot{x} &= Ax + Bu \\ &= (A - BK)x \end{aligned} \tag{4.26}$$

It can be shown that if the pair (A, B) is stablizable then there exists such a K that the state feedback law stabilizes the CLTI system. That is, $(A - BK)$ is a stability matrix.

Difficulty arises in practical implementations of state feedback controllers because the true state x is not always available for control. In the absence of noise, if the linear measurement map $y = Cx$ is invertible then the true state can be recovered from the measured outputs, given that there are as many unique measurements as there are unknown states. However, if this is not the case, then x must be reliably estimated in order for stable feedback to be accomplished. This is the driving factor for the rest of the discussion.

4.4 Output Feedback and State Observers

If only the output y can be measured then state feedback law given by 4.25 cannot be utilized directly. However, If (A, C) is detectable then x can be estimated. The simplest state estimator, as referred to as a *state observer*, is the *open-loop estimator*. The open-loop estimator is simply a copy of the original system which takes the same input as the normal system. That is :

$$\dot{\hat{x}} = A\hat{x} + Bu \tag{4.27}$$

Using this state estimate, define the error e between the true system state x and the state estimate $\hat{x}$ as follows :

$$\begin{aligned} e &:= \hat{x} - x \\ \dot{e} &= A\hat{x} + Bu - (A\hat{x} + Bu) \\ &= Ae \end{aligned} \tag{4.28}$$

The system input is cancelled, for it is equivalent in both the original system and the open-loop estimator. Thus a linear homogeneous system results. As shown in the previous section, if A is a stability matrix then this error system is exponentially stable, meaning that the error between the true state x and the state estimate $\hat{x}$ converges to zero over time.

However, improved performance can be gained by incorporating the system outputs into the state estimation. Consider the estimator given in 4.29, in which the estimated output is defined by a copy of the original system output model except now with the estimated state instead of the true state. The state estimate is calculated by summation of the open-loop estimator with a difference term between this expected output and the actual output.

$$\begin{aligned} \hat{y} &:= C\hat{x} + Du \\ \dot{\hat{x}} &= A\hat{x} + Bu - L(\hat{y} - y), \quad L \in \Re^{n \times m} \end{aligned} \tag{4.29}$$

The additional term $L(\hat{y} - y)$ acts as a correction factor. Again, defining the state estimation error e as :

$$\begin{aligned} e &:= \hat{x} - x \\ \dot{e} &= A\hat{x} + Bu - L(\hat{y} - y) - (Ax + Bu) \\ &= (A - LC)e \end{aligned} \tag{4.30}$$

See that If $(A - LC)$ is a stability matrix then the state estimation error converges to zero exponentially fast. Furthermore, compared to the open-loop estimator, the gain factor L my be designed in such a way that $(A - LC)$ is a stability matrix, even though A alone is not. This is very powerful, because it means that an exponentially stable state estimators may be made for systems which are not inherently stable themselves.

4.4.1 Stabilization via Output Feedback

Consider the CLTI system given by :

$$\begin{aligned} \dot{x} &= Ax + Bu \\ y &= Cx + Du \end{aligned} \tag{4.31}$$

With state estimator given by :

$$\begin{aligned} \dot{\hat{x}} &= A\hat{x} + Bu - L(\hat{y} - y) \\ \hat{y} &= C\hat{x} + Du \end{aligned} \tag{4.32}$$

It has already shown in section 4.3 that even if A is not a stability matrix, there may exist a gain K such that the state feedback law $u = -Kx$ stabilizes the system. It has also been shown that even if A is not a stability matrix, a state estimator of the form given by 4.29 can still produce exponentially stable state estimates $\hat{x}$. Therefore, if the state is not directly available for feedback, one may use the state estimate can be utilized for feedback instead. A controller of this form is known as a *certainty equivalence* controller, and leads to :

$$u = -K\hat{x} \tag{4.33}$$

Combining terms, now have a state estimation model is given in the form of

$$\begin{aligned}\dot{\hat{x}} &= A\hat{x} - BK\hat{x} - L\left(C\hat{x} - DK\hat{x} - y\right) \\ &= \left(A - LC - BK + LDK\right)\hat{x} + Ly\end{aligned} \tag{4.34}$$

Now consider once again the error defined by $e = \hat{x} - x$, with $\dot{e} = (A - LC)e$, as shown in 4.30. Thus :

$$\begin{aligned}\dot{x} &= Ax + Bu \\ &= Ax - BK\hat{x} \\ &= (A - BK)x - BKe\end{aligned} \tag{4.35}$$

From these results a new state-space model can be created with state $x = [x'e']'$, shown below.

$$\begin{bmatrix} \dot{x} \\ \dot{e} \end{bmatrix} = \begin{bmatrix} A - BK & -BK \\ 0 & A - LC \end{bmatrix} \begin{bmatrix} x \\ e \end{bmatrix} \tag{4.36}$$

The diagonal nature of this matrix gives rise to the *separation principal*, which states that gains K and L may be design separately such that $(A - BK)$ and $(A - LC)$ respectively are stability matrices. Thus the the state estimation law and the associated certainty equivalent state feedback law may be designed independently from one another.

4.5 LQR & LQG Control

This section looks to expand the discussion on state and output feedback and introduce notions of optimal control. The goal of Linear Quadratic Regulation (LQR) is to find gain K for state feedback controllers which optimizes the balance of control effort verses system output. Likewise, the goal of Linear Quadratic Gaussian estimation is to find gain L to optimize the state estimation of x given assumptions on noise present in the system.

4.5.1 Linear Quadratic Regulation

Consider the following system

$$\begin{aligned} \dot{x} &= Ax + Bu \\ y &= Cx \\ z &= Gx + Hu \end{aligned} \tag{4.37}$$

Where y is the measured output and z is the output to be controlled (y may equal z).

As mentioned, the LQR problem seeks a solution for K which stabilizes the system, and optimally minimizes the energy of the system. More specifically, one seeks to find $u(t)$ such that the following is minimized :

4.5.2 Linear Quadratic Regulation

$$J_{LQR} \quad := \quad \int_0^\infty y(t)'\bar{Q}y(t) + u(t)'\bar{R}u(t)dt \tag{4.38}$$

The weighting matrices Q and R determine the tradeoff between control energy and output energy. Intuitively, a low energy control input comes at the expense of a higher energy output, and a low energy output necessitates a large control input. These two goals conflict, and LQR seeks to minimize the total energy subject to the weighting defined by the control designer.

A more general quadratic form of the JLQR criterion is given by

$$J_{LQR} \quad := \quad \int_0^\infty x(t)'Qx(t) + u(t)'Ru(t) + 2x'Nu(t)dt \tag{4.39}$$

The criterion given in 4.38 is a special case of 4.39 in which $Q = G'\bar{Q}G, R = H'\bar{Q}H + \bar{R}$, and $N = G'\bar{Q}H$.

As is shown in [12], if a symmetric matrix P can be found which solves the following algebraic Riccati equation

$$A^{'}P + PA + Q - \big(PB + N)R^{-1}(B^{'}P + N^{'}\big) = 0 \tag{4.40}$$

and $(A - BR^{-1}(B'P + N')$ is a stability matrix, then there exists a feedback law of form

$$\begin{aligned} u &= -Kx \\ K &:= R^{-1}\left(B^{'}P + N^{'}\right) \end{aligned} \tag{4.41}$$

which minimizes the JLQR criterion of 4.39. The resulting closed-loop form of the system is then

$$\begin{aligned} \dot{x} &= \left(A - BR^{-1}\left(B^{'}P + N^{'}\right)\right)x \\ \dot{x} &= (A - BK)\,x \end{aligned} \tag{4.42}$$

Since the choice of K in 4.41 minimizes the JLQR criterion, it said to be an *optimal* control.

Assuming that $N := G^{'}H = 0$ then the above algebraic Ricatti equation simplifies to

$$A^{'}P + PA + G^{'}G - PBR^{-1}B^{'}P = 0 \tag{4.43}$$

and again if a symmetric matrix P exists which solves 4.43 and stabilizes $(A - BR^{-1}B'P$, then the optimal control law and resulting closed-loop system simplifies to

$$\begin{aligned} u &= -Kx \\ K &:= R^{-1}B^{'}P \\ \dot{x} &= \left(A - BR^{-1}B^{'}P\right)x \\ \dot{x} &= (A - BK)\,x \end{aligned} \tag{4.44}$$

In this form two important transfer functions can be found which are useful for in describing frequency domain properties of LQR controllers.

$$\begin{aligned}\hat{L}(s) &= K(sI - A)^{-1}B \\ \hat{T}(s) &= G(sI - A)^{-1}B + H\end{aligned} \tag{4.45}$$

These two open-loop transfer matrices are from the process input to controller input, and control input to controlled output, respectively. Many important properties and characteristics of LQR controllers can be obtained via frequency domain manipulations of these transfer functions, [**?**].

4.5.3 Minimum Energy Estimation

As mentioned in 4.4, the full state x is often not available for use in state feedback controllers, and instead a state estimate $\hat{x}$ must be constructed. When the state estimate is used for feedback in place of the true state the resulting controller is said to be *certainty equivalent*. However, the system given by 4.31 is often not exact in practical use of LTI models. Instead, a system of the following form is more appropriate

$$\begin{array}{rcll}\dot{x} &=& Ax + Bu + \bar{B}d, & x \in \Re^n, u \in \Re^k, d \in \Re^q \\ y &=& Cx + n, & y \in \Re^m\end{array} \tag{4.46}$$

Here, terms d and n represent disturbance and measurement noise, respectively. The goal of *Minimum Energy Estimation* (MEE) is to construct an optimal state observer for x which can be used in a certainty equivalent controller. This is accomplished by finding $\bar{x}$, defined by the model in 4.47, which is consistent with past inputs and measurements for the *least* amount of noise d and n.

$$\begin{array}{rcll}\dot{\bar{x}} &=& A\bar{x} + Bu + \bar{B}d, & \bar{x} \in \Re^n, u \in \Re^k, d \in \Re^q \\ y &=& C\bar{x} + n, & y \in \Re^m\end{array} \tag{4.47}$$

The total amount of noise is measured according to the following criterion

$$J_{MEE} \quad := \quad \int_{-\infty}^{t} n(\tau)' Q n(\tau) + d(\tau)' R d(\tau) d\tau \tag{4.48}$$

When an optimal solution for $\bar{x}$ is found, then the MEE state estimate is simply $\hat{x} = \bar{x}$. It can be seen that 4.48 is of a similar form to the JLQR criterion of 4.5.1, and as before, the weighting matrices Q and R play important roles. Varying Q and R in the JMEE criterion effectively changes the balance between the belief in the system outputs versus belief in the system model. When Q is large compared to R, then the noise term n is forced small, measured outputs are trusted, and the resulting state estimator quickly reacts to variations in y. When R is large compared to Q then disturbance d is forced small, the previous state estimates are trusted, and the resulting state estimator reacts slowly to variations in y.

Again, moving to a quadratic criterion, now of the form

$$J_{MEE} \quad := \quad \int_{-\infty}^{t} \left(C\bar{x}(\tau) - y(\tau)\right)' Q \left(C\bar{x}(\tau) - y(\tau)\right) + d(\tau)' R d(\tau) d\tau \tag{4.49}$$

and using arguments similar to that of 4.5.1, it can be shown that if there is a symmetric matrix P which solves the algebraic Ricatti equation given by

$$(-A')P + P(-A) + C'QC - P\bar{B}R^{-1}\bar{B}'P = 0 \tag{4.50}$$

and $(-A - \bar{B}R^{-1}\bar{B}'P$ is a stability matrix, then the minimum energy estimator for 4.46 is given by

$$\begin{aligned} L &:= P^{-1}C'Q \\ \dot{\hat{x}} &= (A - LC)\hat{x} + Bu + Ly \end{aligned} \tag{4.51}$$

With $\hat{x}$ given by 4.51, the convergence of estimator is shown by again defining the error as :

$$
\begin{aligned}
e &= \hat{x} - x \\
\dot{e} &= \dot{\hat{x}} - \dot{x} \\
&= (A - LC)e + \bar{B}d - Ln
\end{aligned}
\tag{4.52}
$$

$(A-LC)$ is a stability matrix, thus $e(t) \to 0$ as $t \to \infty$ when no noise is present, thus the closed loop system is exponentially stable. When noise is present e does not converge to zero, however it is bounded according to d and n, and therefore the closed loop system is BIBO stable.

4.5.4 Linear Quadratic Gaussian Estimation

Assume now that the noise and disturbance present in 4.46 are uncorrelated zero-mean white Gaussian processes. Also, assume that the respective covariance matrices are given by

$$
\begin{aligned}
&E\left[d(\tau)d'(\tau)\right] = \delta(t-\tau)R^{-1} \\
&E\left[n(\tau)n'(\tau)\right] = \delta(t-\tau)Q^{-1}
\end{aligned}
\tag{4.53}
$$

The MEE estimator previously given by 4.51 now describes the Kalman filter. As shown by the previous discussion on the Kalman filter, the estimator minimizes the asymptotic norm of the estimation error.

4.5.5 Combining LQR and LQG For Output Feedback

Consider the following CLTI system, in which disturbance d and measurement noise n are assumed to be zero-mean white Gaussian processes

$$\begin{aligned} \dot{x} &= Ax + Bu + \bar{B}d, \quad & x \in \Re^n, u \in \Re^k, d \in \Re^q \\ y &= Cx + n, & y \in \Re^m \\ z &= Gx + Hu, & z \in \Re^l \end{aligned} \tag{4.54}$$

The optimal feedback controller designed by LQR can be combined with an LQG state estimator to create an *LQG/LQR output feedback controller* of the following form

$$\begin{aligned} u &= -K\hat{x} \\ \dot{\hat{x}} &= (A - LC)\hat{x} + Bu + Ly \\ &= (A - LC - BK)\hat{x} + Ly \end{aligned} \tag{4.55}$$

Since LQR guarantees that $(A-BK)$ is a stability matrix, and LQG guarantees that $(A - LC)$ is a stability matrix, the separation principal guarantees from 4.4 that the resulting closed loop controller is asymptotical stable.

Chapter 5

STABILITY OF THE TOBIT KALMAN FILTER

By leveraging the basic concepts from of the previous chapters it is shown under what conditions the Tobit Kalman filter is a stable estimator for censored data. Behavior of the Tobit Kalman filter as a state observer in both the homogeneous and non-homogeneous case is explored, and it is shown that given certain conditions exponential and BIBO stability can be recovered, despite the presence of censored regions. The Jacobian of a Tobit Kalman observer is derived and it's implications discussed.

5.1 Defining the Tobit State Space

Consider the following homogeneous DLTI system, which is right censored at threshold T :

$$\begin{aligned} \mathbf{x_{k+1}} &= \mathbf{A x_k} + \mathbf{w_k} \\ \mathbf{y_k^*} &= \mathbf{C x_k} + \mathbf{n_k} \\ \mathbf{y_k} &= h(x_k) = \begin{cases} \mathbf{y_k^*}, & \mathbf{y_k^*} \leq \mathbf{T} \\ \mathbf{T}, & \mathbf{y_k^*} > \mathbf{T} \end{cases} \end{aligned} \tag{5.1}$$

with TKF observer as shown in section 3.3 :

$$\begin{aligned} &\mathbf{\hat{x}_{k+1}} = \mathbf{A\hat{x}_k} + \mathbf{L}(\mathbf{y_k} - \mathbf{E}[\mathbf{\hat{y}_k}]) \\ &\mathbf{E}[\mathbf{\hat{y}_k}] = \boldsymbol{\Phi}\left(\tfrac{\mathbf{T}-\mathbf{C\hat{x}_k}}{\sigma}\right)\left[\mathbf{C\hat{x}_k} - \sigma\lambda\left(\tfrac{(\mathbf{T}-\mathbf{C\hat{x}_k})}{\sigma}\right)\right] + \left(\mathbf{1} - \boldsymbol{\Phi}\left(\tfrac{\mathbf{T}-\mathbf{C\hat{x}_k}}{\sigma}\right)\right)\mathbf{T} \end{aligned} \tag{5.2}$$

At any time k, the expectation of the true measurement can be defined as

$$\mathbf{E}[\mathbf{y_k}] = \mathbf{\Phi}\left(\tfrac{\mathbf{T}-\mathbf{C}\mathbf{x_k}}{\sigma}\right)\left[\mathbf{C}\mathbf{x_k} - \sigma\lambda\left(\tfrac{\mathbf{T}-\mathbf{C}\mathbf{x_k}}{\sigma}\right)\right] + \left(\mathbf{1} - \mathbf{\Phi}\left(\tfrac{\mathbf{T}-\mathbf{C}\mathbf{x_k}}{\sigma}\right)\right)\mathbf{T} \tag{5.3}$$

For the purposes of cleaner notion, define the following as

$$\begin{aligned} \gamma &= \Phi\left(\tfrac{T-Cx_k}{\sigma}\right) \\ \lambda &= \lambda\left(\tfrac{T-Cx_k}{\sigma}\right) \\ \hat{\gamma} &= \Phi\left(\tfrac{T-C\hat{x}_k}{\sigma}\right) \\ \hat{\lambda} &= \lambda\left(\tfrac{T-C\hat{x}_k}{\sigma}\right) \end{aligned} \tag{5.4}$$

Here, γ represents the probability of true measurement being uncensored, λ is the Inverse Mills Ratio of the true state, $\hat{\gamma}$ is probability of the expected measurement being uncensored, and $\hat{\lambda}$ is the inverse mills ratio of the state estimate. Using these definitions, the following relation can be found

$$\begin{aligned} \mathbf{E}[\mathbf{y_k}] &= \gamma(\mathbf{C}\mathbf{x_k} - \sigma\lambda) + (\mathbf{1} - \gamma)\mathbf{T} \\ \mathbf{E}[\hat{\mathbf{y}}_\mathbf{k}] &= \hat{\gamma}(\mathbf{C}\hat{\mathbf{x}}_\mathbf{k} - \sigma\hat{\lambda}) + (\mathbf{1} - \hat{\gamma})\mathbf{T} \\ \mathbf{E}[\mathbf{L}(\mathbf{y_k} - \hat{\mathbf{y}}_\mathbf{k})] &= \mathbf{L}\left([\gamma(\mathbf{C}\mathbf{x_k} - \sigma\lambda) + (\mathbf{1} - \gamma)\mathbf{T}] - \left[\hat{\gamma}(\mathbf{C}\hat{\mathbf{x}}_\mathbf{k} - \sigma\hat{\lambda}) + (\mathbf{1} - \hat{\gamma})\mathbf{T}\right]\right) \\ &= \mathbf{L}\left(\gamma\mathbf{C}\mathbf{x_k} - \hat{\gamma}\mathbf{C}\hat{\mathbf{x}}_\mathbf{k} - \gamma\sigma\lambda + \hat{\gamma}\sigma\hat{\lambda} - \gamma\mathbf{T} + \hat{\gamma}\mathbf{T}\right) \end{aligned} \tag{5.5}$$

Therefore 5.2 can be re-written as

$$\hat{\mathbf{x}}_\mathbf{k+1} = \mathbf{A}\hat{\mathbf{x}}_\mathbf{k} + \mathbf{L}\left(\gamma\mathbf{C}\mathbf{x_k} - \hat{\gamma}\mathbf{C}\hat{\mathbf{x}}_\mathbf{k} - \gamma\sigma\lambda + \hat{\gamma}\sigma\hat{\lambda} - \gamma\mathbf{T} + \hat{\gamma}\mathbf{T}\right) \tag{5.6}$$

Re-arranging terms and grouping 5.6 with 5.1 results in the following state-space description of the DLTI system with TKF observer

$$\begin{bmatrix} \dot{x} \\ \dot{\hat{x}} \end{bmatrix} = \begin{bmatrix} A & 0 \\ L\gamma C & A - L\hat{\gamma}C \end{bmatrix} \begin{bmatrix} x \\ \hat{x} \end{bmatrix} + \begin{bmatrix} 0 \\ L\left(\sigma\left(-\gamma\lambda + \hat{\gamma}\hat{\lambda}\right) - (\gamma + \hat{\gamma})\, T\right) \end{bmatrix} \tag{5.7}$$

5.1.1 Effect of the Censoring Limit on the Tobit Kalman Filter

The formulation of 5.7 shows that for open-ended censoring the TKF is inherently a non-linear *time varying* observer, even though the underlying system model is time-invariant. Regardless of the value of x, terms $\hat{\gamma}$ and $\hat{\lambda}$ change in value as $\hat{x}$ evolves. Further illuminated by this formulation however is effect of censoring limit T as it is moved from one extreme to the other, summarized below in table 5.1.

$T \to \infty$		$T \to -\infty$	
$\gamma, \hat{\gamma}$	$\to 1$	$\gamma, \hat{\gamma}$	$\to 0$
$\lambda, \hat{\lambda}$	$\to 0$	$\lambda, \hat{\lambda}$	$\to \infty$
$\mathbf{\hat{x}_{k+1}}$	$\to \mathbf{A\hat{x}_k} + \mathbf{L}\left(\mathbf{Cx} - \mathbf{C\hat{x}_k}\right)$	$\mathbf{\hat{x}_{k+1}}$	$\to \mathbf{A\hat{x}_k}$

Table 5.1: The effecting of right handed censoring limit T on 5.7

The intuitive notion is reinforced that as censoring limit T is increased to ∞ (the no censoring case) then the TKF reduces to the standard minimum energy estimator given by the Kalman filter. In contrast, as censoring limit T is lowered to $-\infty$ (the all-censored case), then the TKF reduces to the open-loop estimator.

As the true state and state observer move deep into the censoring region the TKF observer seemlessly devolves into an open-loop predictor, as defined in 4.27. This is not unexpected. The presence of open-ended censoring regions inherently presents the possibility that the system may move into a region far away from the uncensored region, relative to the noise distributions of Q and R. In such regions, the probability of censoring is extremely high and the censoring value T is repeatedly returned as the measurement. Essentially, no new information is presented to the filter, as the censoring limit is predicted as a measurement and is then returned as a measurement. The filter is left with no better option than to open-loop predict the evolution of the state x based off the system model. From these results it is proposed that if the system to be estimated is open-loop stable, that is A is a stability matrix, then the resulting TKF observer is stable regardless of the level of censoring. The TKF does no worse than an open-loop predictor, and when both censored and uncensored measurements are returned, it is at least as good, if not better than the standard Kalman filter. However, for systems in which A is not a stability matrix, the stability of the accompanying TKF observer cannot be guaranteed. Although, as shown previously, a Tobit-Kalman gain L may be found which stabilizes the filter when near the censoring limit, if the state evolves to deep into the censoring limit then open-loop prediction occurs, and the state estimate may diverge at this time.

5.1.2 Error Convergence of the Tobit Kalman Filter

Going back to the state estimation error of a discrete time noisy homogeneous system, where $e_k = x_k - \hat{x}_k$, for the standard LQG estimator the following system is defined

$$\begin{aligned} \mathbf{x_{k+1}} &= \mathbf{A x_k + w_k} \\ \mathbf{\hat{x}_{k+1}} &= \mathbf{A\hat{x}_k + L(y_k - E[y_k])} \\ \mathbf{y_k} &= \mathbf{C x_k + v_k} \\ \mathbf{E[y_k]} &= \mathbf{C\hat{x}_k} \end{aligned} \tag{5.8}$$

$$\begin{aligned} \mathbf{e_{k+1}} &= \mathbf{x_{k+1} - \hat{x}_{k+1}} \\ &= \mathbf{(A - LC)e_k + w_k - L v_k} \end{aligned}$$

When censoring is present and a T.KF. estimator is utilized, then by use of 5.3 the system and state estimator may be re-modeled as

$$\begin{aligned}
\mathbf{x_{k+1}} &= \mathbf{A x_k + w_k} \\
\mathbf{\hat{x}_{k+1}} &= \mathbf{A \hat{x}_k + L(y_k - E[y]_k)} \\
\mathbf{y_k} &= \gamma(\mathbf{C x_k} - \sigma\lambda) + (\mathbf{1} - \gamma)\mathbf{T} \\
\mathbf{E[y_k]} &= \hat{\gamma}(\mathbf{C \hat{x}_k} - \sigma\hat{\lambda}) + (\mathbf{1} - \hat{\gamma})\mathbf{T}
\end{aligned} \tag{5.9}$$

The state estimation error dynamics can now be redefined as

$$\begin{aligned}
\mathbf{e_{k+1}} &= \mathbf{A x_k + w_k - A \hat{x}_k - L}\left(\gamma(\mathbf{C x_k} - \sigma\lambda) + (\mathbf{1} - \gamma)\mathbf{T} - (\hat{\gamma}(\mathbf{C \hat{x}_k} - \sigma\hat{\lambda}) - (\mathbf{1} - \hat{\gamma})\mathbf{T})\right) \\
&= (\mathbf{A} - \mathbf{L}\gamma\mathbf{C})\,\mathbf{x_k} - (\mathbf{A} - \mathbf{L}\hat{\gamma}\mathbf{C})\,\mathbf{\hat{x}_k} + \mathbf{L}(\sigma(\gamma\lambda - \hat{\gamma}\hat{\lambda}) + (\gamma - \hat{\gamma})\mathbf{T}) + \mathbf{w_k}
\end{aligned} \tag{5.10}$$

Recall that, by 5.5, the definition of γ and λ is given by

$$\begin{aligned}
&\gamma = \Phi\left(\tfrac{T - Cx_k}{\sigma}\right) \\
&\hat{\gamma} = \Phi\left(\tfrac{T - C\hat{x}_k}{\sigma}\right) \\
&\lambda = \lambda\left(\tfrac{T - Cx_k}{\sigma}\right) = \frac{\phi\left(\frac{T - Cx_k}{\sigma}\right)}{\Phi\left(\frac{T - Cx_k}{\sigma}\right)} \\
&\hat{\lambda} = \lambda\left(\tfrac{T - C\hat{x}_k}{\sigma}\right) = \frac{\phi\left(\frac{T - C\hat{x}_k}{\sigma}\right)}{\Phi\left(\frac{T - C\hat{x}_k}{\sigma}\right)}
\end{aligned} \tag{5.11}$$

and therefore 5.10 can be re-written as

$$\begin{aligned}
\mathbf{e_{k+1}} &= (\mathbf{A} - \mathbf{L}\gamma\mathbf{C})\,\mathbf{x_k} - (\mathbf{A} - \mathbf{L}\hat{\gamma}\mathbf{C})\,\mathbf{\hat{x}_k} + \mathbf{L}\left(\sigma(\phi(\tfrac{\mathbf{T - C x_k}}{\sigma}) - \phi(\tfrac{\mathbf{T - C \hat{x}_k}}{\sigma})) + (\gamma - \hat{\gamma})\mathbf{T}\right) + \mathbf{w_k} \\
&= (\mathbf{A} - \mathbf{L}\gamma\mathbf{C})\,\mathbf{x_k} - (\mathbf{A} - \mathbf{L}\hat{\gamma}\mathbf{C})\,\mathbf{\hat{x}_k} + \mathbf{L}(\sigma\mathbf{e}_\phi + \mathbf{e}_\gamma\mathbf{T}) + \mathbf{w_k}
\end{aligned} \tag{5.12}$$

where,

$$\begin{aligned}
&e_\phi = \phi\left(\tfrac{T - Cx_k}{\sigma}\right) - \phi\left(\tfrac{T - C\hat{x}_k}{\sigma}\right) \\
&e_\gamma = \Phi\left(\tfrac{T - Cx_k}{\sigma}\right) - \Phi\left(\tfrac{T - C\hat{x}_k}{\sigma}\right)
\end{aligned} \tag{5.13}$$

By substitution of $\hat{x}_k = x_k - e_k$, equation 5.12 can be written entirely in the form of x_k and e_k, and a complete description of the error dynamics is then given by

$$\begin{aligned}\mathbf{e_{k+1}} = & \left(\mathbf{A} - \mathbf{L}\boldsymbol{\Phi}\left(\tfrac{\mathbf{T}-\mathbf{C}\mathbf{x_k}}{\sigma}\right)\mathbf{C}\right)\mathbf{x_k} - \left(\mathbf{A} - \mathbf{L}\boldsymbol{\Phi}\left(\tfrac{\mathbf{T}-\mathbf{C}(\mathbf{x_k}-\mathbf{e_k})}{\sigma}\right)\mathbf{C}\right)(\mathbf{x_k} - \mathbf{e_k}) \\ & + \mathbf{L}\left(\sigma\left(\phi(\tfrac{\mathbf{T}-\mathbf{C}\mathbf{x_k}}{\sigma}) - \phi(\tfrac{\mathbf{T}-\mathbf{C}(\mathbf{x_k}-\mathbf{e_k})}{\sigma})\right) + \left(\boldsymbol{\Phi}(\tfrac{\mathbf{T}-\mathbf{C}\mathbf{x_k}}{\sigma}) - \boldsymbol{\Phi}(\tfrac{\mathbf{T}-\mathbf{C}(\mathbf{x_k}-\mathbf{e_k})}{\sigma})\right)\mathbf{T}\right) + \mathbf{w}\end{aligned} \tag{5.14}$$

The above error dynamics consist of non-linear and state dependent terms of both x and e, including an error injection term β, defined as

$$\begin{aligned}\beta = & \, \sigma\left(\phi(\tfrac{T-Cx_k}{\sigma}) - \phi(\tfrac{T-C(x_k-e_k)}{\sigma})\right) + \left(\Phi(\tfrac{T-Cx_k}{\sigma}) - \Phi(\tfrac{T-C(x_k-e_k)}{\sigma})\right)T \\ = & \, \sigma e_\phi + e_\gamma T\end{aligned} \tag{5.15}$$

Note that $\phi(\cdot)$ is bounded on $[0, \frac{1}{\sigma\sqrt{2\pi}}]$ and $\gamma(\cdot)$ is bounded on $[0,1]$. Therefore e_ϕ is bounded on $[-\frac{1}{\sigma\sqrt{2\pi}}, \frac{1}{\sigma\sqrt{2\pi}}]$ and γ is bounded on $[-1,1]$. Thus β is bounded by $\pm\left(\frac{1}{\sigma\sqrt{2\pi}} + T\right)$. If, under certain conditions, the asymptotic convergence of the above error, combined with the existence of a unique stationary point at $e = 0$, can be found, then the stability of the Tobit Kalman filter as state estimator with censored data will be proven, for said conditions.

Assume a homogeneous system of the form given by 5.8, in which A is Schur stable, then $x_k \to 0$, as $k \to \infty$. Therefore, the error dynamics go to

$$\begin{aligned}\mathbf{e_{k+1}} = & \left(\mathbf{A} - \mathbf{L}\boldsymbol{\Phi}\left(\tfrac{\mathbf{T}+\mathbf{C}\mathbf{e_k}}{\sigma}\right)\mathbf{C}\right)\mathbf{e_k} + \mathbf{L}\left(\sigma\left(\phi(\tfrac{\mathbf{T}}{\sigma}) - \phi(\tfrac{\mathbf{T}+\mathbf{C}\mathbf{e_k}}{\sigma})\right)\right) \\ & + \mathbf{L}\left(\left(\boldsymbol{\Phi}(\tfrac{\mathbf{T}}{\sigma}) - \boldsymbol{\Phi}(\tfrac{\mathbf{T}+\mathbf{C}\mathbf{e_k}}{\sigma})\right)\mathbf{T}\right) + \mathbf{w} \\ = & \left(\mathbf{A} - \mathbf{L}\boldsymbol{\Phi}\left(\tfrac{\mathbf{T}+\mathbf{C}\mathbf{e_k}}{\sigma}\right)\mathbf{C}\right)\mathbf{e_k} + \mathbf{L}\beta + \mathbf{w}\end{aligned} \tag{5.16}$$

The error dynamics have are now in the form of a state dependent difference equation with a bounded injection term and white Gaussian noise. Sufficient conditions for stability of time-varying linear systems of the form

$$u_{k+1} = M_k u_k, \quad k \in \mathbb{N}_0 \tag{5.17}$$

is shown by [13]. Here M_k represents a sequence of matrices with elements in $\mathbb{C}^{(N\times N)}$. The first assumption is that the frozen systems $u_{k+1} = M_n u_k$ are exponentially stable. Then, if $M \in \Sigma_{K,\omega,\Gamma}$ for some $(K, \omega, \Gamma) \in \mathbb{R}_{\geq 1} \times \mathbb{R}_{\geq 0} \times \mathbb{R}_{>0}$, then

$$||u_k|| \leq K^{k-m} e^{-\omega(k-m)} ||u_m|| \;\; \forall (k, m) \in \{\mathbb{N}_0 \times \mathbb{N}_0 | n \geq m\} \tag{5.18}$$

where $\Sigma_{K,\omega,\Gamma}$ is the class of generators defined by

$$\Sigma_{K,\omega,\Gamma} := \left\{ (M_k) \in (\mathbb{C}^{N\times N})^{\mathbb{N}} \;\middle|\; \begin{array}{l} \forall\, k, m \in \mathbb{N}_0 : ||M_k^m|| \leq K e^{-\omega m} \\ \forall\, k, m \in \mathbb{N}_0 : ||M_k - M_m|| \leq L|k - m| \end{array} \right. \tag{5.19}$$

and $(\mathbb{C}^{N\times N})^{\mathbb{N}}$ is the set of all mapping from $\mathbb{N}$ to $\mathbb{C}^{N\times N}$. Considering only the first term of 5.16, and defining

$$A_k = A - L\Phi(\tfrac{T+Ce_k}{\sigma})C \tag{5.20}$$

a system can be defined of the form

$$e_{k+1} = A_k e_k \tag{5.21}$$

The time-varying system matrix of 5.21 is then considered as a special case of the state dependent system matrix of 5.16, in which the set of all possible sequences of A_k can be formed from the set all possible values of $(A - L\Phi\left(\frac{T+Ce_k}{\sigma}\right)C)$. Note again that $\Phi\left(\frac{T+Ce_k}{\sigma}\right)_{m\times m}$ is diagonal, and

$$0 \leq \Phi_{i,i} \leq 1 \quad \forall\, i \in \mathbb{Z} | 1 \leq i \leq m \tag{5.22}$$

That is, each element of Φ is bounded by $[0, 1]$, corresponding to the 100% censored to 0% censored scenarios pertaining to the specified measurement. Thus, the system matrix of 5.20 is well defined for all possible value of e_k, and

$$\forall (e_k)_{k\in\mathbb{Z}}, \;\; A_k \text{ is exponentially stable}$$

Since A is assumed to be Schur stable, and $(A - LC)$ is designed according to the standard Kalman filter and is assumed to be Schur stable as well, then

$$\forall (A_n)_{n\in\mathbb{N}_0} \in \mathbb{C}^{N\times N}, \;\; e_{k+1} = A_n e_k \;\text{ is exponentially stable} \tag{5.23}$$

Therefore all possible frozen time systems of 5.21 are exponentially stable and the first condition for the stability of 5.21 is met. Next it is noted that

$$\forall\, k, m \in \mathbb{N}_0 : ||A_k - A_m|| \leq ||LC|| \leq L|k-m| \tag{5.24}$$

and

$$\forall\, k, m \in \mathbb{N}_0 : ||A_k^m|| \leq ||A^m|| \leq Ke^{-\omega m} \tag{5.25}$$

Therefore, there exists $A \in \Sigma_{K,\omega,\Gamma}$ for some (K, ω, Γ), and sufficient conditions are met for the bound of form 5.18 for all solutions e of 5.21. Thus, it is proven that the first term of 5.16 is bounded, but it remains to show that $e = 0$ is a unique stationary point. First, it is easily shown via direct substitution that $e = 0$ is a stationary point, for

$$\mathbf{e_{k+1}} = 0 = \mathbf{L}\left(\sigma\left(\phi(\tfrac{\mathbf{T}}{\sigma}) - \phi(\tfrac{\mathbf{T}}{\sigma})\right) + \left(\mathbf{\Phi}(\tfrac{\mathbf{T}}{\sigma}) - \mathbf{\Phi}(\tfrac{\mathbf{T}}{\sigma})\right)\mathbf{T}\right) \tag{5.26}$$

where the zero-mean white Gaussian noise term $\mathbf{w}$ has been omitted. If $e = 0$ is not a unique stationary point then, there must exist a solution to the following

$$\mathbf{e}_\infty = \left(\mathbf{A} - \mathbf{L\Phi}\left(\tfrac{\mathbf{T+Ce_\infty}}{\sigma}\right)\mathbf{C}\right)\mathbf{e}_\infty + \mathbf{L}\left(\sigma\left(\phi(\tfrac{\mathbf{T}}{\sigma}) - \phi(\tfrac{\mathbf{T+Ce_\infty}}{\sigma})\right) + \left(\mathbf{\Phi}(\tfrac{\mathbf{T}}{\sigma}) - \mathbf{\Phi}(\tfrac{\mathbf{T+Ce_\infty}}{\sigma})\right)\mathbf{T}\right) \tag{5.27}$$

for which $e_\infty \neq 0$. Re-arranging 5.27 to move the constant terms to the left side, then the same condition can be restated as

$$-\mathbf{L}(\sigma\phi(\tfrac{\mathbf{T}}{\sigma}) + \mathbf{\Phi}(\tfrac{\mathbf{T}}{\sigma})\mathbf{T}) = \left(\mathbf{A} - \mathbf{L\Phi}\left(\tfrac{\mathbf{T+Ce_\infty}}{\sigma}\right)\mathbf{C} - \mathbf{I}\right)\mathbf{e}_\infty - \mathbf{L}\left(\sigma\phi(\tfrac{\mathbf{T+Ce_\infty}}{\sigma}) - \mathbf{\Phi}(\tfrac{\mathbf{T+Ce_\infty}}{\sigma})\mathbf{T}\right) \tag{5.28}$$

Therefore, if for a fixed level of censoring T, fixed measurement variance σ, Shur stable system matrix A, fixed gain L, and the above condition only being satisfied for $e_\infty = 0$, all sufficient conditions for the convergence of e to a unique stationary point defined by $e = 0$ are met. Thus, the Tobit Kalman filter estimator for censored data meeting these conditions is an asymptotically stable unbiased estimator.

However, the use of a fixed L in 5.28 may not guarantee that $e = 0$ is the only solution. In this case, it is possible for the error dynamics to converge to a non-zero stationary point, and the filter no longer can be said to be unbiased. The error dynamics still converge, as shown, and thus the filter remains stable, although the level of bias may limit its usefulness. For simplicity, consider the scalar case in which $C = I$, $T = 0$, and $\sigma = 1$. It is still assumed that A is Shur and L is designed to be positive semi-definite and $A - LC$ is Shur stable. Condition 5.28 then simplifies to

$$\begin{aligned} -L\phi(0) &= \left(A - L\Phi\left(e_\infty\right) - 1\right) e_\infty - L\phi(e_\infty) \\ -L(\phi(0) - \phi(e_\infty)) &= \left(A - L\Phi\left(e_\infty\right) - 1\right) e_\infty \\ -L\phi_d &= \left(A - L\Phi\left(e_\infty\right) - 1\right) e_\infty \end{aligned} \tag{5.29}$$

For

$$\phi_d = \phi(0) - \phi(e_\infty) \tag{5.30}$$

Note that, $\forall e_\infty$,

$$\begin{aligned} \phi(0) = \tfrac{1}{\sqrt{2\pi}} \geq \phi_d &\geq 0 \\ A &< 1 \\ L &\geq 0 \\ 0 \leq \Phi(e_\infty) &\leq 1 \\ \left(A - L\Phi\left(e_\infty\right) - 1\right) &< 0 \end{aligned} \tag{5.31}$$

Therefore, for a non-zero stationary point to exist, there must exist a non-zero e_∞ which is a solution to 5.29 and meeting the conditions of 5.31. From 5.31 it is apparent that $-L\phi_d < 0$, and since $\left(A - L\Phi\left(e_\infty\right) - 1\right) < 0$, then for 5.29 to hold it must be that

$$e_\infty \geq 0 \tag{5.32}$$

Therefore, if a solution $e_\infty \neq 0$ can be found satisfying the given conditions, then at the very least this bias must be of a known sign. Assuming that $e_\infty > 0$, then

$$\begin{aligned} x_\infty - \hat{x}_\infty &> 0 \\ 0 - \hat{x}_\infty &> 0 \end{aligned}$$

and therefore

$$\hat{x}_\infty < 0 \tag{5.33}$$

That is, for the given example, a biased solution will always result in a state estimate that is below the true state and in the uncensored region. Furthermore, since $e_\infty \geq 0$, and therefore $.5 \leq \Phi(e_\infty) \leq 1$, one can see that

$$\begin{aligned} -L\phi(0) &\leq -L\phi_d \\ -L\phi(0) &\leq (A - L\Phi(e_\infty) - 1)e_\infty \\ -L\phi(0) &\leq -||A - L\Phi(e_\infty) - 1||e_\infty \end{aligned} \tag{5.34}$$

must be satisfied. On the contrary, if $\forall e_\infty$,

$$\begin{aligned} -||A - L\Phi(e_\infty) - 1||e_\infty &< -L\phi(0) \\ -||A - L\tfrac{1}{2} - 1||e_\infty &< -L\phi(0) \end{aligned} \tag{5.35}$$

then the only solution to 5.34 is $e_\infty = 0$, and the filter is unbiased.

The use of a fixed gain L in a filter for censored data is a sub-optimal design. Consider instead of the use of the time-varying optimal Tobit gain instead of a fixed gain L. This places a secondary condition on 5.27, given by,

$$\mathbf{L_{k+1}} = \mathbf{L_k} \tag{5.36}$$

that is, a true stationary point can only be reached if gain L has converged. As defined previously in 3.40 and 3.39, and with the change of variable $\hat{x} = -e$, the optimal Tobit gain at each step is defined by

$$\begin{aligned} \mathbf{E}(\mathbf{p_k}) &= \mathbf{\Phi}(\tfrac{\mathbf{T+Ce}}{\sigma}) \\ \mathbf{L_k} &= \mathbf{\Psi_{k|k-1}C^T E(p_k)^T (E(p_k) C \Psi_{k|k-1} C^T E(p_k)^T + E(p_k v_k v_k^T p_k)^T)^{-1}} \end{aligned} \tag{5.37}$$

which only has a solution to 5.36 should $L_k = 0$ or $E(p_{k+1}) = E(p_k)$. Should $L_k \neq 0$, and $e = 0$, then $E(p_k) = \Phi(\frac{T}{\sigma}) = E(p_{k+1})$, $\hat{x} = 0$, and all Tobit Parameters which are a function of $\hat{x}$ converge, and gain L and covariance P converge to their respective steady state values according to given level of censoring at the origin, as discussed later. Thus $e = 0$ is a stationary point. Should $L_k = 0$, the expectation of being uncensored must be identically zero, the error injection term β of 5.16 is removed, and because A is Shur stable e continues to converge.

It has been shown that the error dynamics of a Tobit Kalman filter estimator, with an inherently Shur stable system matrix and fixed gain, always converges, despite the level of censoring. Furthermore, is has been shown that $e = 0$ is a stationary point of the system, however other stationary points may exist, and conditions for their existence have been given. Likewise, $e = 0$ is also a stationary point for systems with a time-varying Tobit Kalman gain, although tt has yet to be shown however that $e = 0$ is a unique stationary point, and that this point is locally or globally stable. Strong statements with regards to marginally stable and or unstable systems have not yet been completed. In essence, under large degrees of censoring in which approximately $T < Cx - 6\sigma$, nearly all measurements become censored, open-loop prediction ensues, and the Tobit estimator inherits the properties of the underlying system model. Although an unstable system may have a local region region of attraction, especially should the censoring limit be taken to an exceedingly safe limit, it cannot be said to be stable. There remains the finite probability that a state trajectory can be generated which may drive the state and state estimate deep into censoring, at which time the system model no longer permits accurate open-loop estimation.

5.2 Examples of Estimator Convergence Under Differing Initial Conditions

Examples of estimator convergence for the class of stable homogeneous systems, despite the presence of censoring, is shown in the following examples. Useful notions with regard to the behavior of the estimator error dynamics in relation to the initial conditions of the state and state estimate can be gleamed by considering the following possible starting scenarios.

Scenario 1. Completely Uncensored

In this scenario the value of $T \to \infty$ and the system reverts to a completely uncensored case. As seen in previous sections this results in convergence of the TKF estimator to a completely linear and symptomatically stable observer. This can be verified w.r.t. 5.74 by noting that as $T \to \infty$, then

$$\gamma, \hat{\gamma} \to 1$$
$$\lambda, \hat{\lambda} \to 0$$
$$e_\gamma, e_\lambda \to 0$$

and thus the resulting error dynamics go to

$$\mathbf{e_{k+1}} = (\mathbf{A} - \mathbf{LC})\mathbf{e_k} + \mathbf{w}$$

Scenario 2. Completely Censored

Similar to scenario 1, except in the opposing extreme, the value of $T \to -\infty$ and the system reverts to a completely censored case. As seen in previous sections this results in convergence of the TKF estimator to an open loop linear observer. Stability in this case is entirely dependent on the system matrix A. This can be verified w.r.t. 5.74 by noting that as $T \to -\infty$, then

$$\gamma, \hat{\gamma} \to 0$$
$$\lambda, \hat{\lambda} \to \infty$$

and thus the resulting error dynamics go to

$$\mathbf{e_{k+1}} = \mathbf{A}\mathbf{e_k} + \mathbf{w}$$

An example response of the estimator when the state and state estimator are both censored is shown in figure 5.1.

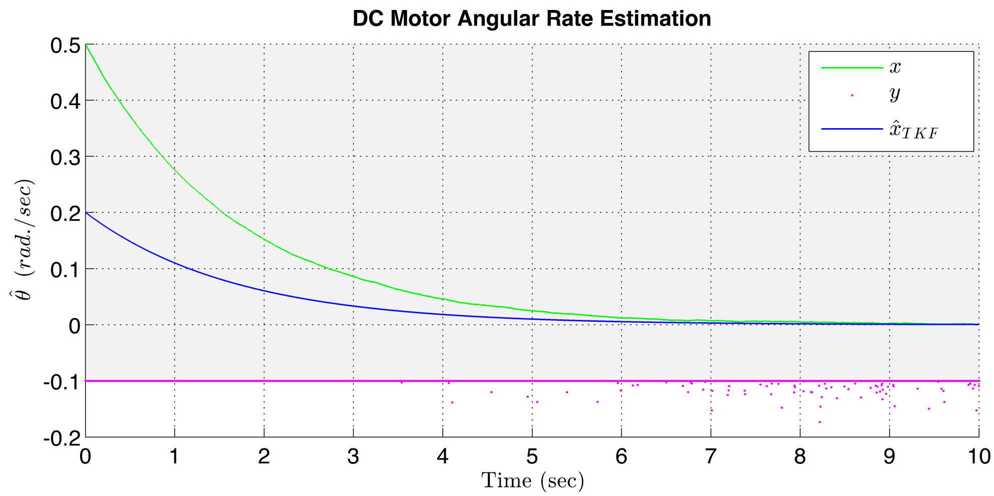

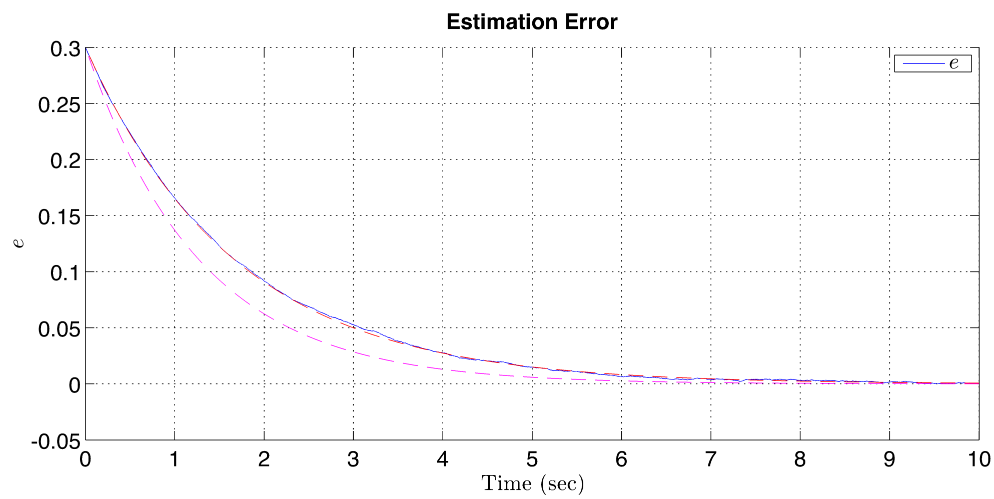

Figure 5.1: Scenario 2. Initial condition response when the state and state estimator are nearly completely censored. The estimator acts as an open-loop predictor, and the error converges.

The bounds of the error convergence are represented by the magenta and red dashed lines. The lower bound of the estimator error, represented in magenta, is given by the convergence of the linear system given that no censoring is present. As given by scenario one, this represents the "best-case" scenario and the dynamics converge to that of the linear LQG estimator. The upper bound of the estimator error, represented in red, is given by the convergence of the linear system given by open-loop prediction. This is the "worst-case" of scenario two, in which nearly all measurements are censored. As expected, when the the state and state estimator start deep in the censored region, the estimation error follows directly on top of the open-loop error bound. Since A is a stability matrix the error converges. However, if A is not a stability matrix, then the upper error bound does not converge, and may diverge.

Scenario 3. True State Uncensored, Estimate Censored

In this more interesting scenario there is now an explicit initial error between state and state estimate. For right handed censoring, if the true state is uncensored and the state estimate is censored, then $\hat{x} > x$, and $\lambda \to 0$. Therefore, $e_\lambda = -\hat{\lambda}$, and

$$\begin{aligned} \gamma &\to 1 \\ \hat{\gamma} &\to 0 \\ e_\gamma &\to 1 \end{aligned}$$

An example response of the estimator for this scenario is shown in figure 5.2.

Contrary to scenario two, in which the error dynamics followed that of the upper error bound, the error dynamics of scenario three follow closely to that of the lower error bound. The uncensored true state results in many uncensored measurements, and the state estimator uses this information to converge to the true state faster than that of scenario two.

Scenario 4. True State Censored, Estimate Uncensored

The opposite to scenario three, whereby the true state is censored and the state estimate is uncensored. Due to right censoring, such a scenario enforces that $\hat{x} < x$, $\hat{\lambda} \to 0$, and therefore $e_\lambda = \lambda$. Since the true state is censored, the censoring limit T is repeatedly returned as a measurement until x reaches near enough to the censoring limit to generate uncensored measurements. Until this point little useful information is presented to the filter, although the lack of uncensored measurements indicates that the true state is above the censoring limit and proportionally far enough away such that

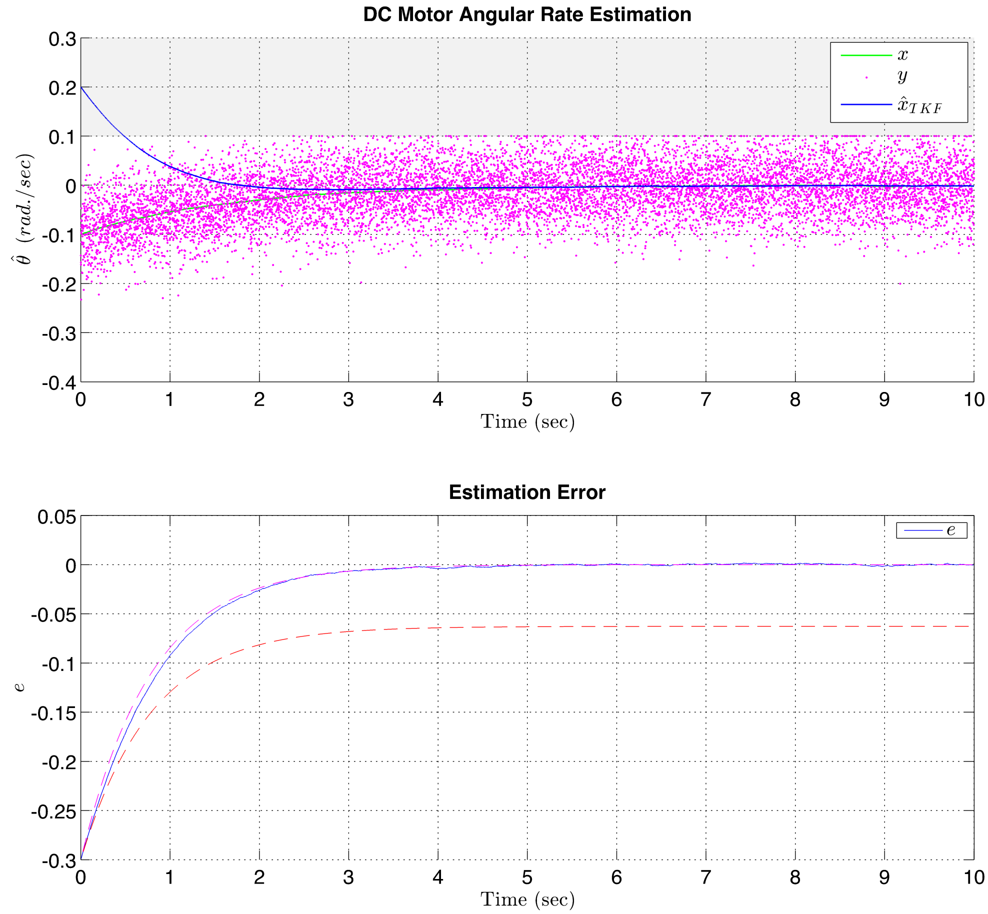

Figure 5.2: Scenario 3. Initial condition response when the true state is uncensored and state estimate is censored.

the noise distribution described by σ is not significant enough to generate uncensored measurements.

$$\gamma \to 0$$
$$\hat{\gamma} \to 1$$
$$e_\gamma \to -1$$

An example response of the estimator for this scenario is shown in figure 5.3. Note that as the true state becomes uncensored, the error dynamics move seamlessly to that of the lower convergence bound as more uncensored measurements become

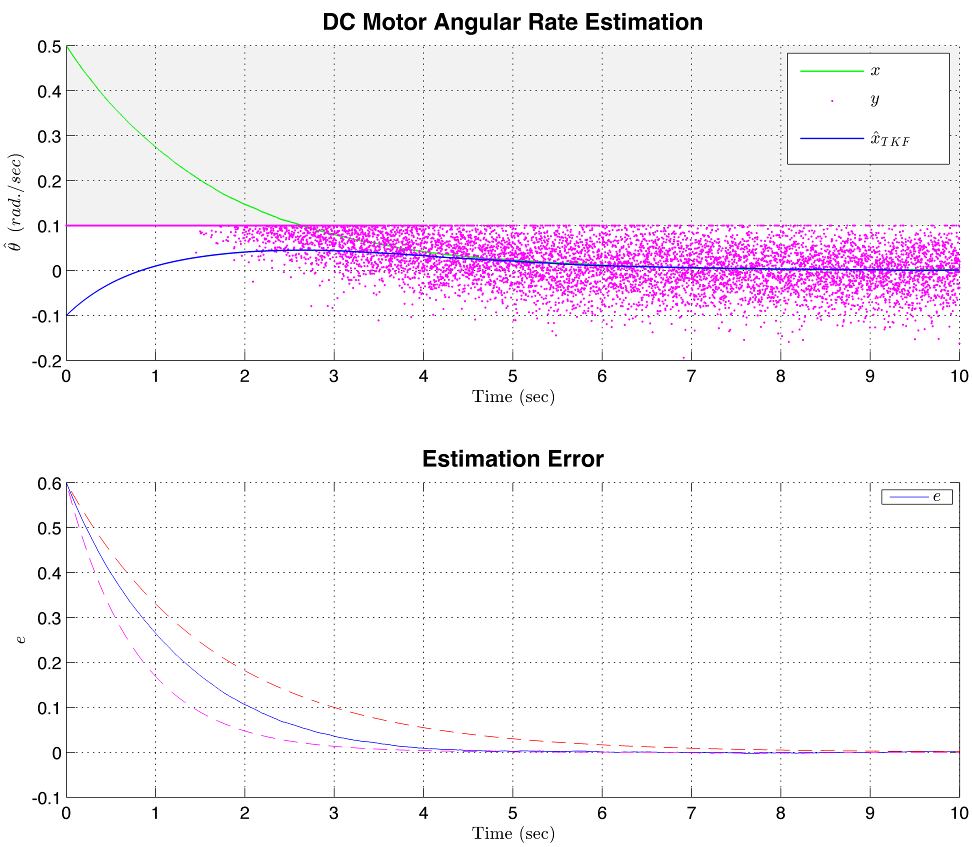

Figure 5.3: Scenario 4. Initial condition response when the true state is censored and state estimate is uncensored.

available. Performance can be improved by using a time-varying TKF gain, with a high initial error covariance which accurately reflects the uncertainty inherent in the initial estimate error.

5.3 The Effect of the Censoring on Internal Stability

Section 4.2.1 discussed the stability of homogeneous systems with respect to initial conditions. It was found that for LTI systems in which A is a stability matrix then the solution for $x(t)$ converges to the origin in finite time, despite the value of $x(0)$, and therefore the system is said to be globally exponentially stable. This result was extended to locally linearized systems in section 4.2.2 by leveraging the system

Jacobian. The effect of censoring on these two results is explained in the following section.

First consider again the following state-space representation of a homogenous system with TKF observer,

$$\begin{bmatrix} \dot{x} \\ \dot{\hat{x}} \end{bmatrix} = \begin{bmatrix} A & 0 \\ L\gamma C & A - L\hat{\gamma}C \end{bmatrix} \begin{bmatrix} x \\ \hat{x} \end{bmatrix} + \begin{bmatrix} 0 \\ L\left(\sigma\left(-\gamma\lambda + \hat{\gamma}\hat{\lambda}\right) - \left(\gamma + \hat{\gamma}\right)T\right) \end{bmatrix} \tag{5.38}$$

As explained previously, increasing levels of censoring force the above formulation into a non-linear relationship due to the presence censoring dependent terms γ and λ, representing the probability of censoring and inverse mills ratio, respectively. Therefore in order to understand the effect of censoring level T on the internal stability of 5.38, the system must first be linearized about an equilibrium point. Then, as shown in section 4.2.2, the system's stability with regards to perturbations away from the equilibrium point can analyzed.

5.3.1 Calculation of the Tobit Jacobian

As a motivating example, first consider the uncensored system LTI system given by

$$\begin{bmatrix} \dot{x} \\ \dot{\hat{x}} \end{bmatrix} = \begin{bmatrix} A & 0 \\ LC & A - LC \end{bmatrix} \begin{bmatrix} x \\ \hat{x} \end{bmatrix} \tag{5.39}$$

Defining state $\mathbf{x} = [x', \hat{x}']'$, then 5.39 has equilibrium point $\mathbf{x^{eq}} = \mathbf{0}$, and can be rewritten in the form of

$$\begin{aligned} \dot{\mathbf{x}} &= f_1(x, \hat{x}) = \mathbf{Ax} \\ \dot{\hat{\mathbf{x}}} &= f_2(x, \hat{x}) = (\mathbf{A} - \mathbf{LC})\hat{\mathbf{x}} + \mathbf{LCx} \end{aligned} \tag{5.40}$$

Then the jacobian is defined as

$$\mathbf{J} \quad = \quad \begin{bmatrix} \frac{\partial f_1}{\partial x} & \frac{\partial f_1}{\partial \hat{x}} \\ \frac{\partial f_2}{\partial x} & \frac{\partial f_2}{\partial \hat{x}} \end{bmatrix} \tag{5.41}$$

Since 5.39 is already a linear system, this results in a trivial Jacobian $\mathbf{J}$ equal to the original system matrix. As shown in section 4.2, the behavior of the system about equilibrium point $\mathbf{x^{eq}}$ can be described by

$$\dot{\delta \mathbf{x}} = \mathbf{J}\delta\mathbf{x} \tag{5.42}$$

where $\delta\mathbf{x} = \mathbf{x} - \mathbf{x^{eq}}$. Here, $\mathbf{J}$ is independent of $\mathbf{x^{eq}}$, and assuming that $\mathbf{J}$ is a stability matrix, then $\mathbf{x}$ will not diverge from the equilibrium point.

The question however, is what happens to an otherwise innocuous system such as this when a censored region is introduced? To understand the effect of censoring on a system such as 5.39, use the system as shown in 5.38. As mentioned in section 5.1.1, this system is inherently non-linear.

With right-handed censoring, the system is now better modeled as

$$\begin{aligned} \dot{\mathbf{x}} &= \mathbf{A}\mathbf{x} \\ \dot{\hat{\mathbf{x}}} &= \mathbf{A}\hat{\mathbf{x}} + \mathbf{L}(-\hat{\gamma}\mathbf{C}\hat{\mathbf{x}} + \gamma\mathbf{C}\mathbf{x} - \gamma\sigma\lambda + \hat{\gamma}\sigma\hat{\lambda} - \gamma\mathbf{T} + \hat{\gamma}\mathbf{T}) \end{aligned} \tag{5.43}$$

so

$$\begin{aligned} \dot{\mathbf{x}} &= f_1(x, \hat{x}) \\ \dot{\hat{\mathbf{x}}} &= f_2(x, \hat{x}) \end{aligned} \tag{5.44}$$

with

$$\begin{aligned} f_1(x, \hat{x}) &= \mathbf{A}\mathbf{x} \\ f_2(x, \hat{x}) &= \mathbf{A}\hat{\mathbf{x}} - \mathbf{L}\hat{\gamma}\mathbf{C}\hat{\mathbf{x}} + \mathbf{L}\gamma\mathbf{C}\mathbf{x} - \mathbf{L}\gamma\sigma\lambda + \mathbf{L}\hat{\gamma}\sigma\hat{\lambda} - \mathbf{L}\gamma\mathbf{T} + \mathbf{L}\hat{\gamma}\mathbf{T} \end{aligned} \tag{5.45}$$

The jacobian is then defined as in 5.41, with

$$
\begin{aligned}
\frac{\partial f_1}{\partial x} &= A \\
\frac{\partial f_1}{\partial \hat{x}} &= 0 \\
\frac{\partial f_2}{\partial x} &= \left[L\gamma\left(\tfrac{\partial}{\partial x}Cx\right) + \left(\tfrac{\partial}{\partial x}L\gamma\right)Cx\right] - \left[L\gamma\sigma\left(\tfrac{\partial}{\partial x}\lambda\right) + L\left(\tfrac{\partial}{\partial x}\gamma\right)\sigma\lambda\right] - L\left(\tfrac{\partial}{\partial x}\gamma\right)T \\
&= L\gamma C + L\phi_x Cx - L\gamma\sigma\left((-\tfrac{1}{\sigma^2})(C(Cx-T))\lambda - \lambda^2\right) - L\phi_x\sigma\lambda - L\phi_x T \\
&= L\left(\phi_x\left(Cx - \sigma\lambda - T\right) + \gamma\left(C + \tfrac{1}{\sigma}\left(C\left(Cx-T\right)\right)\lambda + \sigma\lambda^2\right)\right) \\
\frac{\partial f_2}{\partial \hat{x}} &= A + \left[-L\hat{\gamma}\left(\tfrac{\partial}{\partial \hat{x}}C\hat{x}\right) + -L\left(\tfrac{\partial}{\partial \hat{x}}\hat{\gamma}\right)C\hat{x}\right] + \left[L\hat{\gamma}\sigma\left(\tfrac{\partial}{\partial \hat{x}}\hat{\lambda}\right) + L\left(\tfrac{\partial}{\partial \hat{x}}\hat{\gamma}\right)\sigma\hat{\lambda}\right] + L\left(\tfrac{\partial}{\partial \hat{x}}\hat{\gamma}\right)T \\
&= A - L\hat{\gamma}C - L\phi_{\hat{x}}C\hat{x} + L\hat{\gamma}\sigma\left((-\tfrac{1}{\sigma^2})(C(C\hat{x}-T))\hat{\lambda} - \hat{\lambda}^2\right) + L\phi_{\hat{x}}\sigma\hat{\lambda} + L\phi_{\hat{x}}T \\
&= A - L\left(\phi_{\hat{x}}\left(C\hat{x} - \sigma\hat{\lambda} - T\right) + \hat{\gamma}\left(C + \tfrac{1}{\sigma}\left(C\left(C\hat{x}-T\right)\right)\hat{\lambda} + \sigma\hat{\lambda}^2\right)\right)
\end{aligned}
\tag{5.46}
$$

Now it is shown that,

$$
\mathbf{J} = \begin{bmatrix} A & 0 \\ L\left(\phi_x\left(Cx - \sigma\lambda - T\right) + \gamma\left(C + \frac{1}{\sigma}\left(C\left(Cx-T\right)\right)\lambda + \sigma\lambda^2\right)\right) & A - L\left(\phi_{\hat{x}}\left(C\hat{x} - \sigma\hat{\lambda} - T\right) + \hat{\gamma}\left(C + \frac{1}{\sigma}\left(C\left(C\hat{x}-T\right)\right)\hat{\lambda} + \sigma\hat{\lambda}^2\right)\right) \end{bmatrix}
$$

And thus the local linearization is now

$$
\dot{\delta\mathbf{x}} = \mathbf{J}\delta\mathbf{x} \tag{5.48}
$$

As shown in section 4.2.2, if this local linearization is exponentially stable, then $\mathbf{J}$ must be Hurwitz, and there exists a region about the equilibrium point in which $x(t)$ does not diverge from the equilibrium point for all time. For $\mathbf{J}$ to be Hurwitz one needs $\Re(\lambda) < 0$ for all λ, where λ are the eigenvalues of $\mathbf{J}$; given by the solution to

$$
\begin{vmatrix} \frac{\partial f_1}{\partial x} - \lambda I & \frac{\partial f_1}{\partial \hat{x}} \\ \frac{\partial f_2}{\partial x} & \frac{\partial f_2}{\partial \hat{x}} - \lambda I \end{vmatrix} = 0 \tag{5.49}
$$

5.3.2 Calculation of the Tobit Error Jacobian

Calculation of the Jacobian for the state estimator error dynamics follows from that of section 5.3.1, except now the system as given in section 5.1.2 is utilized, in which

$$
\begin{aligned}
\mathbf{x} &= \mathbf{Ax} + \mathbf{w} \\
\dot{\hat{\mathbf{x}}} &= \mathbf{A}\hat{\mathbf{x}} + \mathbf{L}(\mathbf{y} - \hat{\mathbf{y}}) \\
\mathbf{y} &= \gamma(\mathbf{Cx} - \sigma\lambda) + (\mathbf{1} - \gamma)\mathbf{T} \\
\hat{\mathbf{y}} &= \hat{\gamma}(\mathbf{C}\hat{\mathbf{x}} - \sigma\hat{\lambda}) + (\mathbf{1} - \hat{\gamma})\mathbf{T}
\end{aligned}
$$

$$
\begin{aligned}
\dot{\mathbf{e}} &= \dot{\mathbf{x}} - \dot{\hat{\mathbf{x}}} \\
\dot{\mathbf{e}} &= \mathbf{Ax} + \mathbf{w} - \mathbf{A}\hat{\mathbf{x}} - \mathbf{L}\Big(\gamma(\mathbf{Cx} - \sigma\lambda) + (\mathbf{1} - \gamma)\mathbf{T} - (\hat{\gamma}(\mathbf{C}\hat{\mathbf{x}} - \sigma\hat{\lambda}) + (\mathbf{1} - \hat{\gamma})\mathbf{T})\Big) \\
&= (\mathbf{A} - \mathbf{L}\gamma\mathbf{C})\,\mathbf{x} - (\mathbf{A} - \mathbf{L}\hat{\gamma}\mathbf{C})\,\hat{\mathbf{x}} + \mathbf{L}\sigma(\gamma\lambda - \hat{\gamma}\hat{\lambda} + (\gamma - \hat{\gamma})\mathbf{T}) + \mathbf{w}
\end{aligned}
\tag{5.50}
$$

A new system is then defined in which $x = [x' \;\; e']'$, So that

$$
\begin{aligned}
\dot{\mathbf{x}} &= f_1(x, e) \\
\dot{\hat{\mathbf{e}}} &= f_2(x, e)
\end{aligned}
\tag{5.51}
$$

with

$$
\begin{aligned}
f_1(x, e) &= \mathbf{Ax} + \mathbf{w} \\
f_2(x, e) &= \mathbf{Ae} - \mathbf{L}\gamma\mathbf{Cx} + \mathbf{L}\hat{\gamma}\mathbf{Cx} - \mathbf{L}\hat{\gamma}\mathbf{Ce} + \mathbf{L}\gamma\sigma\lambda - \mathbf{L}\hat{\gamma}\sigma\hat{\lambda} + \mathbf{L}\gamma\mathbf{T} - \mathbf{L}\hat{\gamma}\mathbf{T} + \mathbf{w}
\end{aligned}
\tag{5.52}
$$

and the Jacobian is defined as

$$
\mathbf{J} = \begin{bmatrix} \frac{\partial f_1}{\partial x} & \frac{\partial f_1}{\partial e} \\ \frac{\partial f_2}{\partial x} & \frac{\partial f_2}{\partial e} \end{bmatrix}
\tag{5.53}
$$

with

$$
\begin{aligned}
\frac{\partial f_1}{\partial x} &= A \\
\frac{\partial f_1}{\partial e} &= 0 \\
\frac{\partial f_2}{\partial x} &= -\left[L\gamma\left(\frac{\partial}{\partial x}Cx\right) + \left(\frac{\partial}{\partial x}L\gamma\right)Cx\right] + \left[L\hat{\gamma}\left(\frac{\partial}{\partial x}Cx\right) + \left(\frac{\partial}{\partial x}L\hat{\gamma}\right)Cx\right] \\
&\quad - \left[L\hat{\gamma}\left(\frac{\partial}{\partial x}Ce\right) + \left(\frac{\partial}{\partial x}L\hat{\gamma}\right)Ce\right] + \left[L\gamma\left(\frac{\partial}{\partial x}\sigma\lambda\right) + \left(\frac{\partial}{\partial x}L\gamma\right)\sigma\lambda\right] \\
&\quad - \left[L\hat{\gamma}\left(\frac{\partial}{\partial x}\sigma\hat{\lambda}\right) + \left(\frac{\partial}{\partial x}L\hat{\gamma}\right)\sigma\hat{\lambda}\right] + L\left(\frac{\partial}{\partial x}\gamma\right)T - L\left(\frac{\partial}{\partial x}\hat{\gamma}\right)T \\
\frac{\partial f_2}{\partial e} &= A + \left[L\left(\frac{\partial\hat{\gamma}}{\partial e}\right)Cx\right] - \left[L\hat{\gamma}C + L\left(\frac{\partial\hat{\gamma}}{\partial e}\right)Ce\right] - \left[L\hat{\gamma}\sigma\left(\frac{\partial\hat{\gamma}}{\partial e}\right) + L\left(\frac{\partial\hat{\gamma}}{\partial e}\right)\sigma\hat{\lambda}\right] - L\left(\frac{\partial\hat{\gamma}}{\partial e}\right)T
\end{aligned}
\tag{5.54}
$$

As with the previous Jacobian definition, stability with respect to perturbations away from equilibrium is achieved when J is Hurwitz, that is, when all eigenvalues of J have strictly negative real parts.

5.3.3 Implications of the Tobit Jacobian

In sections 5.3.1 and 5.3.2, the Jacobians of the state/state-estimate and state/state-error systems were derived, and it was noted that in order for the systems to remain stable in the Lyapunov sense it was necessary for the resulting Jacobians to be Hurwitz. There are three main factors which effect the stability of these Jacobians. The first being the underlying, possibly non-linear, system dynamics. The second being the censoring limit T, and the third being the noise parameter σ. The first two may seem to be the most obvious in the traditional sense. For right handed censoring, if T is taken to the extreme upper limit, the system reverts to the uncensored case, as mentioned previously. If, in this uncensored case, the underlying system is linear time invariant and stable, then the resulting Jacobian is trivial, and stable. Thus, regardless of the value of σ, the resulting LQG state estimator is stable with respect to perturbations from equilibrium, as shown in section 4.5.4. From this point on, it is assumed that the underlying uncensored system in consideration is linear and time invariant.

When censoring is present, and a true TKF state estimation formation is used, then it has already been shown that the system model is now truly of a non-linear form. The noise parameter σ plays an important role, signifying how "far" from the censoring region the state and state estimates may be. The ideas of being "deep" into censoring or "deep" into the uncensored region are relative to the noise distribution specified by σ. Thus two systems with identical dynamics, in which one system has a large measurement noise distribution, and one system as a small measurement noise distribution, results in differing notions of stability at differing points. A large measurement noise distribution results in more censored measurements generated for a given fixed state and T. As the state approaches the censoring limit censored measurements are generated sooner and more frequently, however, as the state moves into the censored region more uncensored measurements are generated as well. A small measurement noise distribution means that the state can approach nearer to the censoring limit before censored measurements are generated, but also has the counter affect of quickly causing all measurements to be become censored when the state continues farther into the uncensored region. A tight noise distribution results in the TKF quickly devolving to the open-loop estimator form when in the censored region. While low measurement noise is beneficial in the uncensored case, it has an adverse effect in a censored region, especially for systems with fast dynamics.

To illustrate these concepts consider the stability of the defined TKF Jacobians for a given system as T and σ are varied. For simplicity, first consider the scalar case with $A = -.8$, $C = 1$,and $\sigma = .5$. A stable LQG state estimator of form 5.8 is formed by taking process disturbance variance $\sigma_q = .1$ and solving for optimal LQG gain $L = 0.0246$. Take the equilibrium point to be $x = 0$, and calculate the nominal uncensored Jacobian as

$$\mathbf{J} = \begin{bmatrix} A & 0 \\ LC & A-LC \end{bmatrix} = \begin{bmatrix} -.8 & 0 \\ 0.0246 & -0.82462 \end{bmatrix} \tag{5.55}$$

which has eigenvalues given by $\lambda = [-.8; -0.8246]$. Since L was calculated such that $(A-LC)$ is a stability matrix, the resulting eigenvalues are both negative and the Jacobian is stable, as expected. Now, introducing arbitrary censoring limit T results in a Jacobian of form 5.47. Given the values for A, C, L, σ, and calculating at equilibrium $x = 0$, 5.47 can be simplified to

$$\mathbf{J} = \begin{bmatrix} A & 0 \\ L\left(\phi_x\left(-\sigma\lambda - T\right) + \gamma\left(C - \frac{1}{\sigma}T\lambda + \sigma\lambda^2\right)\right) & A - L\left(\phi_{\hat{x}}\left(-\sigma\hat{\lambda} - T\right) + \hat{\gamma}\left(C - \frac{1}{\sigma}T\hat{\lambda} + \sigma\hat{\lambda}^2\right)\right) \end{bmatrix} \tag{5.56}$$

For the given system, as censoring limit T is progressively lowered the minimum magnitude eigenvalue moves towards the open-loop case, as shown in figure 5.4.

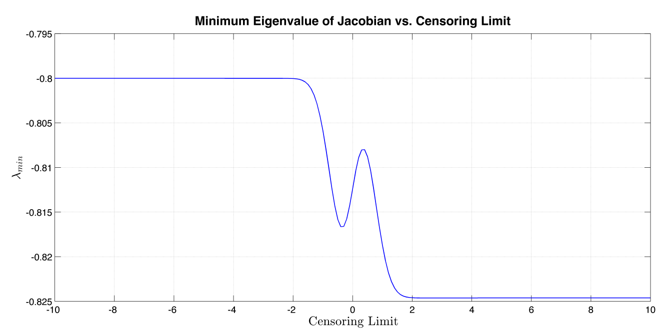

Figure 5.4: Minimum eigenvalue of the Tobit Jacobian as censoring limit T is varied for an inherently stable system.

Again however, since A is a stability matrix, the open-loop estimator case remains exponentially stable, with worst case performance in which the estimator dynamics parallel that of the original system. As seen by eigenvalues of 5.55, when uncensored the estimator dynamics given by LQG are better than that of an open-loop estimator. In the case when T is lowered such that the system is "heavily" censored, then $\lambda \to [-.8; -.8]$, and the state estimate dynamics are that of the original system. Similar results are found when T is varied in the error Jacobian formulation of 5.53, as shown in figure 5.5.

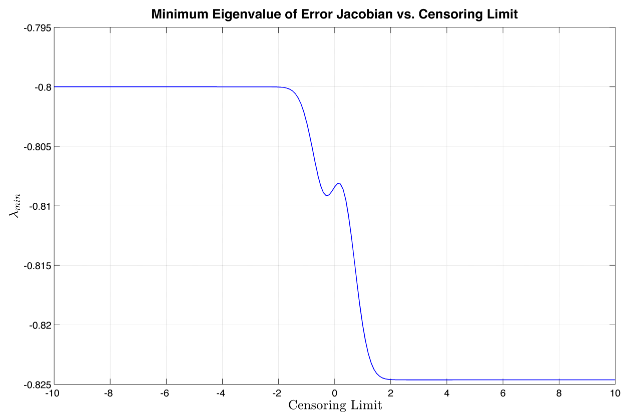

Figure 5.5: Minimum eigenvalue of the Tobit error Jacobian as censoring limit T is varied.

It is evident in figures 5.4 and 5.5 that as T is varied there exists a local disturbance to the trend near $T = 0$. The overall trend, that as T moves from high above $x = 0$ to far below $x = 0$, that the eigenvalues move from the no-censored case the open-loop case, is apparent. However, near $T = x = 0$ the expectation of censoring is 50% regardless of σ. At this point, it appears that it is actually beneficial to be slightly more *censored* than to be slightly more uncensored.

Note however, that in the previous examples, the gain L used at each value of censoring remained that of the uncensored LQG estimator derived from the given examples. However, if one assumes that for a given level of censoring T that the state remains near $x = 0$, then the steady state TKF formulation provides a more optimal value of L via the modified Ricatti equation. By utilizing the updated value of L at each censoring level, the results shown in figures 5.6 and 5.7 are obtained.

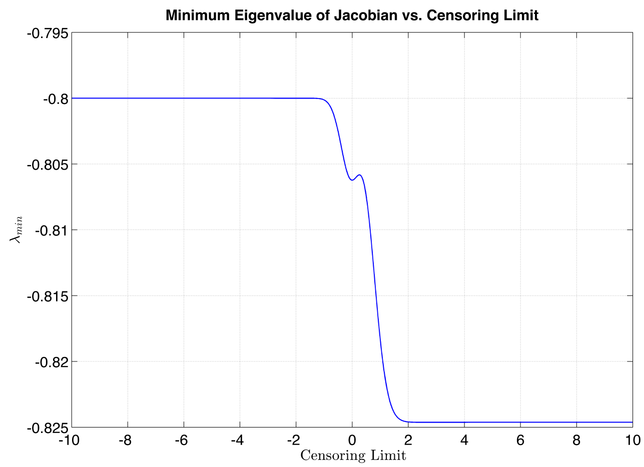

Figure 5.6: Minimum eigenvalue of the Tobit Jacobian as censoring limit T is varied and L is recalculated at each iteration.

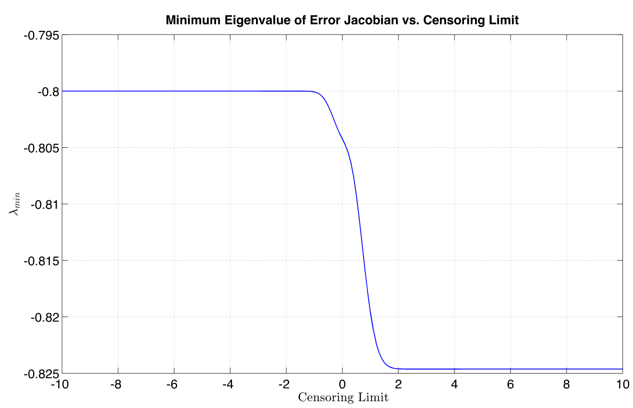

Figure 5.7: Minimum eigenvalue of the Tobit error Jacobian as censoring limit T is varied and L is recalculated at each iteration.

Now, by using the optimum value of L at each level of censoring instead of the naive gain derived from an uncensored LQG estimator, figure 5.7 indicates that the disturbance in the trend near $T = x = 0$ has been alleviated. The error dynamics now follow a smoother trend of more stable performance when uncensored towards open-loop performance when heavily censored.

Consider now a repetition of the above experiment, except T is held fixed at

$T = .5$, and measurement noise variance σ is varied. As shown in 5.8, the minimum Jacobian eigenvalue varies from that of the uncensored case when σ is very small, to that of the 50% censored case when σ is large.

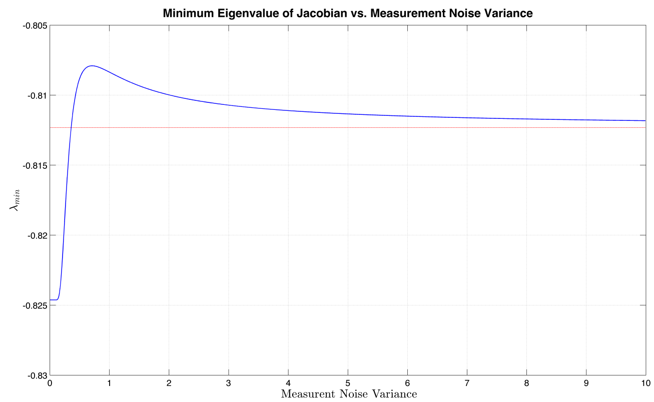

Figure 5.8: Magnitude of the smallest eigenvalue of the Tobit Jacobian as measurement noise variance σ is varied. The red line represents the minimum eigenvalue of 50% censored system.

This is expected, for when x and T are fixed, the "level" of censoring is entirely dependent on the expectation of censoring γ and inverse mills ratio λ, which are now only functions of σ. If σ is very small then the proportional distance from the censoring limit relative to σ increases, and the system behaves as an uncensored system. As σ is increased then the proportional distance to the censoring limit relative to σ decreases, and eventually censored measurements are routinely generated. However, since x and T are fixed, if σ grows large enough that $\sigma >> (T - x)$, then $\gamma \to .5$, meaning that the expectation of censoring reaches a limit of 50%, and the Jacobian eigenvalues converge to that of a 50% censored system.

Again however, note that figure 5.8, represents the eigenvalues of the resulting Jacobian when σ is varied and the naive uncensored gain L is utilized. Therefore, one can see that the minimum eigenvalue actually overshoots that of the 50% censored case and estimator performs worse for values of σ slightly greater than $T - x$. If however, the proper gain L is recalculated at each σ iteration, as done previously when T alone was varied, this effect is no longer seen, as shown in figure 5.9.

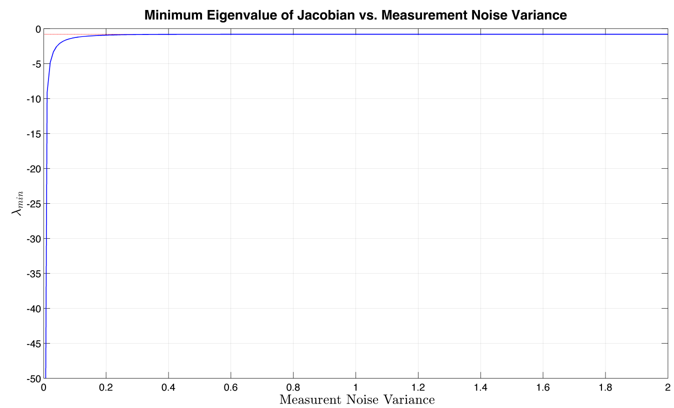

Figure 5.9: Magnitude of the smallest eigenvalue of the Tobit Jacobian as measurement noise variance σ is varied and gain L is recalculated at each iteration. The red line represents the minimum eigenvalue of 50% censored system.

Now, for very small values of σ, the system behaves as if no measurement noise or censoring are present at all. Thus very accurate measurements can be taken of the system output, the minimum eigenvalue is very low, and the state estimator is very quick and stable. However, as σ is increased, the system quickly converges that of a 50% censored system. This however, as per the previous discussion, is entirely expected for larger values of σ enforce that the difference between T and x becomes trivial, and nearly half of all measurements become censored. In this case estimator dynamics revert to that of a 50$ censored system, and the difference between multiple systems with varying levels of σ become trivial, given that $\sigma >> (T - x)$.

5.4 Examples

To illustrate the results of sections 5.1.2, 5.3.1, and 5.3.2, consider the following examples regarding the effects of censoring on the state of a DC motor model and a generic unstable scalar system.

5.4.1 DC Motor Speed Model

For a simplified DC motor angular velocity model with state $\begin{bmatrix}\dot{\theta} \ , \ i\end{bmatrix}'$, then

$$\begin{aligned} \dot{\mathbf{x}} &= \mathbf{A}\mathbf{x} + \mathbf{G}\mathbf{w} \\ \mathbf{y} &= \mathbf{C}\mathbf{x} + \mathbf{v} \end{aligned} \tag{5.57}$$

with the system matrices $\mathbf{A}, \mathbf{G}$, and $\mathbf{C}$ being defined as

$$\mathbf{A} = \begin{bmatrix} \frac{b}{j} & \frac{k}{j} \\ \frac{-k}{l} & \frac{r}{l} \end{bmatrix}, \ \mathbf{G} = \begin{bmatrix} 0 \\ l \end{bmatrix}, \ \mathbf{C} = \begin{bmatrix} 1 & 0 \end{bmatrix} \tag{5.58}$$

where b is the motor friction constant, j is the moment of inertia, k is a force constant, r is resistance, and l is inductance. Notice that angular velocity is the only measurement made. From this point on, unless otherwise noted, take $b = 3.5077\text{E-}6$, $j = 4.2937\text{E-}5$, $k = 9.37\text{E-}3$, $r = 4.27$, and $l = .288\text{E-}6$. A complete description of the homogeneous CLTI system model for DC motor speed control is then given by

$$\begin{aligned} \begin{bmatrix} \ddot{\theta} \\ \dot{i} \end{bmatrix} &= \begin{bmatrix} -0.0817 & 226.6111 \\ -3.3785\text{E}4 & -1.4826\text{E}7 \end{bmatrix} \begin{bmatrix} \dot{\theta} \\ i \end{bmatrix} + \begin{bmatrix} 0 \\ \frac{1}{.288\text{E-}6} \end{bmatrix} w \\ \begin{bmatrix} y \end{bmatrix} &= \begin{bmatrix} 1 & 0 \end{bmatrix} \begin{bmatrix} \dot{\theta} \\ i \end{bmatrix} + v \end{aligned} \tag{5.59}$$

To construct an LQG observer as seen in section 4.5.4 for the above system use the algebraic Ricatti equation to calculate the steady state gain of the Kalman filter associated with the given noise parameters. Taking variance of w and v to be $\sigma_q = .01$ and $\sigma_r = .05$, respectively, then the process and noise covariances are given by

$$\begin{aligned}
\mathbf{Q} &= E\left[(Gw)(Gw)'\right] = (G\sigma_q)(G\sigma_q)' = \begin{bmatrix} .2800\text{E-}4 & .1233\text{E-}4 \\ .1233\text{E-}4 & .0543\text{E-}4 \end{bmatrix} \\
\mathbf{R} &= E\left[vv'\right] = \sigma_r^2 = 0.0025
\end{aligned} \tag{5.60}$$

Solving 4.50 for P yields the minimum energy estimator given by 4.51, resulting in gain L corresponding to the steady gain of the standard Kalman filter for system 5.59.

$$\begin{aligned}
L &= P^{-1}C'Q \\
&= [10.0329 \;\; 0.2257]'
\end{aligned} \tag{5.61}$$

and complete estimator dynamics given by

$$\begin{aligned}
\dot{\hat{\mathbf{x}}} &= (\mathbf{A} - \mathbf{LC})\hat{\mathbf{x}} + \mathbf{Ly} \\
\dot{\mathbf{e}} &= (\mathbf{A} - \mathbf{LC})\mathbf{e} + \mathbf{Gw} + \mathbf{Lv}
\end{aligned} \tag{5.62}$$

Since the maximum eigenvalue of $(A - LC)$ is , the resulting LQG state estimator is exponentially stable. To demonstrate this fact, the evolution of $\dot{\theta}$ and $\hat{\dot{\theta}}$ from the zero initial condition is shown in figure 5.10. As expected, because the system matrix in 5.61 is a stability matrix, the true and estimated angular velocity states do not diverge from the initial condition over time.

However, the introduction of right handed censoring without compensation causes the state estimate $\hat{x}$ to become biased. This is due to the fact that the original LQG estimator assumes a linear measurement model in which $E[y] = E[Cx+v] = Cx$. However, censoring leads to a non-linear measurement model better modeled by 5.3.

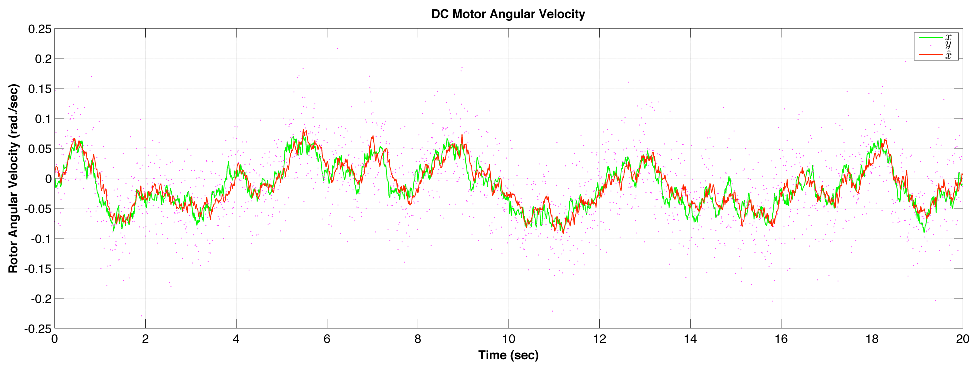

Figure 5.10: Evolution of states $\dot{\theta}$ and $\hat{\dot{\theta}}$ over time without censoring.

The resulting model mismatch results in the LQG estimator incorrectly weighting censored measurements the same as uncensored measurements, biasing the state estimate towards the censoring limit. This result can be seen in figure 5.11.

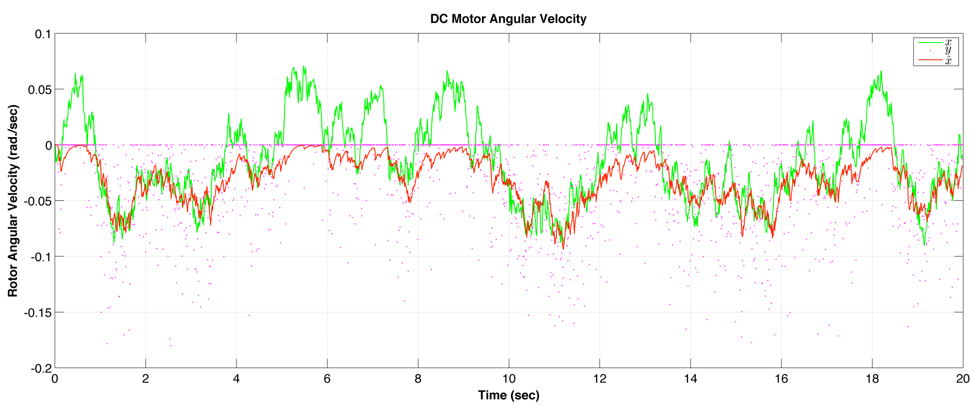

Figure 5.11: Evolution of states $\dot{\theta}$ and $\hat{\dot{\theta}}$ over time with censoring.

To compensate for the censoring present in 5.11 the state estimator must be adjusted to the form given by 5.9 where

$$
\begin{aligned}
\dot{\hat{\mathbf{x}}} &= \mathbf{A}\hat{\mathbf{x}} + \mathbf{L}(\mathbf{y} - \hat{\mathbf{y}}) \\
\hat{\mathbf{y}} &= \hat{\gamma}(\mathbf{C}\hat{\mathbf{x}} - \sigma\hat{\lambda}) + (\mathbf{1} - \hat{\gamma})\mathbf{T}
\end{aligned}
$$

The resulting initial condition response with censoring is shown in 5.12.

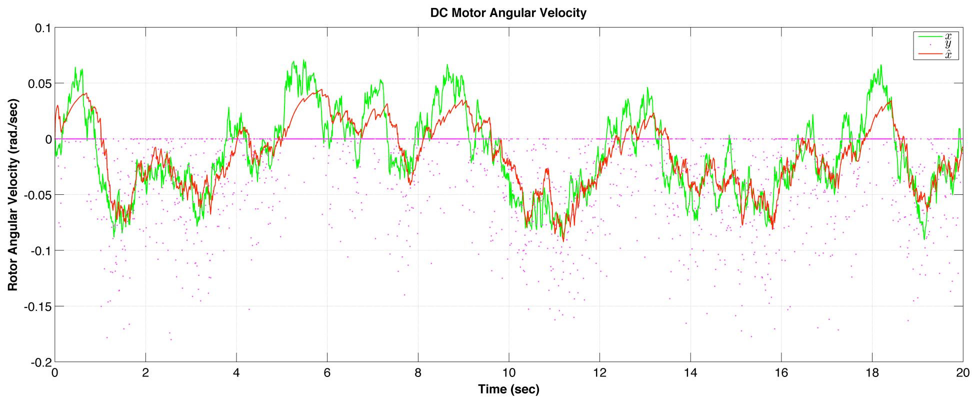

Figure 5.12: Evolution of states $\dot{\theta}$ and $\hat{\dot{\theta}}$ over time with censoring, using a TKF estimator with the same gain as the original uncensored LQG estimator.

Although the same level of censoring is present as in figure 5.11, the new formulation compensates for the censored region and allows for a stable and more accurate state estimation than a naive LQG estimator. However, in figure 5.12, the same gain L is being used as that of the uncensored LQG estimator. In the censored case this gain should be modified to reflect the inherent change in the system model created by the effect of the censored region. Assume that T is constant and that the system remains near the equilibrium point, then it may be assumed that the constant censoring limit results in a near constant proportion of censored measurements being generated. Thus, γ, the expectation of any given measurement being uncensored, and λ, the inverse mills ratio, approach constants over time. Using these constant values the modified algebraic Ricatti equation of 3.4.2 can be solved for a steady state Tobit Kalman gain. For example, should $T = 0$ as in the previous example, and assuming that the system is stable and therefore x remains near 0 as $t \to \infty$, then $E[\hat{\gamma}] = \Phi(0) = .5$. The modified algebraic Ricatti equation results in a new gain value of

$$\begin{aligned} L &= P^{-1}C'Q \\ &= [16.452 \;\; .305]' \end{aligned}$$

This new TKF gain is slightly different from the original uncensored optimal given by 5.61, due the censoring described above. A comparison between estimation with the optimal uncensored gain and the new gain is shown in figure 5.13.

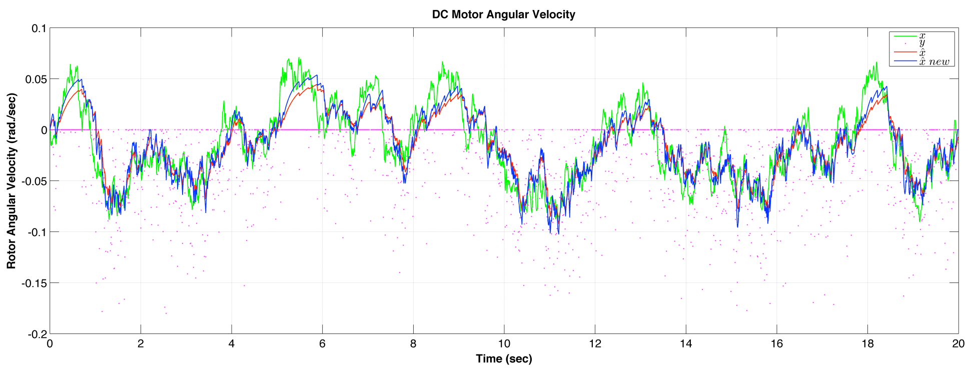

Figure 5.13: Evolution of states $\dot{\theta}$ and $\hat{\dot{\theta}}$ over time with censoring, using a TKF estimator with an updated Tobit gain. The previous $\hat{\theta}$ with the original gain is shown in red, while the new estimate of $\hat{\theta}$ using the updated gain is shown in blue.

The resulting filter with the new Tobit Kalman gain results in a stable unbiased state estimate which compensates for the censored region and has lower error than when the standard LQG gain is utilized.

As discussed earlier, as the censoring limit T is lowered to extreme limits the system enters a state in which nearly all measurements are censored. At such a time γ goes to zero, and the estimator enters the predicted "open-loop" behavior. The result of such an estimator is shown in figure 5.14.

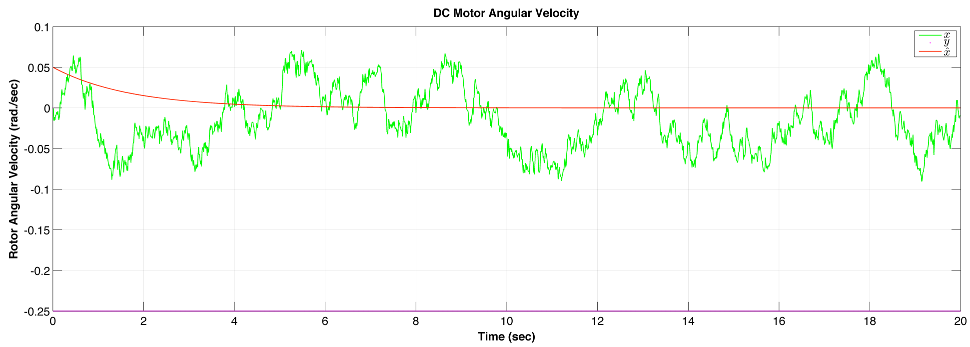

Figure 5.14: Evolution of states $\dot{\theta}$ and $\hat{\dot{\theta}}$ over time with censoring, using a TKF estimator when heavily censored.

As predicted, because A is a stability matrix in this example, the state estimator does not diverge from the true state, however the repeated return of wholly censored measurements is providing almost no useful information. Thus, the state estimator is unable to track with disturbances in the process model, and resorts to open-loop prediction from the initial state estimate. Note here that the initial condition has changed from $[0; 0]$ to $[0; .5]$, meaning that the initial state estimate has an initial error. Since the heavy censoring enforces an open-loop behavior, the state estimate simply converges to the origin in finite time because A is Hurwitz. Also note that the concept of being "heavily" censored is somewhat subjective, in the sense that it relies entirely upon the difference between the censoring limit and the true signal in proportion to the noise parameter σ. Thus, in this scenario, in which $T = -.25$, the censoring limit is 5σ away from the origin, resulting in nearly all measurements to being censored, and thus the signal being "heavily" censored.

5.4.2 DC Motor Position Model

The previous section explored the DC motor speed model and the implication of censoring on the stability of its estimation. The DC motor speed model is convenient due to its inherent open loop stability, and therefore effectiveness at illustrating that the TKF estimator remains stable under certain conditions despite the possibility of heavy censoring. Another similar model is now addressed, that of DC motor angular position. This model is inherently much less stable than the motor speed problem, and therefore is used to demonstrate the effects of censoring in a more dramatic manner.

For a simplified DC motor angular position model with state $\begin{bmatrix}\theta, & \dot{\theta}\ , & i\end{bmatrix}'$, then

$$\begin{aligned} \dot{\mathbf{x}} &= \mathbf{A}\mathbf{x} + \mathbf{G}\mathbf{w} \\ \mathbf{y} &= \mathbf{C}\mathbf{x} + \mathbf{v} \end{aligned} \tag{5.63}$$

with the system matrices $\mathbf{A}, \mathbf{G}$, and $\mathbf{C}$ being defined as

$$\mathbf{A} = \begin{bmatrix} 0 & 1 & 0 \\ 0 & \frac{b}{j} & \frac{k}{j} \\ 0 & \frac{-k}{l} & \frac{r}{l} \end{bmatrix}, \ \mathbf{G} = \begin{bmatrix} 0 \\ 0 \\ l \end{bmatrix}, \ \mathbf{C} = \begin{bmatrix} 1 & 0 & 0 \end{bmatrix} \tag{5.64}$$

where b,j,k,r and l are defined as before in the motor speed model. A complete description of the homogeneous CLTI system model for DC motor postion is then given by

$$\begin{aligned} \begin{bmatrix} \dot{\theta} \\ \ddot{\theta} \\ \dot{i} \end{bmatrix} &= \begin{bmatrix} 0 & 1 & 0 \\ 0 & -0.0817 & 226.6111 \\ 0 & -3.3785\text{E}4 & -1.4826\text{E}7 \end{bmatrix} \begin{bmatrix} \theta \\ \dot{\theta} \\ i \end{bmatrix} + \begin{bmatrix} 0 \\ 0 \\ \frac{1}{.288\text{E-}6} \end{bmatrix} w \\ \begin{bmatrix} y \end{bmatrix} &= \begin{bmatrix} 1 & 0 & 0 \end{bmatrix} \begin{bmatrix} \theta \\ \dot{\theta} \\ i \end{bmatrix} + v \end{aligned} \tag{5.65}$$

Using the same values for process and measurement noise variances as shown previously, now

$$\begin{aligned}\mathbf{Q} &= E\left[(Gw)(Gw)'\right] = \begin{bmatrix} 0 & 0 & 0 \\ 0 & 0 & 0 \\ 0 & 0 & \left(\frac{.01}{.288\text{E-6}}\right)^2 \end{bmatrix} \\ \mathbf{R} &= E\left[vv'\right] = 0.0025\end{aligned} \tag{5.66}$$

Again solving 4.50 for P yields the minimum energy estimator with gain L corresponding to the steady gain of the standard Kalman filter for system 5.65, and given by

$$\begin{aligned}L &= P^{-1}C'Q \\ &= [4.0480 \;\; 8.1931 \;\; -0.0187]'\end{aligned} \tag{5.67}$$

A complete description of the estimator can now be given as in 5.62, and repeated here as

$$\begin{aligned}\dot{\hat{\mathbf{x}}} &= (\mathbf{A} - \mathbf{LC})\hat{\mathbf{x}} + \mathbf{Ly} \\ \dot{\mathbf{e}} &= (\mathbf{A} - \mathbf{LC})\mathbf{e} + \mathbf{Gw} + \mathbf{Lv}\end{aligned}$$

The eigenvalues for the system matrix A are given by

$$\lambda_A = \begin{bmatrix} -14826388.3725128 \\ -0.598070200532675 \\ 0 \end{bmatrix}$$

and the eigenvalues for $(A - LC)$ of the nominal uncensored LQG estimator are given by

$$\lambda_{A-LC} = \begin{bmatrix} -14826388.3725128 \\ -2.32303105520711 - 2.28421305934995i \\ -2.32303105520711 + 2.28421305934995i \end{bmatrix}$$

Therefore, even though the underlying system is only marginally stable, the resulting uncensored LQG state estimator is exponentially stable. To demonstrate this fact, the evolution of θ and $\hat{\theta}$ from the zero initial condition is shown in figure 5.15. As expected, because the system matrix in 5.67 is a stability matrix, the true and estimated angular velocity states do not diverge from the initial condition over time when no censoring is present.

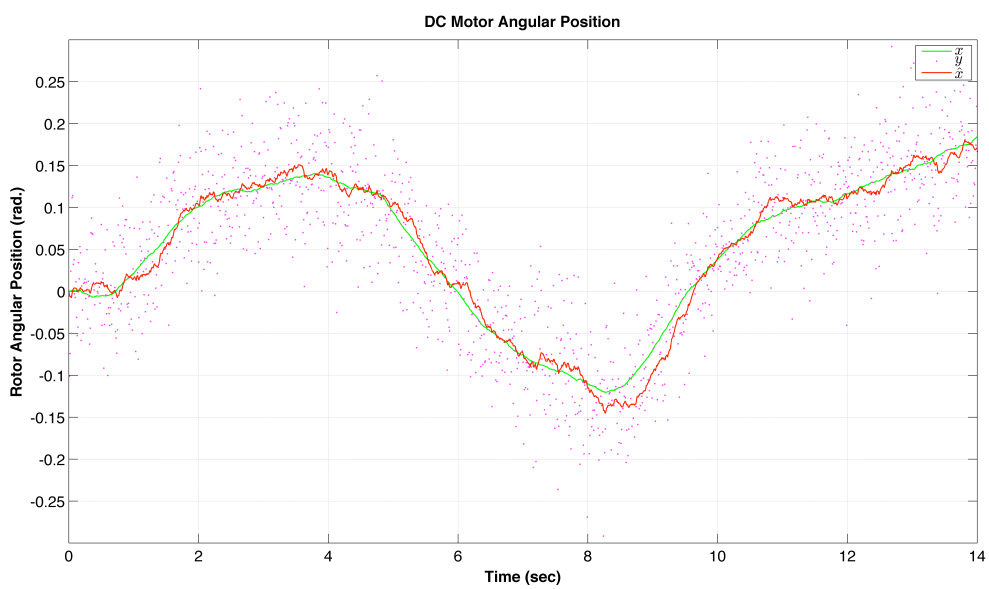

Figure 5.15: Evolution of states θ and $\hat{\theta}$ over time with a TKF estimator and no censoring.

When censoring is introduced the standard estimator is no longer valid, as previously shown, and the TKF estimator of form 5.9 should then be used. If for example, censoring limit $T = 0$ is imposed, then the state estimate evolves as shown in 5.16.

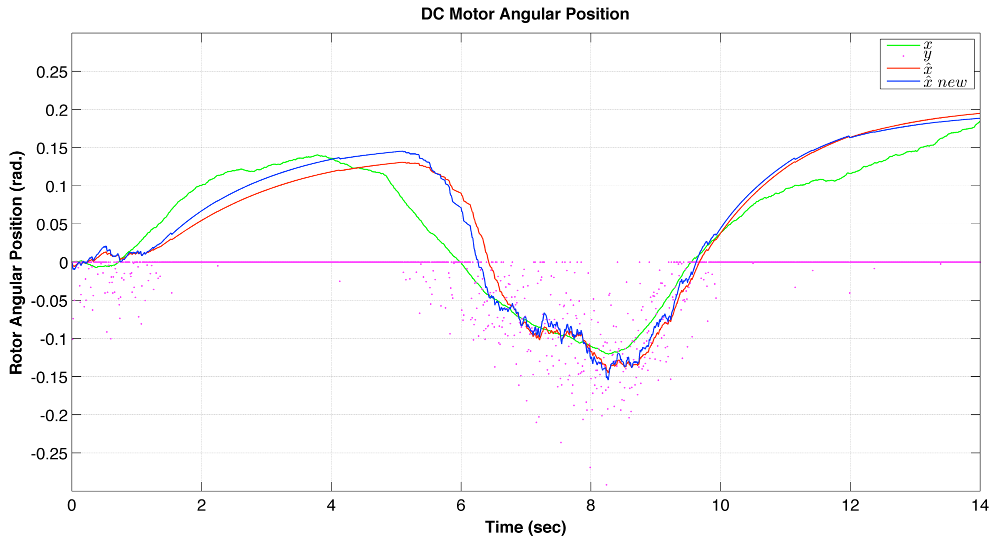

Figure 5.16: Evolution of states θ and $\hat{\theta}$ over time with a TKF estimator and censoring limit $T = 0$. Red is the state estimate when using the original uncensored LQG gain, and blue is the state estimate when using a TKF gain.

As shown in the previous example, there is a noticeable difference between use of 5.9 with the naive uncensored LQG gain L and a new recalculated L based on the censoring statistics. For $T = 0$ modified Ricatti equation may used to estimate a new TKF gain of $L = [7.281, 13.253, -0.0302]'$, resulting the eigenvalues of $(A-LC)$ moving to

$$\lambda_{A-LC} = \begin{bmatrix} -14826388.3725128 \\ -3.9395245780726 - 1.4449381590563i \\ -3.9395245780726 + 1.4449381590563i \end{bmatrix}$$

Should censoring limit T be moves lower to $T = -10deg$ then estimator performance degrades to that shown by 5.17.

Due to the fact that the sever censoring limit provides little valuable information for the first several samples, the estimator cannot do any better than open loop prediction until a noticeable number of uncensored measurements are generated. At

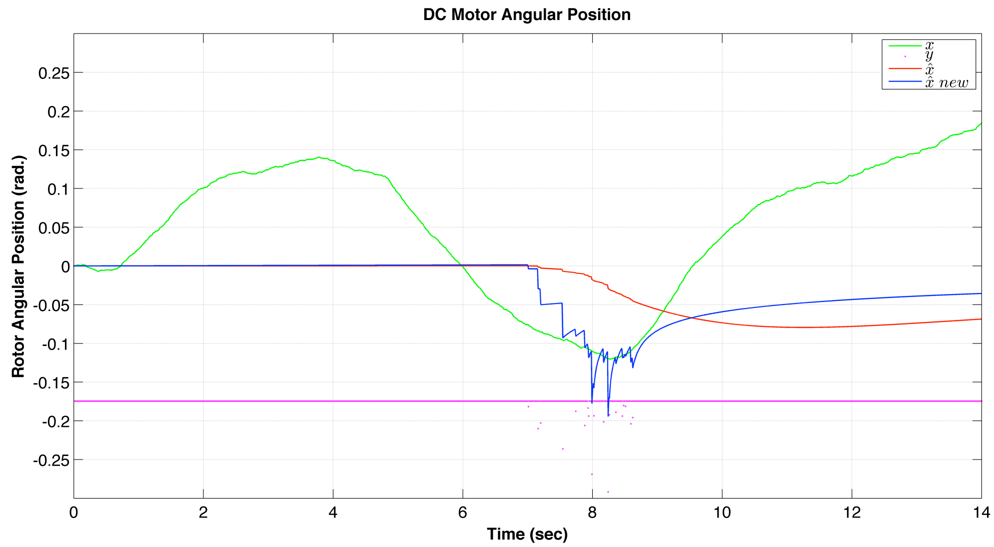

Figure 5.17: Evolution of states θ and $\hat{\theta}$ over time with a TKF estimator and censoring limit $T = -10deg$. Red is the state estimate when using the original uncensored LQG gain, and blue is the state estimate when using a TKF gain.

this point the estimator with the updated gain of $L = [73.1575, 0.6447, -0.0015]$ is able to recover and begin tracking the motor position while it enters the uncensored region, whereas utilization of the original LQG gain provided poorer performance. With updated gain at this level of censoring the eigenvalues of $(A - LC)$ have reduced further to

$$\lambda_{A-LC} = \begin{bmatrix} -14826388.3725128 \\ -73.1486 \\ -0.6070 \end{bmatrix}$$

Now consider the case in which censoring limit $T = -20deg$ and all measurements become censored. At this point $L = [17.7467, 2.3025\text{E} - 10, -5.2485\text{E} - 13]$ and the eigenvalues of $(A - LC)$ are

$$\lambda_{A-LC} = \begin{bmatrix} -14826388.3725128 \\ -17.7467 \\ -0.59807 \end{bmatrix}$$

The eigenvalues of the state estimator in this scenario are approaching that of the original system matrix A given previously. Thus, the estimator is converging to the open-loop estimator, which can be seen in figure 5.18.

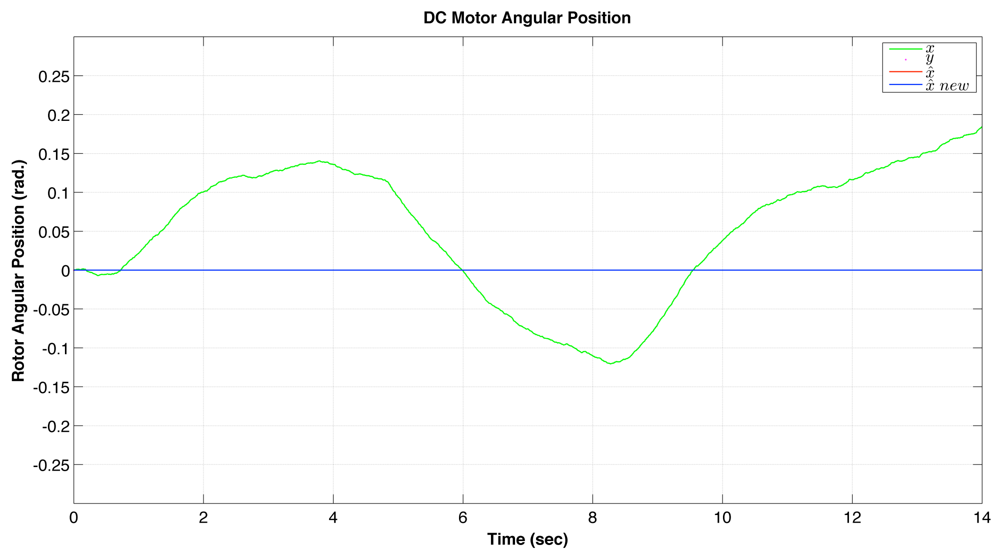

Figure 5.18: Evolution of states θ and $\hat{\theta}$ over time with a TKF estimator and censoring limit $T = -20deg$. Red is the state estimate when using the original uncensored LQG gain, and blue is the state estimate when using a TKF gain.

It is apparent that as the T is lowered from the no-censoring case to the heavily censored case the eigenvalues of the state estimator are approaching that of the original system and the TKF transitions from an LQG estimator to an open-loop predictor. Since the original system is marginally stable, and the TKF is marginally stable as well in the extreme censoring case. In the case when T is such that the system is not heavily censored then the TKF is stable and always performs better than open-loop prediction.

5.5 Changing T to Recover Stability

Consider again a linear time-invariant homogeneous system with a TKF observer as modeled by 5.5 and given below as

$$\begin{aligned}\dot{\mathbf{x}} &= \mathbf{A}\mathbf{x} \\ \dot{\hat{\mathbf{x}}} &= \mathbf{A}\hat{\mathbf{x}} + \mathbf{L}(-\hat{\gamma}\mathbf{C}\hat{\mathbf{x}} + \gamma\mathbf{C}\mathbf{x} - \gamma\sigma\lambda + \hat{\gamma}\sigma\hat{\lambda} - \gamma\mathbf{T} + \hat{\gamma}\mathbf{T})\end{aligned}$$

As mentioned in section 5.3.1, when censoring limit T is constant the resulting TKF observer is non-linear and time-varying. As such, little can be guaranteed in terms of stability and convergence for all times. If the system matrix A is a stability matrix then performance of the observer can be characterized in the extreme cases of complete censoring or no censoring, and stability with regards to perturbation from equilibrium can be calculated, as shown previously.

The deviation from traditional linear analysis is due to the non-linear and state dependent probabilistic terms γ and λ introduced by censoring. Recall that the terms γ and λ represent the expectation of the measurement being uncensored and the inverse mills ratio, respectively, given by 5.5 and repeated here as

$$\begin{aligned}\gamma &= \Phi\left(\tfrac{T-Cx_k}{\sigma}\right) \\ \lambda &= \lambda\left(\tfrac{T-Cx_k}{\sigma}\right) \\ \hat{\gamma} &= \Phi\left(\tfrac{T-C\hat{x}_k}{\sigma}\right) \\ \hat{\lambda} &= \lambda\left(\tfrac{T-C\hat{x}_k}{\sigma}\right)\end{aligned}$$

By definition, each of these terms are entirely dependent on the given measurement noise distribution σ and the difference of the state/state-estimate from the censoring limit T. Therefore, assuming that σ remains constant, if the state and state estimate remain at a constant proportion to the censoring limit then λ and γ remain constant as well. The effect is a convergence of the observer from a time-varying non-linear estimator to a time-invariant linear system with constant disturbance. Such an outcome can be realized in two ways. First, by forcing the true state and state estimate to evolve in such a manner that as $t \to \infty$ then x, $\hat{x} \to \alpha$. Such a system can be realized if A is a stability matrix and $\alpha = 0$. This now describes an open loop stable system and estimator as described previously. The second, and more interesting case, involves defining T such that the constant proportion is maintained regardless of x and $\hat{x}$. Exactly this type of system was described previously in section 3.4.2 in which it was shown that a steady state TKF results.

As shown before, the value of T can be determined at any time by defining an α between $(0, 1)$ such that

$$\mathbf{T} = \mathbf{C}\hat{\mathbf{x}} + \sigma \mathbf{\Phi^{-1}}(\alpha) \tag{5.68}$$

Thus, $\hat{\gamma}$ is then

$$\begin{aligned} \hat{\gamma} &= \Phi\left(\tfrac{T - C\hat{x}_k}{\sigma}\right) \\ &= \Phi\left(\tfrac{C\hat{x} + \sigma\Phi^{-1}(\alpha) - C\hat{x}_k}{\sigma}\right) \\ &= \Phi\left(\Phi^{-1}(\alpha)\right) \\ &= \alpha \end{aligned} \tag{5.69}$$

The error dynamics of the filter, originally defined by 5.10, can now be characterized by

$$\begin{aligned} \dot{\mathbf{e}} &:= (\mathbf{A} - \mathbf{L}\hat{\gamma}\mathbf{C})\mathbf{e} - \mathbf{L}\mathbf{e}_\gamma(\mathbf{C}\mathbf{x} - \sigma\lambda - \mathbf{T}) + \mathbf{L}\gamma\mathbf{e}_\lambda + \mathbf{w} \\ &= (\mathbf{A} - \mathbf{L}\hat{\gamma}\mathbf{C})\mathbf{e} - \mathbf{L}\mathbf{e}_\gamma(\mathbf{C}\mathbf{x} - \sigma\lambda - (\mathbf{C}\hat{\mathbf{x}} + \sigma\mathbf{\Phi^{-1}}(\alpha))) + \mathbf{L}\gamma\mathbf{e}_\lambda + \mathbf{w} \\ &= (\mathbf{A} - \mathbf{L}\hat{\gamma}\mathbf{C})\mathbf{e} - \mathbf{L}\mathbf{e}_\gamma(\mathbf{C}\mathbf{e} - \sigma\lambda - \sigma\mathbf{\Phi^{-1}}(\alpha)) + \mathbf{L}\gamma\mathbf{e}_\lambda + \mathbf{w} \\ &= (\mathbf{A} - \mathbf{L}\gamma\mathbf{C})\mathbf{e} - \mathbf{L}\mathbf{e}_\gamma(\sigma\lambda + \sigma\mathbf{\Phi^{-1}}(\alpha)) + \mathbf{L}\gamma\mathbf{e}_\lambda + \mathbf{w} \end{aligned} \tag{5.70}$$

Assume initial convergence of the filter such that $\gamma \approx \hat{\gamma}$, and $\lambda \approx \hat{\lambda}$, then the error dynamics converge to

$$\dot{\mathbf{e}} = (\mathbf{A} - \mathbf{L}\gamma\mathbf{C})\mathbf{e} + \mathbf{w} \tag{5.71}$$

This form is similar to that of the uncensored LQG estimator, except with the addition term γ, which is assumed to be constant due to the redefinition of T given above. Note that in 5.68 α can chosen such that a desired expectation of being uncensored with respect to the state estimate is accomplished. In short, T is defined in order to set a desired $\hat{\gamma}$. An alternative method of would be set T such that a desired inverse mills ratio $\hat{\lambda}$ results. This can be done by redefining α such that

$$\hat{\lambda} \;=\; -\mathbf{\Phi^{-1}}(\alpha) \tag{5.72}$$

for a desired inverse mills ratio $\hat{\lambda}$, resulting in a T given by

$$\begin{aligned} \mathbf{T} &= \mathbf{C}\hat{\mathbf{x}} + \sigma\mathbf{\Phi^{-1}}(\alpha) \\ &= \mathbf{C}\hat{\mathbf{x}} - \sigma\hat{\lambda} \end{aligned} \tag{5.73}$$

Following the form of 5.70, an alternative description for the estimator error dynamics can be given by

$$\begin{aligned} \dot{\mathbf{e}} &:= (\mathbf{A} - \mathbf{L}\hat{\gamma}\mathbf{C})\mathbf{e} - \mathbf{L}\mathbf{e}_\gamma(\mathbf{C}\mathbf{x} - \sigma\lambda - \mathbf{T}) + \mathbf{L}\gamma\mathbf{e}_\lambda + \mathbf{w} \\ &= (\mathbf{A} - \mathbf{L}\gamma\mathbf{C})\mathbf{e} - \mathbf{L}\mathbf{e}_\gamma(-\sigma\lambda + \sigma\hat{\lambda}) + \mathbf{L}\gamma\mathbf{e}_\lambda + \mathbf{w} \\ &= (\mathbf{A} - \mathbf{L}\gamma\mathbf{C})\mathbf{e} + \mathbf{L}\mathbf{e}_\lambda(\gamma(\mathbf{1} + \sigma) - \hat{\gamma}\sigma) + \mathbf{w} \end{aligned} \tag{5.74}$$

The definitions for T given by 5.68 and 5.73 are entirely analogous. The first defined T such that a desired constant $\hat{\gamma}$ is accomplished, subsequently resulting in a constant $\hat{\lambda}$ as well. The second defines T such that a given constant $\hat{\lambda}$ is accomplished, resulting in a related constant $\hat{\gamma}$ as well. Via either definition, T maintains a constant proportional offset from $\hat{x}$ and either error dynamics of 5.70 or 5.74 can be explored. Although T is maintained at a constant offset from $\hat{x}$, it may fall either below or above $\hat{x}$ depending on the desired level of censoring. Any $\hat{\gamma} < .5$ inherently dictates a $T < \hat{x}$.

It is clear that when T is defined with respect to the state estimate, then the main driver of the error becomes the level of censoring of the *true* state, with an additional term driven by the error between the state and state estimate inverse mills ratios. By looking at 5.74 it becomes apparent that there are four particular scenarios related to the level of censoring and initial conditions that create differing behaviors, and is explored next.

Scenario 1. Completely Uncensored

In this scenario the value of $T \to \infty$ and the system reverts to a completely uncensored case. As seen in previous sections this results in convergence of the TKF estimator to a completely linear and globally symptomatically stable observer. This can be verified w.r.t. 5.74 by noting that as $T \to \infty$, then

$$\begin{aligned} \gamma, \hat{\gamma} &\to 1 \\ \lambda, \hat{\lambda} &\to 0 \\ e_{\lambda} &\to 0 \end{aligned}$$

and thus the resulting error dynamics go to

$$\dot{\mathbf{e}} = (\mathbf{A} - \mathbf{LC})\mathbf{e} + \mathbf{w}$$

Scenario 2. Completely Uncensored

Similar to scenario 1, except in the opposing extreme, the value of $T \to -\infty$ and the system reverts to a completely censored case. As seen in previous sections this results in convergence of the TKF estimator to an open loop linear observer. Stability in this case is entirely dependent on the system matrix A. This can be verified w.r.t. 5.74 by noting that as $T \to -\infty$, then

$$\begin{aligned} \gamma, \hat{\gamma} &\to 0 \\ \lambda, \hat{\lambda} &\to \infty \end{aligned}$$

and thus the resulting error dynamics go to

$$\dot{\mathbf{e}} = \mathbf{A}\mathbf{e} + \mathbf{w}$$

Scenario 3. True State Uncensored, $T > \hat{x}$

In this more interesting scenario there is now an explicit initial error between state and state estimate. The assumption that $\hat{x} \approx x$ is no longer taken for granted. However, in this scenario, since the true state is uncensored one would hope the observer remains stable regardless of its initial state estimate. Since the true state is uncensored then $x < T$. Therefore

$$\begin{aligned} \gamma &\leq \gamma(\tfrac{T-CT}{\sigma}) \\ \lambda &\leq \lambda(\tfrac{T-CT}{\sigma}) \\ e_\gamma &\leq \gamma(\tfrac{T-CT}{\sigma}) - \hat{\gamma} \\ e_\lambda &\leq \lambda(\tfrac{T-CT}{\sigma}) - \hat{\lambda} \end{aligned}$$

and thus the resulting error dynamics go to

$$\dot{\mathbf{e}} = (\mathbf{A} - \mathbf{L}\gamma\mathbf{C})\mathbf{e} - \mathbf{L}\mathbf{e}_\gamma(-\sigma\lambda + \sigma\hat{\lambda}) + \mathbf{L}\gamma\mathbf{e}_\lambda + \mathbf{w}$$

Should the true state be farther in the uncensored region and $x < \hat{x}$, then $\gamma > \hat{\gamma}$ and $\lambda < \hat{\lambda}$, therefore dynamics simplify to

$$\begin{aligned} e_\gamma &> 0 \\ e_\lambda &< 0 \\ \dot{\mathbf{e}} &= (\mathbf{A} - \mathbf{L}\gamma\mathbf{C})\mathbf{e} - \mathbf{L}\|\mathbf{e}_\lambda\|(\gamma(\mathbf{1} + \sigma) - \hat{\gamma}\sigma) + \mathbf{w} \end{aligned}$$

Should the true state be deep in the uncensored region, and thus $x << \hat{x}$, the dynamics simplify to

$$\begin{aligned} \gamma &\to 1 \\ \lambda &\to 0 \\ e_\lambda &\to -\hat{\lambda} \end{aligned}$$

and thus the resulting error dynamics go to

$$\dot{e} = (\mathbf{A} - \mathbf{L}\mathbf{C})\mathbf{e} - \mathbf{L}\hat{\lambda}(\mathbf{1} + \sigma(\mathbf{1} - \hat{\gamma})) + \mathbf{w}$$

An example of this response is shown in figure 5.19.

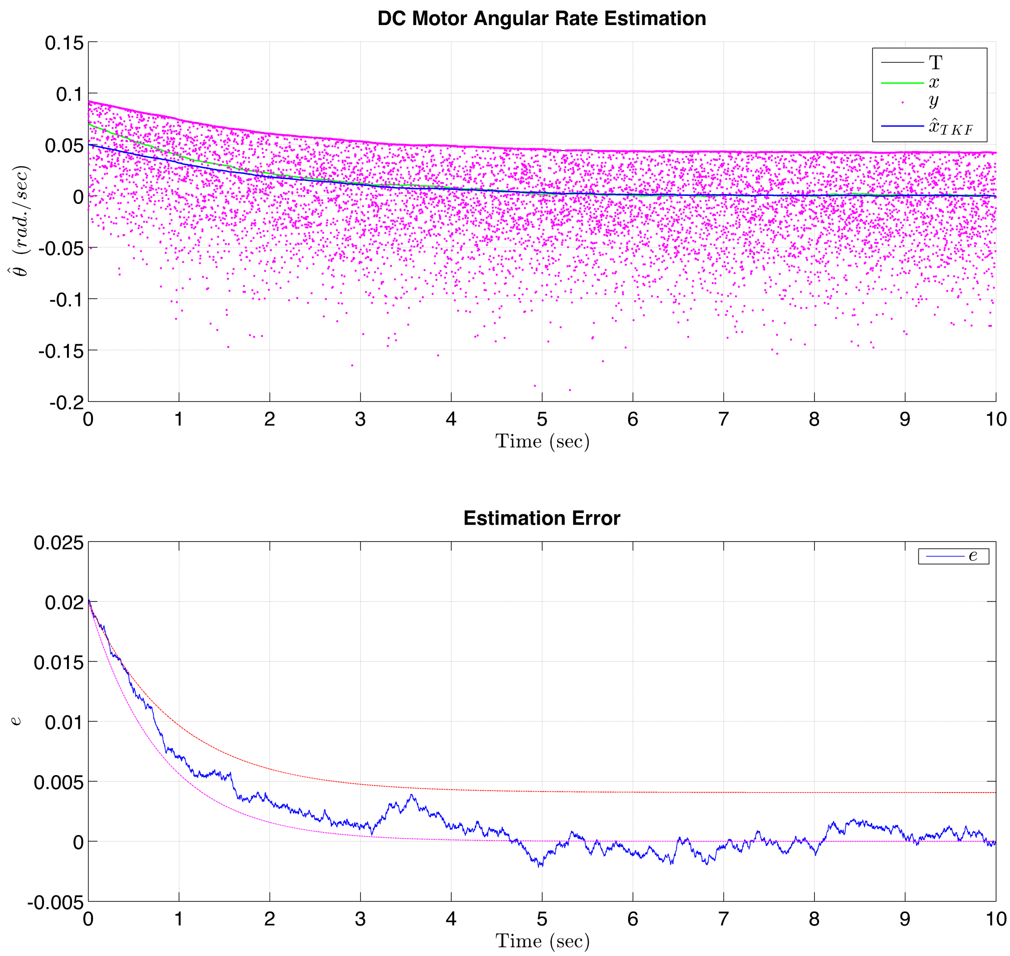

Figure 5.19: Scenario 3. Evolution of states $\dot{\theta}$ and $\hat{\dot{\theta}}$ over time with controlled censoring, using a TKF estimator with an expectation of censoring on $\hat{x}$ of .80.

Scenario 4. True State Uncensored, $T < \hat{x}$

In a similar scenario the true state is again uncensored, but now T is defined to create a heavy degree of censoring relative to $\hat{x}$ and therefore $T < \hat{x}$. As before, since the true state is uncensored then $x < T < \hat{x}$. Therefore it remains that

$$\begin{aligned} \gamma &\leq \gamma(\tfrac{T-CT}{\sigma}) \\ \lambda &\leq \lambda(\tfrac{T-CT}{\sigma}) \\ e_\gamma &\leq \gamma(\tfrac{T-CT}{\sigma}) - \hat{\gamma} \\ e_\lambda &\leq \lambda(\tfrac{T-CT}{\sigma}) - \hat{\lambda} \end{aligned}$$

and thus the resulting error dynamics go to

$$= \quad (\mathbf{A} - \mathbf{L}\gamma\mathbf{C})\mathbf{e} - \mathbf{L}\mathbf{e}_\gamma(-\sigma\lambda + \sigma\hat{\lambda}) + \mathbf{L}\gamma\mathbf{e}_\lambda + \mathbf{w}$$

Further, since $x < T < \hat{x}$, then $\gamma < \hat{\gamma}$ and $\lambda < \hat{\lambda}$. Therefore

$$\begin{aligned} &e_\lambda < 0 \\ &\dot{e} \quad = \quad (\mathbf{A} - \mathbf{L}\gamma\mathbf{C})\mathbf{e} - \mathbf{L}\|\mathbf{e}_\lambda\|(\gamma(\mathbf{1} + \sigma) + \sigma\hat{\gamma}) + \mathbf{w} \end{aligned}$$

If T is defined such to maintain a heavy degree of censoring relative to $\hat{x}$, then $\hat{\gamma} \to 0$, and

$$\dot{e} \quad = \quad (\mathbf{A} - \mathbf{L}\gamma\mathbf{C})\mathbf{e} - \mathbf{L}\|\mathbf{e}_\lambda\|(\gamma(\mathbf{1} + \sigma)) + \mathbf{w}$$

Should x be *deep* in the uncensored region such that $x << T$ then $\gamma \to 1$ and $\lambda \to 0$. Then $e_\lambda \to -\hat{\lambda}$, and

$$\dot{e} \quad = \quad (\mathbf{A} - \mathbf{L}\mathbf{C})\mathbf{e} - \mathbf{L}\hat{\lambda}(\mathbf{1} + \sigma) + \mathbf{w}$$

An example of this response is shown in figure 5.20.

Scenario 5. True State Censored, $T > \hat{x}$

The opposite to scenario three, whereby the true state is censored and the state estimate is partially censored with $T > \hat{x}$. Due to right censoring, such a scenario

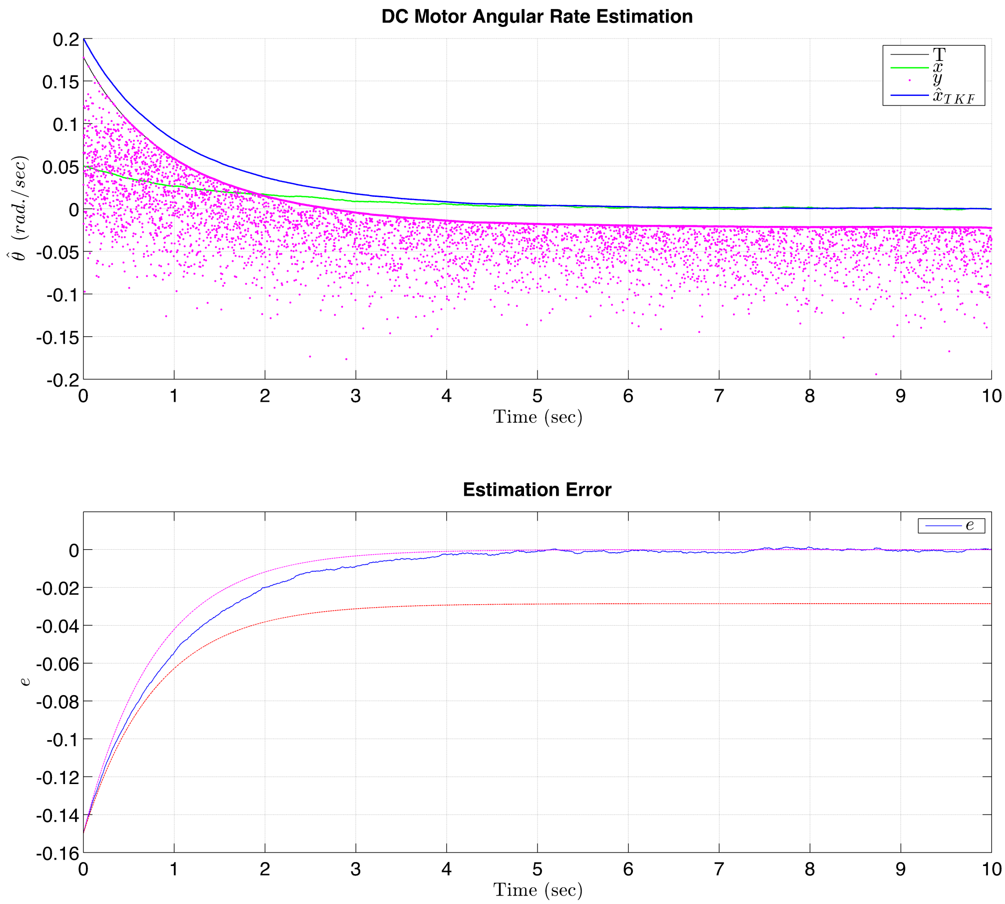

Figure 5.20: Scenario 4. Evolution of states $\dot{\theta}$ and $\hat{\dot{\theta}}$ over time with controlled censoring, using a TKF estimator with an expectation of censoring on $\hat{x}$ of .33.

enforces that $x > T > \hat{x}$, and therefore $\hat{\lambda} < \lambda$, and therefore $e_\lambda > 0$. Since the true state is censored, the censoring limit T is repeatedly returned as a measurement until x reaches near enough to the censoring limit to generate uncensored measurements. Until this point little useful information is presented to the filter, although the lack of uncensored measurements indicates that the true state is above the censoring limit and proportionally far enough away such that the noise distribution described by σ is not significant enough to generate uncensored measurements.

If x is deeply censored, such that $x >> T$, then $\gamma \to 0$. Then

$$\gamma \to 0$$

and thus the resulting error dynamics go to

$$\dot{e} \quad = \quad \mathbf{Ae} - \mathbf{Le}_\lambda(-\hat{\gamma}\sigma) + \mathbf{w}$$

An example of this response is shown in figure 5.21.

Scenario 6. True State Censored, $T < \hat{x}$

Similar to scenario 5, except now T is defined to create a large degree of censoring relative to $\hat{x}$, resulting in $T < \hat{x}$. Should $T << \hat{x}$ then $\hat{\gamma} \to 0$, and

$$\hat{\gamma} \to 0$$

$$\dot{e} \quad = \quad (\mathbf{A} - \mathbf{L}\gamma\mathbf{C})\mathbf{e} + \mathbf{Le}_\lambda(\gamma(\mathbf{1} + \sigma)) + \mathbf{w}$$

If T is much less than both x and $\hat{x}$, then $\gamma \to 0$ as well and the completely censored case of scenario 1 is reached.

An example of this response is shown in figure 5.22.

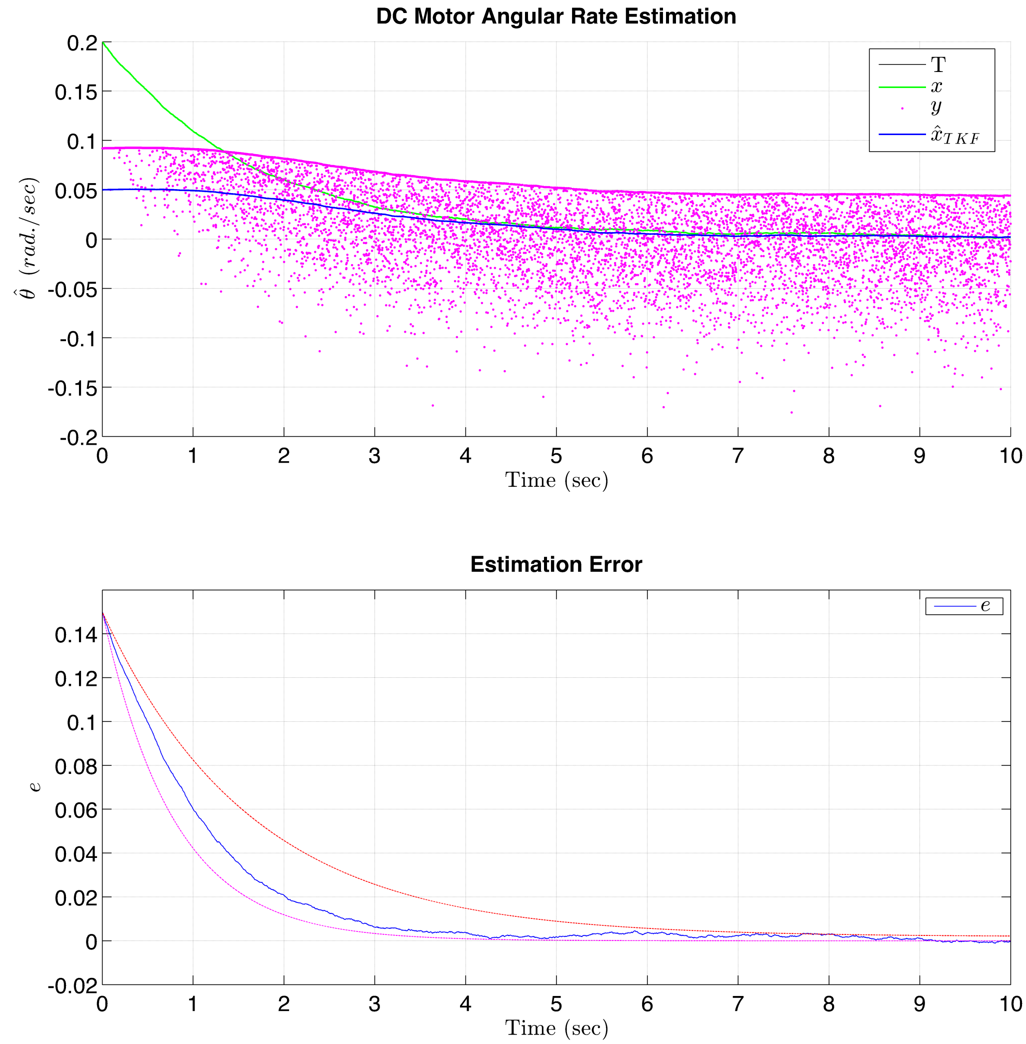

Figure 5.21: Scenario 5. Evolution of states $\dot{\theta}$ and $\hat{\dot{\theta}}$ over time with controlled censoring, using a TKF estimator with an expectation of censoring on $\hat{x}$ of .80.

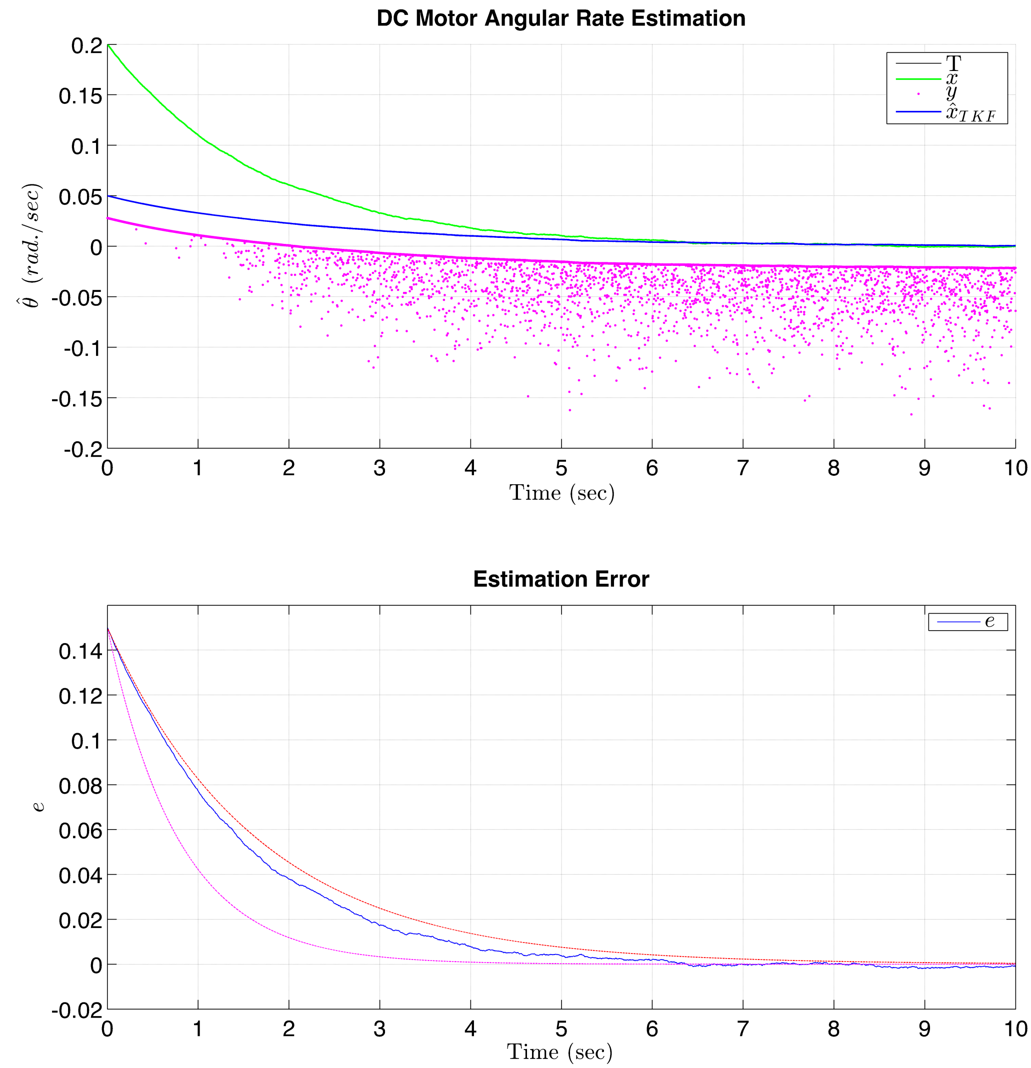

Figure 5.22: Scenario 6. Evolution of states $\dot{\theta}$ and $\hat{\dot{\theta}}$ over time with controlled censoring, using a TKF estimator with an expectation of censoring on $\hat{x}$ of .33.

Chapter 6

OUTPUT FEEDBACK WITH THE TOBIT KALMAN FILTER

In this chapter it is demonstrated via analysis and example how the Tobit Kalman filter can be used in an output feedback system. The previous chapter focused primarily on non-homogenous systems in order to characterize the behavior of the T.K.F. as a state estimator. It is shown how the T.K.F. can be used effectively as a state observer for closed loop control of dynamic systems. The effect of censoring on a standard LQG controlled system is analyzed, and it will be shown how and when such a system becomes unstable due to differing censoring scenarios. It is then shown that use of a T.K.F observer can recover stability under certain conditions. Use of both the standard T.K.F. observer and the time-caring steady state T.K.F. will be discussed, and novel control techniques utilizing T.K.F. specific parameters will be introduced. Effective control of the censoring limits will be demonstrated for multiple unique scenarios, and this concept will be extended with particular application towards computer vision based systems where effective target tracking under a multitude of difficult censoring scenarios may be present.

6.1 Setpoint Control with a State Observer

In chapter four the basic concepts of state feedback and output feedback control were defined and demonstrated, with particular focus on concepts of stability. In section

4.5.5, the LQG output feedback back controller was defined for systems in the form of

$$\begin{aligned} \dot{x} &= Ax + Bu + \bar{B}d, \quad x \in \Re^n, u \in \Re^k, d \in \Re^q \\ y &= Cx + n, \qquad\qquad\qquad\qquad y \in \Re^m \\ z &= Gx + Hu, \qquad\qquad\qquad\qquad z \in \Re^l \end{aligned} \tag{6.1}$$

by utilizing input u defined as

$$u = -K\hat{x} \tag{6.2}$$

where feedback gain K is defined according the LQR design process and is given by 4.41. The LQG state estimator for $\hat{x}$ is defined by 4.51, and the resulting closed loop LQG output feedback controller is then given by

$$\begin{aligned} \dot{x} &= Ax - BK\hat{x} + \bar{B}d \\ \dot{\hat{x}} &= (A - LC - BK)\hat{x} + Ly \end{aligned} \tag{6.3}$$

For uncensored systems the above output feedback controller is guaranteed by the separation principal to result in asymptotically stable closed loop stability. Suppose now instead of driving the system state to the origin it is desired to control system output z to a defined setpoint r. Such a condition is met when state x and input u reach an equilibrium point of (x_{eq}, u_{eq}) for which

$$\begin{aligned} \dot{x} = 0 = Ax_{eq} + Bu_{eq} \\ z = r = Gx_{eq} + Hu_{eq} \end{aligned} \tag{6.4}$$

or

$$\begin{bmatrix} -A & B \\ -G & H \end{bmatrix} \begin{bmatrix} -x_{eq} \\ u_{eq} \end{bmatrix} = \begin{bmatrix} 0 \\ r \end{bmatrix} \tag{6.5}$$

Consider now a change of variables with $\bar{x} := x - x_{eq}$ and $\bar{u} := u - u_{eq}$, with system dynamics mirroring the original system, resulting in

$$\begin{aligned} \dot{\bar{x}} &= A\bar{x} + B\bar{u} \\ \bar{z} &= G\bar{x} + H\bar{u} \end{aligned} \tag{6.6}$$

Application of the LQR design process for the above system then results in

$$\bar{u} = -K\bar{x} \tag{6.7}$$

Thus, the definition for the optimum control input can be found by changing back to the original state and input definitions, resulting in

$$\begin{aligned} u - u_{eq} &= -K\left(x - x_{eq}\right) \\ u &= -K\left(x - x_{eq}\right) + u_{eq} \end{aligned} \tag{6.8}$$

Output feedback for set point control is then constructed by replacing the state feedback term in 6.6-6.8, with the LQG state estimate $\hat{x}$, and thus

$$u = -K\left(\hat{x} - x_{eq}\right) + u_{eq} \tag{6.9}$$

And the LQG estimator of 6.3 is updated with 6.9 to form

$$\dot{\hat{x}} = (A - LC - BK)\hat{x} + BKx_{eq} + Bu_{eq} + Ly \tag{6.10}$$

Using another change of variables, now given by $\bar{x} = x_{eq} - \hat{x}$, the complete LQG output feedback setpoint controller is

$$\begin{aligned} \dot{\bar{x}} &= (A - LC - BK)\bar{x} - L(y - Cx_{eq}) \\ u &= K\bar{x} + u_{eq} \end{aligned} \tag{6.11}$$

6.2 The Tobit Kalman Filter as a State Observer

As discussed previously, the LQG output feedback controller operates under the concept of *certainly equivalence*. In this approach the controller is constructed under principals of optimal state feedback, however state estimates are utilized in place of the true states, which may not be directly available. In the case of LQR, the optimum control law consists of the state feedback term of

$$u(t) = -Kx(t) \tag{6.12}$$

And using certainty equivalence, the following control law is used when the full state cannot be measured,

$$u(t) = -K\hat{x}(t) \tag{6.13}$$

The LQG output feedback controller results from the use of a Kalman filter as a state observer to produce the state estimates utilized by 6.13. The resulting closed loop system is then given by 6.3, with L given by either the optimum Kalman gain or steady state Kalman gain. However, if censoring is present, the measurement model presented 6.16 is no longer valid near or in the censoring region. Thus, as shown previously, the standard Kalman filter produces biased state estimates which then are fed back into the true state dynamics via 6.13. It is shown that the bias induced by censoring can cause certain systems to become unstable when a naive LQG feedback is used when censoring is present.

However, by utilizing the Tobit Kalman filter, unbiased state estimates can be used to construct state estimates for 6.13 when censoring is present. Such a T.K.F. observer is constructed by adding the feedback term of 6.13 to the homogeneous T.K.F. estimator given by 5.6, resulting in the following state estimator formulation

$$\hat{\mathbf{x}}_{\mathbf{k+1}} = (\mathbf{A} - \mathbf{BK})\hat{\mathbf{x}}_{\mathbf{k}} + \mathbf{L}(\mathbf{y}_{\mathbf{k}} - \mathbf{E}[\hat{\mathbf{y}}_{\mathbf{k}}]) \tag{6.14}$$

Here, y_k is the measured system output and $E[\hat{y}_k]$ is dependent on the censoring characteristics of the system. For right censored system considered previously, $E[\hat{y}_k]$ would be defined by

$$\mathbf{E}[\hat{\mathbf{y}}_\mathbf{k}] = \mathbf{\Phi}\left(\tfrac{\mathbf{C}\hat{\mathbf{x}}_\mathbf{k}-\mathbf{T}}{\sigma}\right)\left[\mathbf{C}\hat{\mathbf{x}}_\mathbf{k} + \sigma\lambda\left(\tfrac{(\mathbf{T}-\mathbf{C}\hat{\mathbf{x}}_\mathbf{k})}{\sigma}\right)\right] + \mathbf{\Phi}\left(\tfrac{\mathbf{T}-\mathbf{C}\hat{\mathbf{x}}_\mathbf{k}}{\sigma}\right)\mathbf{T} \tag{6.15}$$

A complete description for a system of form 6.16, subjected to right censoring at T and which utilizes the T.K.F. observer of 6.14 to construct a T.K.F. LQG controller, is then given by

$$\begin{aligned}
\mathbf{x}_\mathbf{k+1} &= \mathbf{Ax} - \mathbf{BK}\hat{\mathbf{x}}_\mathbf{k} + \mathbf{Gw}_\mathbf{k} \\
\hat{\mathbf{x}}_\mathbf{k+1} &= (\mathbf{A}-\mathbf{BK})\hat{\mathbf{x}}_\mathbf{k} + \mathbf{L}(\mathbf{y}_\mathbf{k} - \mathbf{E}[\hat{\mathbf{y}}_\mathbf{k}]) \\
\mathbf{E}[\hat{\mathbf{y}}_\mathbf{k}] &= \mathbf{\Phi}\left(\tfrac{\mathbf{C}\hat{\mathbf{x}}_\mathbf{k}-\mathbf{T}}{\sigma}\right)\left[\mathbf{C}\hat{\mathbf{x}}_\mathbf{k} + \sigma\lambda\left(\tfrac{(\mathbf{T}-\mathbf{C}\hat{\mathbf{x}}_\mathbf{k})}{\sigma}\right)\right] + \mathbf{\Phi}\left(\tfrac{\mathbf{T}-\mathbf{C}\hat{\mathbf{x}}_\mathbf{k}}{\sigma}\right)\mathbf{T} \\
\mathbf{y}^*_\mathbf{k} &= \mathbf{Cx}_\mathbf{k} + \mathbf{n}_\mathbf{k} \\
\mathbf{y}_\mathbf{k} &= h(x_k) = \begin{cases} \mathbf{y}^*_\mathbf{k}, & \mathbf{y}^*_\mathbf{k} \leq \mathbf{T} \\ \mathbf{T}, & \mathbf{y}^*_\mathbf{k} > \mathbf{T} \end{cases}
\end{aligned} \tag{6.16}$$

The error dynamics of 6.16 equal that given by the homogeneous estimator given in 5.10 and repeated in 6.17, for the control law input is cancelled by its equal presence in each term.

$$\begin{aligned}
\mathbf{e}_\mathbf{k+1} &= \mathbf{x}_\mathbf{k} - \hat{\mathbf{x}}_\mathbf{k} \\
&= \mathbf{Ax}_\mathbf{k} - \mathbf{BK}\hat{\mathbf{x}}_\mathbf{k} + \mathbf{Gw}_\mathbf{k} - [(\mathbf{A}-\mathbf{BK})\hat{\mathbf{x}}_\mathbf{k} + \mathbf{L}(\mathbf{y}_\mathbf{k} - \mathbf{E}[\hat{\mathbf{y}}_\mathbf{k}])] \\
&= \mathbf{Ae}_\mathbf{k} - \mathbf{L}\left(\gamma(\mathbf{Cx}_\mathbf{k} - \sigma\lambda) + (\mathbf{1}-\gamma)\mathbf{T}\right) + \mathbf{L}(\hat{\gamma}(\mathbf{C}\hat{\mathbf{x}}_\mathbf{k} - \sigma\hat{\lambda}) + (\mathbf{1}-\hat{\gamma})\mathbf{T}) + \mathbf{Gw}_\mathbf{k} \\
&= \mathbf{Ae}_\mathbf{k} - \mathbf{L}(\gamma\mathbf{x}_\mathbf{k} - \hat{\gamma}\hat{\mathbf{x}}_\mathbf{k})\mathbf{C} + \mathbf{L}(\sigma(\phi-\hat{\phi}) + (\gamma-\hat{\gamma})\mathbf{T}) + \mathbf{Gw}_\mathbf{k}
\end{aligned} \tag{6.17}$$

Where, as defined previously,

$$\begin{aligned}\gamma &= \Phi\left(\frac{T - Cx_k}{\sigma}\right)\\ \hat{\gamma} &= \Phi\left(\frac{T - C\hat{x}_k}{\sigma}\right)\end{aligned} \tag{6.18}$$

$$\begin{aligned}\lambda &= \frac{\phi\left(\frac{T - Cx_k}{\sigma}\right)}{\Phi\left(\frac{T - Cx_k}{\sigma}\right)} = \frac{\phi\left(\frac{T - Cx_k}{\sigma}\right)}{\gamma}\\ \hat{\lambda} &= \frac{\phi\left(\frac{T - C\hat{x}_k}{\sigma}\right)}{\Phi\left(\frac{T - C\hat{x}_k}{\sigma}\right)} = \frac{\phi\left(\frac{T - C\hat{x}_k}{\sigma}\right)}{\hat{\gamma}}\end{aligned} \tag{6.19}$$

$$\begin{aligned}\phi &= \phi\left(\frac{T - Cx_k}{\sigma}\right) = \gamma\lambda\\ \hat{\phi} &= \phi\left(\frac{T - C\hat{x}_k}{\sigma}\right) = \hat{\gamma}\hat{\lambda}\end{aligned} \tag{6.20}$$

Because the control input cancels, and the resulting error dynamics of the T.K.F. LQG controller equals that of the homogeneous state estimator, the same notions of stability can be drawn as defined in 5.1.2. That is, the T.K.F. LQG controller can only remain stable as long as the T.K.F. observer remains stable as well, for the separation principal holds and certainty equivalence is valid. This means that, as can be expected intuitively, unstable systems subjected to a large degree of open-ended censoring cannot be guaranteed global stability. As shown previously there will alway exist a region in which the observer effectively reverts to open-loop prediction, the unstable nature of the system no longer permits a stable and unbiased state estimate, and the resulting closed loop controller is unstable.

However, for inherently stable and or marginally stable systems, the T.K.F. observer has already been shown to be a stable estimator. Thus, via the separation principal, the resulting T.K.F. LQG controller is stable as well. Additional constraints arise on effective performance however as the level of censoring is increased. Under heavy censoring the T.K.F. convergence dynamics slow, and may become slower than that of the LQR feedback control. Although theoretically stable, at such a point the state estimation may be too slow for practical control of the system, and either the control dynamics should be slowed or the level of censoring decreased in order to maintain a fast estimator with respect to the state dynamics. Such concepts and examples of effective closed loop control in the presence of censoring with a T.K.F. observer is demonstrated in the following sections.

In figure 6.1 the closed loop control of an open-loop stable system is shown for varying levels of increasing censoring, utilizing an LQG output feedback controller with both a standard Kalman observer and a Tobit Kalman observer. Here the system is represented by the DC motor speed model given in 5.59. Note that as censoring limit T is lowered the bias induced in the standard Kalman state estimate causes the true state to increase, as a non-zero input is consistently applied to the system. Because the system is open-loop stable the motor velocity does not diverge, however a steady state error is induced. The LQG controller utilizing a Tobit Kalman observer however is able to produce unbiased state estimates despite the presence of censoring, and thus maintains velocity near the origin with minimal performance degradation compared to that of the original uncensored system.

6.2.1 Step Responses Using a T.K.F. Observer

In figure 6.2 the closed loop step response of an open-loop stable system is shown for varying levels of increasing censoring, utilizing an LQG output feedback controller with both a standard Kalman observer and a Tobit Kalman observer. Again, the DC motor speed model is used as given in 5.59. Note that as with figure 6.1, when the censoring limit T is lowered the bias induced in the standard Kalman state estimate causes the true state to increase, as a non-zero input is consistently applied to the system. Because the system is open-loop stable the motor velocity does not diverge, however a steady state error is induced. The LQG controller utilizing a Tobit Kalman

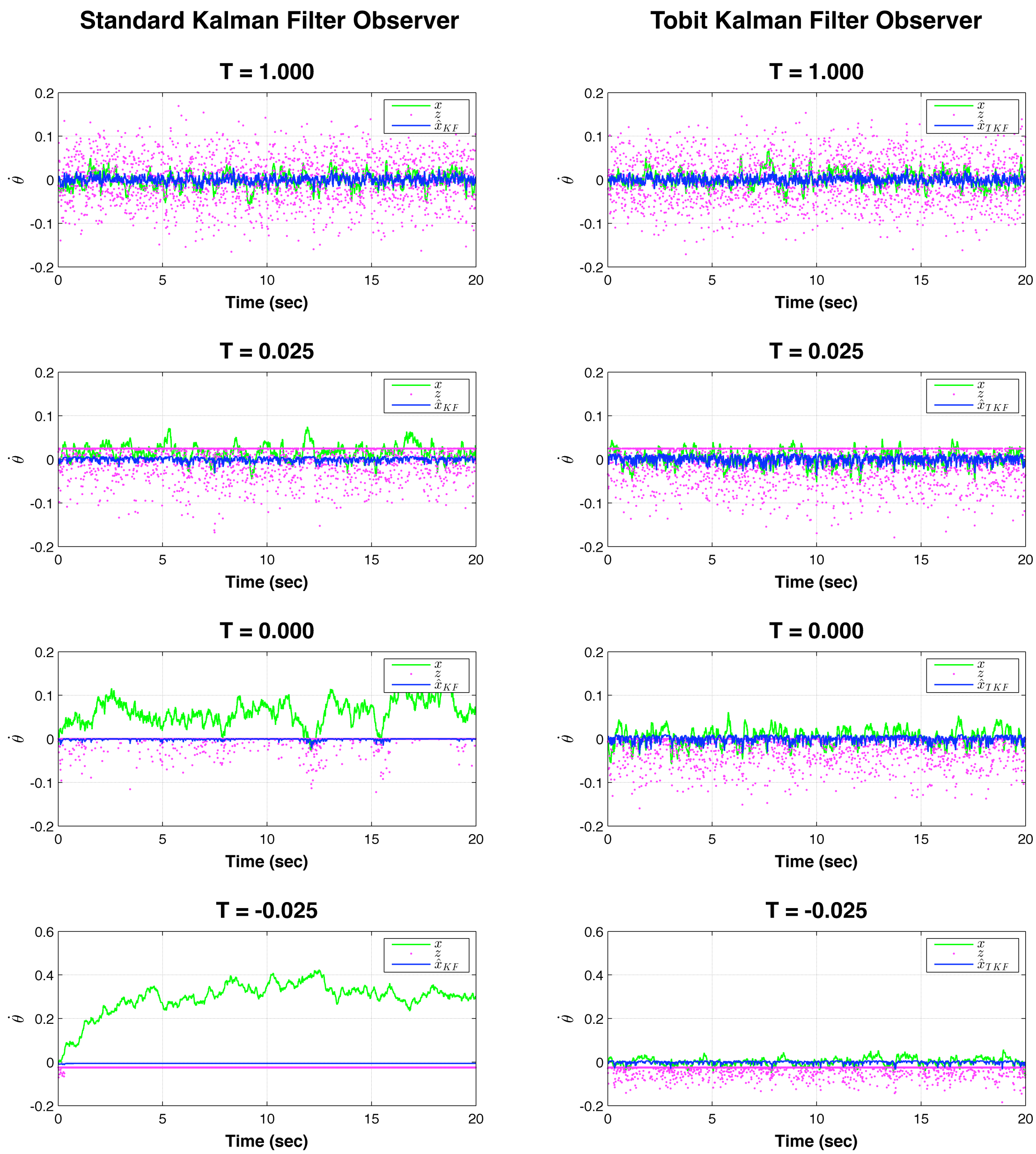

Figure 6.1: Comparison of LQG Control of a stable plant subjected to varying levels of censoring using a standard Kalman observer and a Tobit Kalman observer.

observer however is able to produce unbiased state estimates despite the presence of censoring, and thus maintains velocity near the reference with minimal performance degradation compared to that of the original uncensored system. Thus the Tobit LQG output feedback controller is able to control to reference inputs that are beyond the directly measurable limits of the system's output.

In figure 6.3 the closed loop step response of a marginally stable system is shown with censoring present below the desired reference position. LQG output feedback controllers with both a standard Kalman observer and a Tobit Kalman observer are compared. Here, the DC motor angular position model is used as given in 5.65. When the censoring limit T is lowered a bias is induced in the standard Kalman state estimate and a resulting non-zero input is consistently applied to the system. Because the system is marginally stable, with a pole at the origin, the non-zero input resulting from the standard Kalman estimator bias causes the state to grow unbounded. The LQG controller utilizing a Tobit Kalman observer however is able to produce unbiased state estimates despite the presence of censoring, and thus maintains position near the reference with minimal performance degradation compared to that of the original uncensored system. Even under heavy censoring, growth of the position away from the reference is avoided, and setpoint control to a position within the censored region is possible.

The state estimation error and tracking error of the standard Kalman filter and Tobit Kalman filter observers is shown figure 6.4. It is evident that during the initial free response time prior to the step input that the two controllers operate with the same error order of magnitude. However, as the step input is applied at $t = 4sec$, the controller with a standard Kalman observer begins to diverge in both state estimation and reference tracking. The Tobit Kalman LQG controller however not only fails to diverge in either error, it continues to decrease in both errors as time evolves.

Error covariance during the step response of figure 6.3 is shown in figure 6.5. It is clearly illustrated that standard Kalman observer remain "unaware" of the censoring present on the system output, and thus it's error covariance continues to converge to the

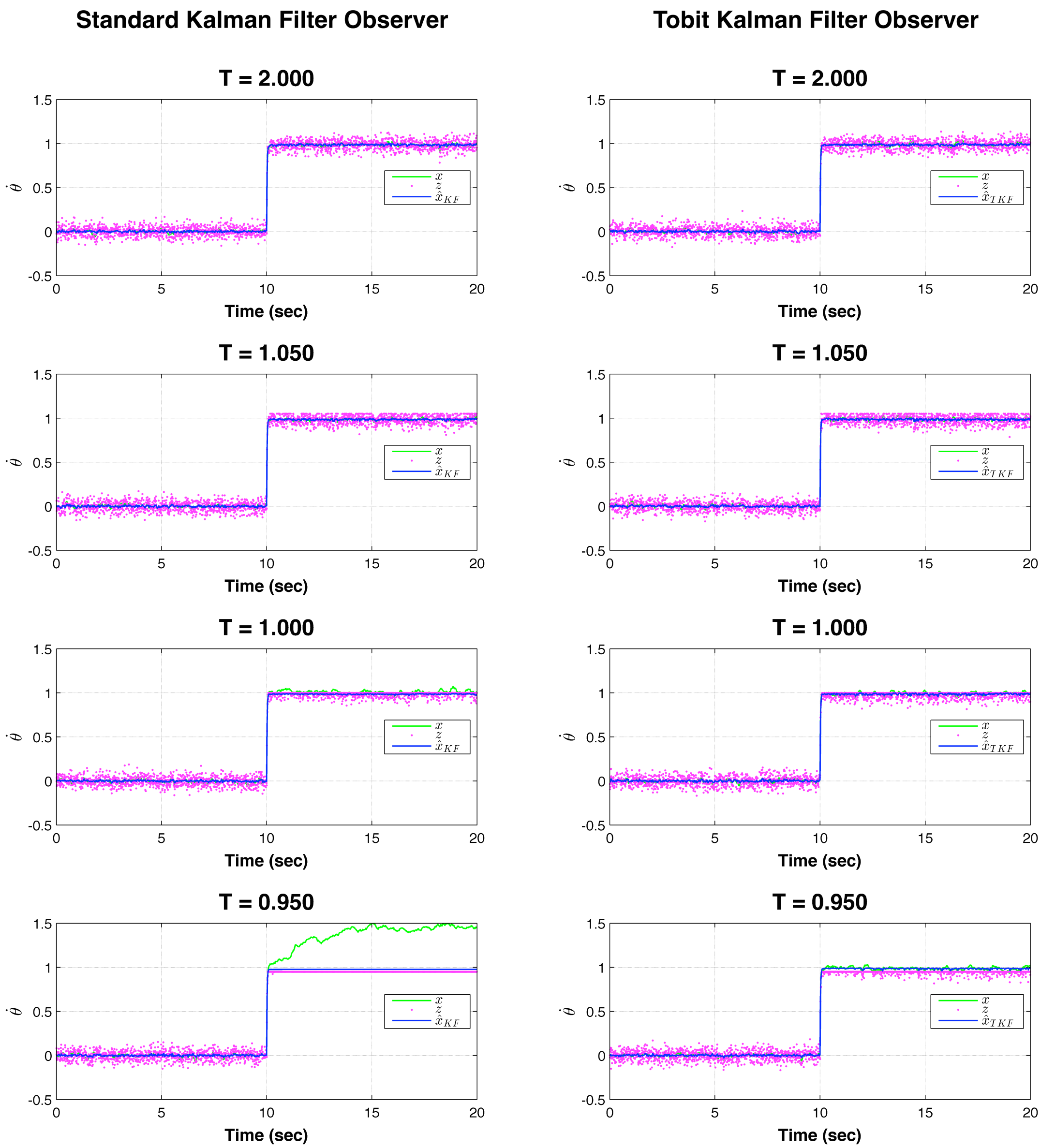

Figure 6.2: Comparison of step responses of LQG controllers subjected to varying levels of censoring on a stable plant, using a standard Kalman observer and a Tobit Kalman observer.

s

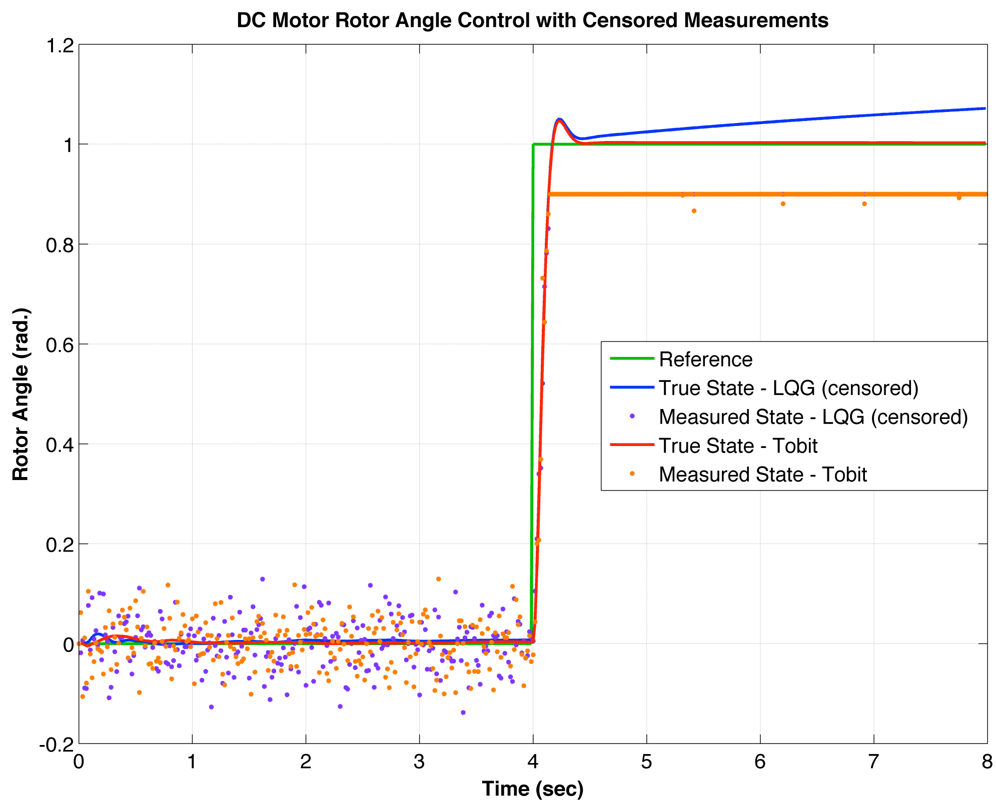

Figure 6.3: Step responses of a marginally stable system subjected to censoring using both a standard Kalman observer and a Tobit Kalman observer

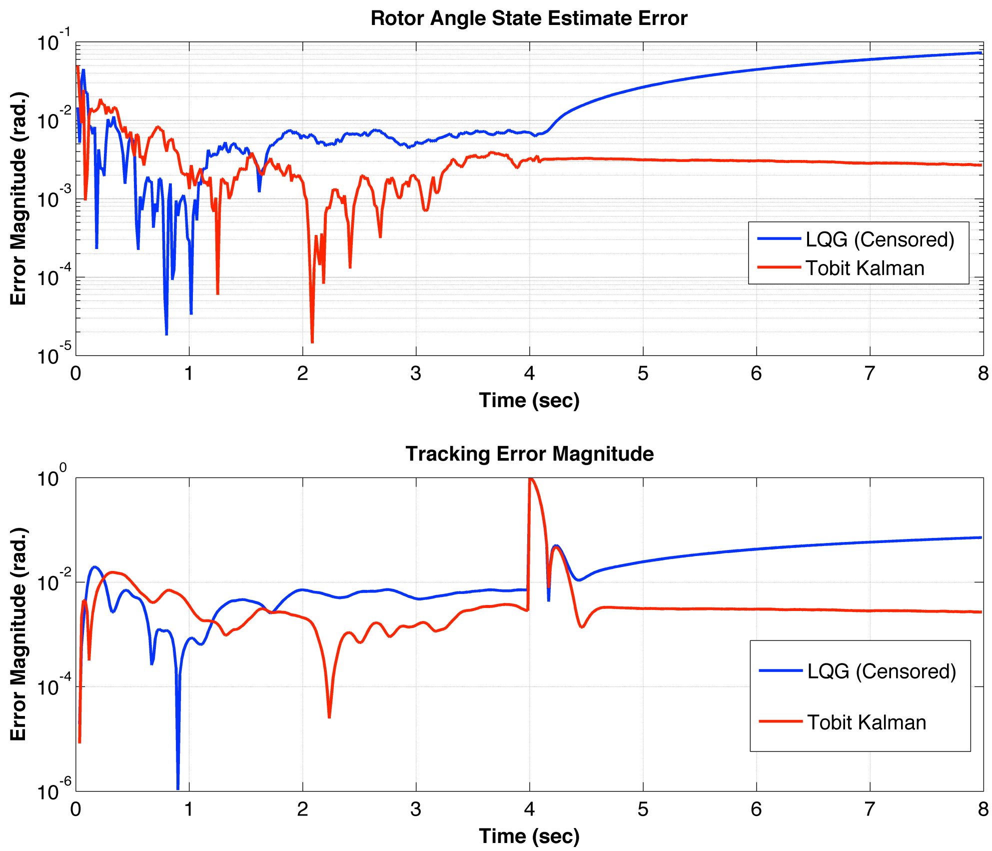

Figure 6.4: State estimate error and reference tracking error while performing LQG controller step response, for both the standard Kalman Filter and Tobit Kalman Filter

uncensored steady state value. The Tobit Kalman observer error covariance however converges to a higher steady state, indicating that censoring is present at a constant level. This is consistent with the fact that the step input combined with a constant censoring limit results in an expectation of censoring that remains constant.

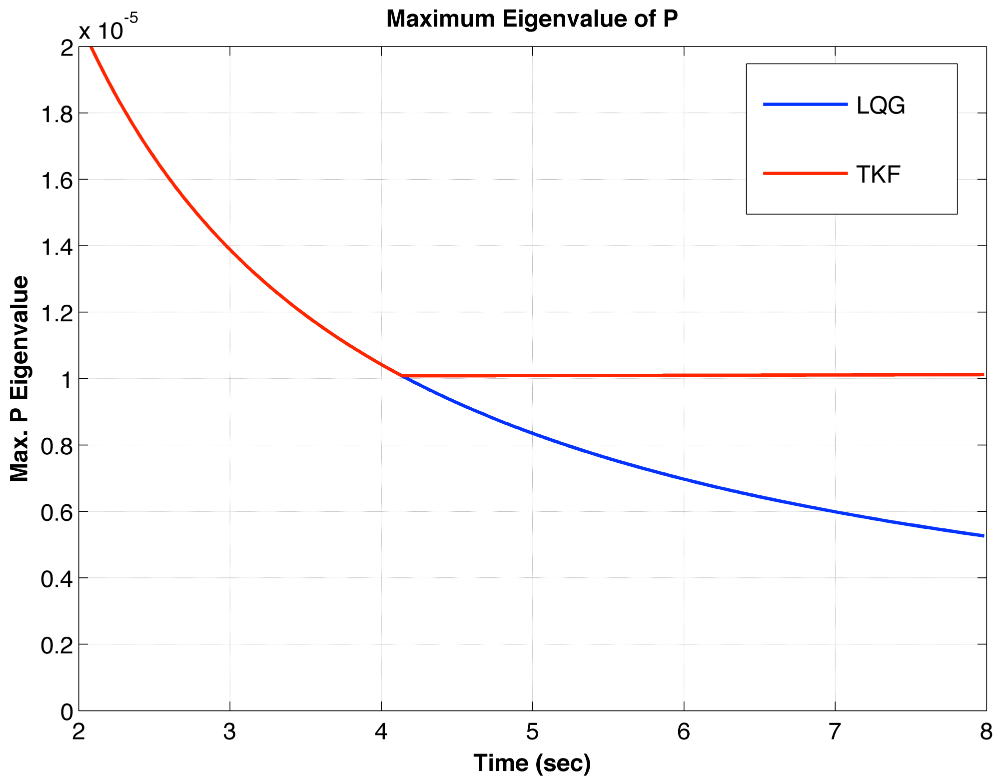

Figure 6.5: State estimate error covariance while performing LQG controller step response, for both the standard Kalman Filter and Tobit Kalman Filter observers. Standard Kalman error covariance continues to converge to the uncensored steady state error covariance, despite the presence of censoring.

This constant expectation of censoring can be calculated, assuming $x = 1$, as

$$\gamma = \Phi\left(\frac{T - C}{\sigma}\right) \tag{6.21}$$

Assuming this constant expectation of censoring, and using the principals of the steady state Tobit Kalman filter as introduced previously, the steady state Tobit Kalman error covariance shown in figure 6.5 can be predicted via the modified algebraic Ricatti Equation.

A more interesting output feedback scenario with a more complicated dynamic model in a censored environment is presented in the next section.

6.3 Mobile Robot Control

6.3.1 Introduction

Often the effect of censored data leads to either engineering the system away from regions where censoring may occur, treating censored measurements as normal measurements, or rejecting censored measurements completely. One common example of this is the censoring of received signal strength (RSS), which results in a drastically reduced ability to accurately estimate vehicle position via range estimates. A Tobit Kalman filter is used to produce a more accurate position estimate despite censoring on RSS, and it is shown how this estimate can be used as feedback in a linear-quadratic-Gaussian (LQG) regulator for position reference tracking.

Effectiveness of the Tobit Kalman filter is shown through simulation of mobile vehicle position estimation using received signal strength (RSS). Using a suitable RF model with known parameters, one can estimate range to a given transmitter. Given range to multiple transmitters with known locations, a position estimate for the receiver can be generated. However, due to the noisy nature of RSS, and a highly nonlinear relationship between signal strength and distance, previous methods of estimating receiver position often artificially censor RSS measurements below a certain limit due to lack of confidence in the measurement [9, 18]. Also, for the same reasons, many RSS indicators only report to a defined lower threshold. It is shown that despite censored RSS measurements, the Tobit Kalman filter produces effective distance to transmitter estimates, and therefore allow for more accurate position estimates with a larger range than typically seen before. By implementing the Tobit Kalman filter as a observer an output feedback controller is constructed which is able to control the vehicle to regions unattainable using the standard Kalman filter.

6.3.2 Mobile Vehicle Motion Model

For simulation purposes the simplified motion model shown below was used to generate vehicle position over time. The model is a two dimensional double integrator with a circular reference input r with radius ζ which starts at $(0, \zeta)$ with frequency ω. LQG regulation was used to implement a closed-loop controller, with performance of the standard Kalman filter and the Tobit Kalman filter as observers being compared.

Position control input is defined as

$$\mathbf{U_p} = \bar{N}r - K_{lqr}\hat{X}_p \tag{6.22}$$

, with $\bar{N}$ being a scaling factor, $\hat{X}_p$ being $(\hat{x}_p, \hat{y}_p)$ state estimates given by (6.43), and K_{lqr} being the optimal solution to the LQG control problem for the motion model outlined by (6.23,6.24). Weighting of output power vs. control effort is determined by the user. By use of the separation principal, feedback gain K_{lqr} is designed separately from that of the observer gain L. When the Tobit Kalman filter is used as an observer closed-loop control remains stable even when signal strength measurements are heavily censored, allowing for stable vehicle motion into regions unreachable by use of the standard Kalman filter alone.

The vehicle motion model can now be fully described by the following :

$$\begin{gathered}\mathbf{X_p(k+1) = A_p X_p(k) + B_p U_p(k) + G_p \sigma_q} \\ \mathbf{Y_p(k) = C_p X(k) + H_p \sigma_r}\end{gathered} \tag{6.23}$$

with

$$\begin{bmatrix} \dot{x}_p \\ \dot{x}_v \\ \dot{x}_p \\ \dot{x}_v \end{bmatrix} = \begin{bmatrix} 1 & \Delta & 0 & 0 \\ 0 & 1 & 0 & 0 \\ 0 & 0 & 1 & \Delta \\ 0 & 0 & 0 & 1 \end{bmatrix} \begin{bmatrix} x_p \\ x_v \\ y_p \\ y_v \end{bmatrix} + \begin{bmatrix} 1 & 0 \\ 0 & 0 \\ 0 & 1 \\ 0 & 0 \end{bmatrix} \begin{bmatrix} U_{p_1} \\ U_{p_2} \end{bmatrix} + \begin{bmatrix} \frac{1}{m}\frac{1}{2}\Delta^2 & 0 \\ \frac{1}{m}\Delta & 0 \\ 0 & \frac{1}{m}\frac{1}{2}\Delta^2 \\ 0 & \frac{1}{m}\Delta \end{bmatrix} \sigma_q \tag{6.24}$$

$$\begin{bmatrix} x_p \\ y_p \end{bmatrix} = \begin{bmatrix} 1 & 0 & 0 & 0 \\ 0 & 0 & 1 & 0 \end{bmatrix} \begin{bmatrix} x_p \\ x_v \\ y_p \\ y_v \end{bmatrix} + \begin{bmatrix} 1 & 0 \\ 0 & 1 \end{bmatrix} \sigma_r \tag{6.25}$$

At each time step k the range to transmitter i is defined as

$$d_i(k) = \sqrt{(x_p(k) - x_i)^2 + (y_p(k) - y_i)^2} \tag{6.26}$$

6.3.3 Radio Frequency Propagation Modeling

At true distance d_i the received signal strength (RSS) relative to transmitter i is modeled as shown in [31] as

$$RSS_i(k) = P_{tx} - PL(d_0) - 10\alpha log_{10}(\frac{d_i(k)}{d_0}) + \eta_{RSS} \tag{6.27}$$

Where P_{tx} is the transmitter power in dBm, α is the path-loss exponent, and

$$PL(d_0) = P_{tx}(1 - FSPL(d_0))$$

is the power loss at reference distance d_0, which is modeled as the free space path loss at d_0 given by

$$FSPL(d_0) = (\frac{4\pi d_0 f}{c})^2$$

Interference, multi-path errors, and fluctuations in transmitter and receiver power are accounted for by η_{RSS}, which has been shown to be accurately modeled as white Gaussian noise independent of d_i [31].

6.3.4 Model for Tracking

In order to arrange this system into a suitable form for tracking with a Tobit Kalman filter, assume a linear state transition model for d_i. For this, use a simple Brownian motion model as given below, because it represents the least informative model possible and highlights the Tobit Kalman filter's ability to provide accurate state estimation despite the lack of strong information about the true system.

$$d_i^*(k) = \beta_i d_i^*(k-1) + \sigma_d \tag{6.28}$$

Letting $\beta = 1$, taking the log_{10} of (6.28) and combining it with (6.27) yields a linear approximation of the system in state space form that is now suitable for Kalman filtering :

$$\begin{aligned} log_{10}(d_i^*(k)) &= log_{10}(d_i^*(k|k-1)) + \eta_d \\ RSS_i(k) &= -10\alpha log_{10}(d_i^*(k)) + (P_{tx} - PL(d_0)) + \eta_{RSS} \end{aligned} \tag{6.29}$$

The constant term $(P_{tx} - PL(d_0)) \approx 0$, and may be omitted. In order to accurately propagate the state estimate for $log_{10}(d_i^*)$ between time steps a correction factor U_{d_i} may be incorporated. A formulation for U_{d_i} is found by noticing that

$$\begin{aligned} d_i^*(k+1) &= \sqrt{(x_p(k+1) - x_i)^2 + (y_p(k+1) - y_i)^2} \\ &\approx (((x_p(k) + \Delta x_v(k)) - x_i)^2 \\ &\quad +((y_p(k) + \Delta y_v(k)) - y_i)^2)^{\frac{1}{2}} \\ &= \beta_i d_i^*(k) \end{aligned} \tag{6.30}$$

with

$$\begin{aligned} \beta_i &= \frac{d_i^* i(k+1)}{d_i^*(k)} \\ &= \sqrt{\frac{((x_p(k)+\Delta x_v(k))-x_i)^2+((y_p(k)+\Delta y_v(k))-y_i)^2}{(x_p(k)-x_i)^2+(y_p(k)-y_i)^2}} \end{aligned} \tag{6.31}$$

Therefore,

$$\begin{aligned} log_{10}(d_i^*(k+1)) &= log_{10}(\beta_i d_i^*(k)) + \eta_d \\ &= log_{10}(d_i^*(k)) + log_{10}(\beta_i) + \eta_d \end{aligned} \tag{6.32}$$

and now define

$$f_{u_i}(X_p) = \frac{1}{2} log_{10}(\beta_i) \tag{6.33}$$

Therefore, by taking $U_{d_i} = f_{u_i}(X_p) = \frac{1}{2} log_{10}(\beta_i)$ the log of distance can be more accurately transitioned between time steps. However, the simplified linear model of the system may be retained by setting $U_{d_i} = 0$, at the expense of reduced performance during censoring due to increased uncertainty in $log_{10}(d_i)$ state propagation.

This leads to the following model for tracking the distances to three transmitters :

$$\begin{aligned} \mathbf{X_d(k+1)} &= \mathbf{A_d X_d(k)} + \mathbf{B_d U_d(k)} + \mathbf{G_d} \boldsymbol{\eta_d} \\ \mathbf{Y_d(k)} &= \mathbf{C_d X_d(k)} + \mathbf{H_d} \boldsymbol{\eta_{rss}} \end{aligned} \tag{6.34}$$

$$\begin{bmatrix} \hat{log}_{10}(d_1) \\ \hat{log}_{10}(d_2) \\ \hat{log}_{10}(d_3) \end{bmatrix} = \begin{bmatrix} 1 & 0 & 0 \\ 0 & 1 & 0 \\ 0 & 0 & 1 \end{bmatrix} \begin{bmatrix} log_{10}(d_1) \\ log_{10}(d_2) \\ log_{10}(d_3) \end{bmatrix} + \begin{bmatrix} 1 & 0 & 0 \\ 0 & 1 & 0 \\ 0 & 0 & 1 \end{bmatrix} \begin{bmatrix} f_{u_1}(X_p) \\ f_{u_2}(X_p) \\ f_{u_3}(X_p) \end{bmatrix} + \begin{bmatrix} 1 & 0 & 0 \\ 0 & 1 & 0 \\ 0 & 0 & 1 \end{bmatrix} \eta_d \tag{6.35}$$

$$\begin{bmatrix} RSS_1 \\ RSS_2 \\ RSS_3 \end{bmatrix} = \begin{bmatrix} -10\alpha & 0 & 0 \\ 0 & -10\alpha & 0 \\ 0 & 0 & -10\alpha \end{bmatrix} \begin{bmatrix} \hat{log}_{10}(d_1) \\ \hat{log}_{10}(d_2) \\ \hat{log}_{10}(d_3) \end{bmatrix} + \begin{bmatrix} 1 & 0 & 0 \\ 0 & 1 & 0 \\ 0 & 0 & 1 \end{bmatrix} \eta_{rss} \tag{6.36}$$

As shown in [31] , σ_d can be modeled as

$$\sigma_d(k) = d_i(k) \frac{\sigma_{rss}}{10\alpha} \tag{6.37}$$

which, when substituted into (6.28), yields

$$\begin{aligned} d_i(k+1) &= d_i(k) + \sigma_d(k) \\ &= d_i(k) + d_i(k)\tfrac{\sigma_{rss}}{10\alpha} \\ &= d_i(k)\left(1 + \tfrac{\sigma_{rss}}{10\alpha}\right) \end{aligned} \tag{6.38}$$

Taking the log_{10} of both sides yields,

$$\begin{aligned} log_{10}(d_i(k+1)) &= log_{10}(d_i(k)\left(1 + \tfrac{\sigma_{rss}}{10\alpha}\right)) \\ &= log_{10}(d_i(k)) + log_{10}\left(1 + \tfrac{\sigma_{rss}}{10\alpha}\right) \end{aligned} \tag{6.39}$$

and therefore an approximation for η_d is made as

$$\eta_d = log_{10}\left(1 + \tfrac{\sigma_{rss}}{10\alpha}\right) \tag{6.40}$$

The full combined system model for tracking vehicle position, velocity, and distance to transmitters can now formed as

$$\begin{aligned} \begin{bmatrix} X_p(k+1) \\ X_d(k+1) \end{bmatrix} &= \begin{bmatrix} A_p & 0 \\ 0 & A_d \end{bmatrix} \begin{bmatrix} X_p(k) \\ X_d(k) \end{bmatrix} + \begin{bmatrix} B_p & 0 \\ 0 & B_d \end{bmatrix} \begin{bmatrix} U_p(k) \\ U_d(k) \end{bmatrix} + \begin{bmatrix} G_p & 0 \\ 0 & G_d \end{bmatrix} \begin{bmatrix} \sigma_q \\ \eta_d \end{bmatrix} \\ \begin{bmatrix} Y_p(k) \\ Y_d(k) \end{bmatrix} &= \begin{bmatrix} C_p & 0 \\ 0 & C_d \end{bmatrix} \begin{bmatrix} X_p(k) \\ X_d(k) \end{bmatrix} + \begin{bmatrix} H_p & 0 \\ 0 & H_d \end{bmatrix} \begin{bmatrix} \sigma_r \\ \eta_{RSS} \end{bmatrix} \end{aligned} \tag{6.41}$$

Finally, estimating range to transmitter i is accomplished by transforming the state $log_{10}(d_i(k))$ by

$$\hat{d}_i(k) = 10^{(log_{10}(d_i(k)))} = d_i^*(k)$$

6.3.5 Estimating Position Using Range Estimates

The circle upon which the receiver lies when at position (x_p, y_p), with range d_i from transmitter i located at position (x_i, y_i) is given by

$$d_i^2 = (x_p - x_i)^2 + (y_p - y_i)^2 \tag{6.42}$$

By using multiple transmitters with known locations, one can estimate the unknown position of the receiver by using range estimates $\hat{d}_i$ to solve for the intersection of these overlapping circles. Expanding (6.42) for multiple transmitters, three for simplicity, yields a linear system as given below.

$$\mathbf{R} = \mathbf{A}\hat{\mathbf{X}}_\mathbf{p}$$

$$\mathbf{R} = \begin{bmatrix} \hat{d_1}^2 - \hat{d_2}^2 \\ \hat{d_1}^2 - \hat{d_3}^2 \\ \hat{d_2}^2 - \hat{d_3}^2 \end{bmatrix}$$

$$\mathbf{A} = \begin{bmatrix} (2x_2 - 2x_1) & (2y_2 - 2y_1) & (x_1^2 + y_1^2 - x_2^2 - y_2^2) \\ (2x_3 - 2x_1) & (2y_3 - 2y_1) & (x_1^2 + y_1^2 - x_3^2 - y_3^2) \\ (2x_3 - 2x_2) & (2y_3 - 2y_2) & (x_2^2 + y_2^2 - x_3^2 - y_3^2) \end{bmatrix} \tag{6.43}$$

$$\hat{\mathbf{X}}_\mathbf{p} = \begin{bmatrix} \hat{x_p} \\ \hat{y_p} \\ 1 \end{bmatrix}$$

Where $\mathbf{R}$ is a vector of squared range estimate differences and $\mathbf{A}$ is a constant matrix dependent on the transmitter locations. Solving the system for $\hat{\mathbf{X}}_\mathbf{p}$ in a least-squares sense yields an estimate $(\hat{x}_p, \hat{y}_p)$ of true receiver position (x_p, y_p). Matrices $\mathbf{R}$ and $\mathbf{A}$ can be expanded to N transmitters by following the above form.

In simulation $\hat{\mathbf{X}}_{\mathbf{p}}$ is then combined with simulated measurements RSS_{m_i}, calculated according to (6.27), to form the censored measurement vector $\mathbf{Z}$ used for the innovation process of the T.K.F.

$$\mathbf{Z} = \begin{bmatrix} \hat{x}_p \\ \hat{y}_p \\ RSS_{m_1} \\ RSS_{m_2} \\ RSS_{m_3} \end{bmatrix} \tag{6.44}$$

$$RSS_{m_i} = \begin{cases} RSS_{m_i}, & RSS_{m_i} > T \\ T, & RSS_{m_i} \leq T \end{cases}$$

The distance estimation states are affected by any censoring imposed on the measured RSS_{m_i}, then affecting the raw distance estimate $\hat{d}_i(k)$, which in turn degrades the localization estimate. By censoring the measured RSS_{m_i} at -90 dBm, the effectiveness of the Tobit Kalman filter compared to the standard Kalman filter is apparent.

6.3.6 Simulation Setup

For the following simulation it was desired to show the capabilities of the Tobit Kalman filter in a general system, not to provide an optimal representation of RSS and its use directly for position estimation and control under realistic dynamics. Therefore, for simplicity, desired vehicle motion was restricted to a circle with constant radius $\zeta = 27$m with ω set to traverse approximately one cycle in the given time period. The RF model has $P_{tx} = 20\ dBm, d_0 = 1, \alpha = 6$, and $\eta_{RSS} = 2$. The number of transmitters was fixed to three with $(x_1, y_1) = (0, 10), (x_2, y_2) = (10, -10), (x_3, y_3) = (-10, -10)$, and $\mathbf{A}$ in (6.43) was constant at all times according to these positions. Initial conditions were set such that velocity $(x_v(0), y_v(0)) = 0$, position $(x_p(0), y_p(0)) = (0, 0)$, $log_{10}(d_i)$ were set to their true values, $\sigma_q = .1$ and $\sigma_r = .05$, and covariance $\Psi = .1$. For solution of the LQG problem for feedback gain K_{lqr}, output control vs. control effort was weighted 1000:1 in the cost minimization, meaning that higher control inputs were favored in exchange for faster response.

As the given example is only meant to be a demonstration for the effectiveness of the Tobit Kalman filter in a censored situation, non-linearities in the formulation of $\mathbf{U_p}$ and $\hat{d}_i$ are ignored. Both effects, while not trivial, are presented to both the standard Kalman filter and the Tobit Kalman filter equally, and therefore a direct comparison between the two remains valid. The following simulation is meant to be a novel approach to the localization problem and does not claim to be the optimal solution.

6.3.7 Results

A two-dimensional representation of the scenario is presented in fig. 6.6, in which the mobile vehicle has traversed the space, attempting to follow the circular reference input using LQG regulation with a Tobit filter based observer. The locations of the three transmitters are noted by the labeled cross marks, with the range at which each transmitter's measured RSS by the vehicle is thresholded (in the absence of η_{RSS}). A standard Kalman filter observer was run in parallel for comparison, but it's state estimate was not used in control feedback. It is readily apparent that the standard Kalman filter can only accurately estimate position when well within the -90 dBm range of all three transmitters, as dictated by (6.43). As the mobile vehicle approaches the thresholded region range to transmitter estimates become heavily biased due to RSS censoring and the least squares position approximation degrades. This censoring on the RSS measurements in shown in fig. 6.7, and it's effect on the estimation of $log_{10}(d_i^*(k))$ for $i = 1$ is shown in fig. 6.8.

Position estimation error is shown in fig. 6.9 as a comparison between the presented filters. For the short period of time in which all three transmitters are uncensored the filter errors converge as the Tobit Kalman filter converges to an uncensored standard Kalman filter. However, for a large majority of the time at least

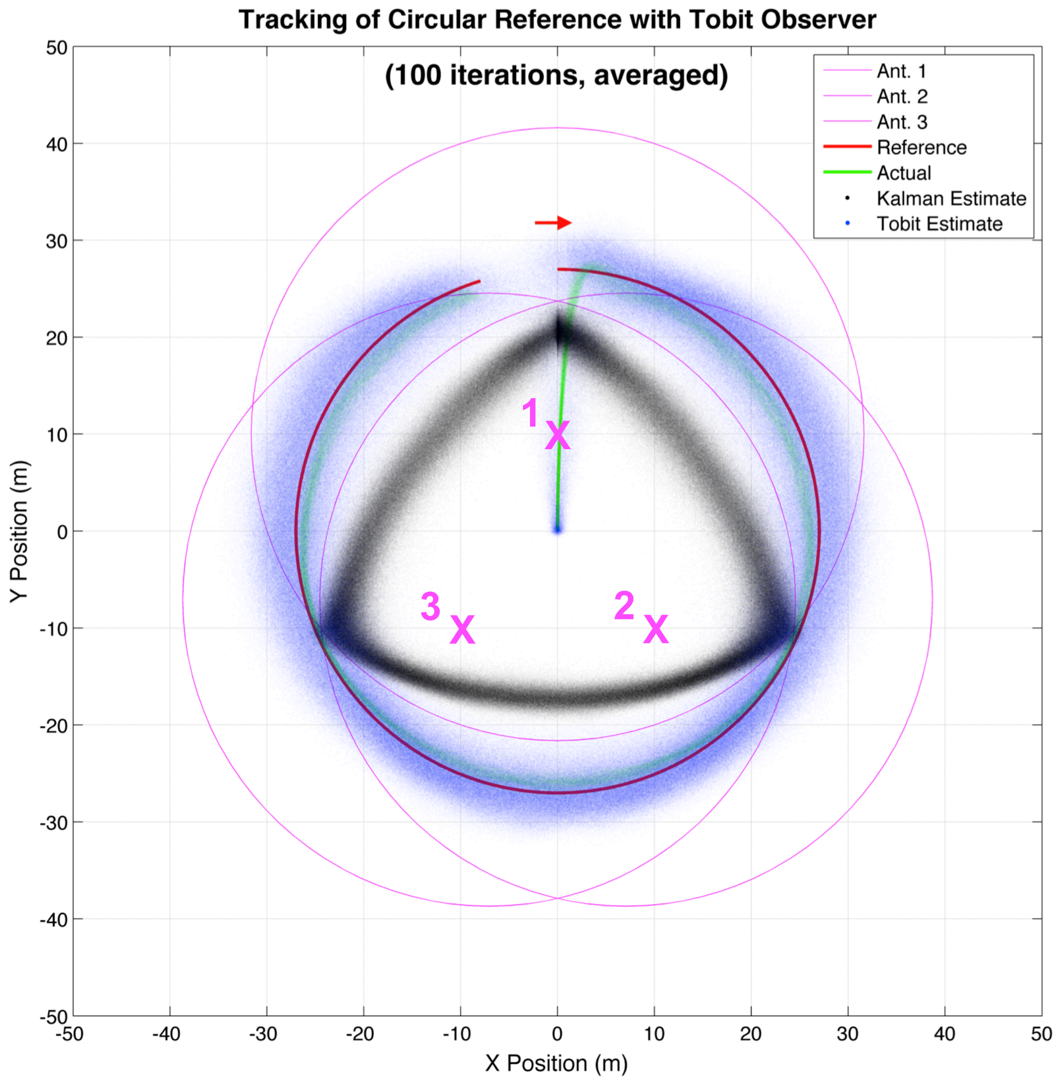

Figure 6.6: Position estimate of the vehicle in 2D space. 100 iterations combined; parameters as given in section 6.3.6. Ranges at which RSS would be censored (-90 dBm) is shown. The standard Kalman filter can only estimate a position when within the -90 dBm range of all three transmitters. The Tobit Kalman filter however successfully propagates a range estimate for any transmitter below this threshold, allowing a more accurate position estimate to be calculated at all times. Closed loop LQG control is stable, and the vehicle adequately tracks the reference trajectory into the censored regions.

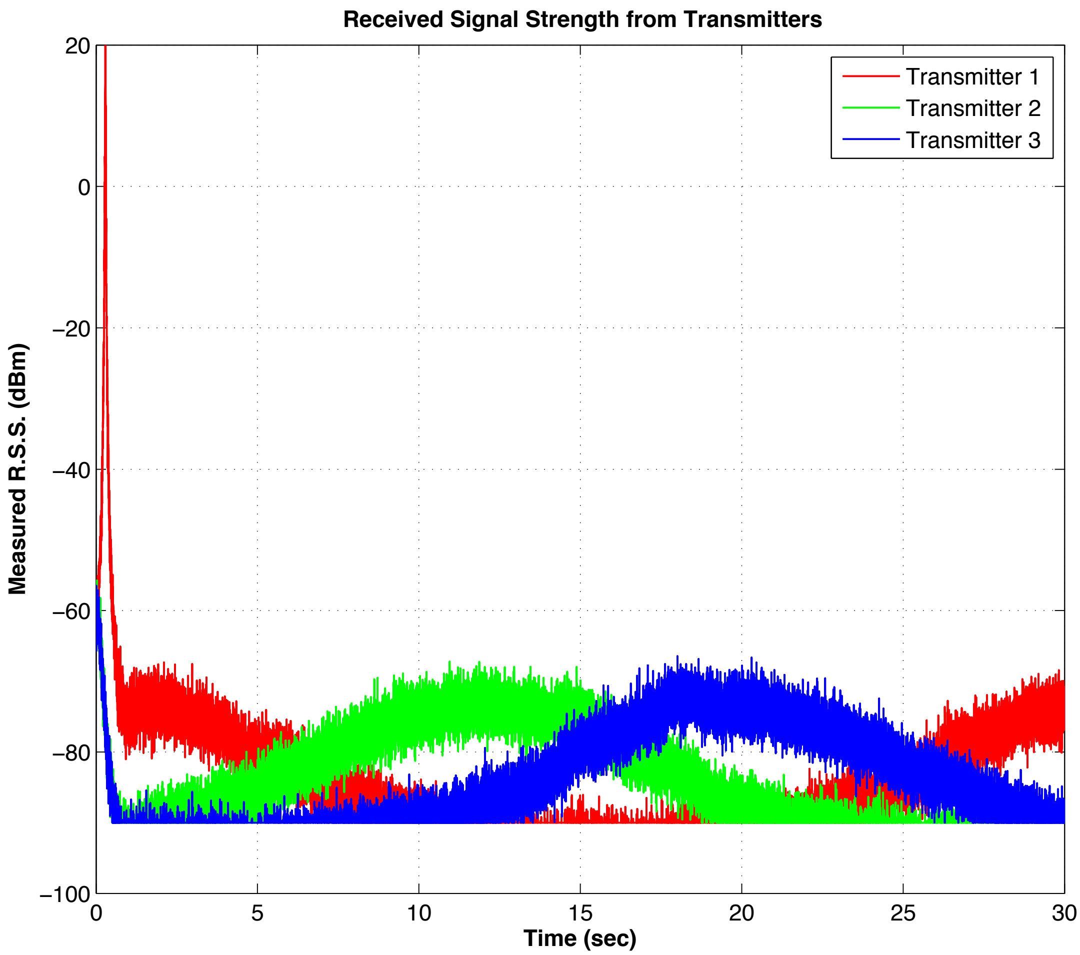

Figure 6.7: Received Signal Strength from all three transmitters vs. time. RSS is only reported to -90 dBm, at which point the measurement is left censored.

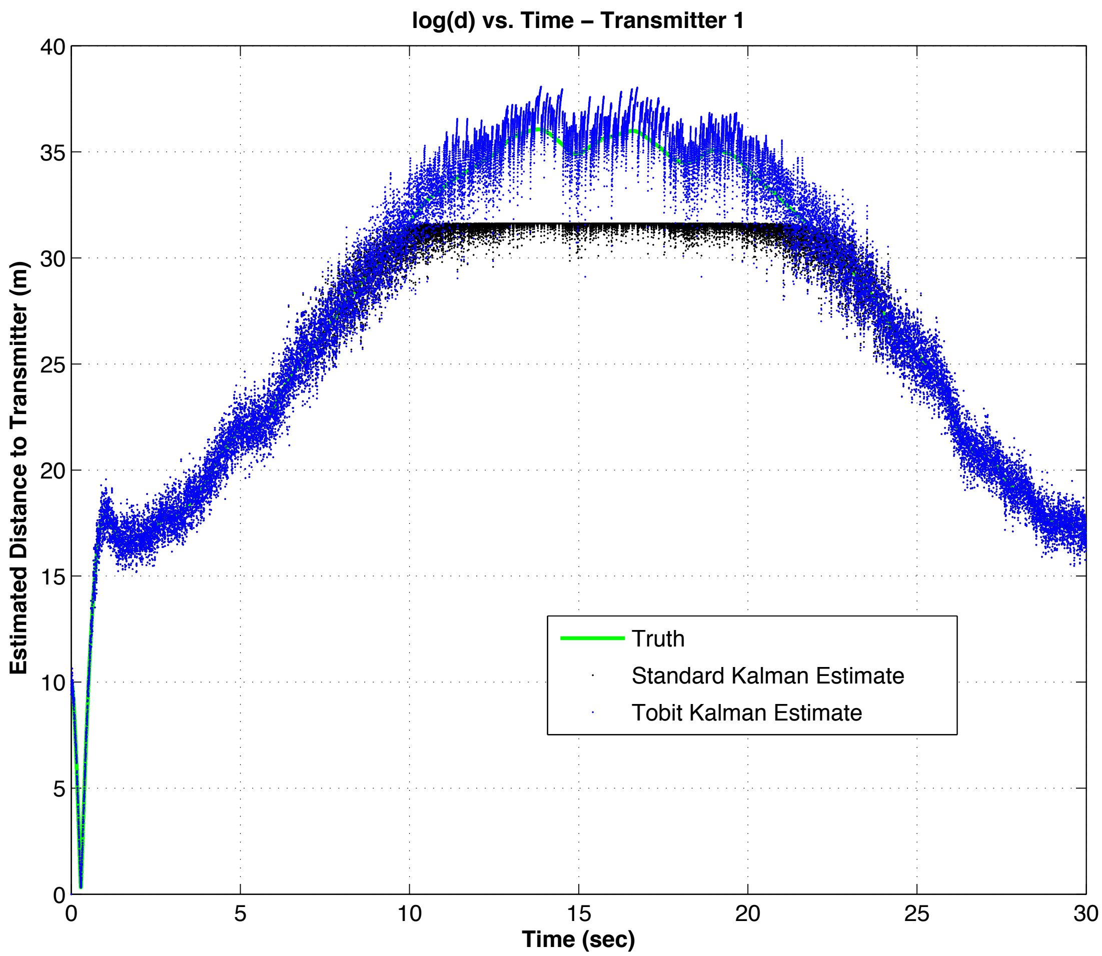

Figure 6.8: Comparison of tracking the state $log_{10}(d_1)$. Censoring in the measurement of RSS_1 results in the standard Kalman filter to fail to adequately track range to transmitter 1, which propagates to a poor position estimate. The Tobit Kalman filter however manages to estimate state values even in the presence of censoring and noise

one transmitter is out of range and often reads as a censored RSS measurement by the vehicle. The standard Kalman filter behaves poorly because its ignorance of censored measurements causes it to trust all measurements with equal weight, even when censored for long periods of time, resulting in a biased estimate. The Tobit Kalman filter is able to generate a state estimate well outside the range of the three overlapping transmitters, and thus is able to maintain a lower position estimate error at nearly all times. Although it is not explicitly shown here, attempting reliable closed-loop LQG control with a standard Kalman filter observer severely restricts the maximum radius ζ of the reference trajectory to within approximately 19m with the given parameters, a nearly 33% reduction in radius compared to that attainable by the Tobit Kalman filter. The bias introduced into the standard Kalman estimate by censoring causes the closed-loop to go unstable if the tracking radius is increased beyond this limit.

The Tobit Kalman filter cannot completely overcome the inherent lack of information that a censored measurement presents, and therefore cannot entirely account for the dynamics of the vehicle's motion with respect to a censored transmitter. At this point the system model becomes an important factor, with more informative models yielding improved state estimates than models with an inherent lack of information. Without an informative dynamic model when measurements are censored the full system behavior is unobservable and cannot be accounted for, but the Tobit Kalman filter does use the information that measurements are censored to its full potential and provides an optimal, real-time, recursive state estimation given the available information.

When the true state of the system is far from the censoring region this formulation converges to the standard Kalman filter. When the true state of the system is near the censoring region, and measurements become censored, the Tobit Kalman filter provides an unbiased state estimation that far outperforms the standard Kalman filter, and effective closed-loop reference tracking is possible. The effectiveness of the Tobit Kalman filter and a potential application for its use is demonstrated by estimation and control of vehicle position using censored received signal strength as a range to transmitter estimate. The Tobit Kalman filter is able to estimate vehicle position with lower

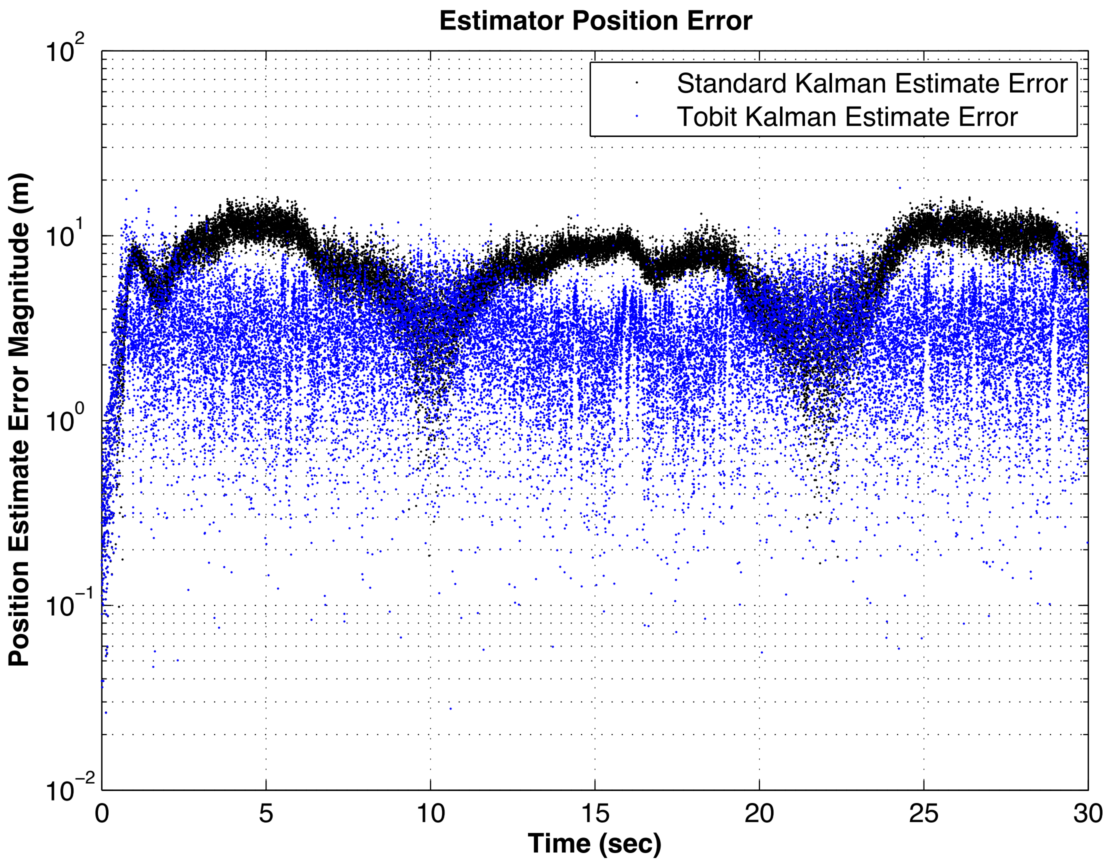

Figure 6.9: Comparison of position error magnitude vs time. As expected, the standard Kalman filter performs poorly because of its ignorance of censored measurements. The Tobit Kalman filter maintains a lower and more consistent mean square error.

mean-squared error despite censored measurements and high noise, while the standard Kalman filter provides a heavily biased and range limited estimate. Is has been shown that in cases where the censoring model is well understood there is a significant amount of information present in what cannot be observed, which is information that can be exploited by the Tobit Kalman filter and has previously largely been ignored.

6.4 Output Feedback With a Steady State Tobit Kalman Filter

In the previous sections output feedback assuming constant censoring limits was assumed. For reasons discussed previously, constant censoring limits impose restrictions on the possible performance of both the Tobit Kalman state estimator and resulting closed loop control using a Tobit Kalman observer. Namely, there may exist open-ended censored regions in which the T.K.F. estimator converges to that of an open-loop predictor, and performance of the subsequent closed loop control depends on the dynamics of the particular system and the desired reference. However, as has be demonstrated in chapter five, the ability to control the censoring limit T may allow the T.K.F. estimator to converge to a steady state and recover global asymptotic stability under certain conditions and assumptions.

For example, consider again the marginally stable DC motor angular position model as used in section 6.2.1. What If, instead of a constant censoring limit T, a variable censoring limit of the form of 5.68 or 5.73 was utilized? The step response shown in figure 6.10 shows such a system, in which a T.K.F. LQG controller is utilized with a censoring T set such that an expectation of censoring of .95 is maintained at all times.

As seen previously, if initial convergence is assumed then the estimator dynamics converge to those given by by 3.4.2. With the addition of a reference input the system becomes

$$
\begin{aligned}
\mathbf{T_k} &= \mathbf{C\hat{x}_k} + \sigma\mathbf{\Phi}(\alpha)^{-1} \\
\mathbf{u_k} &= \mathbf{\bar{N}r_k} - \mathbf{K\hat{x}_k} \\
\mathbf{x_{k+1}} &= \mathbf{Ax_k} + \mathbf{Bu_k} + \mathbf{w_k} \\
\mathbf{\hat{x}_{k+1}} &= (\mathbf{A} - \mathbf{L}\gamma\mathbf{C})\mathbf{\hat{x}_k} + \mathbf{Bu_k} + \mathbf{L}(\gamma\mathbf{Cx_k})
\end{aligned}
\tag{6.45}
$$

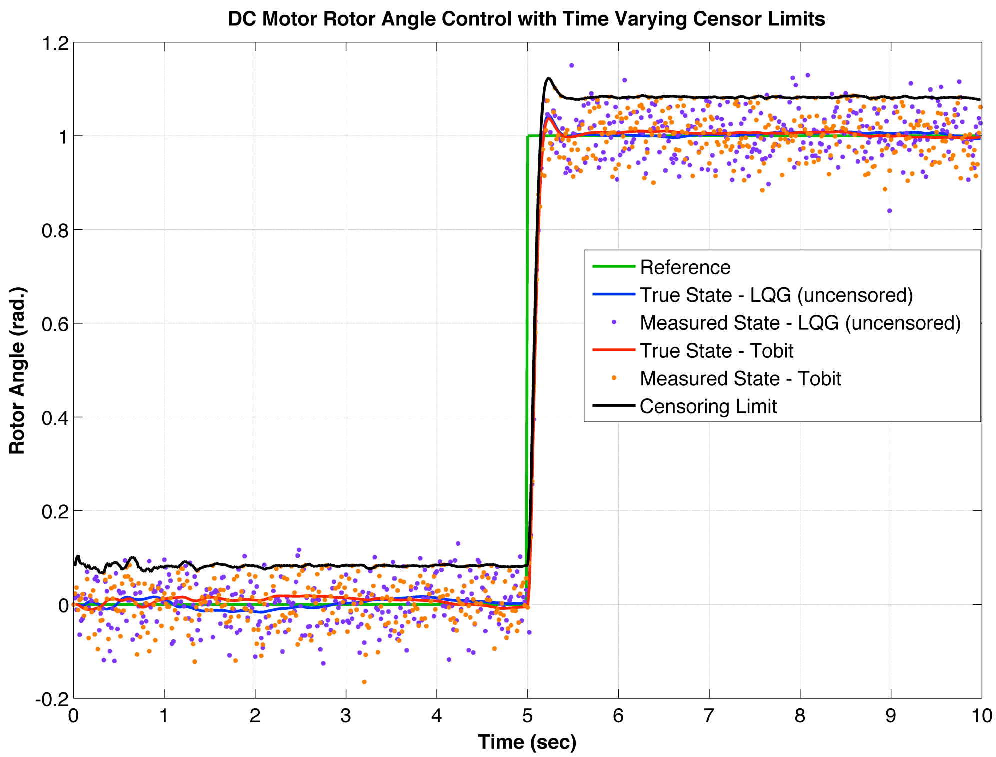

Figure 6.10: Step response of a Tobit LQG controller with censoring limit T set to maintain an expectation of censoring of .95. Response of an LQG controller with an *uncensored* standard Kalman filter observer is shown for comparison.

Note in figures 6.10,6.11 that an expectation of being *uncensored* for 95% of the measurements is maintained for a relatively low censoring limit. Thus, if maintaining a high censoring limit T to avoid censoring entirely has an associated cost, it may be very beneficial to use a Tobit Kalman observer and smartly control the censoring limit

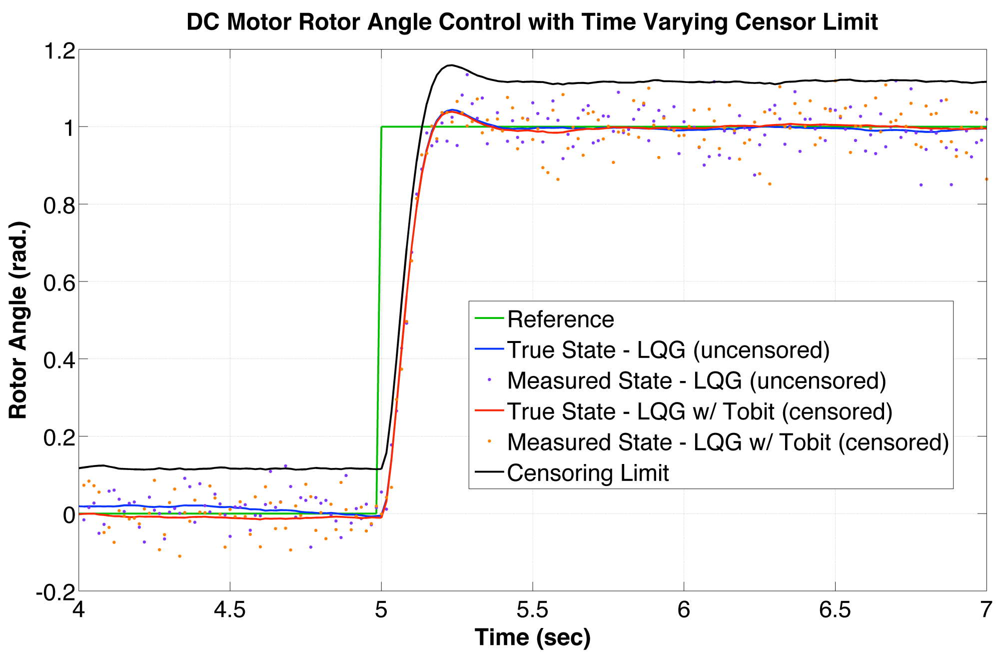

Figure 6.11: Detailed view of the step response of a Tobit LQG controller with censoring limit T set to maintain an expectation of censoring of .95. Response of an LQG controller with an *uncensored* standard Kalman filter observer is shown for comparison.

according to the above rule. As shown, even when censored is purposefully allowed, minimal degradation of estimation and control performance can be achieved by using a Tobit Kalman observer.

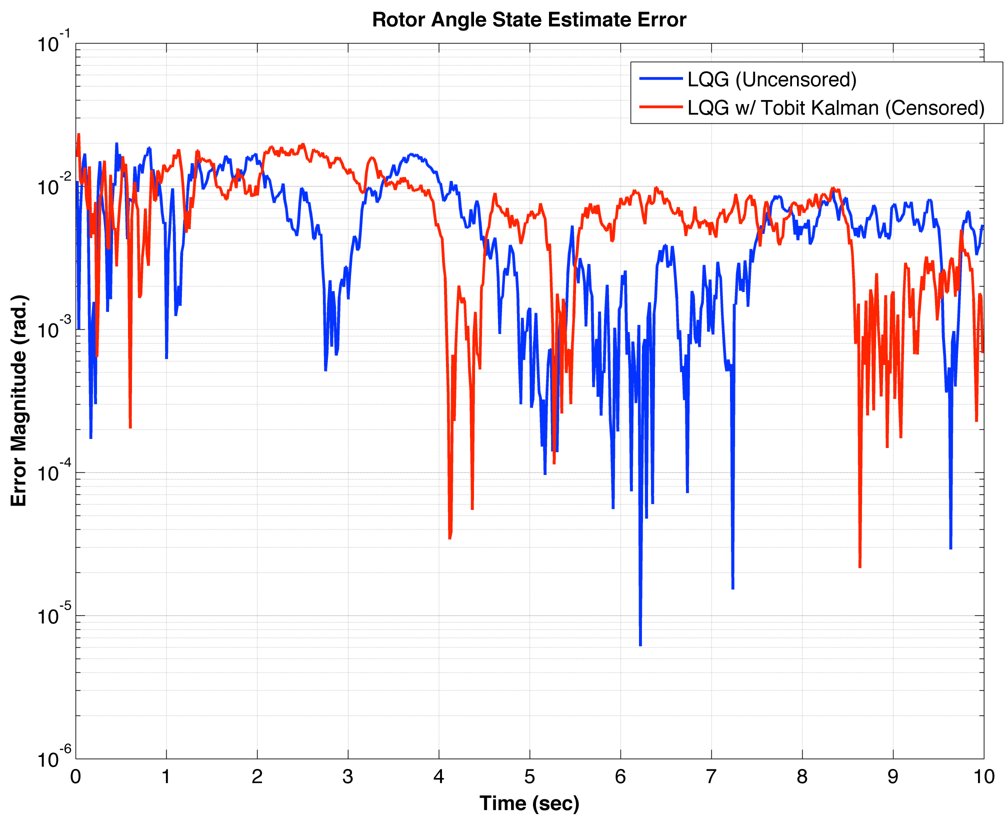

Figure 6.12: Comparison of state estimation error of a Tobit Kalman filter with 5% *censored* measurements, and an *uncensored* standard Kalman filter, for the step response in figure 6.10.

In figure 6.12 the state estimation error between the *uncensored* Kalman filter and the 5% *censored* Tobit Kalman filter is shown. It is apparent that even though the Tobit observer has some degree of censored measurements, the state estimation error remains indistinguishable from that of the standard Kalman observer. Likewise, tracking error between the two observer follows a similar pattern, as shown in figure 6.13.

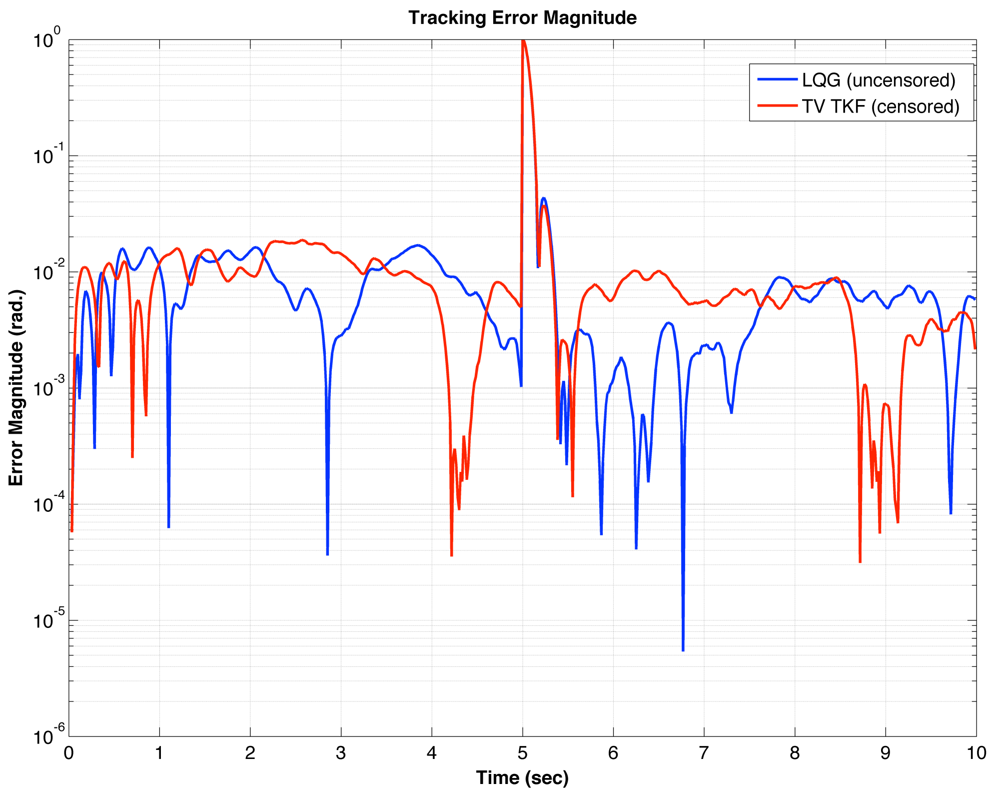

Figure 6.13: Comparison of reference tracking error of a Tobit Kalman filter with 5% *censored* measurements, and an *uncensored* standard Kalman filter, for the step response in figure 6.10.

6.4.1 Transfer Function Comparisons Using the Steady State T.K.F. Observer

As previously calculated in 5.5, a steady state T.K.F. in which T is varied according to 5.68 or 5.73, results in a predictable expectation of censoring, inverse mills ratio, Tobit update gain, and Tobit error covariance. As such, the transfer function of the uncensored LQG controller can be modified to include these new Tobit filter parameters and calculate transfer function of steady state Tobit LQG Controllers for a given level of censoring.

First, consider the uncensored steady state LQG output feedback controller given by 6.3. The negative-feedback transfer matrix is given by

$$\hat{C}(s) = K(sI - A + LC + BK)^{-1}L \tag{6.46}$$

and the transfer matrix from control input u to output y is

$$\hat{P}(s) = C(sI - A)^{-1}B \tag{6.47}$$

The resulting closed loop transfer matrix from r to output y is then

$$\hat{y} = \hat{P}(s)(I + \hat{C}(s)\hat{P}(s))^{-1}(N + \hat{C}(s))\hat{r} \tag{6.48}$$

If T is defined as according to 5.68, where here α is renamed ED, then

$$T = C\hat{x} + \sigma\Phi^{-1}(ED)$$

$$\begin{aligned}
\hat{\gamma} &= ED \\
\hat{\lambda} &\to \frac{\phi(\Phi^{-1}(\hat{\gamma}))}{\hat{\gamma}} \\
C &\to \hat{\gamma}C \\
L &\to L_{Tobit} \\
\Psi &\to \Psi_{Tobit}
\end{aligned} \tag{6.49}$$

If the standard uncensored Kalman gain is utilized instead of this new Tobit gain, then the transfer functions for the corresponding L.Q.G. Tobit output feedback controller change from 6.46 & 6.47 to

$$\begin{aligned} \hat{C}(s) &= K(sI - A + L\hat{\gamma}C + BK)^{-1}L \\ \hat{P}(s) &= \hat{\gamma}C(sI - A)^{-1}B \end{aligned} \tag{6.50}$$

As the expectation of censoring $\hat{\gamma} = ED$ is lowered, and the offset of the censoring limit T from the state estimate progressively shrinks, then the transfer functions of 6.50 change accordingly. In figure 6.14 a comparison of the step responses of the DC motor angular velocity model under increasingly heavy expectations censoring is shown.

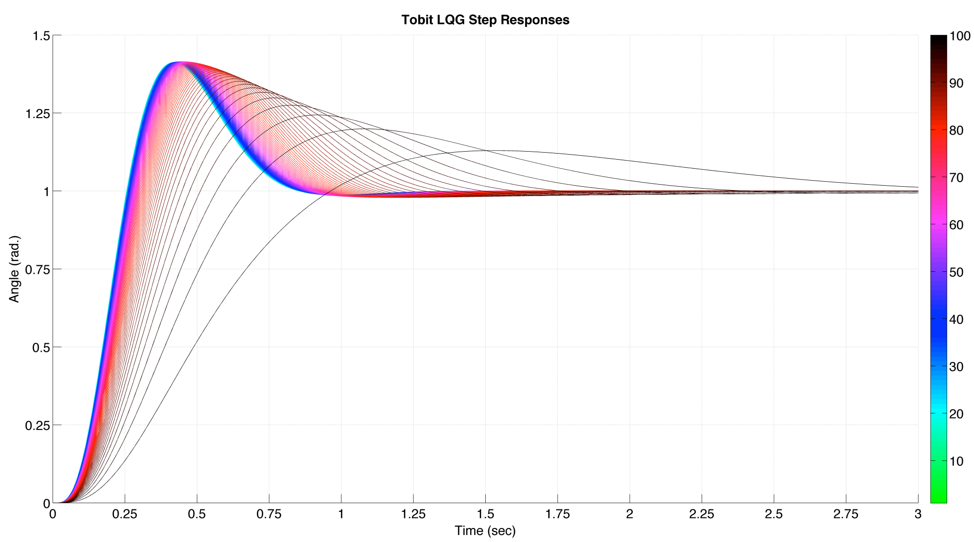

Figure 6.14: Comparison of step responses generated via the transfer functions of steady state Tobit LQG controllers under varying levels of censoring. Color meter represents expectation of censoring, with 0 being entirely uncensored, and 100 being entirely censored. Note that as censoring increases, step performance decreases.

As expected, when the censoring level increases the step dynamics slow. At the extreme levels of censoring the Tobit observer behaves as an open loop estimator and the step response reflects such a system. Of note here however, is that little performance degradation is seen until a very large degree of persistent censoring is induced, namely that of nearly 90% or greater censored measurements. In figure 6.15 the bode plots for the same scenario is presented. Again, as expected, the magnitude and phase plots for the given system degrade as the expectation of censoring is increased. As before, the performance loss due to censoring is minimal until very large persistent censoring is present.

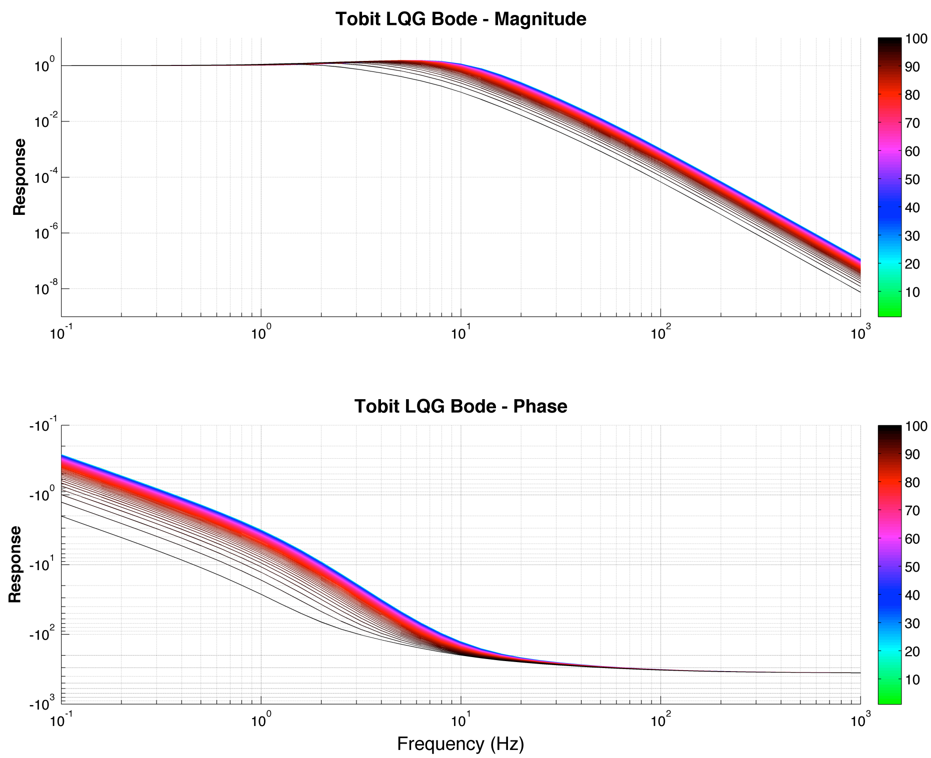

Figure 6.15: Comparison of bode plots generated via the transfer functions of steady state Tobit LQG controllers under varying levels of censoring. Color meter represents expectation of censoring, with 0 being entirely uncensored, and 100 being entirely censored. Note that as censoring increases, magnitude and phase responses decrease.

6.5 Controlling Uncertainty Using Tobit Parameters

As has been extensively discussed previously, when censoring is present the Tobit Kalman filter provides more information with regards to the current level uncertainty and filter performance than the standard Kalman filter and similar estimators. The standard Kalman filter assumes a linear system output model, which is subjected to zero-mean measurement noise, and is available at all times. As such, the standard Kalman filter converges to a calculable steady state gain and error covariance which may be determined via the algebraic Ricatti equation, as has been shown. However, the presence of censoring breaks both the linear measurement model and zero-mean measurement noise assumptions. All measurements are weighted equally, despite the clear difference in information a censored vs. non-censored measurement presents. As shown, naive use of the standard Kalman filter when censoring is present results in a biased and uninformative filter that not only cannot accurately estimate the true system state but also converges to an incorrect error covariance that leaves no indication of true estimator uncertainty.

The Sinopoli et. al. formulation of the Kalman filter for when measurements are dropped is a potential first approach towards the handling of censored measurements. That is, when censored measurements are read they are assumed to contain no valuable information and are then ignored, and the state *a priori* prediction step is performed without an *a posteriori* correction. However, in this case, a string of repeated censored measurements results in a rapidly increasing state estimate error covariance which over-estimates the true uncertainty of the system. A bias is also induced, for censored measurements are not utilized at all, and uncensored measurements are weighted more heavily.

The Tobit Kalman filter, however, utilizes the information that censored measurements present. The frequency of arrival between censored and uncensored measurements create a weight between the expected value to be seen and the actual measurements observed. The calculated expectation of censoring and inverse mills ratio also provide valuable information with regards to the state's estimated location and expected measurement. As censoring varies the Tobit Kalman filter measurement variance, gain, and error covariance updates accordingly. No longer is the estimation uncertainty a defined steady state quantity; with censored measurements it becomes a dynamic element. The expectation of censoring, inverse mills ration, and error covariance, is now information available from the Tobit Kalman filter which can be directly leveraged as feedback for the update censoring limits in order improve estimation performance according to specified criteria. It is shown in sections 6.6 and 6.7 how parameters unique to the Tobit Kalman filter can be used in novel estimation techniques to influence state estimation performance and uncertainty.

6.6 Estimation with Multiple Censored Regions

In this section the effect of taking multiple simultaneous measurements of the system output, each with independent censoring characteristics, is considered. As more simultaneous measurements are taken of the same system state, the Bernoulli approximation of the expected measurement becomes more accurate. Furthermore, differing censoring characteristics can be applied to independent measurements, allow for a sensor fusion type system which does not rely upon a rederiviation of the Tobit Kalman filter gain and error covariance terms. Each measurement's expectation of censoring, inverse mills ratio, and variance is calculated according to that measurement's respective censoring model, and the Tobit Kalman gain and *a posteriori* update calculations remain unchanged.

An example of such a system is given in 6.51 as

$$\begin{aligned} \mathbf{x_{k+1}} &= \mathbf{A}\mathbf{x_k} + \mathbf{G}\mathbf{w} \\ \mathbf{y_k} &= \mathbf{C}\mathbf{x_k} + \mathbf{H}\mathbf{v} \end{aligned} \tag{6.51}$$

with

$$\begin{bmatrix} \dot{x} \end{bmatrix} = \begin{bmatrix} .99 \end{bmatrix} \begin{bmatrix} x \end{bmatrix} + \begin{bmatrix} 1 \end{bmatrix} w \tag{6.52}$$

$$\begin{bmatrix} y_1 \\ y_2 \end{bmatrix} = \begin{bmatrix} 1 \\ 1 \end{bmatrix} \begin{bmatrix} x \end{bmatrix} + \begin{bmatrix} 1 & 0 \\ 0 & 1 \end{bmatrix} \begin{bmatrix} v_1 \\ v_2 \end{bmatrix} \tag{6.53}$$

In essence, the output vector is stacked with multiple measurements of the same state. Here, two separate measurements are defined, the first being subjected to right censoring, and the second being subjected to left censoring. The censoring limit is common among both censoring regions such that $T = 0$ for each, resulting in measurements defined by

$$Z = \begin{bmatrix} z_1 \\ z_2 \end{bmatrix}$$

where

$$\begin{aligned} z_1 &= \begin{cases} y_1, & y_1 < T \\ T, & y_1 \geq T \end{cases} \\ z_2 &= \begin{cases} y_2, & y_2 > T \\ T, & y_2 \leq T \end{cases} \end{aligned} \tag{6.54}$$

Estimated measurements are defined by $\hat{Y} = C\hat{X}$, and with thus for the given C, $\hat{y} = \hat{x}$. The full expectation of censoring and inverse mill ratio is then given by

$$\begin{aligned} \gamma &= \begin{bmatrix} \Phi\left(\frac{T-\hat{y}}{\sigma_r}\right) & 0 \\ 0 & \Phi\left(\frac{\hat{y}-T}{\sigma_r}\right) \end{bmatrix} \\ \lambda &= \begin{bmatrix} \frac{\sigma_r \phi\left(\frac{T-\hat{y}}{\sigma_r}\right)}{\gamma_{11}} \\ \frac{\sigma_r \phi\left(\frac{T-\hat{y}}{\sigma_r}\right)}{\gamma_{22}} \end{bmatrix} \end{aligned} \tag{6.55}$$

Variance is calculated according to the following,

$$V = \begin{bmatrix} \sigma_r^2 \left(1 - \lambda_{11}^2 - \lambda_{11} \left(\frac{T-\hat{y}}{\sigma_r}\right)\right) & 0 \\ 0 & \sigma_r^2 \left(1 - \lambda_{21}^2 - \lambda_{21} \left(\frac{T-\hat{y}}{\sigma_r}\right)\right) \end{bmatrix} \tag{6.56}$$

and the expected measurement vector is then consistent with the size of the actual observed measurement vector, with each expected measurement being a bernoulli random variable with an expected value calculated according to their respective elements of γ and λ.

$$E\left[y\right] = \begin{bmatrix} \gamma_{11}\left(\hat{y} - \sigma_r \lambda_{11}\right) + \left(1 - \gamma_{11}\right) T \\ \gamma_{22}\left(\hat{y} + \sigma_r \lambda_{21}\right) + \left(1 - \gamma_{22}\right) T \end{bmatrix} \tag{6.57}$$

Innovation is then calculated in the same manner as the standard Tobit Kalman filter, by taking the error between the observed system output and expected measurements.

$$Innovation = Z - E\left[y\right] \tag{6.58}$$

Using the newly calculated value of V given by 6.56, the structure of the Tobit gain formulation and *a posteriori* state and error covariance update remain unchanged. As such, the state estimate is produced via the combined information from both measurements. The estimation of such a brownian system, with both left and right censoring present independently, is shown in figure 6.16.

The system state is accurately estimated throughout all space, even though the first measurement is entirely right censored at $T = 0$ and the second is entirely left censored at $T = 0$ as well. Although neither measurement can sense the entire space, their combined information is accurately and automatically combined via the stacked Tobit Kalman formulation, enabling accurate state estimation at all times and smooth transitioning from one region to another.

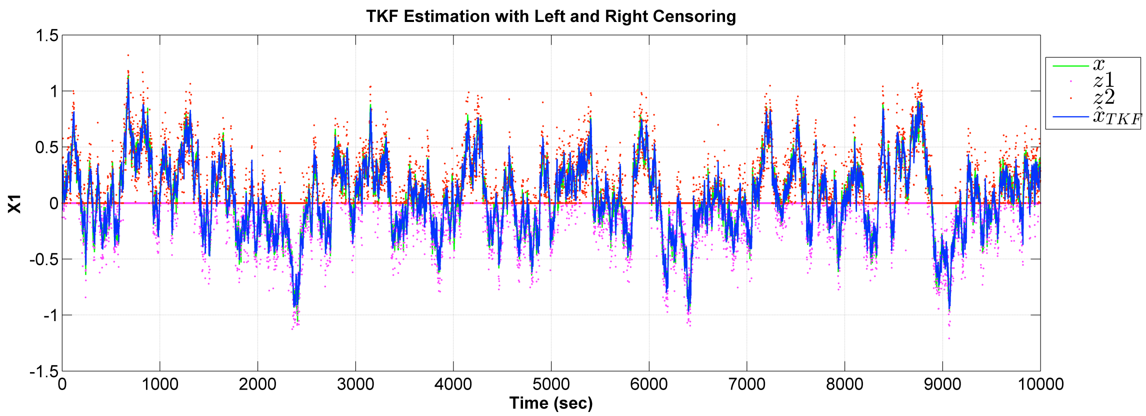

Figure 6.16: Estimation of a scalar brownian system with a Tobit Kalman filter in which both left and right censoring are present, each defined at the same censoring threshold. In this arrangement, the censoring limits combine such that the entire space can be "seen", and the resulting state estimate seamlessly tracks through the entire space.

A similar measurement system can considered, in which multiple independent measurements are made of the same system output, each with identical censoring characteristics. This is equivalent to taking multiple simultaneous samples, and since measurement noise is assumed to be independent between samples the proportion of censored vs. uncensored measurements allows for a more accurate estimate of the censored measurement distribution at the current state value. Thus, a more accurate estimate the state can be formed without the need for differing censored regions and subsequent sensor technologies. A comparison between estimation of the same brownian motion model with a varying number of concurrent right-hand censored measurements is shown in figure 6.17, and in detail in figure 6.18.

It is especially evident in figure 6.18 that as more measurements are used the Tobit filter is able to more confidently and more accurately estimate the true system state in the censored region. This is further verified in figure 6.19, in which it shown that the mean squared estimation error decreases as a function of the number of concurrent measurements increases, as would be expected.

Now consider the same model as in 6.51, but with each measurement being

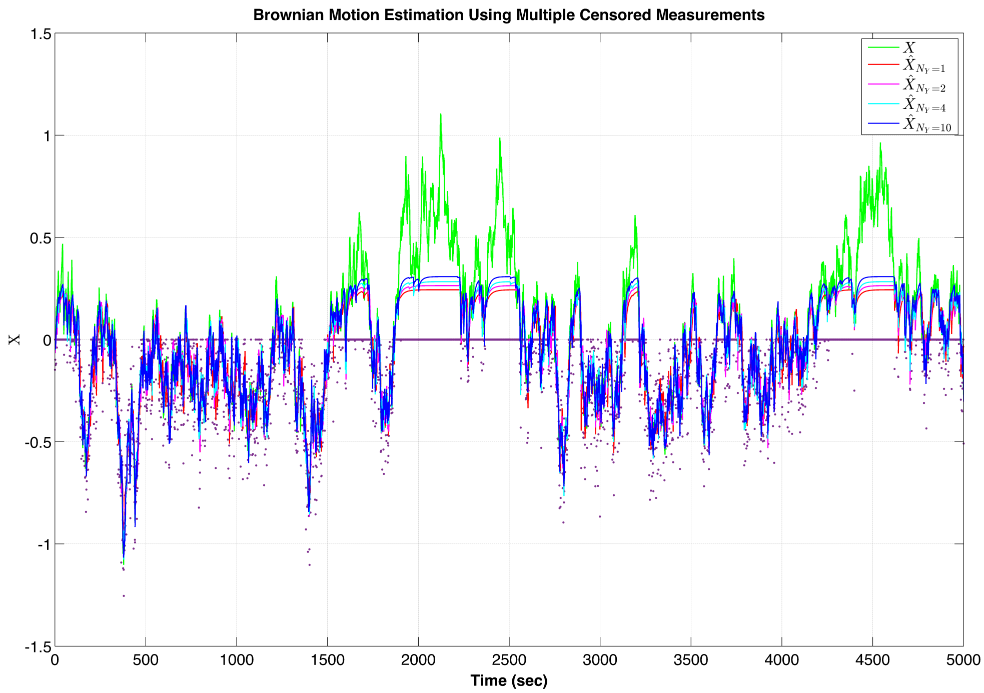

Figure 6.17: Estimation of a scalar brownian system with a Tobit Kalman filter in which multiple measurements are taken concurrently, each with independent noise but subjected to the same censoring model. N_y represents the number of concurrent measurements used for a given estimate iteration. A single representative set of measurements in shown by purple markers to indicate the censoring model present.

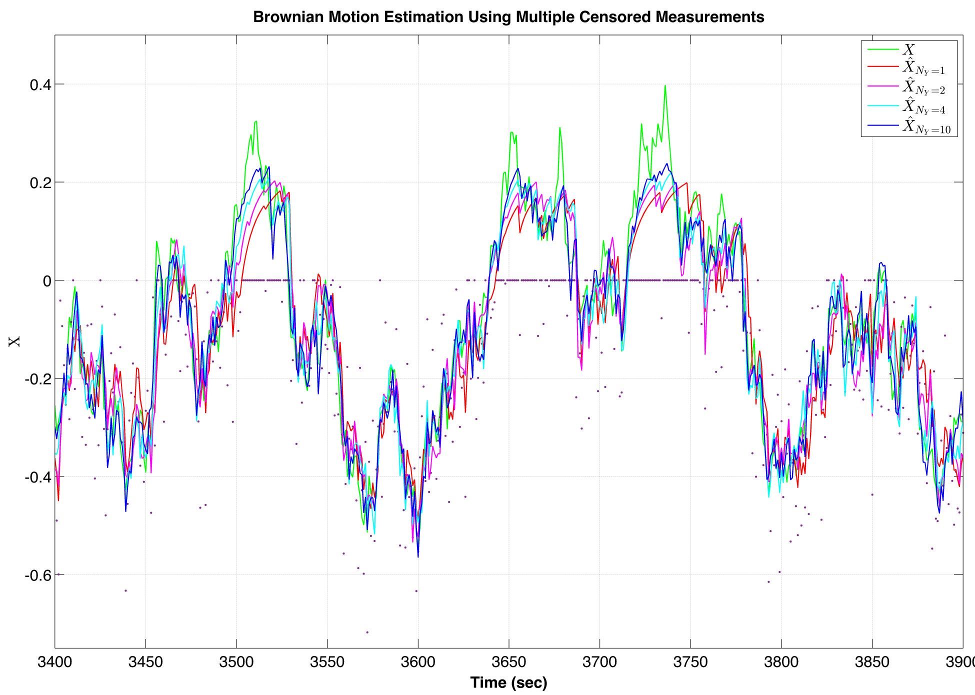

Figure 6.18: Detail view of figure 6.17. As more measurements are used the state estimation in both the uncensored and censored regions is improved. A single representative set of measurements in shown by purple markers to indicate the censoring model present.

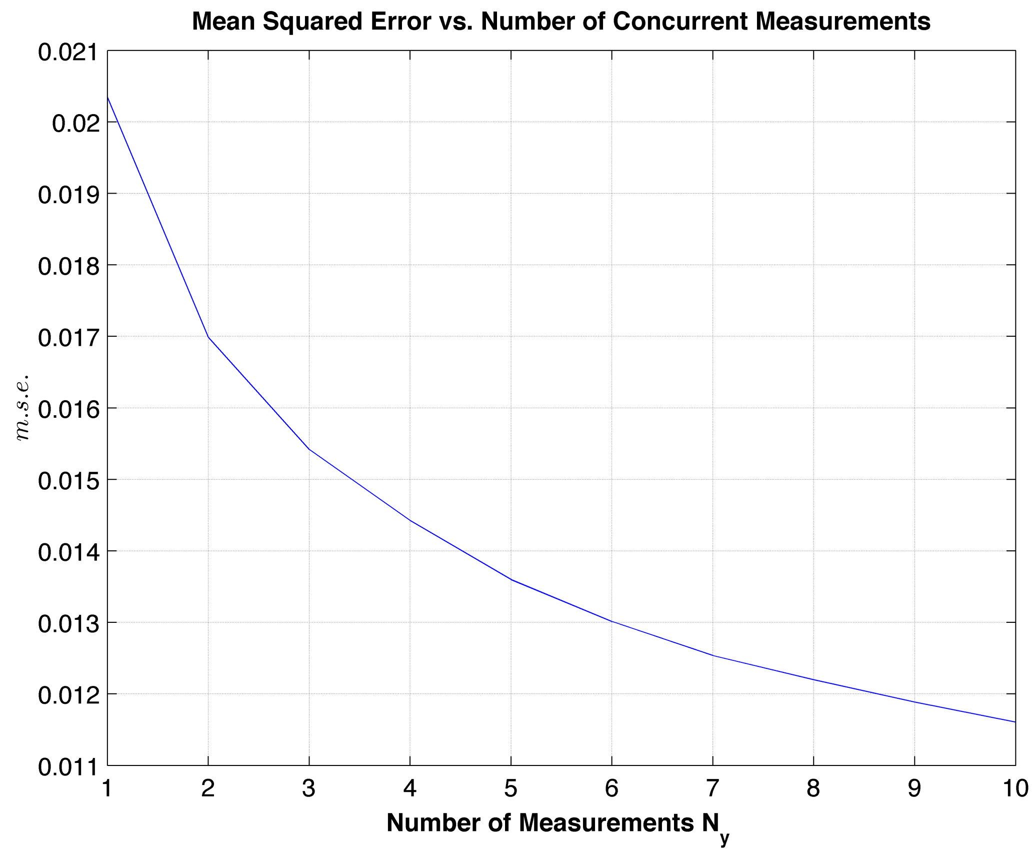

Figure 6.19: Mean squared error of the brownian state estimation as a function of the number of concurrent censored measurements used.

subjected to independent saturation regions. That is, output y_i is uncensored when it lies between lower and upper censoring limits defined by T_{l_i} and T_{h_i}. This in effect creates multiple uncensored "windows", or fields of view (FOV). Any measurements outside of these fields of view, whether they be above or below, are censored. The censoring fields of view may or may not be overlapping. The measurement model is now given by

$$Z = \begin{bmatrix} z_1 \\ z_2 \end{bmatrix}$$

with

$$z_i = \begin{cases} y_i, & T_{l_i} < y_i < T_{h_i} \\ T_{l_i}, & y_i \leq T_{l_i} \\ T_{h_i}, & y_i \geq T_{h_i} \end{cases} \tag{6.59}$$

As with the previous discussion, the expectation of being uncensored γ, the inverse mills ratio λ, and variance V must be correctly defined for each independent measurement according to that measurements censoring model. This leads to the following for multiple saturation regions,

$$\begin{aligned} \gamma_i &= \Phi\left(\tfrac{T_{h_i}-\hat{y}}{\sigma_r}\right) - \Phi\left(\tfrac{T_{l_i}-\hat{y}}{\sigma_r}\right) \\ \gamma_{h_i} &= 1 - \Phi\left(\tfrac{T_{h_i}-\hat{y}}{\sigma_r}\right) \\ \gamma_{l_i} &= \Phi\left(\tfrac{T_{l_i}-\hat{y}}{\sigma_r}\right) \\ \lambda_i &= \frac{\phi\left(\frac{T_{h_i}-\hat{y}}{\sigma_r}\right)-\phi\left(\frac{T_{l_i}-\hat{y}}{\sigma_r}\right)}{\gamma_i} \end{aligned} \tag{6.60}$$

$$V_{i,i} = \sigma_r^2\left(1 - \lambda_i^2 + \left(\tfrac{\hat{y}\lambda_i}{\sigma_r}\right) + \left(\frac{T_{l_i}\Phi\left(\frac{T_{l_i}-\hat{y}}{\sigma_r}\right)-T_{h_i}\Phi\left(\frac{T_{h_i}-\hat{y}}{\sigma_r}\right)}{\gamma_i}\right)\right) \tag{6.61}$$

Due to the saturation censoring model the expected measurement is defined slightly differently, however the overall form of weighting T vs. the uncensored measurements remains. The innovation equation and subsequent Tobit gain and update equation are unchanged.

$$E\left[y_i\right] = \gamma_i\left(\hat{y} - \sigma_r\lambda_i\right) + \gamma_{l_i}T_{l_i} + \gamma_{h_i}T_{h_i} \tag{6.62}$$

$$Err_y = Z - \begin{bmatrix} E\left[y_1\right] \\ E\left[y_2\right] \end{bmatrix} \tag{6.63}$$

In figure 6.20 the same brownian motion used previously is estimated, now with two independent and non-overlapping saturation censoring regions. The Tobit filter is able provide accurate state estimates both in and between the censoring regions. The error covariance accurately reflects the total information presented by the two concurrent measurement models and estimation between censored and uncensored regions remains smooth at all times.

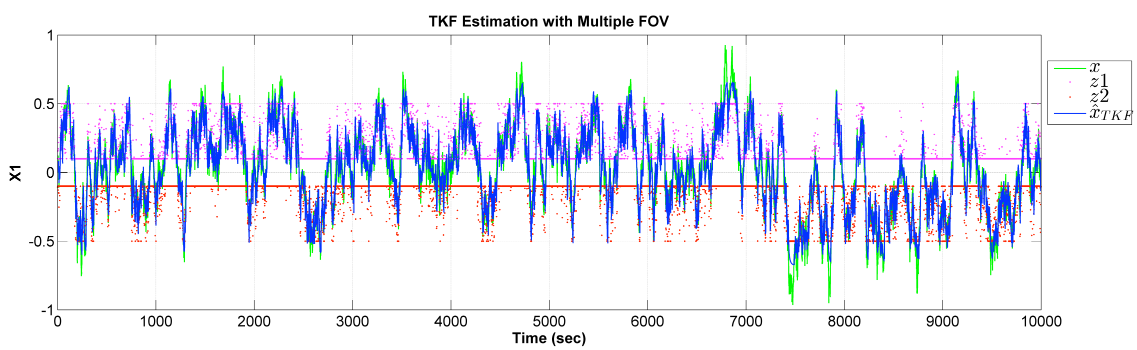

Figure 6.20: Estimation of a scalar brownian system with a Tobit Kalman filter in which two non-overlapping saturation censoring regions are present.

6.7 Application of the T.K.F. and Censored Feedback Control Towards Novel Computer Vision Techniques

The previous section discussed the estimation of a brownian system in which two independent saturation censored measurements where utilized in the Tobit Kalman filter. It was noted that such a measurement model, as given by 6.59, in effect creates two independent "fields of view" for the same system state. In this section it is discussed how this concept can be applied to computer vision based target tracking, in which a known camera model creates a saturation region in which the target can be observed. Unique advantages of the Tobit filter, as discussed previously, allow novel tracking techniques to be explored for one or more targets. The goal of such a system is depicted in 6.21.

Here it desired to visually track one or more targets which may be of similar appearance, and may exit the field of view. The edges of the camera system's field of view define censoring limits, for which targets can be measured while inside the field of view, and cannot be measured while outside the field of view. Although a target outside the field of the view cannot be directly observed, a known dynamic model can be used accurately predict its expected evolution until uncensored measurements can taken again. Such a problem was first explored in section 2.2, where it was demonstrated how a Kalman filter framework can be used to accomplish such a goal for stationary targets. The drawback however, was that the Sinolpoli et. al. method employed at that time suffered from a rapidly growing error covariance while the target is outside the field of view. Therefore it was possible to unrealistically snap to a target response when censored for a long period of time, opening the possibility for false detection and target identification confusion. It was also assumed that the targets were fixed, and therefore had no dynamic model of their own evolution, and that the movement of the camera would permit an accurate estimation of the target's position within the imaging plane. It is shown in the following sections and examples how a Tobit Kalman estimator can be used in a vision based system in order to rectify these deficiencies and track moving targets which enter and exit the field of view.

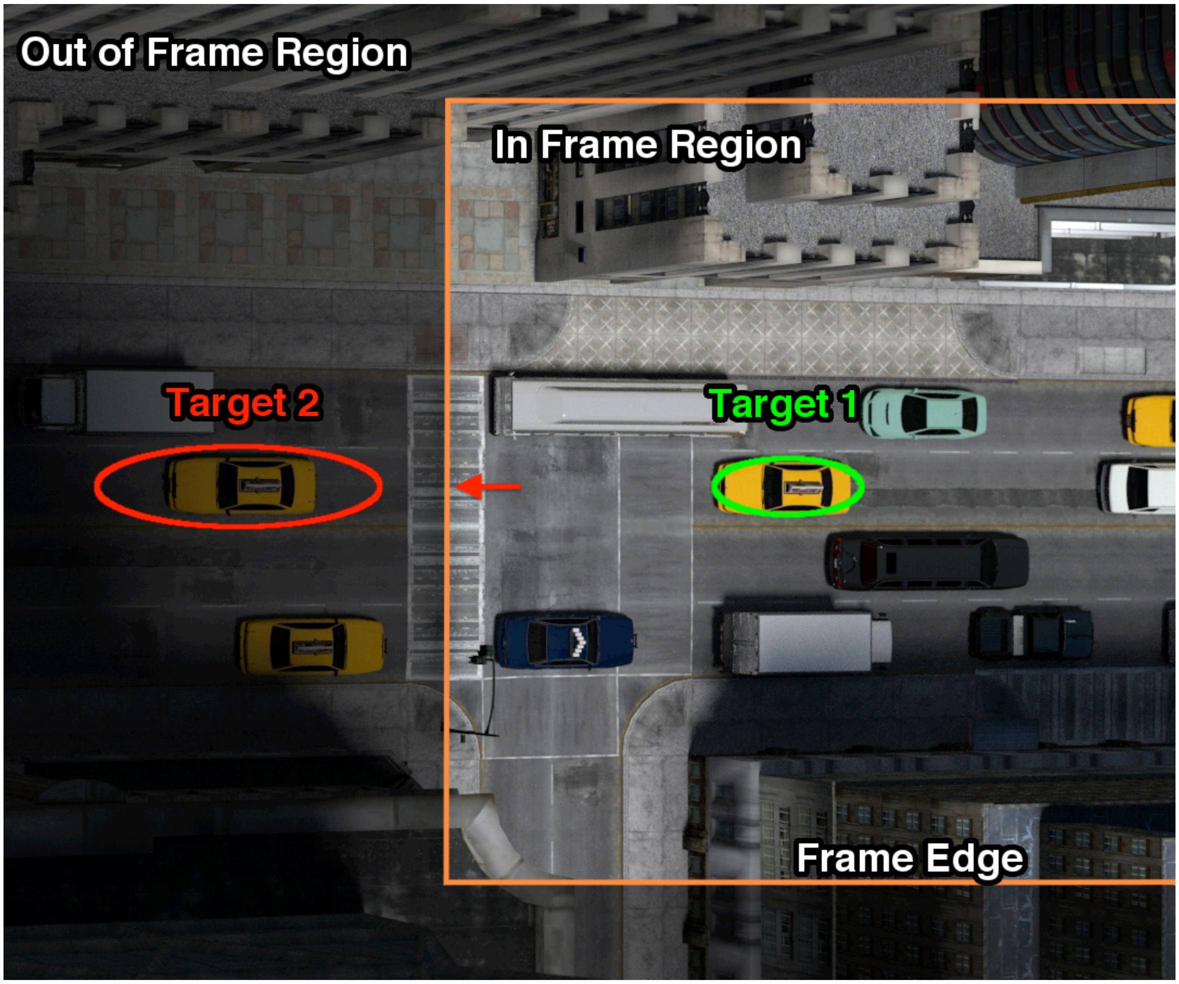

Figure 6.21: Tracking of multiple targets in a congested environment using an airborne vision based sensing system

6.7.1 Saturation Censoring in a Vision Based System

Assume that there exists an airborne camera system which is pointing towards the ground at a known position and attitude. Furthermore, assume that the imaging system is calibrated such that it's intrinsic camera matrix is well defined. Projection of the left and right edges of the camera frame onto the ground create left and right censoring limits on the ground, which is assumed to be a plane. A saturation region can then be formed in the units of this ground plane, for which targets can be observed. Such a scenario is shown in figure 6.22.

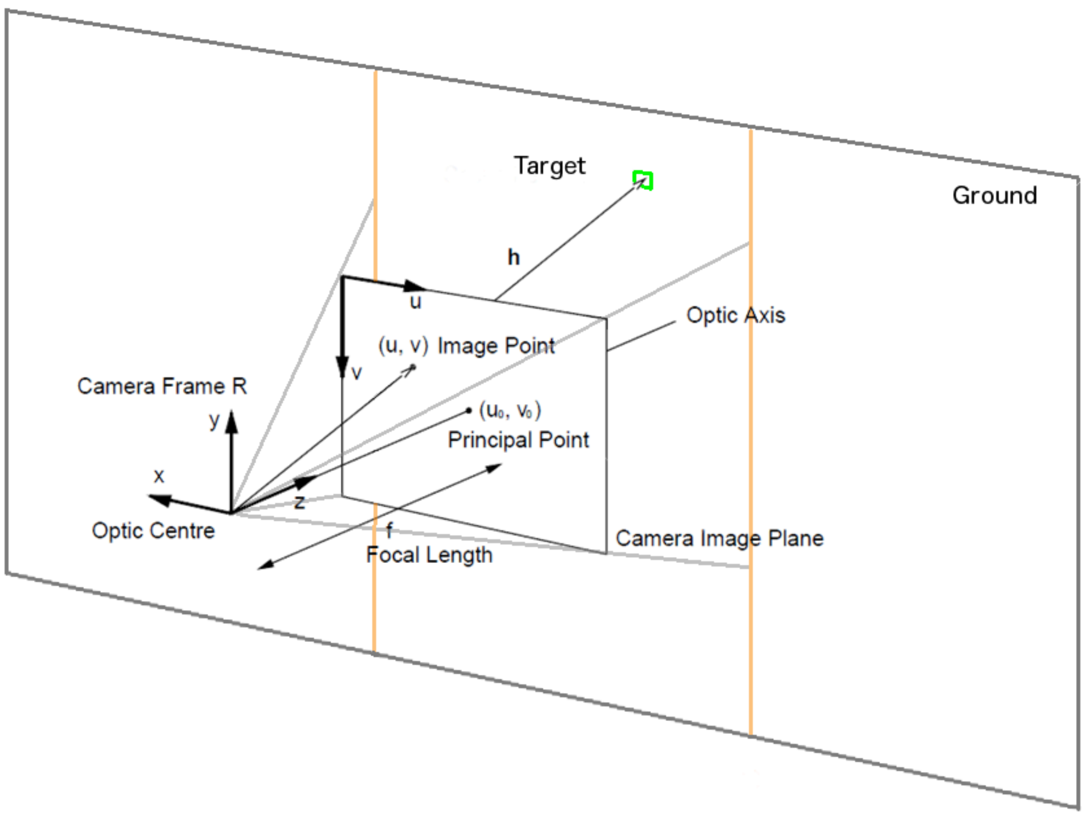

Figure 6.22: Projection of airborne camera frame boundaries onto the ground. Left and right field of view limits can be used to implement the Tobit saturation censoring model for target tracking and estimation.

The target's state dynamics can be formed in the reference frame of the ground plane, and its output can be measured via the vision based system. A Tobit Kalman filter for saturation censoring can be utilized to incorporate the left and right censoring restraints imposed by the limited horizontal field of view of camera. Incorporation of all four camera edges is called *frame censoring*. Although a more accurate and generic censoring model, frame censoring requires a two dimensional state motion model, a much more complicated censoring model with cross-correlation between censored measurements, and a larger array of assumptions to be made with regard to the target's evolution in the censored region. Assume for the purposes of the following discussion that the camera and target are restricted to one axis of motion. That is, assume that the target only moves in a horizontal motion with respect to the imaging plane and only the left and right saturation limits imposed by the camera field of view are relevant.

6.7.2 Tracking Targets Between Multiple Fields of View

Consider first the following constant velocity motion model for a single target, which is subjected to random disturbances in velocity.

$$\begin{aligned}\mathbf{X(k+1)} &= \mathbf{AX(k)} + \mathbf{G}\sigma_{\mathbf{q}} \\ \mathbf{Y(k)} &= \mathbf{CX(k)} + \mathbf{H}\sigma_{\mathbf{r}}\end{aligned} \tag{6.64}$$

with

$$\begin{bmatrix} \dot{x}_p \\ \dot{x}_v \end{bmatrix} = \begin{bmatrix} 1 & \Delta \\ 0 & 1 \end{bmatrix} \begin{bmatrix} x_p \\ x_v \end{bmatrix} + \begin{bmatrix} \frac{1}{2}\Delta^2 \\ \Delta \end{bmatrix} \sigma_q \tag{6.65}$$

$$\begin{bmatrix} y_{p_1} \\ y_{p_2} \end{bmatrix} = \begin{bmatrix} 1 & 0 \\ 1 & 0 \end{bmatrix} \begin{bmatrix} x_p \\ x_v \end{bmatrix} + \begin{bmatrix} 1 & 0 \\ 0 & 1 \end{bmatrix} \sigma_r \tag{6.66}$$

Assume two camera systems are present in the environment, in a manner consistent with that described the previous section, which create two separate non-overlapping saturation censoring regions on the ground plane of the target. Projection of left and right frame limits of camera i onto the ground then create censoring limits T_{h_i} and T_{l_i}, respectively. Measurements z_i are then assumed to come from the vision based system according to model given previously in 6.59, and given by

$$z_i = \begin{cases} y_{p_i}, & T_{l_i} < y_{p_i} < T_{h_i} \\ T_{l_i}, & y_{p_i} \leq T_{l_i} \\ T_{h_i}, & y_{p_i} \geq T_{h_i} \end{cases} \tag{6.67}$$

As with before, estimated measurements given by $\hat{Y} = C\hat{X}$, and therefore with the given C, $\hat{y} = \hat{x}_p$, and the expectation of being uncensored and the inverse mills ratio are then defined by

$$\begin{aligned} \gamma_i &= \Phi\left(\frac{T_{h_i} - \hat{y}}{\sigma_r}\right) - \Phi\left(\frac{T_{l_i} - \hat{y}}{\sigma_r}\right) \\ \gamma_{h_i} &= 1 - \Phi\left(\frac{T_{h_i} - \hat{y}}{\sigma_r}\right) \\ \gamma_{l_i} &= \Phi\left(\frac{T_{l_i} - \hat{y}}{\sigma_r}\right) \\ \lambda_i &= \frac{\phi\left(\frac{T_{h_i} - \hat{y}}{\sigma_r}\right) - \phi\left(\frac{T_{l_i} - \hat{y}}{\sigma_r}\right)}{\gamma_i} \end{aligned} \tag{6.68}$$

with the measurement variance is given by

$$V_i = \sigma_r^2 \left(1 - \lambda_i^2 + \left(\frac{\hat{y}\lambda_i}{\sigma_r}\right) + \left(\frac{T_{l_i}\Phi\left(\frac{T_{l_i} - \hat{y}}{\sigma_r}\right) - T_{h_i}\Phi\left(\frac{T_{h_i} - \hat{y}}{\sigma_r}\right)}{\gamma_i}\right)\right) \tag{6.69}$$

Each expected measurement is then formed as

$$E\left[y_i\right] = \gamma_i\left(\hat{y} - \sigma_r\lambda_i\right) + \gamma_{l_i}T_{l_i} + \gamma_{h_i}T_{h_i} \tag{6.70}$$

and the innovation is then the difference between the observed position from the vision based detector and the expected target measurement given by 6.70.

$$Ey_i = z_i - E\left[y_i\right] \tag{6.71}$$

Tobit gain and update equations remain unchanged. Demonstrated in figure 6.23 is the tracking of a single target which is moving from one field of view to another, with no over-lap between the censored regions. At the beginning of the target trajectory only the right camera can observe the target, between approximately 13 to 18 seconds neither camera can directly observer the target, and from 18 to 30 seconds only the left camera can observe the target. It appears that target position estimation remains consistent throughout the entire trajectory of the simulation, despite the transition from one censoring to another.

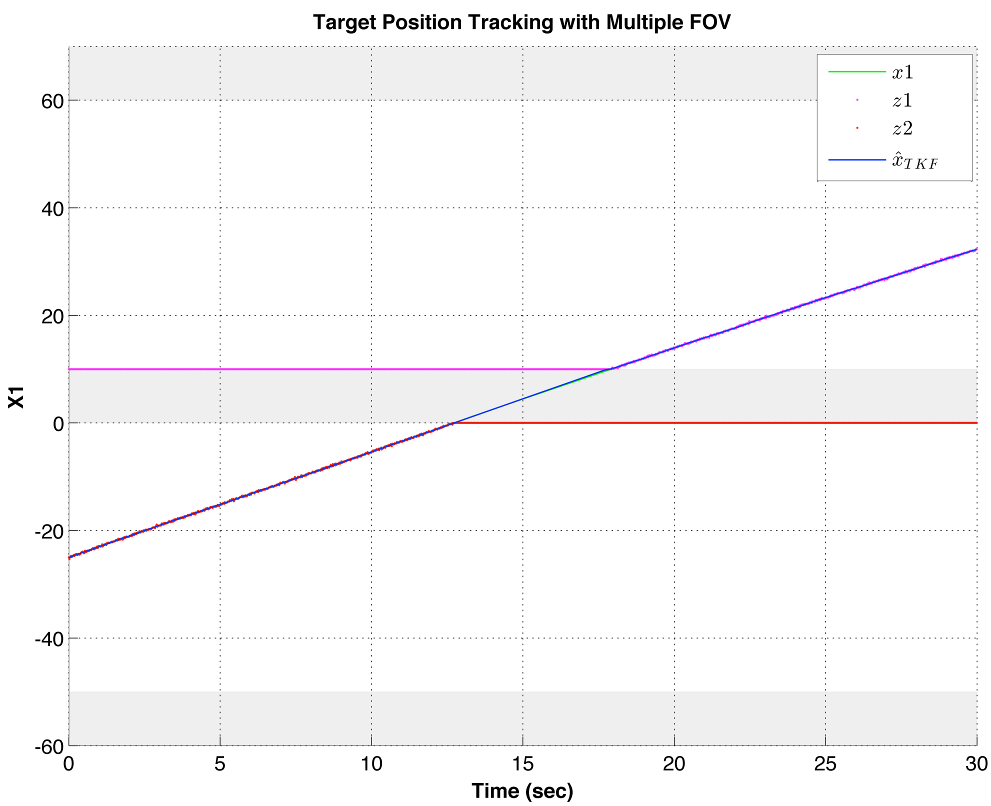

Figure 6.23: Tracking of target position between two non-overlapping fields of view using a stacked measurement vector with independent saturation censoring regions.

It is evident in figure 6.23 that while the target is outside the field of view of both censored regions, the target's velocity cannot be estimated. This is because of the limitations of the target dynamical model, for as the position becomes entirely censored the filter must resort to pure prediction based on the constant velocity assumption.

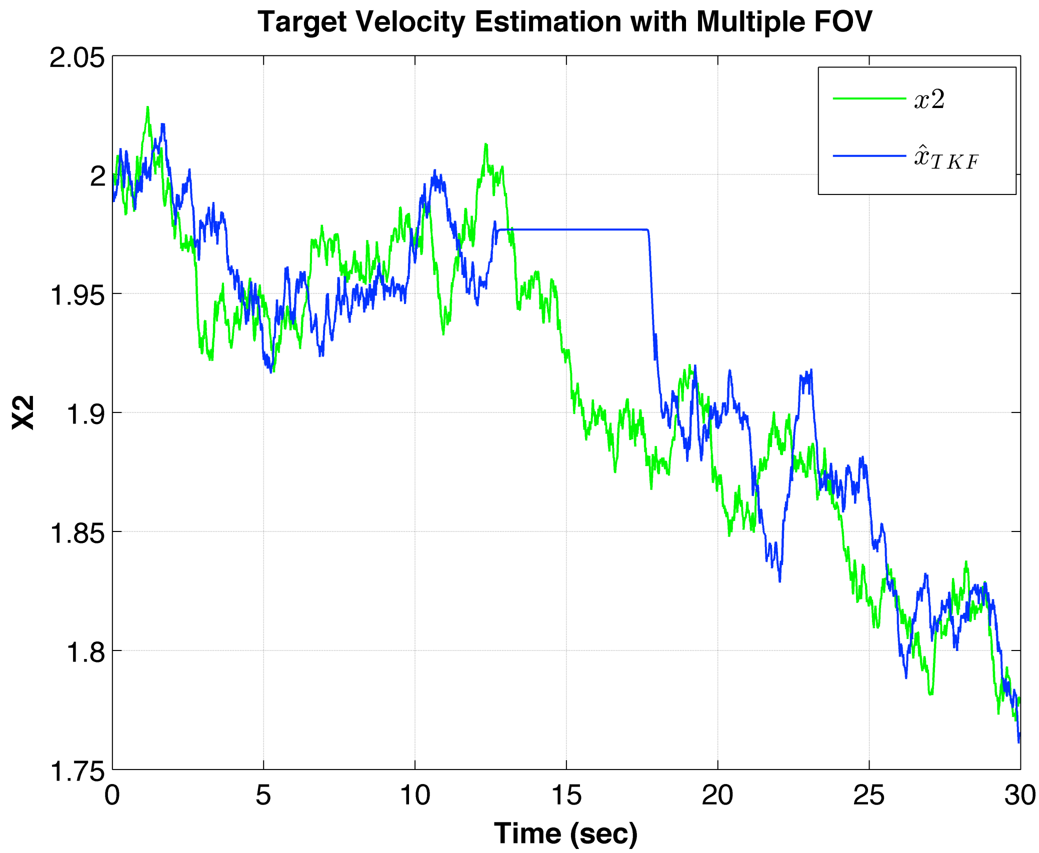

Figure 6.24: Estimation of target velocity between two non-overlapping fields of view using a stacked measurement vector with independent saturation censoring regions. Due to limitations in the dynamic model, velocity is propogated while target position is censored.

A more detail view provided by 6.25 shows the transition of the target from the censored region into the saturation region of the left camera. Position estimation error has increased in the censored region since the disturbances in the velocity cannot be observed. The filter has over estimated the velocity of the target, as is evident from figure 6.24, and expects the target to enter the uncensored region earlier than in truth.

However, when the target is not observed as predicted the estimate begins to correct itself and move toward the true position. The estimate then converges to the true state in the uncensored region of the left camera.

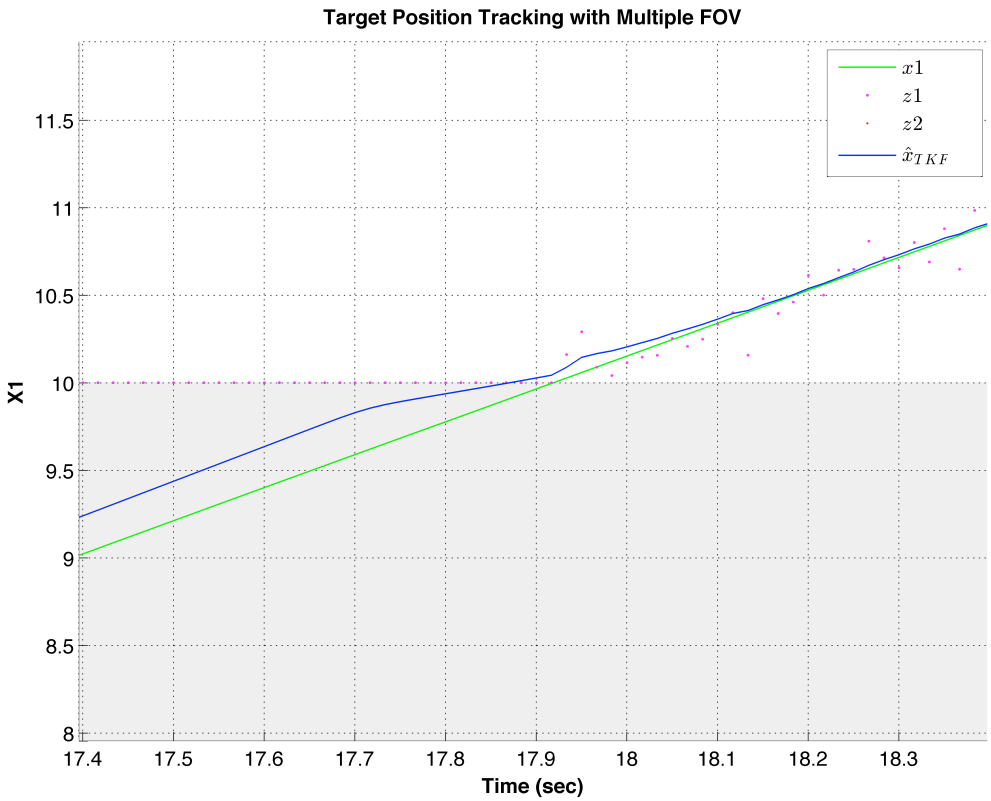

Figure 6.25: Detail view of figure 6.23 in the area near when the target exits the censored region between the two fields of view. Notice that while censored the target position error has grown, however the estimated position moves towards the true position as the estimate approaches the censored region and uncensored measurements are not observed.

The error covariance of the estimator is shown in figure 6.26. Error covariance converges to that of the uncensored Kalman filter while the target remains far from the censored regions. However, uncertainty grows as the target enters the censored area between the non-overlapping uncensored region. Position uncertainty grows more rapidly than that of velocity, although both fall rapidly as the second censoring limit approaches and the target is observed.

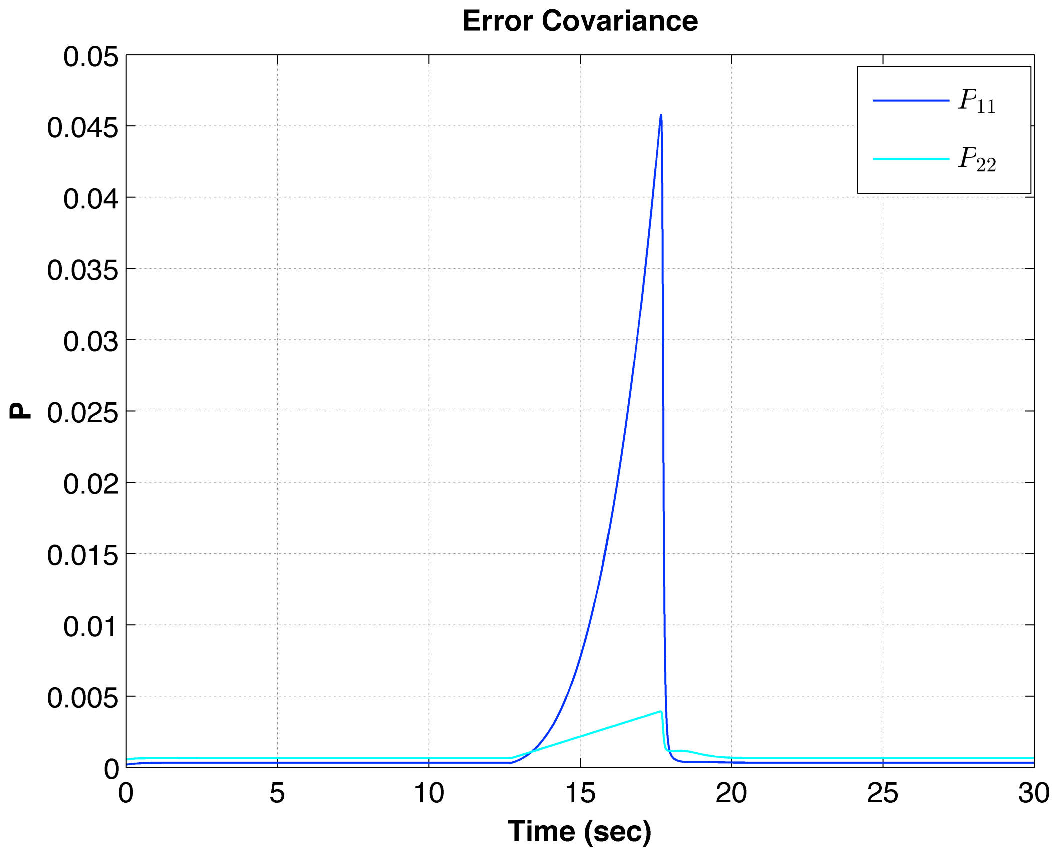

Figure 6.26: Error covariance while tracking of target between two non-overlapping fields of view using a stacked measurement vector with independent saturation censoring regions. Note that uncertainty grows while target moves through the censored region, but quickly recovers as the target approaches and enters the second field of view.

Repeating the same scenario, expect with over-lapping saturation censored regions, is shown in figure 6.27. In contrast to the previous simulation in which there existed a region where neither camera could measure the target position, there now exists a region in which both cameras can detect the target concurrently. As such, it would be expected that target velocity can now be estimated at all times, and in the common field of view of each camera the uncertainty of the filter decreases.

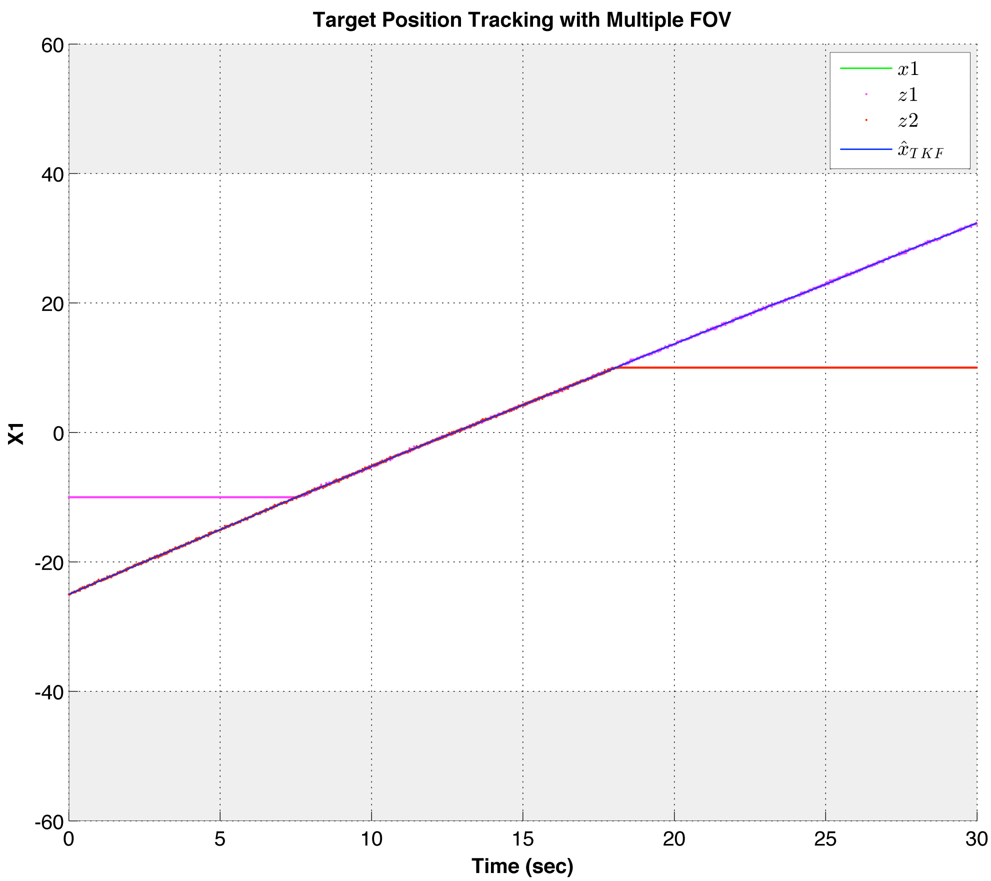

Figure 6.27: Tracking of target position with two overlapping fields of view using a stacked measurement vector with separate saturation censoring regions.

It is verified in figure 6.28 that velocity can indeed be measured at all times. This is unsurprising, for even the existence of touching yet non-overlapping uncensored regions, such that in the first left & right censoring example, allowed for accurate state estimation in the transition between each region.

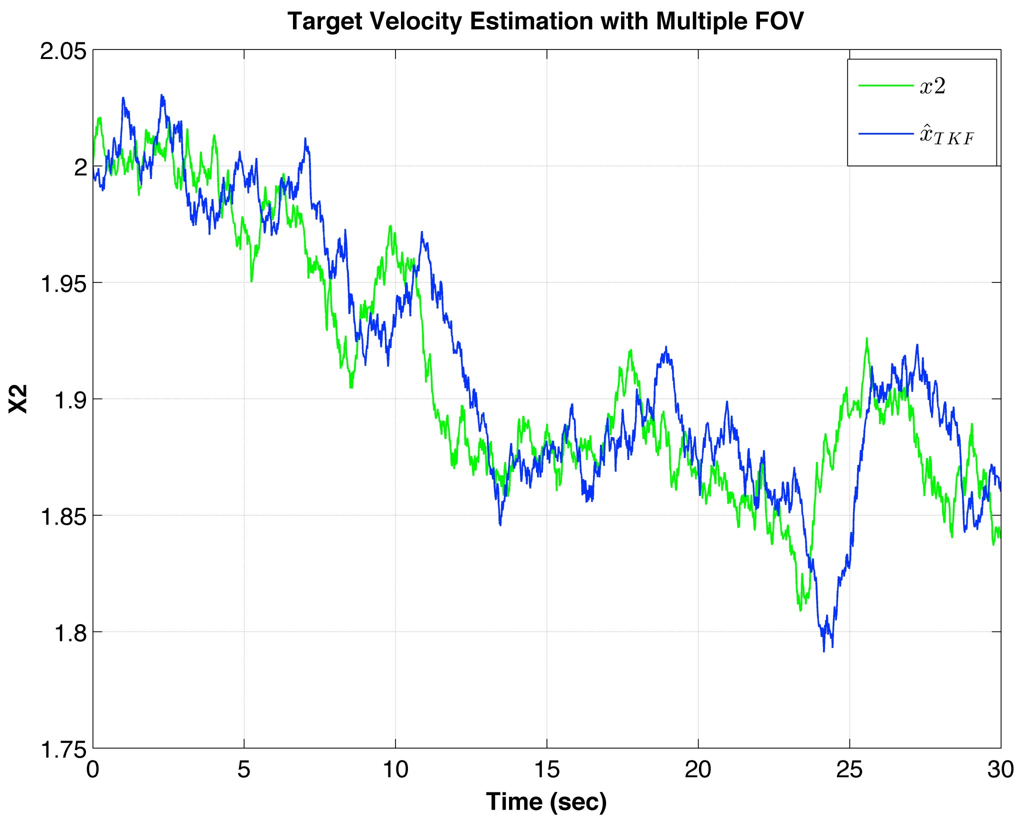

Figure 6.28: Estimation of target velocity with two overlapping fields of view using a stacked measurement vector with separate saturation censoring regions.

In figure 6.29 a detailed view of the transition into the over-lapping uncensored region is shown. At this point the filter is effectively presented with twice as much information regarding the state as was previously available, since both cameras can now contribute a meaningful position measurement. The state estimate appears to tighten around the true state in this overlapping region.

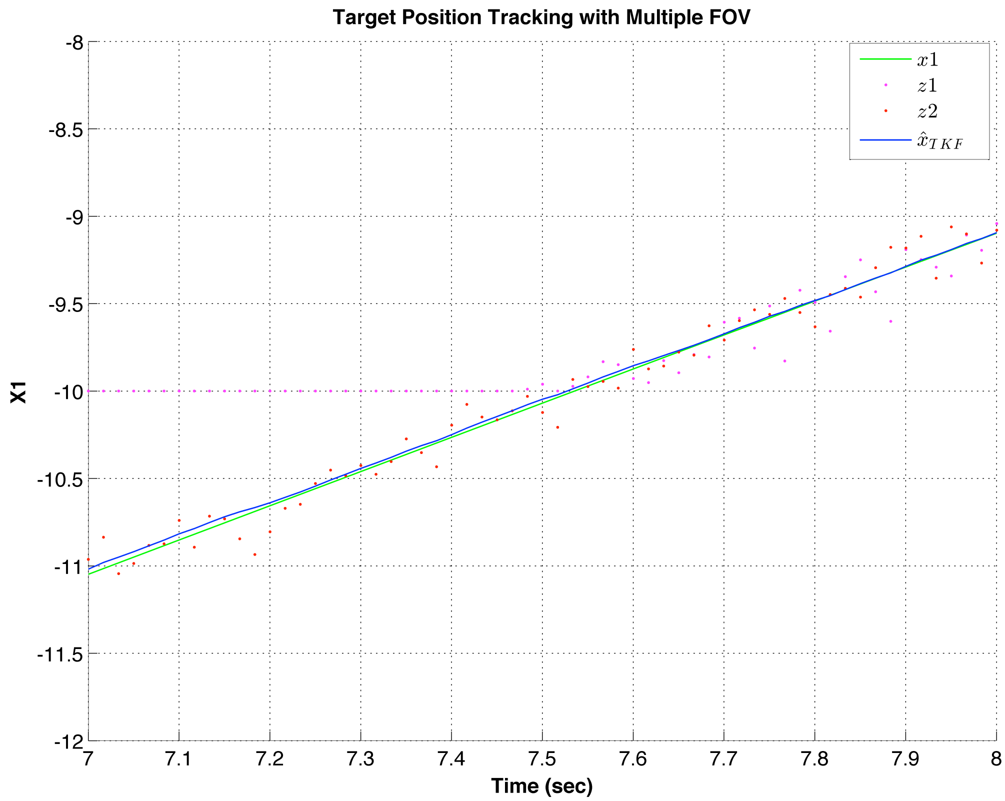

Figure 6.29: Detail view of figure 6.27 in the area near when the target enters the overlapping region between the two fields of view.

The reduction in filter uncertainty while in the overlapping uncensored region is confirmed in 6.30. While in either the left or right camera's field of view exclusively, the error covariance converges to the steady state of an uncensored standard Kalman filter with a single measurement. However, when in the overlapping uncensored region the error covariance for both position and velocity is reduced significantly. These steady state error covariances can be predicted by the Ricatti equation by either considering a single measurement, with no censoring, or two measurements, again with no censoring.

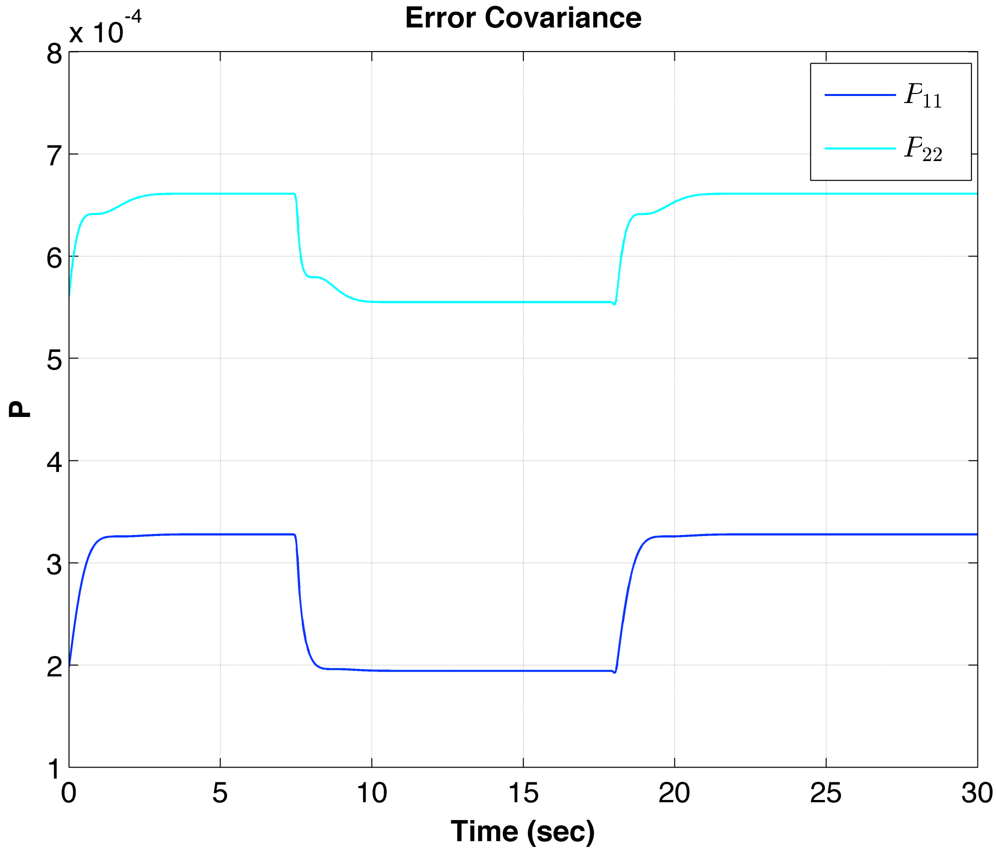

Figure 6.30: Error covariance while tracking of target with two overlapping fields of view using a stacked measurement vector with separate saturation censoring regions. Note that uncertainty reduces while target moves through the region in which the fields of view overlap.

In the previous example the tracking of a single target with multiple stationary fields of view was considered. However, there are additional useful scenarios that can be explored. The first being, can the camera be automatically controlled such that a target is tracked according to a given condition? The second being, how can multiple targets be tracked simultaneously? These questions are not necessarily mutually exclusive, for if two targets are desired to be tracked with a single field of view, but are diverging from each other, how should the camera react?

6.7.3 Automatic Panning Using Tobit Parameters

In this section the principals of the steady state Tobit Kalman filter are applied to the vision based target tracking problem. In the previous section the methodology behind considering a vision based tracking system as a censored Tobit Kalman problem was introduced for stationary cameras, and thus, stationary censoring limits. However, in previous sections such as 5.5 and 6.4, the ability of the Tobit Kalman filter to dictate a variable censoring limit and maintain a steady state estimator has been demonstrated. By controlling the ground based saturation censoring limits for a vision based system, and thus the camera's position and attitude, automatic panning motions can be found which accomplish a multitude of differing scenarios which may be desired.

For example, consider the same constant velocity motion model for a single target as used previously in 6.64. Assume that the target tracking begins far from censoring, and it is known that the target moves from right to left with an unknown velocity but given measurement noise variance σ. Suppose it is desired to automatically move the camera such that there is at least a 99.99% probability that the target does not exit the left edge of the camera's field of view. Mathematically speaking, this scenario is equivalent to the steady state Tobit Kalman definition given previously in which the censoring limit T is defined to maintain an offset from the state estimate according to a desired expectation of being uncensored. That is,

$$\begin{aligned}\mathbf{T^*_{h_k}} &= \mathbf{C\hat{x}_k} + \sigma\mathbf{\Phi^{-1}}(\mathbf{.9999}) \\ \mathbf{T_{h_k}} &= f(T^*_{h_k}) = \begin{cases} \mathbf{T_{h_0}}, & \mathbf{T^*_{h_k}} \leq \mathbf{T_{h_0}} \\ \mathbf{T^*_{h_k}}, & \mathbf{T^*_{h_k}} > \mathbf{T_{h_0}} \end{cases}\end{aligned} \tag{6.72}$$

The rule given by 6.74 enforces that when the camera's field of view is projected on the ground the resulting saturation region's high censoring limit is maintained such that the expectation of the target measurement being uncensored is at least 99.99%. In other words, if the saturation censoring limit T_h given above is accomplished, the target measurement is only censored .01% of the time. It assumed that for a given desired censoring limit on the ground that a camera position and attitude can be calculated to meet the given condition. For simplicity, T_{l_k} is set to $T_{h_k} - 50$, representing a camera moving at a constant altitude in a purely translational motion at a fixed focal length to accomplish the desired offset between censoring limits. An example of such a scenario is shown in 6.31.

As similar scenario is considered in figure 6.32, in which both the left and right ground censoring limits are controlled such that the target is maintained directly in the middle of the field of view at all times. The size of the window around the target, and resulting offsets of T_h and T_l from the state, the dictated again by a desired expectation of measurement censoring. Such a rule is then given by

$$\begin{aligned}\mathbf{T_{h_k}} &= \mathbf{C\hat{x}_k} + \sigma\mathbf{\Phi^{-1}}(\tfrac{\mathbf{1}}{\mathbf{2}}(\mathbf{ED}+\mathbf{1})) \\ \mathbf{T_{l_k}} &= \mathbf{C\hat{x}_k} + \sigma\mathbf{\Phi^{-1}}(\mathbf{1} - \tfrac{\mathbf{1}}{\mathbf{2}}(\mathbf{ED}+\mathbf{1}))\end{aligned} \tag{6.73}$$

where ED represents the desired expectation of censoring. Since the target is maintained in the middle of the field of view the measurement noise distribution is equally censored on both tails, and therefore the inverse mill ratio remains zero. With expectation of censoring maintaining a constant value, and inverse mills ratio being zero, the variance converges as well, and a steady Tobit Kalman filter results. As with before, the given expectation of being uncensored can be used calculate a steady state

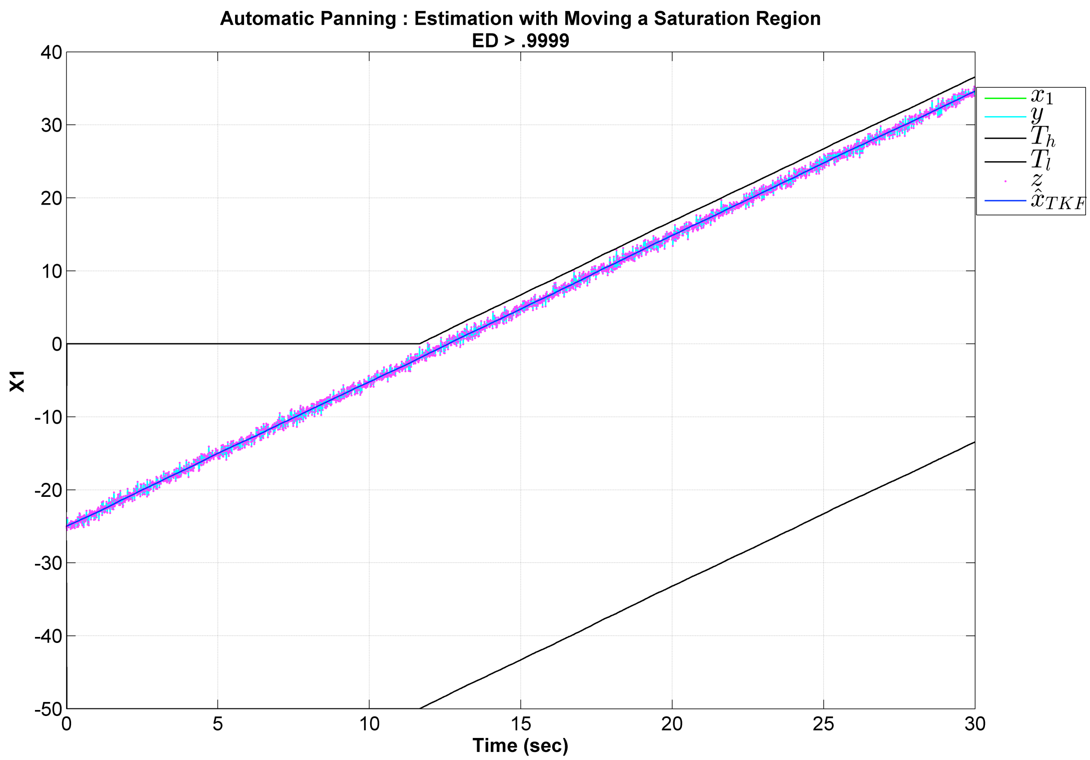

Figure 6.31: Automatic translation of FOV using a steady state saturated Tobit Kalman filter, using the expectation of being uncensored (ED) to control camera limits.

Tobit gain and error covariance, which can be considered in the design process to set ED to maintain or exceed a certain level of desired uncertainty.

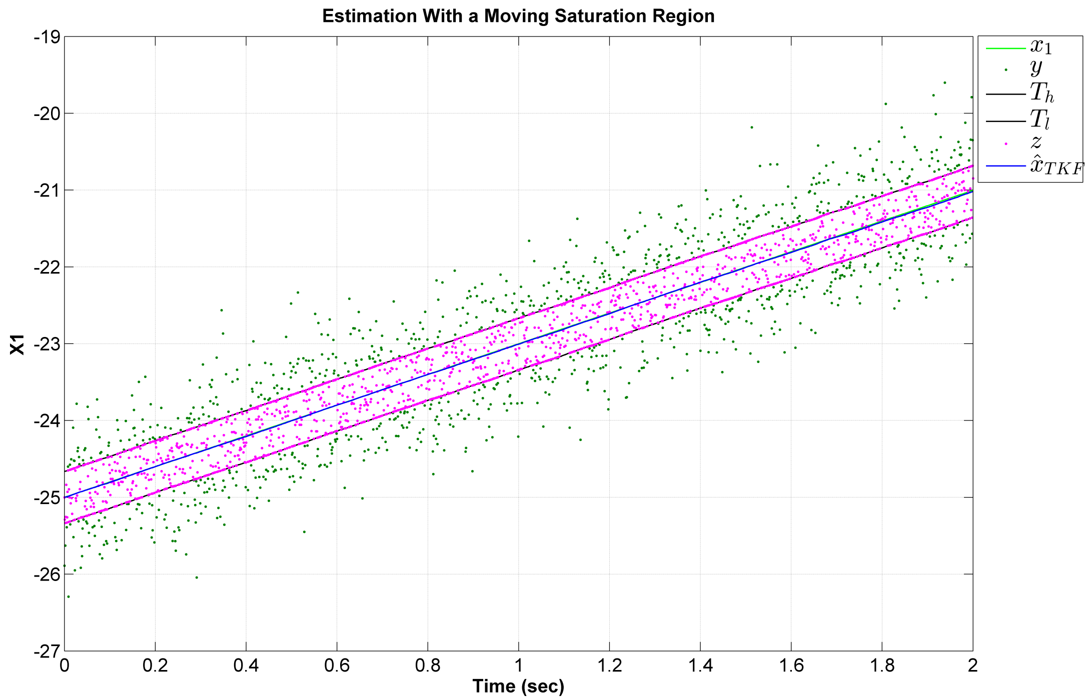

Figure 6.32: Automatic translation of FOV using a steady state saturated Tobit Kalman filter, using the expectation of censoring (ED) to center target within FOV and track with target.

Complications arise in the above scenarios when it is desired to simultaneously track one or more targets. For N targets and $M \geq N$ independent fields of view it may be possible to track all given targets via a smartly stacked measurement vector, as seen previously. However, if $M < N$, then there exists scenarios in which the target states may diverge, and a fixed size censoring limit will not be able to observe both targets simultaneously. At such a time a panning motion would then need to be induced in order to selectively look at each target. Two methods for achieving such motions are put forward in the following examples. Each method uses a Tobit parameter based feedback to influence censoring limits T_h and T_l such that the saturation censored region is moved to reduce target uncertainty.

The method for tracking multiple targets is analogous to the previous examples, in that the inverse mills ratio λ is used as a feedback to control the combined censoring limits of the camera's saturation censoring region. As mentioned in the previous example, when the target is centered in the field of view the inverse mills ratio goes to zero, as there is an equal expectation of the being on the left or right of the field of view. When two targets are present one can extend the stacked measurement example for stacked states as well. Whereas before in 6.27 a stacked measurement vector was used to create multiple fields of view of the same state, the analogous example can created in which multiple independent states can be stacked as well. These states can be measured independently, with these measurements subjected to either the same or differing censoring models. When using a stacked state vector, with a corresponding stacked measurement vector, multiple inverse mills ratios need be calculated, one for each independent measurement. By attempting to drive the combined inverse mills ratio to zero the censoring region tries to keep both targets centered in the FOV, and effectively attempts to drive each target to the same expectation of censoring as well. Should the imager focal length and position be fixed, then the only method for controlling these censoring limits is to pan the camera. Such a generated panning motion can be seen in6.33, in which the following update law for T is used

$$T_h(k) = T_h(k-1) - K(\lambda_1(k) + \lambda_2(k)) \tag{6.74}$$

where K is a proportional gain and

$$\lambda_i \quad = \quad \frac{\phi\left(\frac{T_h - \hat{y}_i}{\sigma_r}\right) - \phi\left(\frac{T_l - \hat{y}_i}{\sigma_r}\right)}{\gamma_i} \tag{6.75}$$

The filter attempts to update T_h such that the combined inverse mills ratio of the targets is reduced. Censoring limit T_l is found in relation to T_h according to the camera model. If both targets are well within the field of view then target measurements will be unbiased and the inverse mills ratios negligible, no change in T_h occurs, and the camera remains stationary. However, should target i move nearer to a censored region, that it is it approaches the edge of the field of view, then the respective λ_i pushes the desired censoring limit in such a manner as to reduce the expectation of censoring.

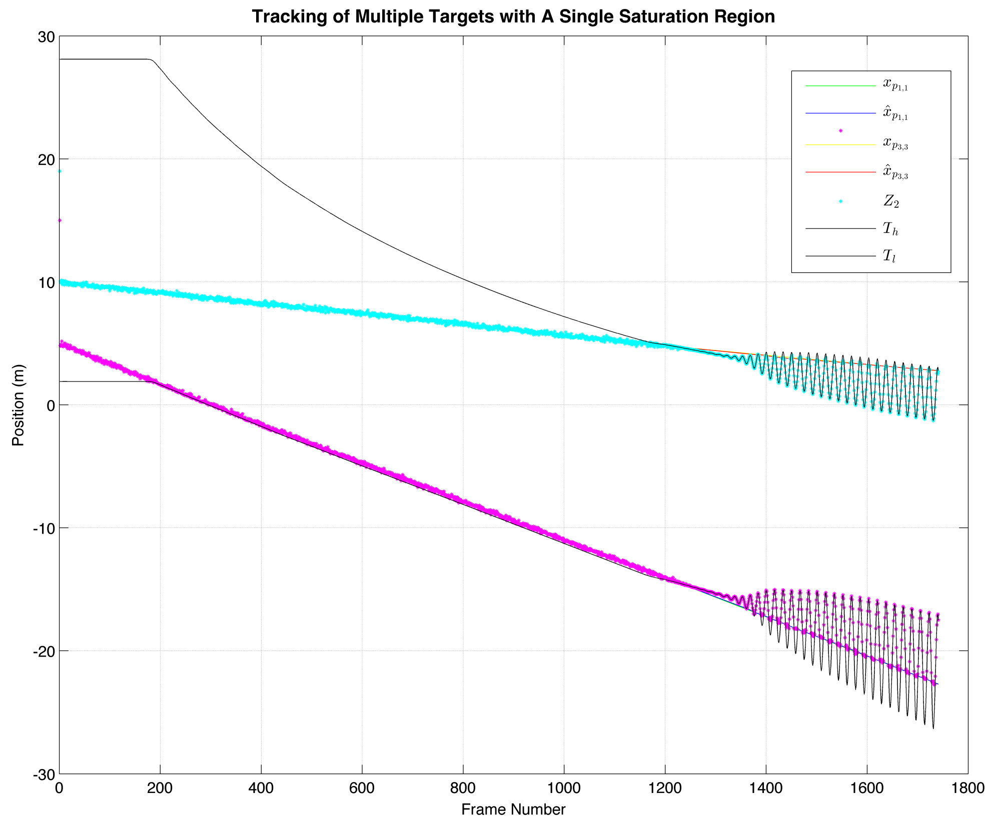

Figure 6.33: Automatic panning of a solitary FOV using a saturated Tobit Kalman filter, using the inverse mill ratio to control camera limits in order to estimate multiple targets.

In the given example the trajectories of the two targets begin in a similar manner, however the first target nears the edge of the field of view early on. The censoring limit T_h automatically compensates for this via the λ feedback, and the camera is panned to accomplish the desired censored limit and keep both targets in the field of view. However, because the second target is moving significantly slower, it begins to exit the opposite side of the field of view. Focal length is fixed so the separation between the T_h and T_l censoring limits cannot be expanded by increasing the field of view directly. Such an action may be undesirable, for the effective pixels on target are reduced and the vision algorithm may suffer accordingly. Therefore a panning motion is induced, for when the saturation limits are adjusted to view one target, the inverse mills ratio of the other target grows. Eventually λ_2 grows to such an extent that the saturation limits are forced to moved towards the offending second target, thereby causing λ_1 of the first target to grow. This balancing act is continued indefinitely, with the oscillations becoming greater in magnitude.

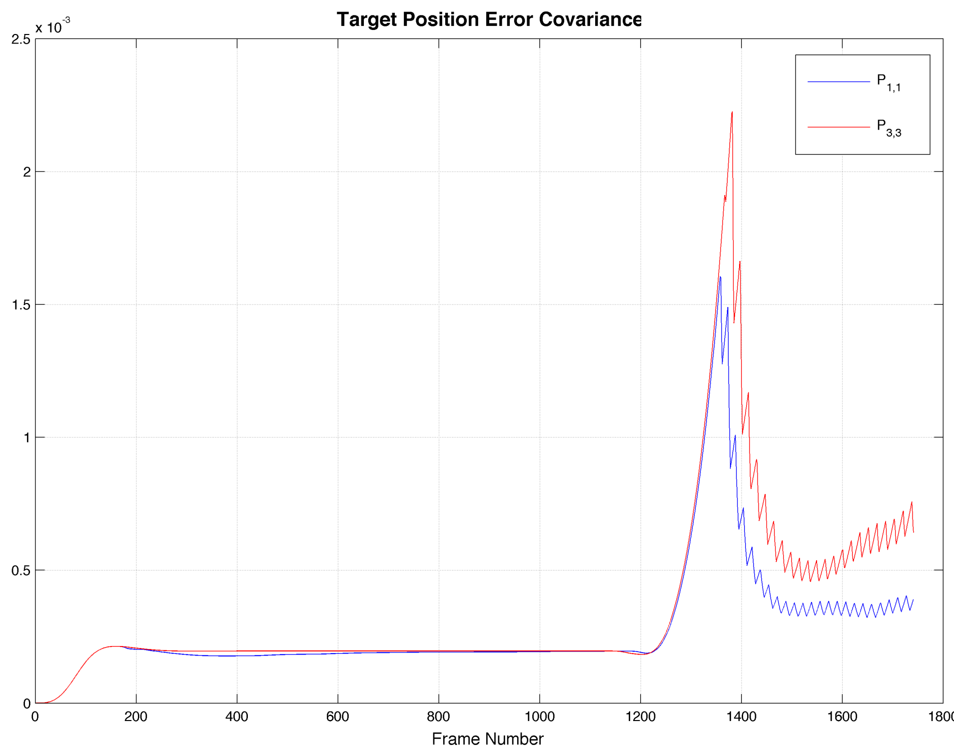

Figure 6.34: Error covariance of a saturated Tobit Kalman filter while using the inverse mill ratio to control camera limits in order to estimate multiple targets.

In figure 6.34 the error covariance for the above example is shown. The error covariance initially converges, as the both targets remain in the field of view and are not subjected to censoring. Eventually however, near the 1200 frame mark, the separation between targets has grown significantly large enough that both targets can no longer be contained in a fixed field of view. For a short period of time the inverse mills ratio feedback term has not accumulated enough to enforce a significant change in the censoring limit, thus the camera remains stationary, both targets are censored, and the error covariance grows rapidly. However, the feedback term eventually gains enough influence to begin the panning motion, in which each target is observed over alternating short time steps. At this time, the error covariance for each target is reduced. The error covariance for the first target remains lower as it remains uncensored for a larger proportion of the panning motion, as is evident in figure 6.33.

As shown in figure 6.34, and mentioned previously, the Tobit Kalman filter error covariance provides a meaningful measure of the quality of the current state estimate. This is valuable information that is not present in the standard Kalman Filter, which converges to a steady state, or is otherwise less informative, such as in the Sinopoli et. al Kalman filter in which the error covariance grows unnecessarily fast. Therefore, can this information be leveraged for use directly in the control of the censoring limits, as seen previously? Such a system is presented in figure 6.36, in which a similar scenario was constructed as to the previous example, except T_h is now updated according a feedback which incorporates the error covariance directly, with intent of driving the field of view in such a manner that a desired P confidence interval is always maintained. Such an update law takes the form of

$$T_h(k) = T_h(k-1) - K\left((P_{1,1}(k-1) - P_{ref_1}) - (P_{3,3}(k-1) - P_{ref_2})\right) \tag{6.76}$$

where, gain, K is a tuned proportional gain. The reference error covariances P_{ref_i} represent desired levels of uncertainty. These can be taken either as the optimal uncensored values, calculated according the steady state standard Kalman filter, or can be artificially set higher to reflect a more forgiving camera controller. For instance, setting P_{ref_i} higher than the uncensored value allows for the respective target to exit the field of view and remain censored until the error covariance grows to such a level that the feedback term then engages. For example, it is possible to designate these reference values according to the associated confidence interval of the state, such that the censoring limit is updated in order to maintain a 95% confidence that the target is within a given radius of the target estimate. Should an accurate dynamic model of the target be available, then the error covariance grows rather slowly even when the target is completely censored. Feedback on P therefore remains low, the censoring limit is not driven harshly at first, and unnecessary camera motion is avoided until error uncertainty grows to prescribed unacceptable level. In such a scenario the filter is in essence controlling uncertainty. An example of the motion induced by such a design is shown in figure 6.35 for a single target, and in figure 6.36 for multiple targets.

It is apparent in figure 6.35, that by directly using the error covariance as feedback, it is possible to allow the target to exit the field of view and still safely maintain a desired level of target location uncertainty. Thus the target object does not have to be strictly within the field of view at all times, and optimal techniques for practical control of the camera, such as power, bandwidth, field of view, etc., can be considered. The extension to two targets is shown in figure 6.36. A similar result is found as in that of 6.33, in which a panning motion is induced to alternatively view each target and reduce the total error uncertainty. Since the error covariance is used directly instead of the expectation of censoring, the targets are allowed more time in the censored region before uncertainty grows to an unacceptable level.

A more optimal feedback term for the adjustment of T_h would perhaps seek a motion which minimizes this error covariance over time with less of an oscillatory component, and which takes into account the dynamics of the panning motion itself and its effect on the camera system. Infinitely large and unrealistically fast panning oscillations need to be avoided in order to maintain vision algorithm performance and implement such a camera controller in a practical manner. Also the extension to

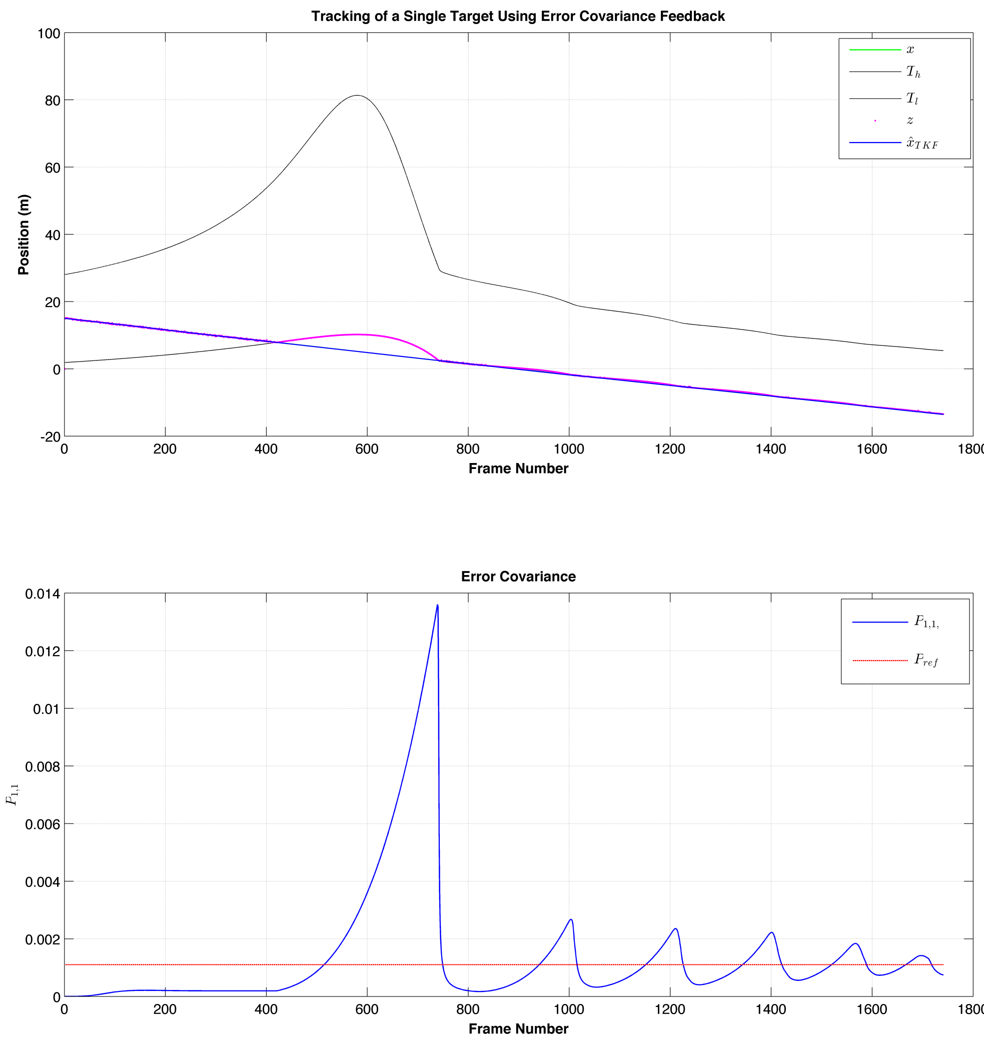

Figure 6.35: Automatic panning of a solitary FOV using a saturated Tobit Kalman filter, using the error covariance to control camera limits in order to maintain a desired level of target location uncertainty.

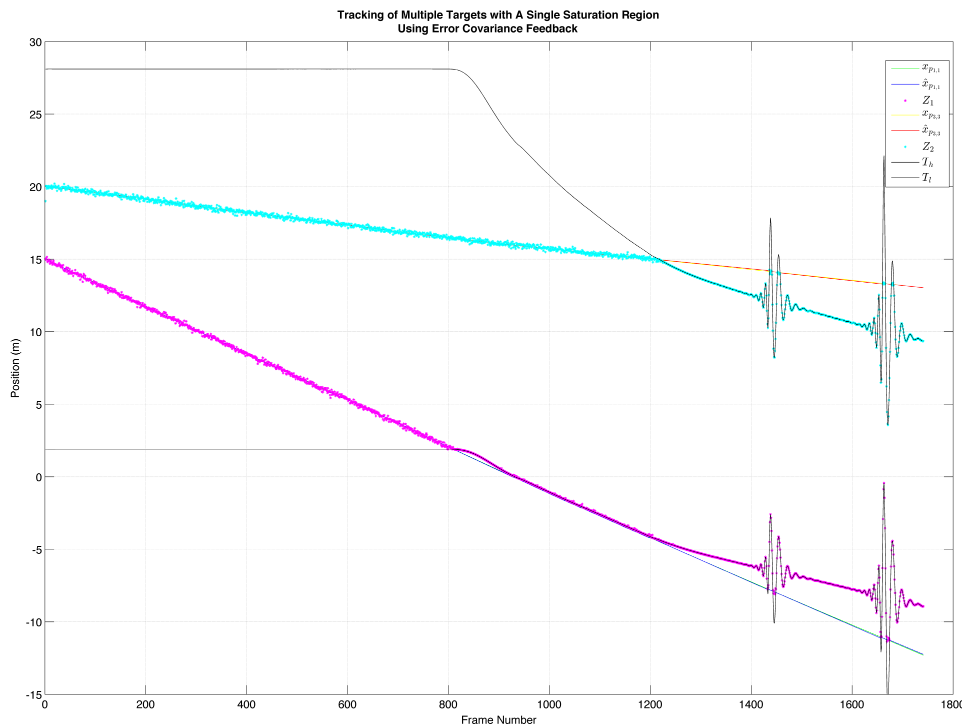

Figure 6.36: Automatic panning of a solitary FOV using a saturated Tobit Kalman filter, using the error covariance to control camera limits in order to track multiple targets.

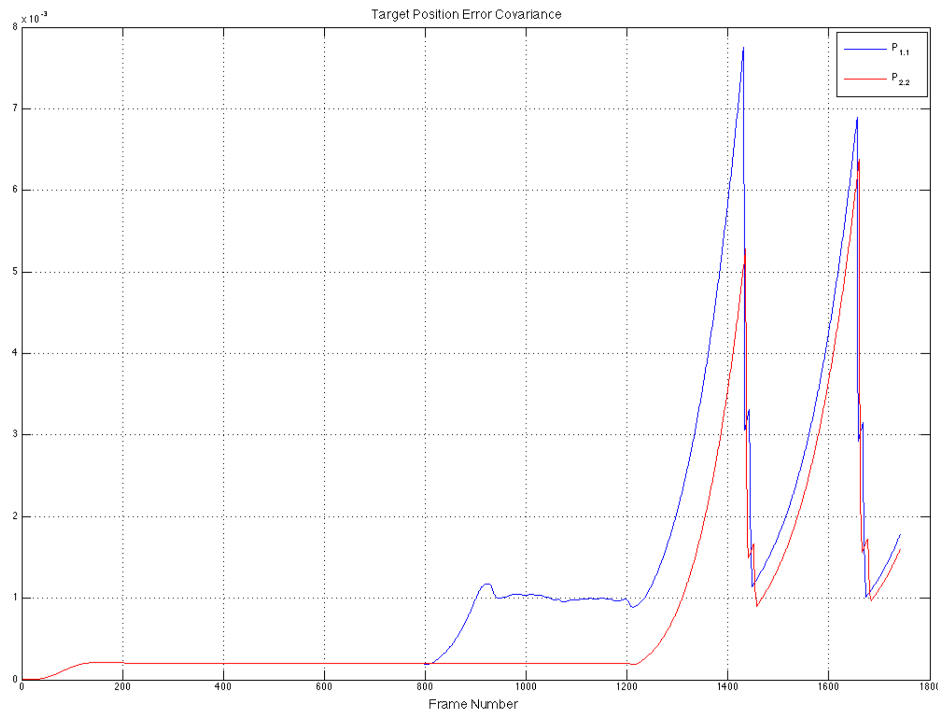

Figure 6.37: Error covariance while controlling camera FOV limits in order to track multiple targets.

the optimal tracking of N targets should be considered, and the usefulness of frame censoring over saturation censoring considered. Such concepts will be explored in future work.

Chapter 7

CONCLUSION AND FUTURE WORK

In this work a thorough introduction to the topic of estimation and control with censored data has been presented. Handling of censored data has largely been an under valued topic in many engineering disciplines, despite its practical relevance and common occurrence. Specifically addressed was the topic of output censoring in state-space dynamical systems, with the specific intent of deriving a recursive real-time estimator with application to practical control systems. In doing so the traditional method of recursive estimation via the Kalman filter was first introduced, with a discussion on the effects of censored measurements on such an estimator. Novel techniques were introduced for handling of censored measurements in vision based tracking system, without modification to the original Kalman filter framework.

The Tobit Kalman filter was derived, which utilizes a new measurement expectation model to re-derive the Kalman gain, measurement variance, and *a posteriori* state estimate and error covariance update. The effectiveness of the Tobit Kalman filter as a state estimator in the presence of censored data was demonstrated, and multiple censoring models were defined. A steady state Tobit Kalman filter was introduced which, assuming the censoring level can be changed, allows for convergence of the Tobit Kalman filter's gain, error covariance, and expectation of censoring, given certain conditions. After a brief introduction to basic linear control theory concepts, the stability of the Tobit Kalman filter estimator was discussed. It was shown that for inherently stable systems, in which the system matrix is stable, the Tobit Kalman filter always provides a stable state estimate despite the level of censoring present. For systems which are unstable, local stability of the estimator may be possible, depending on the censoring characteristics.

Given a stable Tobit Kalman estimator, an effective close loop LQG based output feedback controller was formed using the T.K.F. as a state observer. New control possibilities were introduced, one of which includes set point control to references within a censored region, a previously unacheivable result using traditional linear methods. Control using the steady state Tobit Kalman filter was demonstrated as well, and it was shown that high levels of censoring can be tolerated with stable systems with minimal degradation in control performance. Using the steady state Tobit Kalman filter observer, the effective performance of the resulting LQG output feedback controller can be analyzed for differing levels of expected censoring.

Novel estimation techniques were then discussed which utilize parameters unique the Tobit Kalman filter. Namely, the implications of multiple censoring regions was discussed via the sampling of multiple concurrent measurements. It was demonstrated how multiple censored measurements can be combined in a single filter to reduce estimator uncertainty. Particular attention was focused on the application of vision based tracking, in which it was demonstrated how saturation censoring can be used to model an airborne imager. Filter formulations were introduced for the tracking of one or more targets which exit the field of view, and automatic control of the camera saturation limits was demonstrated.

7.1 Future Work

The work presented here provides an exciting foundation for a large variety of both theoretical and applications based future research. From the stability analysis of more complicated non-linear systems subjected to censoring, to the simultaneous tracking of multiple targets using distributed censoring regions, the possibilities are truly endless. The implications of censored data and its effect on control systems is still a largely undervalued topic, despite its ubiquitous nature in nearly all of engineering and natural sciences. The questions raised throughout the development of the previous topics only adds more to the list of still unexplored areas. The way we think of censoring, and classify new problems in a censored formulation, is ever changing and evolving. Censored data is no longer relegated to simple saturated accelerometers or poor RF receivers, which are then ignored or shyed away from. The value of these censored measurements can now begin to be harnessed for ever newer techniques of estimation and control, examples of which are given by, but limited to, the following

Optimal Distribution of Multiple Censored Regions
The topic of multiple censored regions was introduced in 6.6 for stationary limits, and then leveraged in section 6.7 for moving censoring limits. There remains extensive research to be done in both of these topics. For instance, can a greedy algorithm be used to optimally distribute multiple censored regions throughout a given space such that total estimation error is minimized over all possible state trajectories? Can these regions be moved in real-time in an optimal fashion? Can swarm coverage be controlled to an increased area by incorporating censored communication between individual elements? Sensor fields of view may not need to overlap, and state uncertainty can be estimated and possibly controlled while inside the censored regions, as demonstrated in 6.7.

Optimal Tracking of Multiple Simultaneous Targets with a Limited FOV
An extension to the topic of tracking multiple targets with a limited field of view, as introduced in 6.7, has numerous applications to surveillance and optimal control. More optimal and stable panning motions should be found for increased effectiveness of automated surveillance. The concept of "controlling uncertainty", a unique property of the Tobit Kalman filter, should be leveraged and refined. Associating cost with particular tracking motions or tracking errors can lead to automatic priority assignment of multiple targets.

Frame Censoring with the Tobit Kalman Filter
The realization of frame censoring represents the most general and powerful censoring model for vision based tracking and detection systems. Extensions to multiple dimensions will lead a generic censoring model independent of potential application. However, the framework for censored measurement modeling and propagation for such a system is still in its infancy, and stability criteria is as of yet undefined. The possibility of more complicated censoring limits, of variable size and shape, need to be considered and the implications derived.

The Quantized Tobit Kalman Filter
Taking the idea of multiple censoring regions to the extreme results in the quantized Tobit Kalman filter, in which all of space is made up discrete bins with adjacent bounds. Now every measurement is an occluded measurement, with its value dependent upon the underlying continuous state, its noise distribution, and the distribution of occlusion regions. Can such a system be constructed with a

purpose? Perhaps to purposefully induce dithering such that optimal reconstruction of a continuous signal can be performed via estimation with Tobit Kalman filter with discrete measurements?

Sensor Fusion using the Tobit Kalman Filter

Introduced in section 6.6, the use of multiple censored regions with multiple censoring models presents unique applications towards new sensor fusion techniques. How can the Tobit Kalman filter be used to optimally combine the information present in an array of poor, possibly censored, measurements? In parallel to that of optimal distribution of censored regions, how can multiple different censoring models be optimally combined to maximize the information of the underlying system, with minimal cost?

Estimation and Control with Categorical Data

Exploration of non-traditional ways of classifying censored data leads to an entirely new field of advanced signal processing of categorical and survey data. How can one process measurements that are not truly numerical in nature, and yet still relate to a given underlying state to be estimated? What other systems and processes can be re-defined in a censored framework?

Non-linear Analysis of the Tobit Kalman Filter Estimator

Application of the Tobit Kalman filter to non-linear system will be explored. The state dependent nature of various Tobit parameters lends itself more naturally to a non-linear framework for more robust stability analysis. The study of conditions for global exponential stability of Tobit Kalman estimators of time-varying systems. Incorporation of possible non-linear censoring limit dynamics, as well as censoring limit uncertainty. Is there an applicable parallel to that of the E.K.F. for the Tobit Kalman filter, and if so, under what conditions?

Non-linear Control with a Tobit Kalman Filter Observer

Incorporation of advanced non-linear control techniques, coupled with T.K.F. estimators, for novel control techniques of both linear and non-linear systems subjected to persistent censoring. Moving away from LQG control to more robust control techniques. Guaranteeing control specifications for given levels of expected censoring and classes of inputs.

Adaptive & Network Control with a Tobit Kalman Observer

Coupling of Tobit Kalman estimation with concepts of optimal adaptive control, creating systems which can react to sudden changes in censoring. Network control of multiple agents, each potentially subjected to censoring. How long can a network node be censored before too much information is lost and the network fails? Can network converge exceed that of traditional techniques if information is allowed be censored?

BIBLIOGRAPHY

[1] T Amemiya. Regression analysis when the dependent variable is truncated normal. *Econometrica: Journal of the Econometric Society*, pages 997–1016, 1973.

[2] T Amemiya. The estimation of a simultaneous-equation tobit model. *International Economic Review*, pages 169–181, 1979.

[3] Christophe Andrieu and Arnaud Doucet. Particle filtering for partially observed gaussian state space models. *Journal of the Royal Statistical Society: Series B (Statistical Methodology)*, 64(4):827–836, 2002.

[4] Herbert Bay, Andreas Ess, Tinne Tuytelaars, and Luc Van Gool. Speeded-Up Robust Features (SURF). *Computer Vision and Image Understanding*, 110(3):346–359, June 2008.

[5] G Bishop and G Welch. An introduction to the kalman filter. *Proc of SIGGRAPH, Course*, 8:27599–23175, 2001.

[6] G Calzolari and G Fiorentini. Estimating variances and covariances in a censored regression model. *Statistica No. 53*, pages 323–339, 1993.

[7] R.T Carson and Y Sun. The Tobit model with a nonzero threshold. *The Econometrics Journal*, 10(3):488–502, 2007.

[8] T Cipra and R Romera. Kalman filter with outliers and missing observations. *Test*, 6(2):379–395, 1997.

[9] Tian He et al. "range-free localization schemes for large scale sensor networks.". *Proceedings of the 9th annual international conference on Mobile computing and networking*, 2:81–95, 2003.

[10] A Gern, U Franke, and P Levi. Robust vehicle tracking fusing radar and vision. In *International Conference on Multi-Sensor Fusion and Integration for Intelligent Systems*, pages 323–328. VDI/VDE Soc. Meas. & Autom. Control, 2001.

[11] JB Hampshire and J.W Strohbehn. Tobit maximum-likelihood estimation for stochastic time series affected by receiver saturation. *Information Theory, IEEE Transactions on*, 38(2):457–469, 1992.

[12] João P Hespanha. *Linear systems theory.* Princeton university press, 2009.

[13] Adrian T Hill and Achim Ilchmann. Exponential stability of time-varying linear systems. *IMA journal of numerical analysis*, 31(3):865–885, 2011.

[14] C Hue, J P Le Cadre, and P Pérez. Tracking multiple objects with particle filtering. *Aerospace and Electronic Systems, IEEE Transactions on*, 38(3):791–812, July 2002.

[15] Rudolph Emil Kalman. A new approach to linear filtering and prediction problems. *Transactions of the ASME–Journal of Basic Engineering*, 82:35–45, 1960.

[16] S Kar, B Sinopoli, and J.M.F Moura. Kalman filtering with intermittent observations: Weak convergence to a stationary distribution. *Automatic Control, IEEE Transactions on*, 57(2):405–420, 2012.

[17] Zia Khan, T Balch, and F Dellaert. MCMC-based particle filtering for tracking a variable number of interacting targets. *IEEE Trans. Pattern Anal. Machine Intell.*, 27(11):1805–1819, 2005.

[18] Y. M. Kwon, K. Mechitov, S. Sundresh, W. Kim, and G. Agha. "resilient localization for sensor networks in outdoor environments.". *Proceedings 25th IEEE International Conference on Distributed Computing Systems*, pages 643–652, 2005.

[19] J.F McDonald and R.A Moffitt. The uses of Tobit analysis. *The review of economics and statistics*, 62(2):318–321, 1980.

[20] Stephen J McKenna, Sumer Jabri, Zoran Duric, Azriel Rosenfeld, and Harry Wechsler. Tracking Groups of People. *Computer Vision and Image Understanding*, 80(1):42–56, October 2000.

[21] D Reid. An algorithm for tracking multiple targets. *Automatic Control, IEEE Transactions on*, 24(6):843–854, 1979.

[22] C Schmaltz, B Rosenhahn, T Brox, J Weickert, D Cremers, L Wietzke, and G Sommer. Occlusion modeling by tracking multiple objects. *Pattern Recognition*, pages 173–183, 2007.

[23] W Schnedler. Likelihood estimation for censored random vectors. *Econometric Reviews*, 24(2):195–217, 2005.

[24] B Sinopoli, L Schenato, M Franceschetti, K Poolla, M I Jordan, and S S Sastry. Kalman filtering with intermittent observations. *Automatic Control, IEEE Transactions on*, 49(9):1453–1464, 2004.

[25] B Sinopoli, L Schenato, M Franceschetti, K Poolla, M.I Jordan, and S.S Sastry. Kalman filtering with intermittent observations. *Automatic Control, IEEE Transactions on*, 49(9):1453–1464, 2004.

[26] R.J Smith and R.W Blundell. An exogeneity test for a simultaneous equation Tobit model with an application to labor supply. *Econometrica: Journal of the Econometric Society*, pages 679–685, 1986.

[27] S.C Smith and P Seiler. Estimation with lossy measurements: jump estimators for jump systems. *Automatic Control, IEEE Transactions on*, 48(12):2163–2171, 2003.

[28] Davide Spinello and Daniel J Stilwell. Nonlinear estimation with state-dependent gaussian observation noise. *IEEE Transactions on Automatic Control*, 55:1358–1366, 2010.

[29] H Tao, H Sawhney, and R Kumar. A sampling algorithm for tracking multiple objects. *Vision Algorithms: Theory and Practice*, pages 347–387, 2000.

[30] J Tobin. Estimation of relationships for limited dependent variables. *Econometrica: Journal of the Econometric Society*, pages 24–36, 1958.

[31] Jeffrey Vander Stoep. Design and implementation of reliable localization algorithms using received signal strength. *Diss. University of Washington*, 2009.

[32] Alper Yilmaz, Omar Javed, and Mubarak Shah. Object tracking. *ACM Comput. Surv.*, 38(4):13–es, December 2006.

[33] Tao Zhao and R Nevatia. Proceedings of the 2004 IEEE Computer Society Conference on Computer Vision and Pattern Recognition, 2004. CVPR 2004. In *Proceedings of the 2004 IEEE Computer Society Conference on Computer Vision and Pattern Recognition, 2004. CVPR 2004.*, pages 406–413. IEEE, 2004.